AN INVESTIGATIVE APPROACH TO EXPLORE OPTIMUM ASSEMBLY PROCESS DESIGN FOR ANNULAR TARGETS CARRYING LEU FOIL

A Thesis presented to
the Faculty of the Graduate School
at the University of Missouri – Columbia

In Partial Fulfillment

of the Requirements for the Degree

Master of Science

---

by

ANNEMARIE HOYER

Dr. A. Sherif El-Gizawy, Thesis Supervisor

DECEMBER 2013

The undersigned, appointed by the Dean of the Graduate School,

have examined the thesis entitled

AN INVESTIGATIVE APPROACH TO EXPLORE OPTIMUM ASSEMBLY PROCESS DESIGN FOR ANNULAR TARGETS CARRYING LEU FOIL

presented by Annemarie Hoyer,

a candidate for the degree of Master of Science in Mechanical Engineering,

and hereby certify that, in their opinion, it is worthy of acceptance.

_____

Professor A. Sherif El–Gizawy

_____

Professor Gary Solbrekken

_____

Professor Stephen Montgomery-Smith

_____

Professor Robert A. Winholtz

ACKNOWLEDGEMENTS

This thesis topic has been a great adventure for me. I thoroughly enjoyed working on this project and meeting all of those involved at MURR, ORNL, and Y-12. I thank all for this awesome opportunity to make a difference.

To express my thanks to individuals, I would like to say my biggest supporter was Emily Ferner Elmore, my cousin-by-marriage – you helped me achieve my goals and were the ever-present voice of comfort and guidance when I needed it most. I would also like to thank the undergraduate honor research students that helped out in the machine shop and those that became my support group to bounce ideas off. Jacob Harris and Andrew Gunn, your helping hands and contributions were greatly appreciated.

Secondly, I'd like to thank the graduate students from my lab that helped me as well: Ph.D candidate Shane Corl (FDM parts), Master's candidate Zhentao "Daniel" Xie (Hydroforming FEA modeling), Master's candidate Amer Krvavac (Hydroforming topic), Ph.D candidate Brian Graybill (FEA modeling of target – I'm still not judging you). You all are the reason I feel included at the office, my second home.

Next, I'd like to thank the guys that work for Dr. Solbrekken – Master's candidate Philip Makrarewicz and Ph.D candidate Srisharan Garg Govindarajan. I would have been lost without Philip's guidance and constant help; he was also a great person to bounce ideas off. Sri was an excellent source of reference material as well as a person that seemed to just know everyone. I'm excited to spend the summer working at ORNL with you!

I would also like to send a shout out to the ETS technicians that helped me: Ghassan Al Bahhash (you make the best parts in the fastest time – thanks!), Brian Samuels (no one welds like Brian), and Rex Gish (thanks dealing with my dumb questions and teaching

me the importance of drawing sheets and tolerances. I had no idea the financial difference between metric and English units were so difficult).

Next, I would like to thank the team that helped fund this project – John Creasy (project manager Y-12), Barak Tjader (project manager Y-12), Chris Bryan (project manager ORNL – thanks for the job this summer!), Steve Sherman (project manager ORNL), Thomas Watkins (XRD training and testing – epic triangle symbol!).

Next, I want to thank the individuals here at home responsible for running this project. Charlie Allen became my go-to person for historical questions on this project. He also seems to know everyone involved in this project and continues to help by securing funding. I see a trip to Germany in the future to research sputtering. Also, a huge thank you to Dr. Solbrekken for allowing me to help out with your project – this has really opened my eyes to the importance of what we do. Thank you!

Lastly, I want to thank Dr. El-Gizawy for this awesome opportunity to work with a great research team and to meet such great people. I have learned so much and am especially grateful to take part in this important work. I would like to send one more thank to the gentlemen reading my thesis, Dr. El-Gizawy, Dr. Solbrekken, Dr. Winholtz and Dr. Montgomery-Smith. Your time and patience is much appreciated.

"The will to conquer is the first condition of victory." – Grimm

"Don't bother just to be better than your contemporaries or predecessors. Try to be better than yourself." – William Faulkner

TABLE OF CONTENTS

LIST OF FIGURES

Figure Page

LIST OF TABLES

NONMENCLATURE

e^-	beta particle
ν_e	electron antineutrino
γ	gamma ray
σ_{dr}	drawing stress, Pa
σ_{fr}	forming stress, Pa
Q_{dr}	drawing ratio
Q_{fr}	forming ratio
ε	strain
δ	inhomogeneity factor
μ	coefficient of friction
α	half angle of draw plug
L	length of plug, mm
a_0	internal diameter of inner tube
a_1	maximum plug diameter
M	moment due to stress distribution
I	section area moment
c	distance from neutral axis to outer beam
S_y	yield strength
h_p	depth of plastic region

SN_N	signal to noise, nominal the better
SN_L	signal to noise, larger the better
SN_S	signal to noise, smaller the better
y	sample measurement
n	number of samples
S^2	variance
σ_H	hoop stress
F	force
t	radial thickness
l	axial length of cylinder
d	interplanar spacing
v	Poisson's ratio
E	Young's modulus
ϕ	azimuthal angle
ψ	tilt angle
D_{tube}	tube diameter
X	x data point probe result
Y	y data point probe result
D_{probe}	probe diameter

AN INVESTIGATIVE APPROACH TO EXPLORE OPTIMUM ASSEMBLY PROCESS DESIGN FOR ANNULAR TARGETS CARRYING LEU FOIL

Annemarie Hoyer

Dr. A. Sherif El-Gizawy, Thesis Supervisor

ABSTRACT

Technetium-99m is the most widely used nuclear isotope in the medical field, with nearly 80 to 85% of all diagnostic imaging procedures. The daughter isotope of molybdenum-99 is currently produced using weapons-grade uranium. A suggested design for aluminum targets carrying low-enriched uranium (LEU) foil is presented for the fulfillment of eliminating highly enriched uranium (HEU) for medical isotope production. The assembly process that this research focuses on is the conventional draw-plug process which is currently used and lastly the sealing process. The research is unique in that it is a systematic approach to explore the optimal target assembly process to produce those targets with the required quality and integrity.

Conducting 9 parametric experiments, aluminum tubes with a nickel foil fission-barrier and a surrogate stainless steel foil are assembled, welded and then examined to find defects, to determine residual stresses, and to find the best cost-effective target dimensions. The experimental design consists of 9 assembly combinations that were found through orthogonal arrays in order to explore the significance of each factor. Using probabilistic modeling, the parametric study is investigated using the Taguchi method of robust analysis. Depending on the situation, optimal conditions may be a

nominal, a minimized or occasionally a maximized condition. The results will provide the best target design and will give optimal quality with little or no assembly defects.

CHAPTER 1

INTRODUCTION

MOTIVATION

On August 8, 2005, the United States under President George W. Bush signed the Energy Policy Act of 2005 at Sandia National Laboratories in Albuquerque, New Mexico. "This legislation promotes dependable, affordable, and environmentally sound production and distribution of energy for America's future" [1]. Section 630 of the policy mandates a study to be done by the National Academy of Sciences (NAS) that validates the technical and economic feasibility of converting molybdenum – 99 (Mo – 99) for production with low enriched uranium (LEU). Out of the National Nuclear Security Administration (NNSA), the office of Global Threat Reduction Initiative (GTRI) states their mission is to reduce and protect vulnerable nuclear and radiological material located at civilian sites worldwide. This research focuses on the conversion process; more specifically, the conversion of high enriched uranium (HEU) targets to LEU medical isotope targets. The program to reduce use of HEU in the civilian sphere was initiated in 1978 and still continues today. In 1992, the United States passed the Schumer Amendment to the Energy Policy Act that limited U.S. exports of HEU to facilities that met several conditions: (1) lack alternative LEU production process, (2) agree to switch to LEU when possible and (3) the U.S. had to be actively developing an alternative LEU production process suitable for the facility. These efforts will result in the permanent threat reduction by minimizing and, to the extent possibly, eliminating the need for HEU in civilian applications [2]. Thus, a source of nuclear weapons material is removed. Dr. Peter Karamoskos states that "the world is heading in

a very dangerous direction. Far from the threat of nuclear weapons having receded with the downfall of the Soviet Union and the end of the cold war, the world stands at the brink of a second nuclear age" [3]. Due to the accelerating spread of nuclear weapons, nuclear know-how and nuclear materials, the nuclear threat is very much a real one. The two most widespread uses of HEU are as research reactor fuel and as targets for the production of medical isotopes; and is thus prone to theft in the civilian sector more so than military or weapons production facilities. With low concentrations of Uranium – 235 isotopes, LEU cannot be used in nuclear weapons. In addition, it has been discussed that decommissioning or converting reactors to use LEU is less expensive than improving physical protection requirements to levels for HEU protection. Although operating costs should be the same or less for LEU processing, the conversion from HEU will be a significant cost to current producers.

The conversion of molybdenum – 99 production from HEU to LEU would increase reliability of molybdenum – 99 supplies in one important respect: namely it would remove longer-term uncertainties associated with the continued availability of HEU for molybdenum – 99 production – using the same reactors and same or similar processes [4]. One strategy to achieve this goal is to use a target that utilizes a LEU foil. Currently, molybdenum – 99 production uses HEU in a powder dispersion target. This method, conventionally used for fuel rods and plates, combines fine particles of aluminum and HEU to bond into a rigid plate during irradiation [5]. The highly desired isotope, Technetium 99m (Tc-99m), is one of the decay by-products in the production of molybdenum – 99 and is derived from weapons-grade HEU.

Weapons grade HEU poses a significant terrorist nuclear proliferation threat. In accordance to GTRI, all molybdenum – 99 production must switch from using HEU to LEU; though, this switch will increase safety, it is also the motivating factor behind the switch from the dispersion target to the foil target [6]. Incidentally, all of the United States supply of molybdenum – 99 is entirely supplied by foreign countries: Canada, the Netherlands, South Africa and Belgium. For this reason, the University of Missouri is attempting to become one of the larger suppliers of molybdenum – 99 that will naturally lead to a domestic supply of the most needed medical isotope and as well providing to international countries.

What does this mean for the U.S. as a nation? In order to eliminate HEU from any and all processes, a new source must be found suitable to replace. However, HEU is not only used as a medical isotope, but also it is still used as reactor fuel for three of the seven nuclear reactors around the world that produce molybdenum – 99. Also, three of the four molybdenum – 99 processing facilities use HEU targets with the fourth (South Africa) in the process of converting to LEU. One major advantage to LEU is that it is produced by the dilution of HEU. By adulterating all HEU possible, the abundant weapons grade uranium would be converted to non-weapons grade. All feasibility tests up-to-date state that the conversion process is possible with some success stories. The biggest obstacles besides some technical difficulties lie with commercialization of molybdenum – 99 production. Some other obstacles include the larger space required for the number of targets to be irradiated so that more targets filled with LEU foil are produced in order to match the amount produced using HEU targets. In addition, the higher volume of waste produced by the process can also prove to be a slight obstacle as well [7].

APPLICATION

Nuclear medicine uses radioisotopes for research diagnosis and treatment of diseases, such as cancer and other types of illnesses. Some medically relevant radioisotopes include Actinium – 225, Carbon – 11, Iodine – 123 and Strontium – 82. However, nearly 80 – 85 % of diagnostic imaging procedures in nuclear medicine use the daughter isotope of molybdenum – 99, Technetium – 99m. The "m" indicates that this is a metastable nuclear isomer. This much usage roughly estimates as 30 million diagnostic imagining procedures annually [8]. Scientists continue to find new uses for Technetium – 99m in the imaging field, especially with the high rate of developing cancer patients. The earliest detection is a large factor in recovery chances. With Technetium – 99m, the detection of cancer cells/tumors is noninvasive, with is an advantage for the medical world.

The most popular nuclear medical isotope is indeed Technetium – 99m and it is well suited to be used as a radioactive tracer because it can be easily detected in the human body via medical equipment. It emits 140 keV gamma rays and has a very short half-life of 6 hours, which poses many problems. Because of such a short half-life, Technetium – 99m cannot be transported over large distances nor can it sit on the shelf until needed. The parent isotope, molybdenum – 99, has a longer half-life of 66 hours, and thus makes this isotope the best phase for travel. During this phase of radioactivity, the molybdenum – 99 isotope is shipped to radiopharmacies and hospitals in radiation-shielded cartridges known as technetium generators as seen in Fig. 1-1 [4]. Generator systems were developed in 1958 by Brookhaven National Lab (BNL), when scientists accidently discovered that molybdenum – 99 could generate Technetium – 99m [9].

Fig. 1-1. Technetium Generators [4].

molybdenum – 99 decay into Technetium – 99m by emitting a beta particle and an antineutrino. The decay process results in Technetium – 99m as described in Eq. (1-1), with the e^- as the beta particle emitted and v_e as the electron antineutrino [6]. Furthermore, the Technetium – 99m similarly undergoes a transition phase, emitting a gamma ray to yield Technetium – 99, shown by Eq. (1-2).

$$^{99}\mathrm{Mo} \rightarrow {}^{99m}\mathrm{Tc} + e^- + \mathbf{v}_e \tag{1-1}$$

$$^{99m}\mathrm{Tc} \rightarrow {}^{99}\mathrm{Tc} + \gamma \tag{1-2}$$

Unlike the previous parent isotopes, Technetium – 99 has a long half-life of 214,000 years. Unfortunately, Technetium – 99 has no significant industrial use; however, it has been proposed that Technetium – 99 be used for optoelectronic devices and nanoscale nuclear batteries. With such a short time frame from irradiated targets to injections of Technetium – 99m, the entire process takes approximately in the range of 5 to 20 days, depending on the processing facility, shipping distances and availability and frequency of transportation. See Table 1-1 for breakdown of times. Sadly, even though the extraction process can recover a highly pure product, more than half of the molybdenum – 99 decays during the phase of target irradiation.

Table 1-1. Typical Process Times for Mo-99 and Tc-99m Supply Chains [4].

Process Steps	**Typical process times (hr)**
U-235 target irradiation and cooling	130 - 168 (5-7 days)
Shipping and Processing of target to extract Mo-99	6 - 28
Mo-99 packaged and shipped	6 - 12
Tc-99m generator prepared and packaged	12
Tc-99m generator shipped	1 - 24
Tc-99m generator used by hospital or radiopharmacy	168 - 336 (7 - 14 days)

As stated before, there are no domestic suppliers in the U.S. for molybdenum – 99 and all isotopes are shipped from foreign countries. Prior to its shutdown, the reactor in Canada was producing nearly 60 % of the U.S supply of molybdenum – 99 and 40 % of the world supply, depending on global reactor production schedules [10]. MDS Nordion as a supplier was ideal for U.S. supply due to the country's proximity, even as the plant continued to use HEU targets and reactor utilized LEU reactor fuel. Over the past few years, MDS Nordion has at one point supplied 100 % of the U.S supply of molybdenum – 99. Operating since 1957, the National Research Universal (NRU) reactor in Canada was replaced with the Multipurpose Applied Physics Lattice Experiment (MAPLE) reactors that went into effect in the mid-1990s. However, after commission in 2000, the MAPLE reactors announced in 2003 that the reactors had a positive coefficient of reactivity which meant the reactors could become unstable and uncontrollable. Five years later and millions of dollars spent on investigations and

modifications, the cause of the positive coefficient could not be identified. In May of 2008, the MAPLE project was terminated. The NRU reactor continues to be a leader in molybdenum – 99 supply, but is scheduled for shut-down by end of 2015, with no backup reactor available to come online before then. The MAPLE reactors are shown in Fig. 1-2 [11].

Fig. 1-2. MAPLE 1 and 2 reactors, and New Processing Facility, at AECL Chalk River Laboratories (NRU and NRX reactors are behind, on the left and right, respectively) [11].

Other foreign producers of molybdenum – 99 include the Netherlands. Mallinckrodt produced approximately 40 % of the U.S. supply of molybdenum – 99 and about 25 % of the world supply [4]. At the Petten site, production began in late 1998 and targets are irradiated in 3 reactors: (1) the High Flux Reactor (HFR) located at Petten, (2) the Belgian Reactor II located at Mol, Belgium and (3) Osiris reactor located in Saclay, France. Through Mallinckrodt, the Institute National des Radioelements (IRE) in Belgium produces molybdenum – 99 for U.S. use and separately produces approximately 20 % of the world supply of molybdenum – 99. Targets are irradiated in one of the three reactors mentioned for the Petten site. However, the Petten reactor, HFR, was shut down for several lengthy periods: once in 2008, another in 2010 and then again in November 2011 due to repairs of the cooling system. Also, the IRE in 2008 shut down briefly after I-131 was unexpectedly vented through a stack. With the two to three major producers of molybdenum – 99 out of service, the need to develop new molybdenum – 99 production systems

because the highlight of many energy policies. During this time, the radiopharmaceutical companies and hospital were in desperate need of molybdenum – 99 with no supplier, creating a global molybdenum – 99 shortage.

The last supplier of molybdenum – 99 is NTP Radioisotopes out of South Africa. This supplier produces 10 % of the world supply of molybdenum – 99 and provides back up supplies to the U.S market [4]. Targets are irradiated in the Safari – 1 reactor which is currently undergoing conversion of HEU fuel to LEU. On December 6, 2010, Lantheus Medical Imaging, a molybdenum – 99 producer, received the first shipment of FDA – approved LEU-produced medical isotopes from NTP [12].

Today, there are four reactors that utilize LEU targets with a fifth slowly emerging. The Australian Nuclear Science and Technology Organization (ANSTO) reactor was using LEU targets with LEU fuel in 2007, with Lantheus Medical as the molybdenum – 99 processor in 2009. Besides South Africa and Australia using LEU targets, Argentina was the first institution to turn from HEU to LEU targets commercially, not just for research. Having produced molybdenum – 99 with HEU targets since 1985, the reactor in Argentina, Commision Nacional De Energia Atomica (CNEA), switched in 2002 towards LEU targets due to difficulties of obtaining HEU. Lastly, the BATAN reactor in Serpong, Indonesia demonstrated the irradiation, disassembly and processing of LEU targets in 1995 and has produced as many as 2000 targets annually. On a joint research project with Argonne National Lab (ANL) since 1992, BATAN was a resource to irradiate research targets and remove LEU foil post irradiation [13]. NTP, ANSTO, CNEA and BATAN are the four reactors using LEU targets and either using or

currently converting to LEU fuel. The fifth reactor is University of Missouri Research Reactor (MURR). With funding from Y-12 National Security Complex, College of Engineering researchers are working through technical issues of LEU targets and irradiation, while MURR is in the process of converting to LEU fuel. In a presentation about GTRI's molybdenum – 99 Program on December 5, 2011, Parrish Staples provided the following Fig. 1-3 about U.S. supply matrix as of 2010 to help distinguish what reactors and producers are using HEU/LEU fuel and/or HEU/LEU targets.

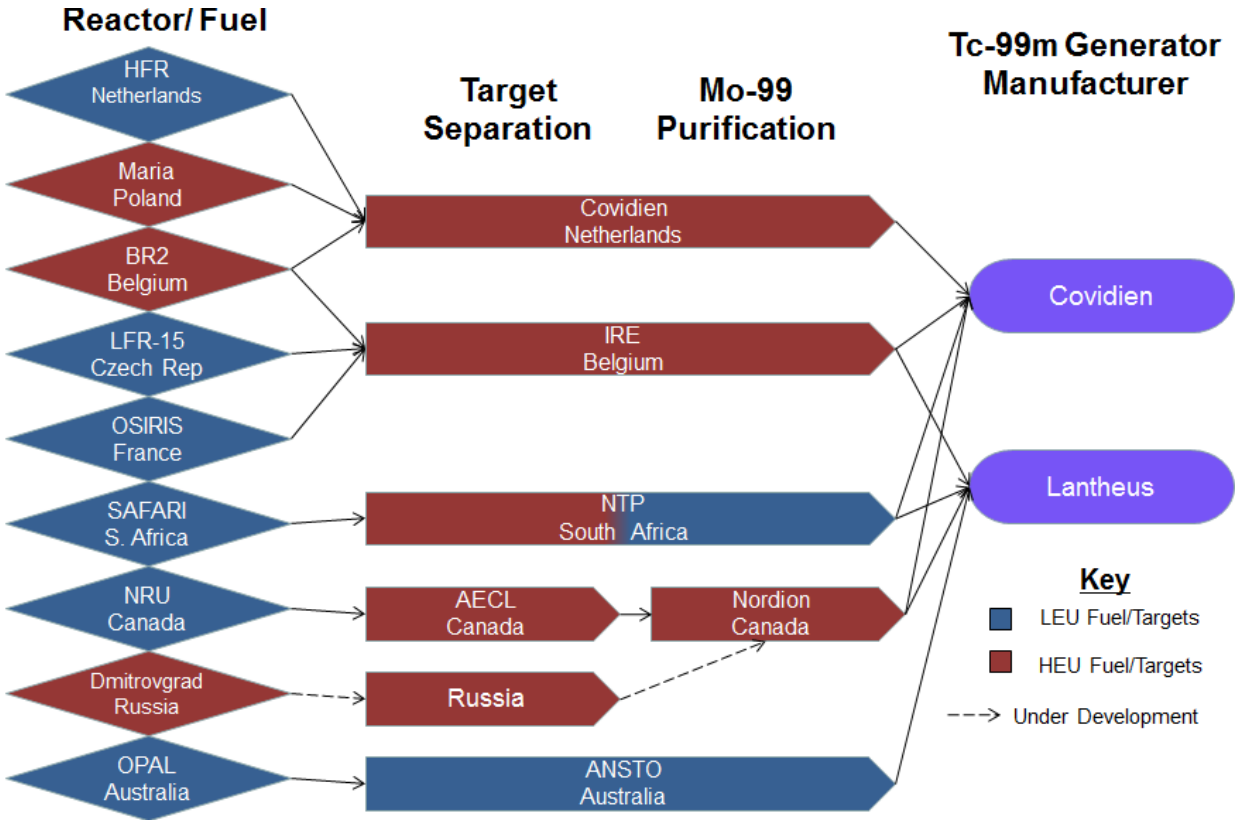

Fig. 1-3. Current U.S. Mo-99 Supply Matrix [14].

Even though NTP has slowly been supplying molybdenum – 99, our major target producer will go offline by the end of 2015 due to the age of the reactor. Because NRU in Canada supplies the majority of molybdenum – 99, it is imperative that new LEU methods are found. It is because of this new deadline that scientists and politicians are working to have a U.S. domesticated system

of molybdenum – 99 production in place by 2016. In fact, Belgium, France and the Netherlands have announced with the U.S. a common understanding to help minimize the use of HEU in the production of medical isotopes [15]. Even places like Iran are interested in supporting their nuclear program, one of the most polarizing issues in the one of the world's most volatile regions. The New York Times reports that "while American and European officials believe Tehran is planning to build nuclear weapons, Iran's leadership says that its goal in developing a nuclear program is to generate electricity without dipping into the oil supply it prefers to sell abroad and *to provide fuel for medical reactors*" [16].

BACKGROUND

This research study will focus strictly on the assembly and fabrication of targets and will not discuss the irradiation of those targets. Two processes have been developed at the University of Missouri with a third concept that MU is collaborating with Forschungs-Neutronenquelle Heinz Maier-Leibnitz (FRM II) out of Munich, Germany. The two means of assembly that have been designed at the University of Missouri are a swaging and a hydroforming process. While hydroforming is still in the feasibility stage, the experiments and results reported will only be applicable to the swaging process. The swaging experimented assembly method will be discussed in detail in Chapter 2, Literature Review along with previous experiments done by other labs. The third and last concept as part of the collaboration that has just begun its feasibility stage is a sputtering process and work is done in a joint research project with graduate students at FRM II.

The swaging process has been a common idea, but no institution has successfully found a working combination. Two years ago, 2011, the first feasibility tests were done at Mizzou, using

the Argonne National Lab working drawing of target dimensions. Our initial setup included a draw plug and a drawing die, as shown in Fig. 1-4. The plug is orange, the inner tube is blue, the outer tube is red, and lastly, the drawing die is yellow. The function of the die is to ensure uniform deformation and prevent tube rupture.

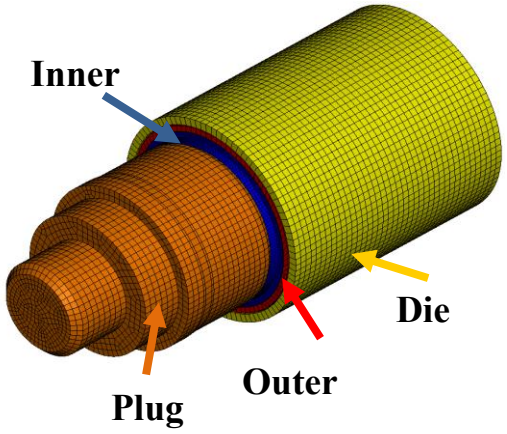

Fig. 1-4. Draw die setup with inner and outer target tubes.

All feasible tests showed promising efforts. However, as with any new system, there were some flaws and defects. The biggest issue was the amount of gaps, shown in Fig. 1-5. Gaps create a problem for thermal properties and allow heat convection to the uranium foil, which then could in turn cause the uranium to bond with the barrier. However, it has been suggested that some gap around the foil edges would be a positive attribute to provide space the fission gases during irradiation.

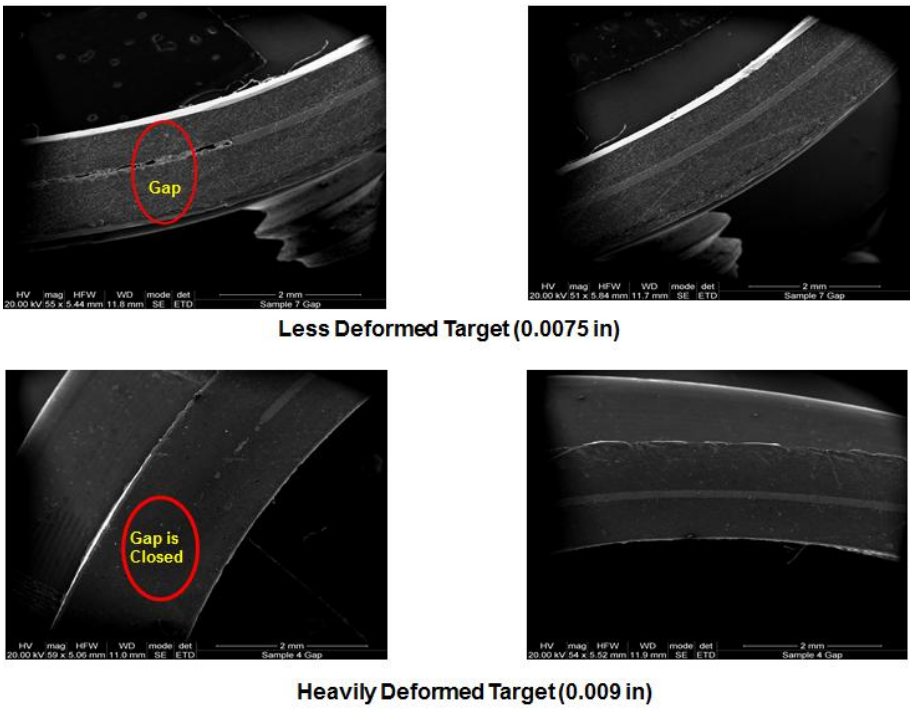

Fig. 1-5. Air gaps illustrated in the cross-section of the foil area.

With this new information, the next step is to optimize the target dimensions/ratios for proposed system. An experimental matrix was designed using the Taguchi optimization method.

As with all research projects, there are several goals associated with this work. Because there is no domestic U.S. molybdenum – 99 producer or supplier, one goal is to create a simple system that can produce as many as 5000 targets annually. Ideally, MURR would be the first internal supplier. The second goal is to create a system that is cost effective and that can be shared with third world countries. It has been suggested that the new LEU targets should cost similarly to HEU targets. If cost can be reduced, that would make this system more sufficient for third world countries. The third and last goal is to create a system that is flexible to material, tube diameter and tube length. The proposed system will be able to accommodate all of these goals.

CHAPTER 2

LITERATURE REVIEW

CURRENT PRODUCTION

Ninety five to ninety eight percent of the world's supply of molybdenum – 99 is produced by just four organizations: MDS Nordion, Mallinckrodt, Institute National des Radioelements Belgium and Nuclear Technology Products Radioisotopes (NTP) [4]. The four organizations listed are considered large-scale production because they supply more than 1000 6-day curies of molybdenum – 99 per week to the market on routine basis. Each producer uses their own process of assembling targets and later extracting molybdenum – 99, but all suppliers produce nearly pure molybdenum – 99 product. This poses a problem because none of these organizations have a home base in the United States. All of molybdenum – 99 must be imported and therefore billions of dollars are spent to neighboring countries. One of the goals as set by the U.S. Department of Energy is to provide molybdenum – 99 in-house, so to speak. In addition to providing 50% of domestic needs of molybdenum – 99, the U.S. also hopes to provide 50% of the world's supply of molybdenum – 99.

TARGET DEVELOPMENT

The research described here will focus on the irradiated targets. "The 'target' used for molybdenum – 99 production is a material containing uranium – 235 that is designed to be irradiated in a nuclear reactor" [4]. In detail, the assembly process will be explained as well as the swaging process. However, it is necessary to revisit the history of the target selection and assembly to avoid making similar and unnecessary mistakes. "One way to categorize the world's molybdenum – 99 production is by the type of target used" [17]. For example, the

Australian Nuclear Science and Technology Organization (ANSTO) uses a target consisting of slightly enriched UO_2 pellets. This is very specific to LEU targets as denoted by the descriptors "slightly enriched." Target that still utilize HEU are one of the three following states: (1) Miniature Al-clad fuel plates containing U-Al alloy (UAl_x) dispersion fuel [Argentine National Atomic Energy Commission (CNEA), National Institute of Radioelements (IRE) of Belgium, Mallinckrodt in the Netherlands, etc.]. (2) Pins containing U-Al alloy [Atomic Energy of Canada, Limited (AECL)], or (3) a thin film of UO_2 coated on the inside of a stainless steel tube [National Atomic Energy Agency (BATAN) of Indonesia and Sandia National Laboratories (SNL)]. Use of an electrodeposited UO_2 layer on the inner surface of a stainless steel cylinder, which is used as both a target and a dissolver, is part of the so-called Cintichem process, developed by Union Carbide [18].

It important to note here that there is no literature or previous work done to systematically study the assembly process. Many countries have created their targets with a "trial and error" approach, but none provided a scientific approach behind their targets assembly process. Additionally, there is no literature that covers the effects of the drawing process and the welding process together. Thus, the research reported here is original and innovative in the field of molybdenum – 99 targets.

One of the leading national labs in the initial design of annular targets is Argonne National Labs. Argonne concentrated on the design shown in Fig. 2-1, where a thin (125 μm thick) uranium metal foil is sandwiched between slightly tapered inner and outer tubes.

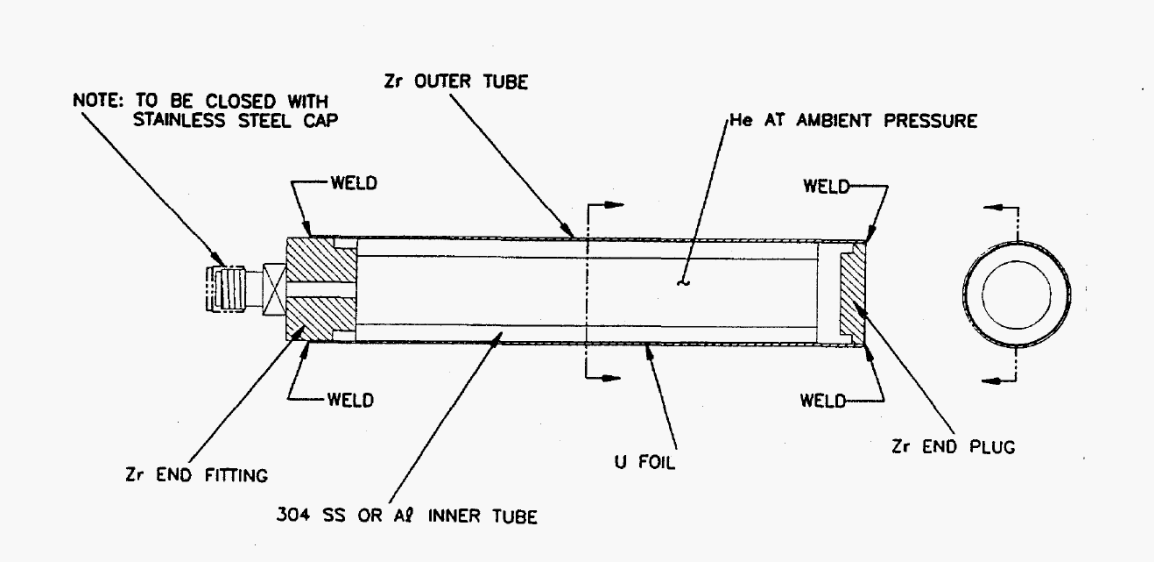

Fig. 2-1. Argonne National Lab Drawing of U-Metal Foil Target [17].

This design was chosen in order to increase the molybdenum-99 yield while decreasing the amount of waste. The inner tube was preferentially made of a material with a larger thermal expansion coefficient than that of the outer tube material in order for differential thermal expansion to assist in maintaining good thermal contact between the foil and the tubes. Additional reasoning behind this design is that once cooled, the disassembly process will be easier because the inner tube will shrink more than the outer tube.

Argonne chose several different types of tubing materials as well as discovering the need for additional metal foil to protect the uranium foil. As will be discovered, one of the biggest issues was the uranium bonding to the cladding material and thus making disassembly difficult.
In summer of 1995, four targets were assembled and disassembled. The first sample consisted of a zirconium outer tube and an aluminum inner tube. Zirconium has a much lower thermal expansion coefficient than aluminum. However, in spite of an aluminum oxide barrier on the inner tube, the uranium reacted with the aluminum and could not be removed. On the flip side, metallography showed no apparent interaction of the uranium with the zirconium outer tune, on

which a thin zirconium oxide barrier had been placed. Argonne then assumed that zirconium was a suitable target tube material. The second target sample used a zirconium outer tube because of the promising results from the first sample and an aluminum inner tube, coated with flame-sprayed zirconium layer; thereby, retaining all the features of the first design and adding a zirconium layer between the uranium and aluminum to prevent interaction [17]. A third sample was created using zirconium as the material for the outer tube and magnesium as the material for the inner tube. Lastly, at this time, a fourth sample was made with zirconium for the outer tube material and the inner tube material as well. In the fourth sample, obviously there was no thermal expansion difference present due to the same material being used, but this was necessary to prove the nonbonding of uranium foil and zirconium. After irradiation, the last three samples (2^{nd}, 3^{rd} and 4^{th} sample) were examined to determine performance of the materials. The results showed that the uranium foil had bonded to the inner tube of each sample tested. Argonne surmised that the explanation was that the high fission rate in the uranium and correspondingly high recoil atom flux at the uranium–target tube interface lead to an efficient atomic intermixing at the interface. The results concluded that uranium bonding by this mechanism will occur with any material.

In August of 1996, four more targets were assembled and irradiated to test two basic concepts. The latter two samples will demonstrate firstly the importance of uranium foil bonding with the inner tube and secondly the viability of the fission–fragment barrier concept. The first sample was a zirconium outer tube with an austenitic stainless steel inner tube. Stainless steel was chosen because the uranium foil will bond to the inner tube with the foil and will be harvested together from the zirconium after irradiation. Additionally, stainless steel does not dissolve in

acid; therefore, only the uranium foil will dissolved, thus decreasing waste material. Results from this first sample showed that the uranium foil had bonded with the zirconium, which was unexpected. Therefore, with the foil bonding to both inner and outer tubes, the inner tube could not be extracted. To overcome the uranium bonding with the cladding material, a thin recoil–absorbing barrier foil of approximately 10 μm thickness were placed between the uranium and one or both target tubes. Argonne expected the foil to bond with the uranium but not with the tubes, since the fission fragments will not penetrate the barrier. Since the barrier foils must be dissolved with the uranium foil, only certain materials such as nickel, copper, iron and zinc are allowed. The second sample utilized nickel foil on both sides of the uranium foil with an aluminum inner tube with un-oxidized surfaces. It is unclear what the outer tube material, but it was assumed that zirconium was used. Results showed that the inner tube with foils was easily extractable, but the foils could not be removed, indicating bonding, presumably by diffusion, of the nickel to the aluminum. It was surmised that an introduction of an aluminum oxide layer will help prevent such bonding. The last two samples used a stainless steel inner tube with a zirconium outer tube. The third sample used nickel foil only between the uranium and outer tube. As expected, the foil bonded with the stainless steel, but the inner tube with foil was extractable. With this case, the inner tube could be put in acid and the uranium/nickel foils dissolved. The fourth and last sample used copper barrier foils on both sides of the uranium foil. Results indicated that the inner tube with foils was easily extractable and the foil sandwich was easily removed from the inner tube.

In August of 1998, several tests were run with different barrier foil thicknesses as well as barrier material. Table 2-1 shows the results of those tests. The importance of this table helps to

distinguish which combinations of foil and tubing materials work well. From there, thermal and mechanical properties are then reviewed to pinpoint specifically the appropriate combination.

Table 2-1. Characteristics of LEU Metal-Foil Targets Irradiated in the RSG-GAS Reactor during August 1998[a] [19].

Target		Barrier		Inner Tube	
No.	Inner Wall	Material	Thickness, μm	Extractable?	Foil Removed?
1	304 SS	Zn foil	15	Yes	Yes
2	304 SS	Ni foil	15	Yes	Yes
3	304 SS	Zn plate	17[b]	Yes	Yes
4	304 SS	Ni plate	11	Yes	Yes
5	304 SS	Al foil	23	Yes	No
6	Al	Al foil	23	No	-
7	Zr	Zn foil	15	Yes	Yes
8	Zr	Zn foil	15	Yes	No

a. All targets had an outer cylinder wall of zirconium.
b. By weight, calipers gave a thickness of 21 μm. The plating density of zinc on the uranium foils has always been lower than theoretical.

It was discovered through the test results in Table 2-1 that electroplated uranium crumpled to pieces during disassembly and the zinc foils were found to be very brittle. However, the positive solution that was determined was that the nickel foils were "springy and easily handled" [19]. From this knowledge, the barrier material selected to use was the nickel foil.

The last piece to determine for the target material was the tubing material. From the conclusions, "future targets will likely be fabricated with zirconium or aluminum on both inner and outer walls" [19]. Because aluminum is inexpensive and easier to machine, all tests will be run using Al 6061-T6. Therefore, the final target material will be aluminum for inner and outer tubing and nickel foil for the barrier foil. Due to safety measures, researchers used stainless steel surrogate foil with similar material properties to that of uranium foil as far as thermal coefficients and yield stress.

However, there were still problems with this composition. The biggest issue is finding the right dimensions to reduce assembly time but still ensure assembly effectiveness and correct deformation. Another issue that arose was that "unfortunately, the lack of bonding between the LEU foil and cladding creates the potential for heat transfer restricting gaps to form" [20]. The final design that Argonne National Laboratories proposed is shown in Fig. 2-2.

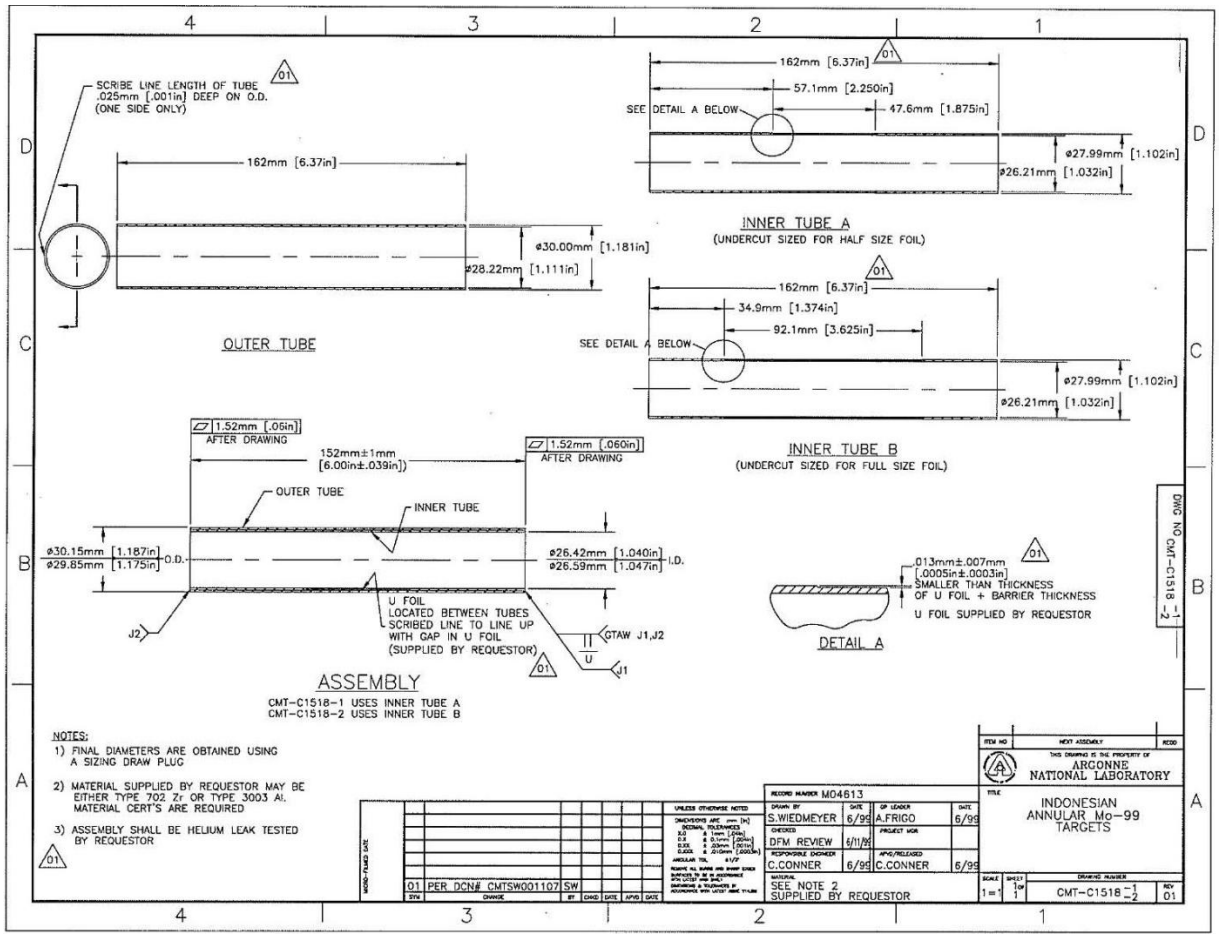

Fig. 2-2. Argonne National Laboratory Target with Dimensions and Tolerances[1].

It is important to remember that the target must satisfy several requirements to be successful: (1) it must be properly sized to fit into the irradiation position inside the reactor, (2) it must contain a sufficient amount of U – 235 to produce the required amount of molybdenum – 99 when it is

[1] Used courtesy of Argonne National Laboratory (1999).

irradiated, (3) it must have good heat transfer properties to prevent overheating which could lead to target failure, (4) the target must provide a barrier to the release of radioactive products, especially fission gases, during and after irradiation, and (5) the target materials must be compatible with the chemical processing steps that will be used to recover and purify molybdenum – 99 after the target is irradiated [4].

PREVIOUS DESIGN

Argonne National Lab was one of the first labs to define dimensions and tolerances for their target design. However, their overall dimensions and tolerances were very tight; thus, very expensive to manufacture. Through research at University of Missouri, graduate students were able to define the tolerances more loosely. This helped make the assemblies easier to put together and yet still substantial. The depth cut tolerances were relaxed from 0.0003 inches to 0.00075 inches. The diameter tolerances were changed to 0.001 inch while the overall length was given a tolerance of 0.125 inches. This was important so that the targets could be made faster and cheaper, yet researchers are still able to assemble the targets efficiently and effectively with the surrogate foil and nickel sandwich. Tips and assembly tricks have been used to overcome assembly issues.

Since sealing the ends is part of the assembly process, tungsten inert gas (TIG) welding was suggested because of its versatility and efficiency. However, an electro-beam (EB) weld study was completed as well. EB welding is more precise and would be a very good suggestion for places that do not have proficient TIG welders or for suppliers that are handling large-scale orders. A good representation of TIG welding is shown in Fig. 2-3. More discussion will cover the welding issues and suggestions in later chapters.

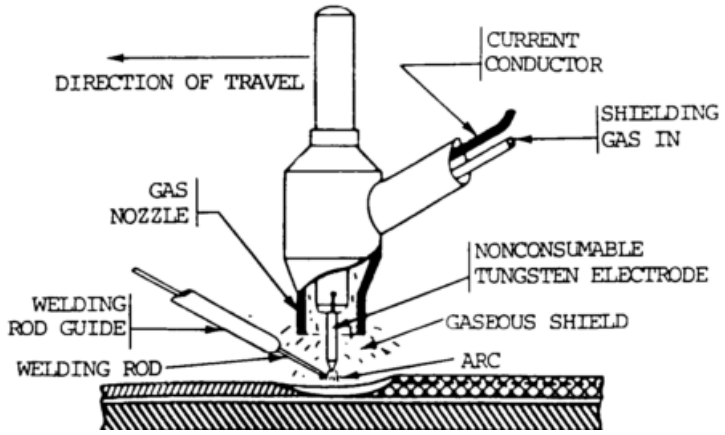

Fig. 2-3. Illustration of TIG welding [21].

Lastly, once targets are irradiated, there will need to be a form of disassembly process. Purchased by the U.S Department of Energy from Cintichem, Inc., the Cintichem process has proven to be very effective by dissolving targets and acquiring the molybdenum-99. The process has since been modified for dissolving using alkaline conditions rather than acidic solutions. This process may be effective, but the waste content is very high. Additional research at the University of Missouri is being done to provide a disassembly device that will efficiently and effectively cut the targets without creating metal chips or shavings. Because of the plastic/elastic deformation discussed in section titled "Target Assembly Processes," the outer tube will spring apart and expose the nickel sandwiched uranium foil.

DEMAND PROJECTIONS

Because the process to produce molybdenum – 99 is quite involved (machining targets, time to assembly, cleaning, irradiate, disassembly, etc.), one would expect the cost for producing molybdenum – 99 to be expensive. Currently, the average cost per dose of Technetium – 99m is approximately $9.05; however, those costs continue to increase due to the demand and short supply of molybdenum – 99. Once a stable supply of molybdenum – 99 can be found through

irradiation of LEU foil, the costs per dosage will also decrease, making non-invasive approach must more feasible that being just equivalent to invasive surgery in terms of financial costs. Procedures that use Technetium – 99m range from one brand TechneLite® from just over 2 MBq/kg (0.05 mCi/kg) for a single pediatric thyroid imaging to 1110 MBq (30 mCi) for a single blood pool imaging of the heart (Bristol-Myers Squibb 2005). The Nuclear Energy Agency predicts an average annual growth rate of 1.1% to 3.0 % increase of the number of imaging procedures, being 35 % increase by 2020 and a 50 % increase by 2030 [22].

TARGET ASSEMBLY PROCESSES

The original HEU targets favored the flat plate setup. Research has been done to assess whether or not this would work for LEU as well. While the research for the flat is on-going along with the research for annular targets; however, studies are showing both processes valid. However, the promise that annular targets can hold more LEU foil is very attractive.

The swaging assembly process works by deformation via draw plug, which is based on a metal forming process already in use. The plug is pushed through the assembled target with foil, deforming as it proceeds through. The important aspect is that the amount of deformation for the inner and outer tube is not equal. The inner tube, the tube in direct contact with the draw plug, is deformed plastically. Plastic deformation means the deformation is not in the elastic region and the structure stays deformed permanently. The outer tube, the tube not in contact with the draw plug, is deformed elastically. This is important for disassembly purposes. With the ends removed and a longitudinal cut, the outer tube will spring apart because it is elastic still and reveal the foil for easy access. Therefore, the forming pressure is a vital part in validating this approach. Below, Fig. 2-4 shows the swaging process.

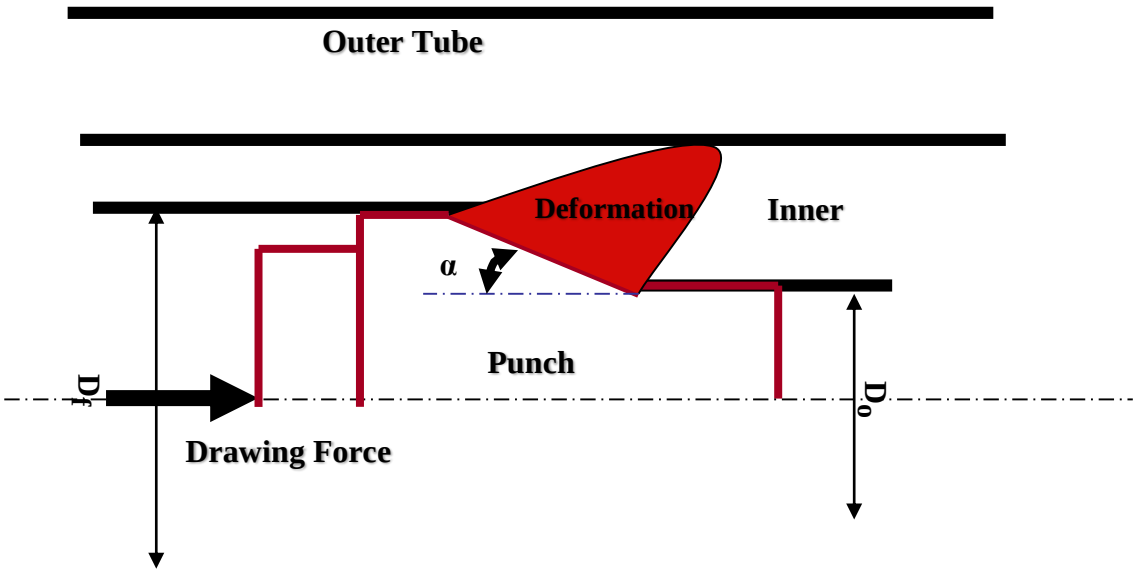

Fig. 2-4. Swaging Process Analysis [23].

Like most research, the method to validating work is to compare theoretical calculations with computer simulations to actual laboratory experiments. Computer simulation results will not be presented here because the working model is in its early stages. First, theoretical calculations were done to decide if this method of deformation was possible. Knowing the yield stress σ_{fm} for aluminum 6061-T6, the drawing stress can be calculated by using Eq. (2-1).

$$\sigma_{dr} = \sigma_{fm} Q_{dr} \tag{2-1}$$

The unknown here is Q_{dr}, the drawing ratio. The drawing ratio is a combination of the forming ratio, the strain and δ , the inhomogeneity factor

$$Q_{dr} = Q_{fm} \delta\varepsilon \tag{2-2}$$

To calculate the forming ratio, see Eq. (2-3), where μ is the coefficient of friction between workpiece and die, while α is the half angle of the draw die

$$Q_{fm} = 1 + \mu \cot \alpha \tag{2-3}$$

To calculate the inhomogeneity factor, see Eq. (2-4), where the *L* represents the length of the plug and the equation for *h* is shown in Eq. (2-5). The variables in Eq. (2-5) are the inner internal diameter a_0 and the maximum plug diameter, a_1.

$$\delta = 0.88 + 0.12\frac{h}{L} \tag{2-4}$$

$$h = \frac{\left(a_0 + a_1\right)}{2} \tag{2-5}$$

Lastly, the final equation for the drawing stress calculation is strain, ε shown in Eq. (2-6), where the variables here are cross-sectional area of the inner and outer tube assembled and the cross-sectional area of the outer and plug.

$$\varepsilon = \ln\left(\frac{\left[\text{OuterOD}^2 - \text{InnerID}^2\right]}{\left[\text{OuterOD}^2 - \text{PlugOD}^2\right]}\right) \tag{2-6}$$

Substitute Eq. (2-3), Eq. (2-4), and Eq. (2-6) into Eq. (2-2) [24]. Preliminary results showed drawing stresses near 105 MPa, with a drawing force of 1566 N (352 lb-f) [23]. One problem that was discovered was how to handle a negative strain value. Analysis behind discovering a negative strain proved that in order for the value not to be negative, the deformed inner diameter had to be at least the same as the plug diameter, or smaller with springback allowed. Larger deformed inner diameters meant the plug diameter is not in contact with the inner tube.

When the sample is subjected to externally applied loads, the resultant internal stresses can build up, causing the sample to have residual stresses. The simplest definition of residual stresses is the stresses that remain in the sample after it has been deformed and all external forces removed. The deformation must be non-uniform across the material cross-section in order to give rise to residual stresses. Without knowing how much residual stresses exist, the samples will be tested

using x-ray diffraction method (XRD analysis). Here, the sample is irradiated with a beam of monochromatic x-rays over a variable incident angle range. Interaction with atoms in the sample results in diffracted x-rays when the Bragg equation is satisfied. Resulting spectra are characteristic of chemical composition and phase. The technique uniquely provides phase identification (e.g. graphite or diamond), along with phase quantification, percent crystallinity, crystallite size and unit cell size. For layered materials, Grazing Incidence XRD (GIXRD) allows compositional depth profiling of phases within the structure. This method of testing is preferred because it is non-destructive. The equation for finding residual stresses in a very simplistic example is displayed in Eq. (2-7).

$$\sigma_{x(\text{res})} = \begin{Bmatrix} \left(\frac{M}{I} - \frac{S_y}{c - h_p}\right) y & 0 \le y \le \left(c - h_p\right) \\ \frac{M}{I} - S_y & \left(c - h_p\right) \le y \le c \end{Bmatrix} \tag{2-7}$$

where M is the moment due to the stress distribution, I is the second area moment, c is the distance from the neutral axis to an outer beam, S_y is the yield strength and h_p, shown in Fig. 2-5, is the depth of plastic region.

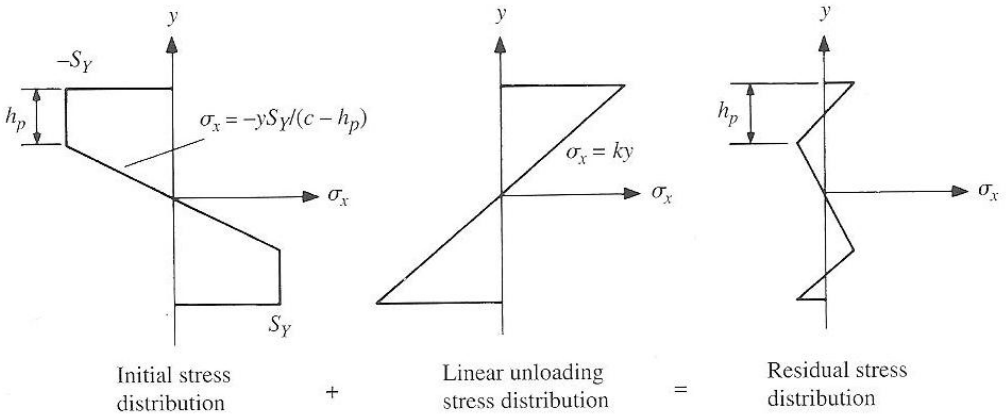

Fig. 2-5. Unloading tends to follow a linear path that is equivalent to superimposing a linear unloading stress distribution over the initial stress distribution [25].

Due to the complexity of finding residual stresses, all samples will undergo extensive XRD testing at Oak Ridge National Laboratories located in Oak Ridge, TN. However, additional work is being done with annular targets, including finite element models as well as thermal models as shown in Fig. 2-6.

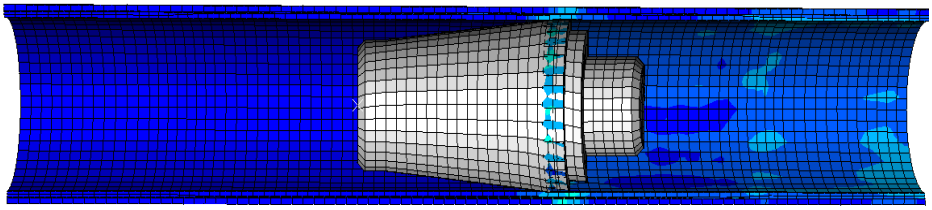

(a)

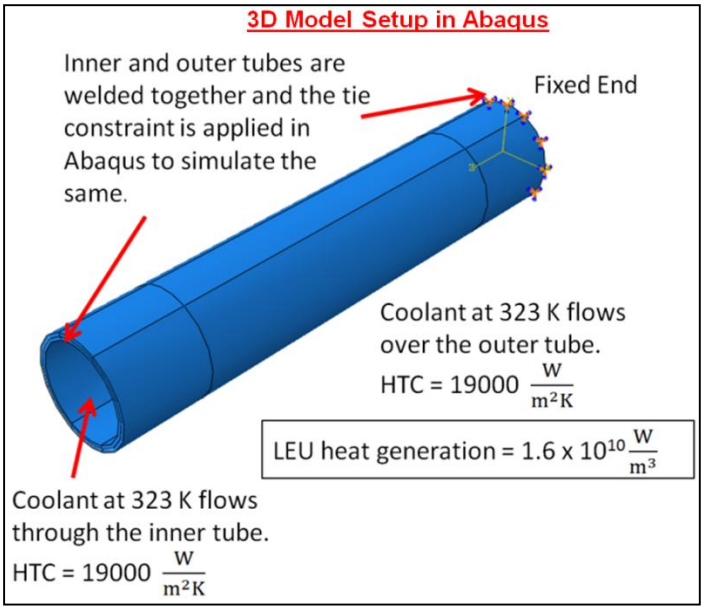

(b)

Fig. 2-6. Finite Element Model (a) and Thermal Analysis Model (b) of on-going research.

LITERATURE CONCLUSION

Even though there is an avid number of technical papers available for this research project as a whole, none really focus closely on the targets themselves. Many papers cover processes such as chemical irradiation, disassembly and perhaps a few will discuss material considerations. Therefore, due to lack of publish works on target optimization, the results here are truly unique and one of the first in this field.

Over the next few years, as reactors begin to switch fuel types and more companies in the private sector see the need for molybdenum – 99 suppliers, the switch from HEU to LEU will start to become more obvious. The demand for molybdenum – 99 now is slowly rising due to the functionality and effectiveness of molybdenum – 99, but lack of domestic suppliers means that shipments to hospitals are being imported from other countries.

Luckily, the U.S. Department of Energy continues to fund this project with the belief that the knowledge that comes from research will help create a more stable environment with expenditures being domestic, rather than financing operations outside of the United States. This project is showing promising results as well as a preview into the future production of molybdenum – 99.

CHAPTER 3

METHOD OF INVESTIGATION

EXPLANATION OF TECHNIQUES

The objective of this research is to systematically explore and optimize the target assembly process in order to produce those targets with the required quality and integrity. To do so, various techniques were used to study and make analyses of the tube design. To clarify those techniques, the beginnings of this chapter will be spent explaining and defining what those methods are and how they can be used appropriately.

The goal of this project was to find a quality target that assemblies quickly, has little or no defects, seals 100%, and a design that will increase target production. One of the several methods used to meet these objectives was to utilize a robust design, which greatly improves engineering productivity by consciously considering the noise factors, or rather, environmental variation during the product's usage, manufacturing variation and component deterioration. This approach focused on improving the fundamental function of the product or process by facilitating flexible designs and concurrent engineering. It is a powerful method that reduces cost and improves quality. The Robust design method is also known as the Taguchi Method, discovered by Dr. Genichi Taguchi in the early 1980s [26]. This approach is most commonly referred as parameter designs and is more efficient and effective in experimental design and statistical data analysis.

The first step was to determine the experimental design, or rather the set of experiments. An experimental matrix was designed to evaluate the performance of the product, in this case, the

tube design. One table was made for the controllable factors and the uncontrollable factors. The factors were contained in an orthogonal array, a table of integers whose column elements represent the low, medium and high levels of the column factors. Factors might be wall thickness, relief area length, amount of deformation while the levels would be multiple steps within that factor (i.e. deformation – little deformation, more deformation, and most deformation). The purpose of the noise factor array was to create variability so that controllable factor levels that are least sensitive are identified.

Once results were gathered, the Taguchi method also has techniques for analyzing those results called robust analysis. Generally, each preferred output required individual analysis. The responses obtained from different experiments were analyzed using statistical response tables and graphical representation of the mean effects of each parameter on any particular output of the assembled target. The response analysis helped in identifying those parameters that have the greatest impact on process variability and its level of performance. Depending on where the outputs fall, the scaled variation was analyzed using an appropriately chosen signal-to-noise ratio (SN). The ratios were derived from the quadratic loss function. The transformation method was used to convert the measured response into an S/N ratio, which are performance measures that optimize a process. The S/N ratio analysis also provided a sensitivity measurement of a process at various levels of both controllable factors and uncontrollable or noise factors. The optimum process design was achieved when the S/N ratio was maximized. In other words, it was the process condition at which the variability, resulting from the uncontrollable factors, was minimized. There are three SN functions, see Eq. (3-1), Eq. (3-2), and Eq. (3-3). Those responses were plotted to get response graphs.

Nominal the best

$$SN_N = 10\log\left(\frac{\overline{y^2}}{S^2}\right) \tag{3-1}$$

Larger the Better

$$SN_L = -10\log\left(\frac{1}{n}\sum_{i=1}^{n}\frac{1}{y_i^2}\right) \tag{3-2}$$

Smaller the better

$$SN_S = -10\log\left(\frac{1}{n}\sum_{i=1}^{n}y_i^2\right) \tag{3-3}$$

In the above equations, y_i represents a single experimental result for one factor and one level, *n* is the number of samples, and S^2 is the variance.

Other methods that were included in the study consist of analysis of variance (ANOVA), which used standard statistical analysis techniques so that design engineers can determine how much variation affects the region of interest and which factors are associated. ANOVA predicted the relative significance of the design parameters and gave the percentage of contribution of each fact; thus, providing a quantitative measure of various factors on design performance.

Another form of analysis that was done was reliability analysis. Because the research focuses on the targets, rather than the assembly rig, a portion of the reliability study was done on the tube design. Two forms of reliability tests were made: Failure Mode and Effect Analysis (FMEA) and Accelerated Life Testing. FMEA, done on the assembly rig, offers a subjective deterministic reliability to detect flaws and which errors are more devastating than others. FMEA does not offer solutions, but merely points out potentially catastrophic errors. The purpose of accelerated life testing was to induce field failure in the laboratory at a much faster rate by providing a harsher, but nonetheless, representative environment. In such a test, the product was expected to

fail in the lab just as it would have failed in the field—but in much less time. In order to complete many experiments, a MATLAB script was written to simulate the forming process. Montecarlo simulation is a computerized mathematical technique that relied on repeated random sampling to obtain numerical results and took into account for risk in quantitative analysis and decision making. The technique is used by professionals in such widely disparate fields as finance, project management, energy, manufacturing, engineering, research and development, insurance, oil & gas, transportation, and the environment. The random sampling usually varied about a current working value and can be derived from probabilistic densities, such as normal and lognormal distributions.

FORMS OF MEASUREMENTS

There were four major forms of measurements: calipers, computer numerical control (CNC) machine, *ImageJ* pixel measurements and a pressure gauge. Digital calipers used were accurate to ±0.0005 inches while the CNC probing machine was accurate to ± 0.0001 inches. Many of the microscope pictures were measured using *ImageJ*, which compares the amount of pixels to the magnification scale. Instructions for using *ImageJ* are shown in Appendix A: *ImageJ* Instructions. The microscopes used on this project were the scanning electron microscope (SEM) and the optical microscope, located at the Electron Microscopy Core Facility in the Department of Veterinary Pathobiology and at Lafferre Hall materials lab at the University of Missouri. A third microscope, a stereomicroscope, was located in Building 4508 of Oak Ridge National Laboratory and was used to obtain the EB weld specimens.

Throughout this project, one of the most vital aspects was the cleanliness of the targets. Several times during the assembly process, the samples were rinsed with acetone and washed using a

Cole-Parmer 08895-14 ultrasonic bath with heater. The bath was roughly a 1:1 mixture of 99.5% pure acetone and deionized water. The foil pieces were also cleaned thoroughly. One of the biggest issues was welding. Several hours were spent machining the tubes, cleaning them, cutting foil, assembling the targets, lubricating, deforming, and facing the edges. Nearly two targets in nine would fail during welding. Once strict cleaning procedures were installed, the failure rate reduced to zero. Once again, cleanliness is stressed as a very important approach for this particular project.

RESIDUAL STRESS TESTING – HOOP VS. LONGITUDINAL

Of the many outputs obtained, the most valuable output from this study was residual stresses. Residual stresses are those that remain in the target after assembly. This post-forming state was important as it can either aid or hinder the disassembly process. Because the target was cut longitudinally for disassembly, a tensile residual stress state in the outer tube was desired, such that the outer tube "springs" open instead of collapsing after being cut. Due to the geometry shape of the targets, cylindrical objects can develop several types of stresses once deformed. It should be noted that the targets undergo some stress recovery during welding due to accompanying heat. Cylindrical objects, like the assembled targets, can develop several types of stresses once deformed. Two stresses that were of interest were hoop stress and longitudinal stress. The hoop stress is the force exerted circumferentially (perpendicular both to the axis and to the radius of the target) on every particle in the cylinder wall. Because the targets do not fit the requirements for a thin-walled vessel, hoop stress is commonly written as the following:

$$\sigma_H = A + \frac{B}{r^2} \tag{3-4}$$

with A and B as constants of integration based on boundary condition, and *r* as the radius at the point of interest in the cylinder.

Assuming the cylinder is subjected to an internal pressure P and the external pressure is zero, the boundary conditions are used solve for the Lame constants and solve for hoop stress are

$$\sigma_H = \frac{\mathrm{Pr}^2}{\left((r+t)^2 - r^2\right)}\left[1 + \frac{(r+t)^2}{r^2}\right] \tag{3-5}$$

To better describe the stress, a diagram is provided. Below, Fig. 3-1 shows the directions of both hoop stress and longitudinal stress.

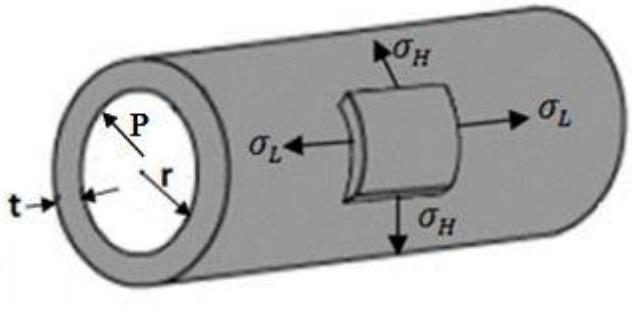

Fig. 3-1. Hoop stress (σ_H), axial stress (σ_L), pressure *P*, radius *r* and thickness *t* [27].

Both hoop and axial stresses were measured and recorded. The robust analysis will show the best target with the nominal residual hoop stress and minimized longitudinal stress.

In order to evaluate the stress in the targets, x-ray diffraction was used. Table 3-1 lists the details of the experimental conditions for the x-ray measurements. Briefly, a single axis (β) goniometer [28] was employed for the stress measurements using the "Ω-goniometer geometry" [29]. A goniometer is an instrument that either measures an angle or allows an object to be rotated to a precise angular position. The 311 lattice reflection from the aluminum phase was utilized for the strain measurements. During scanning, the incident beam and detectors were oscillated ±3°

about the β axis to improve particle statistics. Specimen alignment was accomplished using a contact probe. Goniometer alignment was ensured by similarly examining a aluminum powder puck (low stress). The maximum observed peak shift for the (331) reflection of AL (~150 °2θ) was less than 0.04 °2θ for Ω tilting as described in Table 3-1.

Table 3-1. Experimental conditions of the x-ray measurements made on the PROTO iXRD system.

Parameter	Condition
Equipment	PROTO iXRD Portable Residual Stress Measurement System MGR40 gonioneter head Two position sensitive scintillation detectors (PSSDs), 18.5° 2θ range each.
Power	80 W, 20 kV, 4 mA
Radiation	Co Kα, λ = 1.788965 Å
Aperture size	0.5, 1.0, 2.0, 3.0, 4.0 mm round, 0.5 x 3, 0.5 x 5, 1 x 5,1.5 x 5, 2 x 5 mm
Source to specimen distance	96 mm
Specimen to detector distance	40 mm
Tilt Axis/Axes	Ω, a max of 11 ψ tilt/detector: -41.8 to 18.2° ψ and -18.2 to 41.8°ψ
Oscillation Axis/Axes X, Y, Z, Azimuthal ranges	Each with 132 mm, ±180° φ
2θ Scans	0.036° 2θ step/channel, range 149.8 to 168.3° 2θ, 10 scans at 0.5 sec/scan

The data was analyzed with the XrdWin software [30]. The peaks were fit with a Pearson VII function to the upper 85% of the peak to determine their location. The fully expanded equation relating strain to stress in terms of the goniometer tilt and axes is: [29]

$$\varepsilon_{\phi\psi} = \frac{d_{\phi\psi} - d_0}{d_0} = \frac{(1+\nu)}{E}\left\{\sigma_{11}\cos^2\phi + \sigma_{12}\sin 2\phi + \sigma_{22}\sin^2\phi - \sigma_{33}\right\}\sin^2\psi + \frac{(1+\nu)}{E}\sigma_{33} - \frac{\nu}{E}\left\{\sigma_{11}+\sigma_{22}+\sigma_{33}\right\} + \frac{(1+\nu)}{E}\left\{\sigma_{13}\cos\phi + \sigma_{23}\sin\phi\right\}\sin 2\psi \quad (3\text{-}6)$$

This equation may be reduced to Eq. (3-7), assuming $\sigma_{33} = \phi = 0$.

$$\varepsilon_{\phi\psi} = \frac{(1+\nu)}{E}\sigma_{\phi}\sin^2\psi + \frac{(1+\nu)}{E}\sigma_{13}\sin 2\psi - \frac{\nu(\sigma_{11}+\sigma_{22})}{E} \tag{3-7}$$

Furthermore, $d_{\phi\psi}$ simplifies to Eq. (3-8).

$$d_{\phi\psi} = \frac{(1+\nu)}{E}\sigma_{\phi}\sin^2\psi d_0 + \frac{(1+\nu)}{E}\sigma_{13}\sin 2\psi d_0 - \frac{\nu(\sigma_{11}+\sigma_{22})}{E}d_0 + d_0 \tag{3-8}$$

Here, ε, d, ν, E, and σ are the strain, interplanar spacing, Poisson's ratio, Young's modulus and stress, respectively. The variables ϕ and ψ refer to the azimuthal angle and tilt angle while the subscript 0 refers to a strain-free state, respectively. The strain-free interplanar spacing, d_0, was taken as 1.1788965 Å due to the radiation source, refer to Table 3-1. The values for E and ν were taken as 216 GPa and 0.276, respectively. Equation (3-8) is in the form of an ellipse: $y = A\sin^2\psi + B\sin 2\psi + C$.

PREPARATIONS

Many of the samples were destroyed for viewing cross-sections until the microscope. Nearly all samples were etched or sanded and polished. In order to view the influence of the weld on the target/foil, the quartered samples were etched in a solution for 60 seconds. For recipe and instructions, please see Appendix B: Etching Formula [31]. For samples that were cleaned and polished, several size sand grits were used, ranging from 350 grit size to 2500 grit size for polishing. Aluminum oxides were used in the polishing stage, rather than a polymer compound which did nothing to improve visibility. To speed up the process, a Dremel 4000 was used for finer detail work.

In addition, to help aid in improving the roundness, machinist used an expanding mandrel (no. 6 1 to 1.25"), produced by Interstate. The mandrel is directly responsible for all measurements

made at the University of Missouri. It was discovered that the main reason behind poor targets due to improper roundness was that the tubes were not machined with this tool. Efforts here will show that roundness is no longer an issue once this tool was used.

Fig. 3-2. Expanding mandrel used to ensure proper roundness in machined targets.

COMPUTER AIDED DESIGN/MATLAB

One computer program that was especially helpful on this project was SolidWorks 2013 [32], a computer aided design (CAD) software. The tubes are built in the part software and imported to drawing sheets for machining. All tube designs are shown in Appendix C: Tube Drawings. Several designs are included there, including designs that were made especially for the longer foil samples. SolidWorks was also used to produce CAD models of the draw plugs made for this research. Those drawings may be found in Appendix D: Plug Drawings with machining instructions. Lastly, SolidWorks was also used to create the assembly rig. Drawings are provided in Appendix E: Assembly Rig.

Another program used was MATLAB [33]. In addition to the targets, several draw plugs were made for this research. A short code for calculating dimensions of the draw plug depending upon option of keeping the same deformation angle or keeping the length of the plugs consistent. Appendix F: Function *dimens* shows the complete code. MATLAB was also used to write and run the reliability study.

MATERIALS

Lastly, this section will state all target materials used. The tubes were made from aluminum 6061-T6 drawn tubes, inner tube stock size 1.125 inches x 0.058 inches x 1.009 inches at 96 inches and outer tube stock size 1.250 inches x 0.083 inches x 1.084 inches at 96 inches. Foil order is shown in Appendix G: Foil Order. The surrogate foil to the uranium is stainless steel 304 foil (Fe/Cr18/Ni10). The fission-barrier foil is 99.9 % Nickel foil. Safety specifications are included in Appendix H: Foil Safety. Cleaning solutions are 99.5% acetone and deionized water with lint-free micro-clothes.

INVESTIGATIVE APPROACH

This section will outline the steps to assemble the targets, beginning with machined tubes. For complete drawings for experiments, see Appendix C: Tube Drawings.

Step 1: Machine tubes.

Step 2: Verify measurements are within the drawing specifications.

Step 3: Initial 99.5% acetone rinse, soak each tube in ultrasonic bath of 1-to-1 99.5% acetone/deionized mixture for 10 minutes each.

Step 4: Rinse each tube with 99.5% acetone, dry with lint-free micro-clothes.

Step 5: Cut stainless steel foil, rinse with 99.5% acetone.

Step 6: Cut nickel foil, rinse with 99.5% acetone.

Step 7: Wrap nickel foil around stainless steel foil.

Step 8: Assemble foil with inner and outer target tubes (a pipe clamp or rubberband may be helpful).

Step 9: Mark foil gap middle and engrave sample.

Step 10: Seal off ends with tape (painters tape is easy to remove).

Step 11: Spry inner surface of inner tube with graphite spray, let dry 5 minutes.

Step 12: Remove tape from ends before deforming.

Step 13: Deform using the swaging process. Fig. 3-3 shows the draw plug setup.

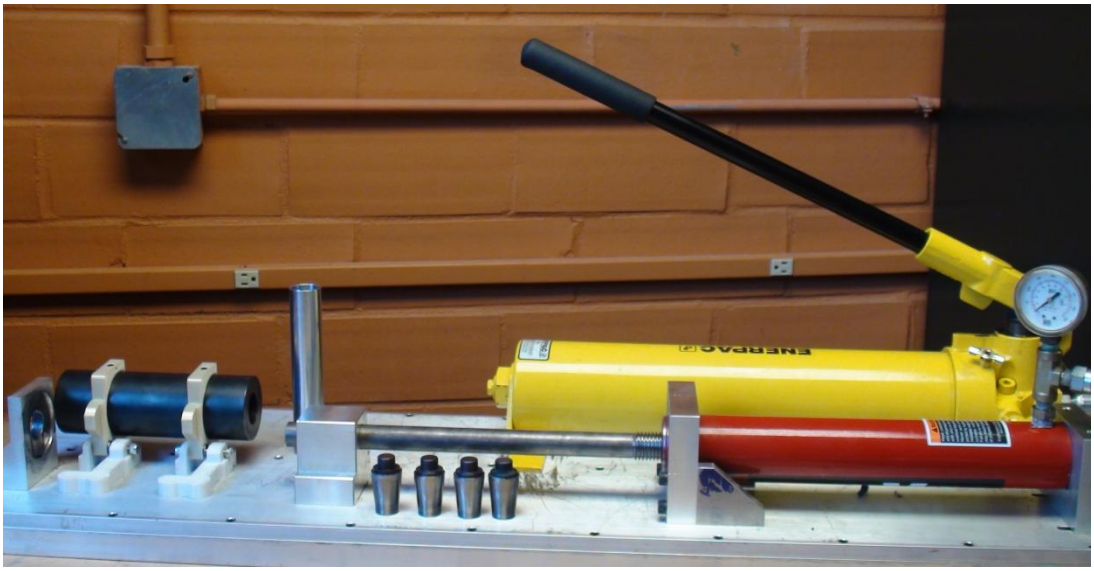

Fig. 3-3. Draw Plug Rig.

Step 14: Initial cleaning with denatured alcohol or acetone (toothbrush may be helpful).

Step 15: Ultrasonic bath soak again.

Step 16: Set target in oven at 300 º F for 2 to 3 hrs.

Step 17: Prepare ends for welding by facing target ends on the lathe machine.

Step 18: TIG/EB weld target ends. Fig. 3-4 illustrates the TIG welding setup.

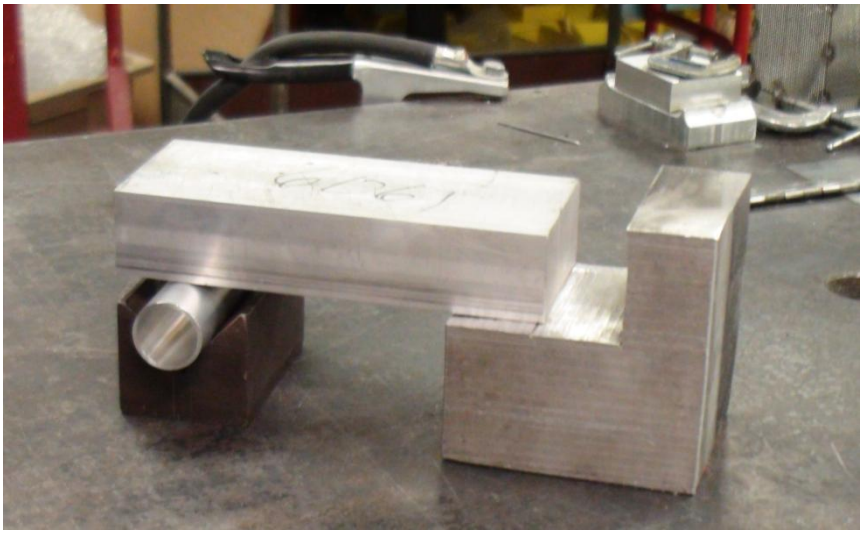

Fig. 3-4. TIG welding setup.

DESIGN AND CONSTRAINTS

Lubrication

There were many design constraints that were instilled during this process. One was the type of lubrication was necessary during the draw plug process. Without lubrication, the draw piece smears the inner surface of the target and galls the material badly. Galling is a form of wear caused by adhesion between sliding surfaces. When a material galls, some of it is pulled with the contacting surface, the draw plug in this case, especially if there is a large amount of force compressing the surfaces together. Galling is caused by a combination of friction and adhesion between the surfaces, followed by slipping and tearing of crystal structure beneath the surface. This will generally leave some material stuck or even friction welded to the adjacent surface, while the galled material may appear gouged with balled-up or torn lumps of material stuck to its surface. Fig. 3-5 illustrates some of the results of galled material.

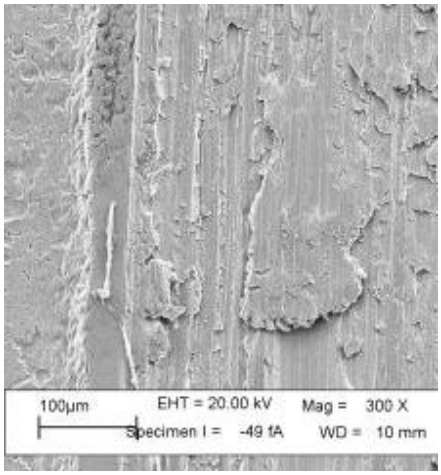

Fig. 3-5. Example of galled aluminum.

The material smears and perhaps may destroy the crystal structure, thus compromising the integrity of the sample. Fig. 3-6 is a target that was deformed without any lubrication and clearly marks are visible.

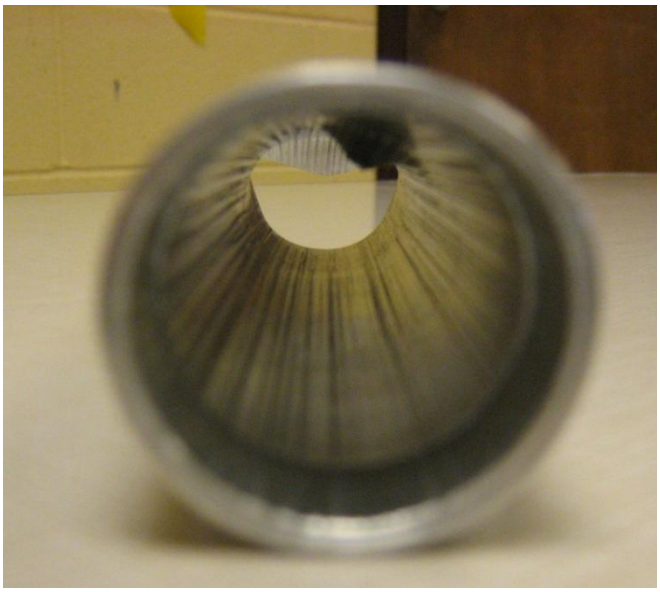

Fig. 3-6. Galled sample, no lubrication used.

Galling to the inner surface of the target is not so much as important as the draw plug receiving the smeared material. With build-up of aluminum 6061-T6 material, the plugs would need to be cleaned after each use to prevent such build-up that would naturally lead to ununiformed deformation. However, with the use of lubricant, the amount of galling may be reduced. Once

graphite lubricate was used, the marks no longer showed on the samples. Fig. 3-7 shows a target that is partially disassembled, notice the point mark that was made by the longitudinal cutting wheel from the disassembly device.

Fig. 3-7. Perfect sample with lubrication used.

With the correct lubrication, the sample performs well. Initially, the very first lubrication that was used was dishwashing soap; however, that proved to have unfavorable effects on the welding process. Thus, dishwashing soap was eliminated from the process and graphite lubricant was used instead. For extra precautions, the target ends were covered with painters' tape to prevent graphite from running between the inner and outer tubes. Once deformed, it would be very difficult to remove any unwanted graphite stuck between the tubes.

Welding (Pros/Cons of TIG and EB welding)

Since sealing is part of the assembly process, a study was done to determine an appropriate process. As stated above, the targets were difficult to TIG weld due to contaminants between the tubes. Once the ultrasonic cleaning was added to the process, the welds were more consistent.

However, once the ultrasonic cleaning solution was added, the welds were not consistent and repeatedly failed to seal. It was concluded that any substances that were a strong alkaline or strong acid could not be used to clean the targets. Therefore, a neutral pH fluid was used to clean the targets and a volatile liquid was chosen to effectively evaporate all traces. Acetone is a widely used laboratory cleaner and was ideal for this situation. Once acetone was added one-to-one with deionized water, the targets welded great each time. Below, Fig. 3-8 shows a poor weld due to contaminants. Contaminants were, but not limited, to paper particles, dust, oxide layers, leftover lubricant, and leftover cleaning substance.

Fig. 3-8. Example of poor TIG weld due to contaminants.

Once contaminants were removed from the tubes, the welds were near flawless each time. Below, Fig. 3-9a and Fig. 3-9b show the result of an acceptable weld. This issue was also a problem for EB welding, even though the target was under a vacuum during the weld process. A possible explanation might be that the heat will cause outgassing of molecules absorbed on surfaces.

(a) Top view of TIG weld. (b) Side view of TIG weld.
Fig. 3-9. Example of acceptable TIG weld.

TIG welding is acceptable if producing fewer than 1000 targets per year. However, for high scale production, a more precise method may be warranted in order to produce more targets faster. Electron beam welding (EBW) is a fusion welding process in which a beam of high-velocity electrons is applied to two materials to be joined. Often, the weld is performed under vacuum conditions to prevent dissipation of the electron beam. With the target under vacuum, weld flaws are less likely to appear compared to contaminants affecting TIG welding. Below, Fig. 3-10a and Fig. 3-10b show a representation of the weld itself as well as a target end sample that was EB welded. The weld is clean, precise, and does not leave a mound of welded material, known as a hump, around the edges that is visible with the TIG welded targets.

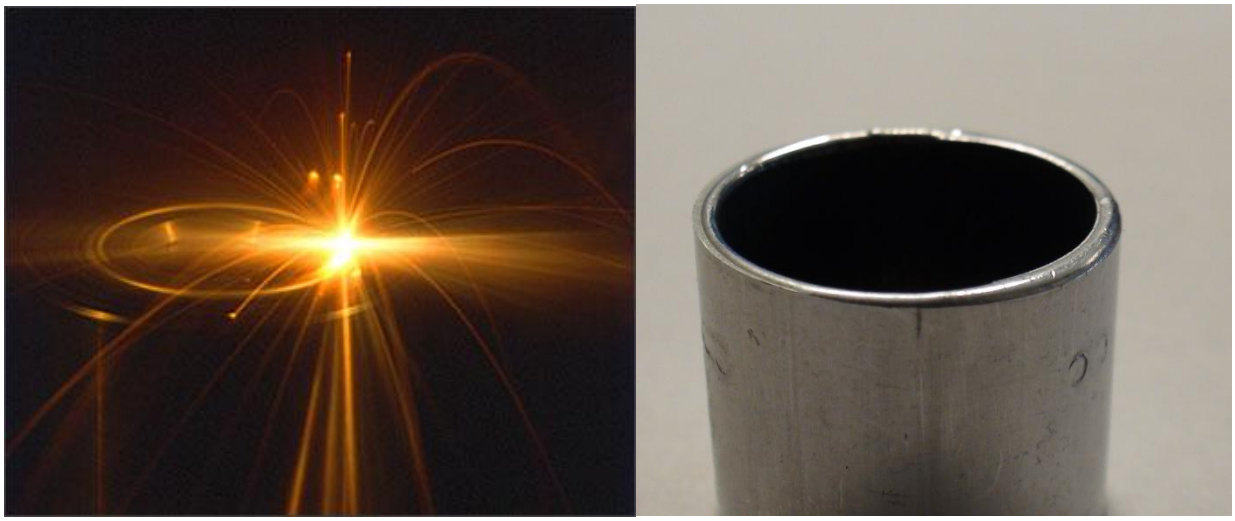

(a) Electron beam weld process. (b) Target sample with electron beam weld.

Fig. 3-10. Example of Electron Beam weld.

TIG welding

TIG welding is very inexpensive when compared to the requirements of EB welding. However, aluminum is one of the hardest materials to weld; therefore, the technician must be well trained with experience handling this material. TIG welding also requires some pre-machining before the ends are sealed. The amount of deformation to the targets forces the tubes to elongate to different lengths, with differences as much as 0.03 inches. Once the ends are equal, there is still a wide range of mistakes that can be made TIG welding. The heat affected zone is fairly large due to the long heat transfer time because penetration of the work material into the joint is required. Lastly, the output quality is very average and it is common to see material distortion due to the low controllability of TIG welding.

EB welding

EB welding is very precise and highly controllable. The resultant small heat affected zone due to low heat transfer time is favorable in that if the foil length were to increase, the welding process

will not have a large impact on uranium foil housed in the aluminum tubes. The beam spends such a short time on the joint, that there is little or no time for heat transfer except for that to melt the area under the beam. The part is easier to handle due to manipulator set up which does not exist in TIG welding. The output quality of EBW is excellent. However, the cost of precision is high, compared to TIG welding.

Table 3-2 summarizes the pros and cons of TIG versus EB welding. Depending on the yield expected, TIG welding is appropriate for low volume, but for mass production, EB welding is suggested. Equipment cost is relative in comparison to the equipment cost of a reactor or hot cell.

Table 3-2. Pros and cons of TIG and EB welding.

TIG	EBW
Less Training Required	Training Required
Easy to make Mistakes	Highly Controllable
High Energy Input	Low Energy Required
High Heat Affected Zone	Low Heat Affected Zone
Material Distortion	Minimal Material Distortion
$400 (cost of 9 targets)	$1,500 (cost of 9 targets)
Pre-Machining Required	No Pre-Machining Required
Average quality	High Quality

In order to get the best EB weld, a technician must first turn the ends down on the lathe. Using the following settings from Table 3-3, the weld technician should track the joint first while increasing the beam current to get a good weld in the center.

Then the technician should lower the beam current slightly and move the beam to the outer edge and breakdown the corner while blending with the center weld. Next step requires that the technician move to the inside edge to do the same thing.

To improve appearances, the technician may increase or decrease the current and/or the beam focus as needed.

Sometimes there can be contaminates that blow out at the joint. The target may need to cool between passes and run back over weld/joint several times to seal.

Table 3-3. EB weld parameters.

Voltage	100 kV
Beam Current	Manual mA up to ~1.5 mA, Pulsed at 20 Hz
Focus	Defocus -0.020 from sharp
Rotary Sped	~ 15-20 IPM

Deformation

Another design constraint that exists with the assembly process is to ensure the plastic deformation of the inner tube, but elastic deformation of the outer tube. This process is known as autofrettage. This technique is usually done on a single vessel that is subjected to pressure, causing internal portions of the part to yield and internal compressive residual stresses result. Examples of parts manufactured using autofrettage are pressure pump cylinders, gun barrels, and fuel injections systems for diesel engines. When autofrettage is used for strengthening gun barrels, the barrel is bored to a slightly undersized inside diameter, and then a slightly oversized die is pushed through the barrel. The amount of initial under-bore and size of the die are calculated to strain the material past its elastic limit into plastic deformation, sufficiently far that the final strained diameter is the final desired bore. The deformation process is illustrated in Fig. 3-11.

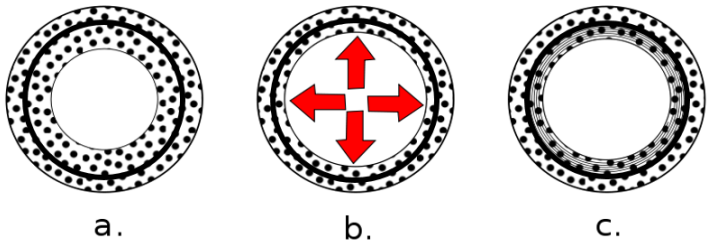

Fig. 3-11. The tube (a) is subjected to internal pressure past its elastic limit (b), leaving an inner layer of stressed metal (c) [34].

The relief depth for the foil area is one of the variable subjects. However, with deep relief depths, there is less material to deform. There must be enough material in order to complete deform the outer tube elastically without rupturing the inner tube, due to too little material. The reliability based Monte Carlo study will show whether the optimal target condition can be machined properly so to avoid material rupture during deformation.

Design Revision

One of the issues that arose was found during the assembly of the larger foil tests. As the surface of the foil increased, so did the surface area that comes into contact with the tubes during insertion. With increased surface area, the friction increased; thus, a good assembly was prevented. Below, Fig. 3-12 shows a target that failed to assembly properly due to too much foil.

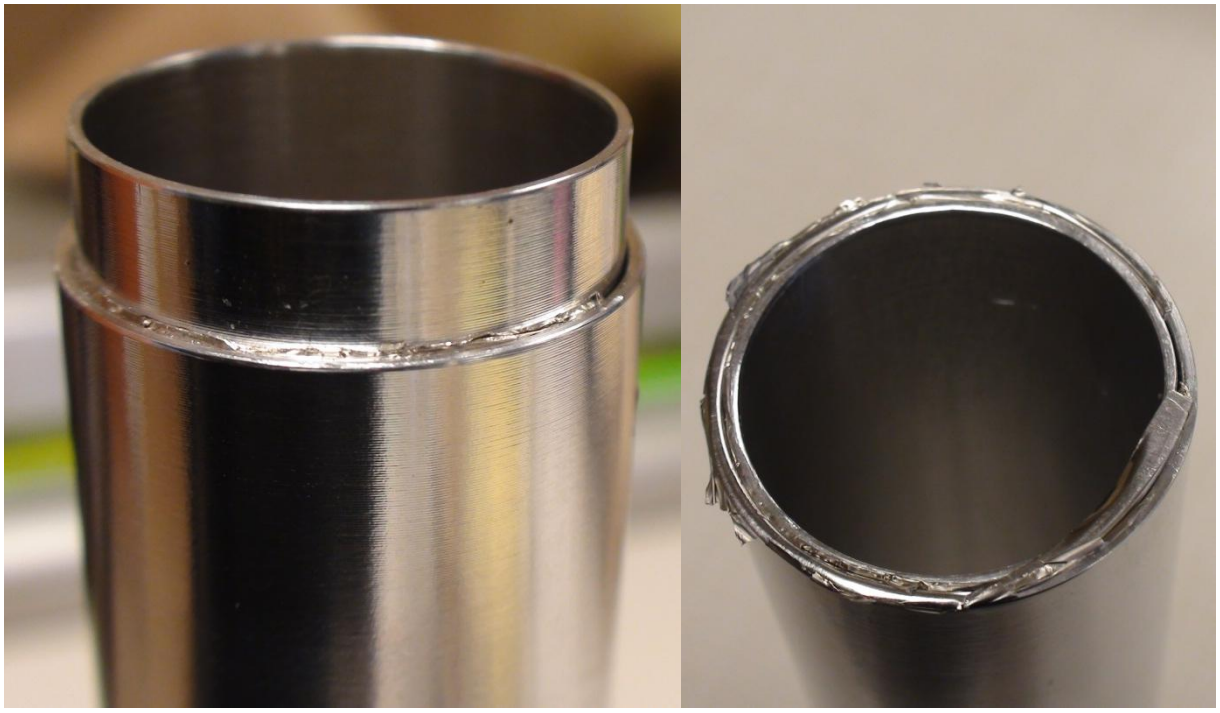

Fig. 3-12. Example of target with longer foil that failed to assembly.

This created a big issue in that the tests could not be completed if the target would not assemble. One of the solutions was to add material to one relief end of the inner tube and bore out the extra material from relief end from outer tube. This new feature prevented the foil from passing the relief end lip and made assembling the targets much quicker. Below, Fig. 3-13 is a drawing of the new design, used for sample 1.

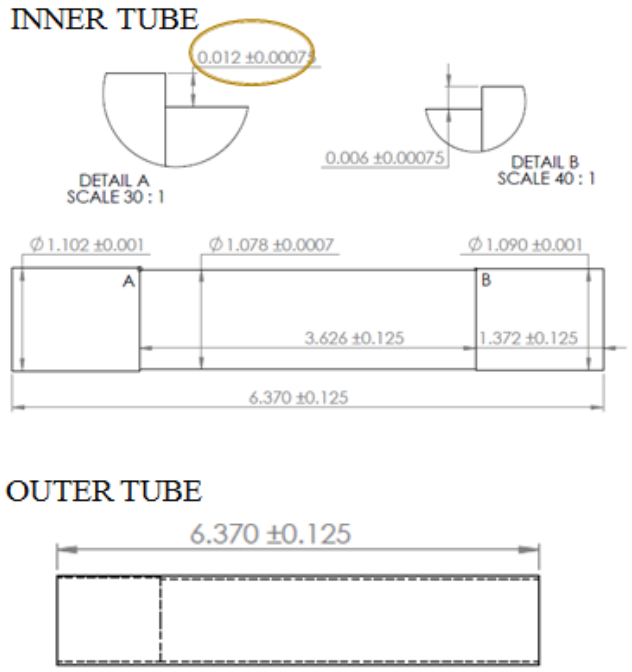

Fig. 3-13. Example of new end design for tubes.

As a result, the new targets are better improved and easier to nest with longer foil options. Because this feature worked so well for the longer foil cases, the idea was added to all target drawings. The next figure, Fig. 3-14, shows sample 4 that has a foil length of 5.244 inches that assembled very nicely. Complete drawings are available in Appendix C: Tube Drawings.

Fig. 3-14. Sample 4 longer foil case that assembled well with the new added feature.

DESIGN OF EXPERIMENTS

The basis of this research is to vary dimensions of the targets and amount of deformation to discover the optimal condition that would consistently produce the best target. In order to systematically test the targets, a parametric study was created to have four factors with three levels each. The variables include the amount of deformation, relief area depth, cutting foil gap, and distance from target ends to the relief area. The levels ranged from low, medium and high conditions. The importance of testing at low, medium and high levels is to find the factor that is most sensitive, thus helping to find the best condition and eliminate insensitive factors. Table 3-4 lays out the factors with their different levels, three per factor. The symbols in the table are illustrated in Fig. 3-15.

Table 3-4. Factors and their alternative levels.

Factors	Number of Levels		
	1	2	3
A. Amount of Deformation, inch	0.009	0.010	0.011
B. Depth of Relief Area, (t_R), inch	0.006	0.007	0.008
C. Cutting Gap,(g) inch	0.500	0.300	0.150
D. Distance from Target End to Relief area, (We) inch	1.372	0.750	0.500

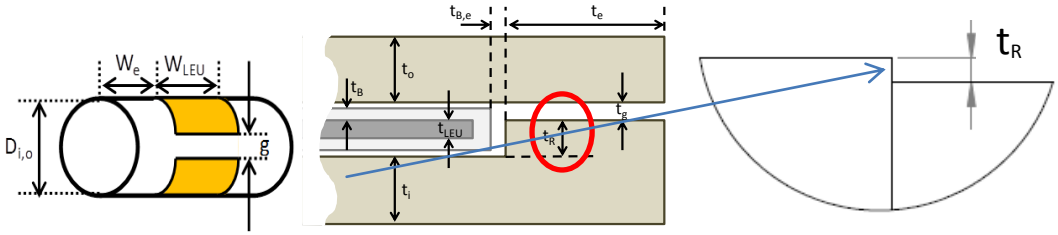

Fig. 3-15. Illustration for Table 3-4 symbols.

With this set of experiments, Table 3-5 shows the experimental log, a total of 9 tests per matrix. The outputs from this analysis are the optimal forming pressure, residual stresses, roundness, presence of defects, such as cracks, unnecessary gaps, heat affects from welding, etc. One set of experiments may be used for multiple output results such as cracks and heat affects, but most outputs will require a single experiment set per output. The nine samples from the matrix set were created four times for testing, plus a master set. Therefore, forty targets were machined, assembled and welded, complete with nickel and stainless steel foil. The process is outlined in the investigative approach section of this chapter.

Table 3-5. Experimental log for parametric analysis.

Exp. No.	A Punch Size (in)	B Relief Depth (in)	C Gap (length of foil), (in)	D Distance to Relief Area (foil width), (in)
1	0.009	0.006	0.500 (2.805)	1.372 (3.500)
2	0.009	0.007	0.300 (3.080)	0.750 (4.744)
3	0.009	0.008	0.150 (3.223)	0.500 (5.244)
4	0.010	0.006	0.300 (3.087)	0.500 (5.244)
5	0.010	0.007	0.150 (3.230)	1.372 (3.500)
6	0.010	0.008	0.500 (2.874)	0.750 (4.744)
7	0.011	0.006	0.150 (3.237)	0.750 (4.744)
8	0.011	0.007	0.500 (2.880)	0.500 (5.244)
9	0.011	0.008	0.300 (3.074)	1.372 (3.500)

As stated previously, the outputs for this parametric study are forming pressure, residual stress, roundness and presence of defects. The forming pressure should be minimized but should still satisfy the assembly requirements (i.e. plastic/elastic deformation in their respective areas). Residual stresses should exist, but should be conservative. Extreme residual stresses may lead to premature failures and could compromise the integrity of the target as a whole. TIG welds become very difficult to add if the surfaces of the tubes are under extreme stresses. However, some residual stress is necessary in order for the outer tube to spring apart after dissection. Another output is roundness. Roundness was an issue for assembly. Without near perfect roundness, the tubes were very difficult to slide together, adding more time to the overall assembly process. This inefficiency needed to be eliminated, for a smooth and effortless process. Roundness is not necessary an output to the parametric study, but rather a control aspect, still necessary to the project. Thus, roundness as an output from the robust analysis was eliminated. The last output is the presence of defects. Clearly, the targets should have very few defects. The presence of defects again may compromise the targets during the deformation

stage, irradiation or possibly, the disassembly process. Wanting to maximize the foil area, longer foil length leave very little distance to the weld. The heat from the weld process may destroy the foil or even cause the fission process. This mishaps need to be avoided. Another defect is the presence of gaps between the foil and the tube surfaces. Too many air gaps prevent correct heat transfer between the surfaces. As a result, the heat flow begins to cluster in the gap regions and the heat transfer is constricted across the interface [6]. This phenomenon is illustrated in Fig. 3-16.

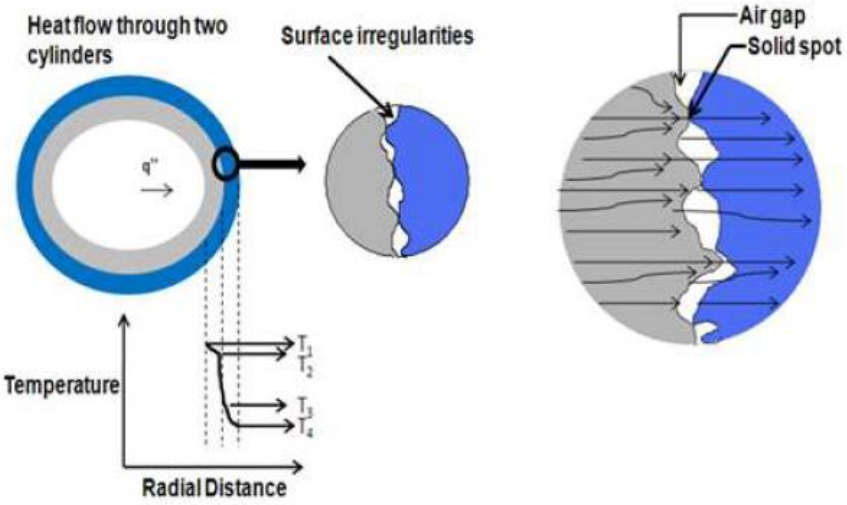

Fig. 3-16. Heat flow through a joint and temperature drop at the interface [6].

However, some air gaps are necessary to provide room for fission gases to expand. The amount of gas is unknown, but future experiments will be run in order to determine a quantity of the gases produced. Thus, few air gaps are necessary, just not large air gaps. Based on the amount of heat generated, the allowable gap space is proportional.

DATA COLLECTION

Each output requires data to make a collective conclusion. Forming pressures were recorded during the deformation process, via digital gauge. Residual stresses were found by x-ray

diffraction after welding. Once tubes undergo the heating process that will simulate the irradiation process, the targets are tested again for residual stress to find the changes during irradiation. Roundness was found though CNC measurements and tolerances added to the original tube drawings. Defects were found by sectioning each target to review the cross-section of the foil area and the weld area. Samples were viewed under the SEM as well as the optical microscope.

Like all research, assumptions were made. Those include, but are not limited to the following: (1) the stainless steel 304 foil has similar properties to the low-enriched uranium, (2) the forming pressure is the same as the pressure required to push the draw plug through the tubes, (3) at any surface, there is at most two layers of nickel foil, (4) the heat from the weld is quickly dissipated to the nearby surfaces (see outlined instructions for welding process setup), (5) the cross-section represent the effects of the entire target, and lastly, (6) all material cracks near the ends are attributed to the welds.

CHAPTER 4

RESULTS AND DISCUSSION

Data from all nine experiments is compiled and analyzed. The results of the experiments are studied to determine the impact of the dimensions on the reliability and efficiency of the assembly draw-plug process. The optimal conditions were found through robust analysis. Experimental results are present in the results tables for the following outputs.

OUTPUT 1 – FORMING PRESSURE

The first output as a result of the robust analysis is forming pressure. The forming pressure here is merely for quality control purposes and can control the amount of deformation of the target. Obviously, more pressure will lead to more deformation. Since the scenario changes for each target, each physical model should be compared to a verified ABAQUS model to ensure that the target is not under desired deformation. High deformation pressure may affect the target negatively during welding and once the target undergoes irradiation.

Experimental Results

Sample 1 has the following factors: smallest deformation, smallest relief depth, largest foil gap, largest distance to relief area. Below, Fig. 4-1 plots the peak pressures during deformation. The pressure here is the required pressure to drive the plug through the target, not the actual deformation pressure. The peak pressure was found to be 628 PSI.

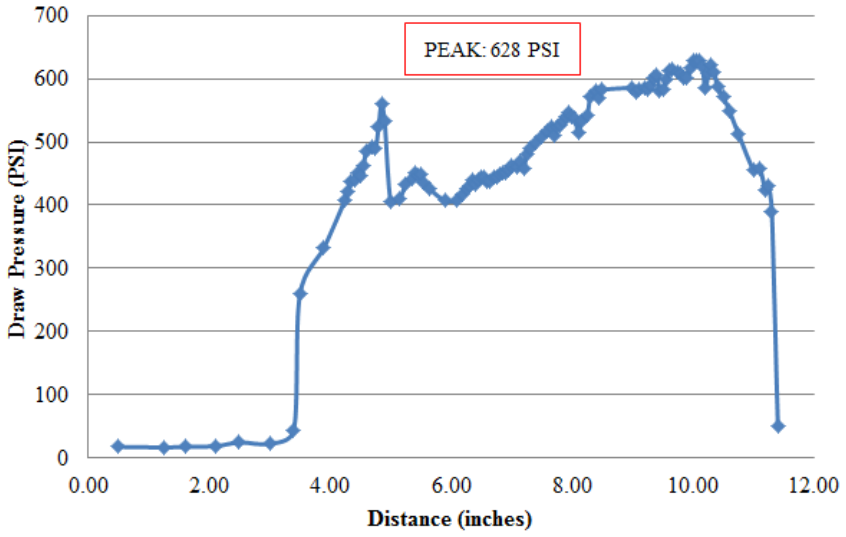

Fig. 4-1. Plot of maximum peak pressure during swaging, sample 1.

Sample 2 has the following factors: smallest deformation, middle relief depth, middle foil gap, middle distance to relief area. Below, Fig. 4-2 plots the peak pressures during the deformation process. Again, pressure plotted here is the required pressure, not the actual deformation pressure. Peak pressure was found to be 445 PSI.

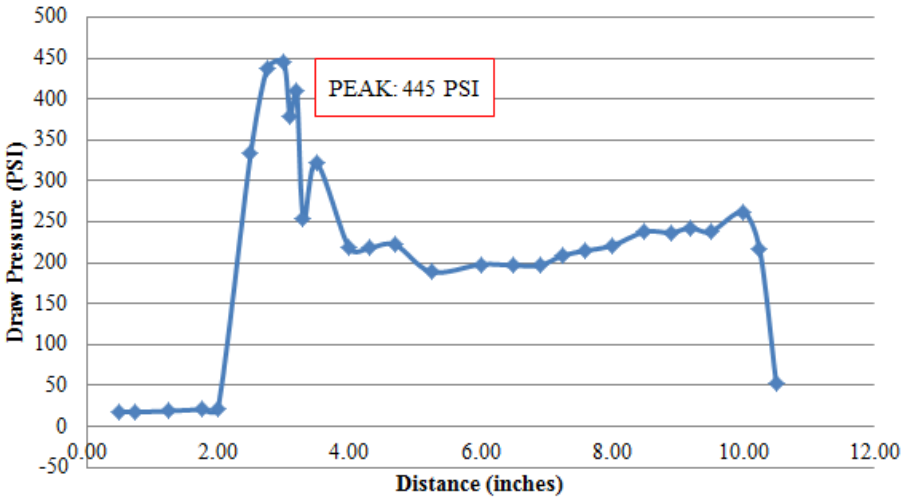

Fig. 4-2. Plot of maximum peak pressure during swaging, sample 2.

Sample 3 was assembled with the following factors: smallest deformation, largest relief depth, smallest foil gap, smallest distance to relief area. The maximum required pressure was found to be 644 PSI, with plots shown in Fig. 4-3.

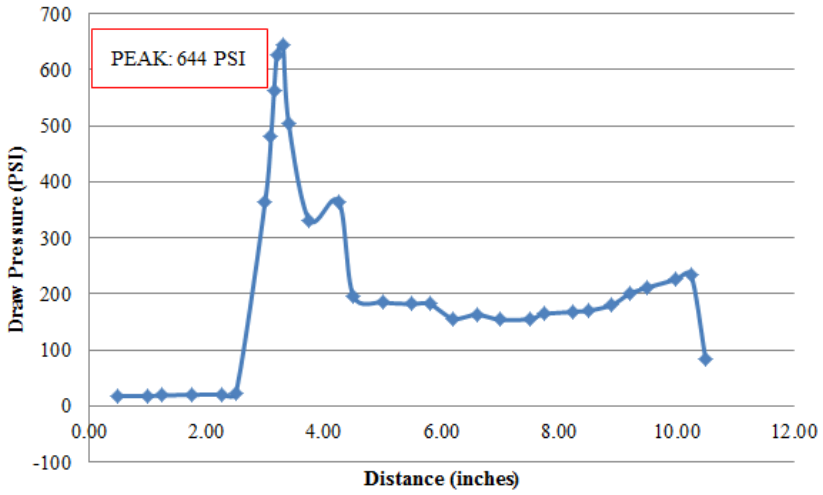

Fig. 4-3. Plot of maximum peak pressure during swaging, sample 3.

Sample 4 was assembled with the following factors: middle deformation, smallest relief depth, middle foil gap, smallest distance to relief area. The maximum required pressure was found to be 409 PSI, with the graph shown in Fig. 4-4.

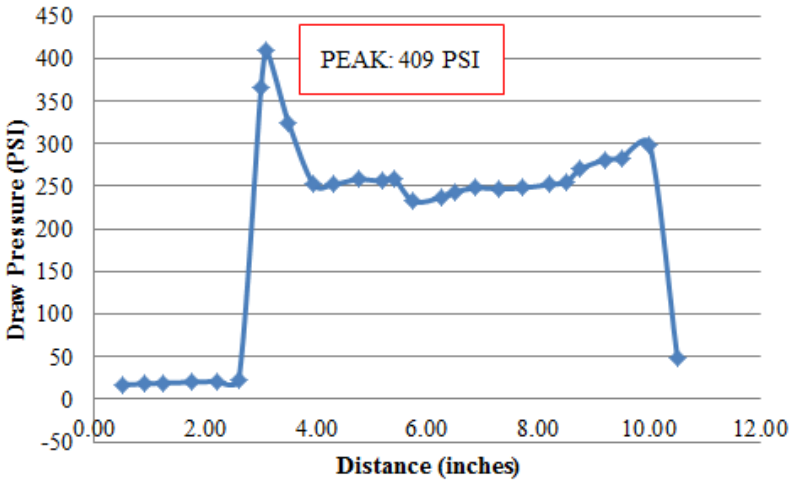

Fig. 4-4. Plot of maximum peak pressure during swaging, sample 4.

Sample 5 was assembled with the following factors: middle deformation, middle relief depth, smallest foil gap, largest distance to relief area. The maximum required draw pressure was found to be 467 PSI, as shown in the graph in Fig. 4-5.

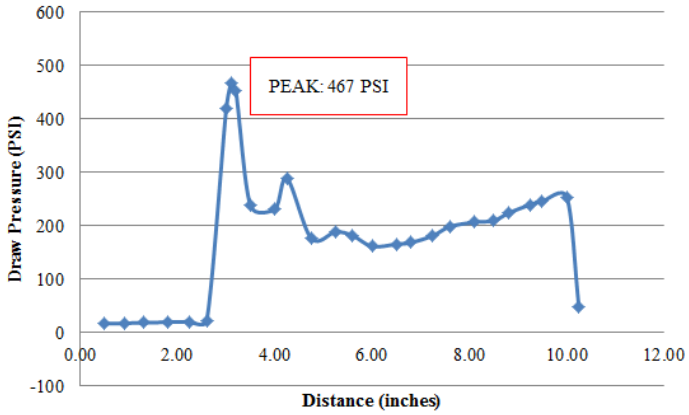

Fig. 4-5. Plot of maximum peak pressure during swaging, sample 5.

Sample 6 was assembled with the following factors: middle deformation, largest relief depth, largest foil gap, middle distance to relief area. The maximum required pressure was found to be 424 PSI, shown in Fig. 4-6.

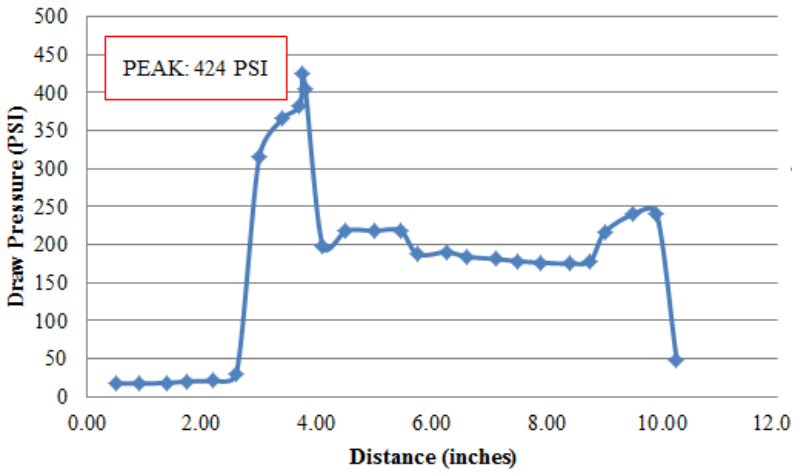

Fig. 4-6. Plot of maximum peak pressure during swaging, sample 6.

Sample 7 was assembled with the following factors: largest deformation, smallest relief depth, smallest foil gap, middle distance to relief area. The maximum required pressure was found to be 806 PSI, shown in Fig. 4-7.

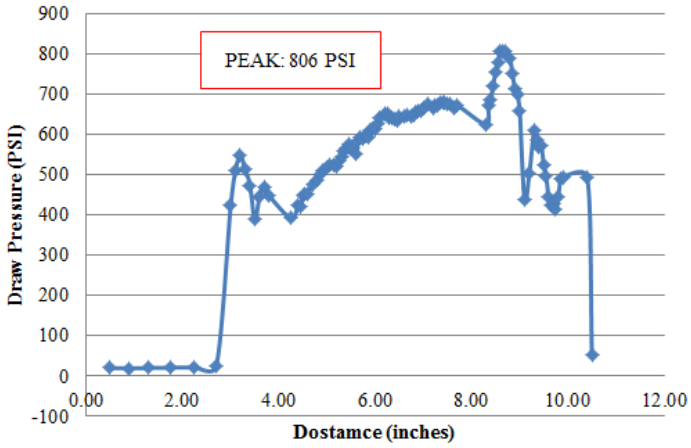

Fig. 4-7. Plot of maximum peak pressure during swaging, sample 7.

Sample 8 was assembled with the following factors: largest deformation, middle relief depth, largest foil gap, smallest distance to relief area. The maximum required pressure was found to be 474 PSI, shown in Fig. 4-8.

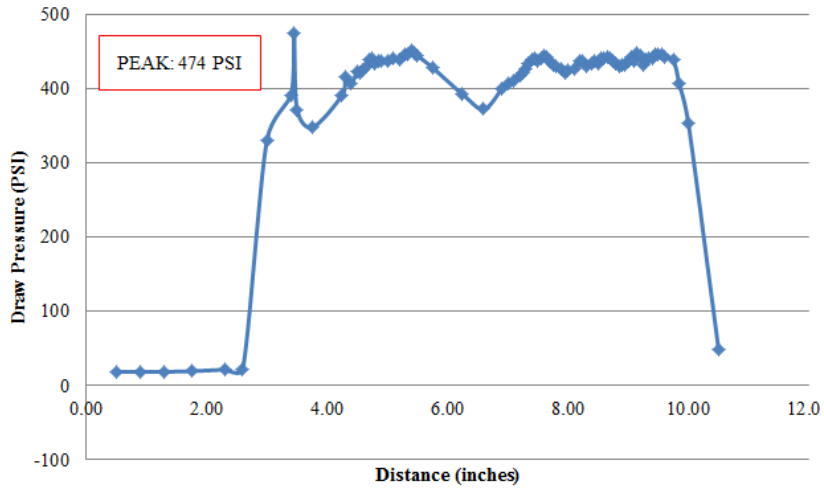

Fig. 4-8. Plot of maximum peak pressure during swaging, sample 8.

Sample 9 was assembled with the following factors: largest deformation, largest relief depth, middle foil gap, largest distance to relief area. The maximum required pressure was found to be 756 PSI, shown in Fig. 4-9.

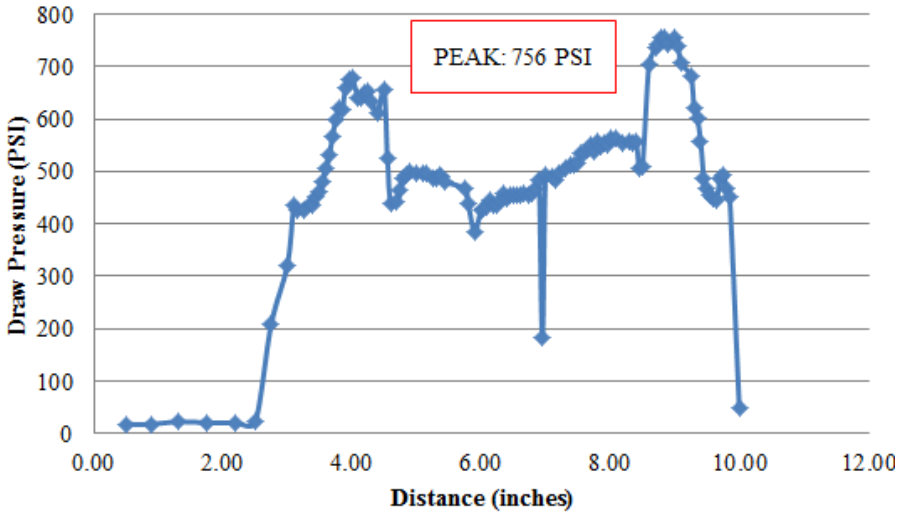

Fig. 4-9. Plot of maximum peak pressure during swaging, sample 9.

The maximum peaks plotted above represent the most pressure required to drive the draw plug through the target. The lubrication used in samples 1, 5 through 9 was dry graphite, while sample 2 through 4 was spray-on graphite. The lower pressures may be partial to better

lubrication. However, it was expected to see higher pressures with targets samples that used later plug sizes.

OUTPUT 2 - ROUNDNESS

The second output to the analysis is roundness. However, since none of the factors or their levels will affect the roundness, this particular condition will be excluded from robust analysis. More importantly, the roundness affects the ease of assembly. Better roundness will evidently lead to faster assembly time. The goal is to determine appropriate roundness tolerances that may be applied to the tube drawings. Initially advice from the College of Engineering machining technicians suggested that the roundness of the contact surfaces were more important and thus should have tighter tolerances than surfaces that do not interact. The internal surface of the inner tube will be made round by the draw-plug during deformation. Lastly, the external surface of the outer tube does not contribute to any process. Once again, all targets made at the University of Missouri used an expanding mandrel that help ensure proper roundness.

Initial measurements were made to verify that the machined tubes were fabricated within the designated diameter tolerances. Preliminary results did not show any large changes in diameters; however the three diameter measurement is not enough to definitively describe the roundness projections. Table 4-1 displays the measurements made with calipers.

Table 4-1. Static measurements of 18 tubes used in first run of experiments[2].

	Inside Tube								Outside Tube					Foil		
Measure Device	#	OD (in)	OD Relief (in)	Relief Circum (in)	Relief Length (in)	ID (in)	Length (in)	Thick (in)	#	ID (in)	Length (in)	Thick (in)	OD (in)	Length (in)	Width (in)	Thick (in)
		1.088	1.051	3.302		1.022		0.036		1.104		0.040	1.181			
Calipers	1	1.088	1.052	3.305	3.626	1.023	6.375	0.039	1	1.106	6.344	0.041	1.181	3.500	2.805	0.009
		1.088	1.052	3.303		1.020		0.036		1.106		0.041	1.181			
		1.089	1.074	3.374		1.024		0.039		1.105		0.042	1.179			
Calipers	2	1.089	1.075	3.377	4.875	1.024	6.344	0.037	2	1.104	6.375	0.042	1.179	3.500	3.080	0.008
		1.088	1.075	3.377		1.024		0.035		1.106		0.041	1.179			
		1.088	1.071	3.365		1.025		0.036		1.104		0.039	1.180			
Calipers	3	1.088	1.072	3.368	5.374	1.025	6.344	0.036	3	1.104	6.375	0.042	1.180	3.500	3.223	0.007
		1.089	1.072	3.368		1.025		0.037		1.105		0.040	1.180			
		1.088	1.077	3.383		1.029		0.037		1.104		0.041	1.180			
Calipers	4	1.088	1.076	3.380	5.372	1.026	6.344	0.035	4	1.104	6.375	0.041	1.180	3.500	3.087	0.009
		1.088	1.077	3.383		1.028		0.036		1.104		0.041	1.180			
		1.089	1.075	3.377		1.025		0.035		1.106		0.040	1.179			
Calipers	5	1.088	1.076	3.380	3.620	1.025	6.375	0.035	5	1.106	6.344	0.040	1.179	3.500	3.230	0.008
		1.089	1.076	3.380		1.024		0.036		1.106		0.040	1.179			
		1.088	1.072	3.368		1.025		0.036		1.109		0.040	1.181			
Calipers	6	1.088	1.072	3.368	4.865	1.025	6.375	0.036	6	1.108	6.375	0.039	1.181	3.500	2.874	0.009
		1.088	1.071	3.365		1.025		0.036		1.109		0.039	1.182			
		1.090	1.076	3.380		1.025		0.036		1.104		0.041	1.180			
Calipers	7	1.089	1.078	3.387	4.890	1.025	6.375	0.036	7	1.104	6.344	0.040	1.180	3.500	3.237	0.009
		1.090	1.077	3.383		1.025		0.037		1.105		0.041	1.180			
		1.091	1.074	3.374		1.025		0.036		1.106		0.041	1.179			
Calipers	8	1.091	1.073	3.371	5.375	1.025	6.359	0.036	8	1.106	6.375	0.040	1.179	3.500	2.880	0.008
		1.091	1.074	3.374		1.025		0.035		1.106		0.040	1.180			
		1.087	1.074	3.374		1.029		0.036		1.104		0.040	1.180			
Calipers	9	1.088	1.072	3.368	3.636	1.026	6.375	0.037	9	1.104	6.375	0.041	1.179	3.500	3.074	0.009
		1.088	1.074	3.372		1.028		0.036		1.106		0.041	1.180			

Tubes marked in RED are INSIDE tubes

Tubes marked in BLUE are OUTSIDE tubes

[2] Note: The pink highlighted data is later used to compare to another form of measurements

The measurements from Table 4-1 were helpful, but did not guarantee roundness. The static measurements indicated that the tubes were within specifications outlined in the drawing sheets. The more accurate method available was to use a probe measurement device. To further investigate roundness, each tube was measured using a digitize method via a probe attachment. Due to the tight tolerances of the tubes, a vice for the inner tube and another vise for the outer tube were fabricated to prevent deformation during measurements. In Fig. 4-10, the experimental setup of the CNC machine is shown complete with the two additional vices made. The drawings of the vice assembly and parts are available in Appendix I: Vice Drawings.

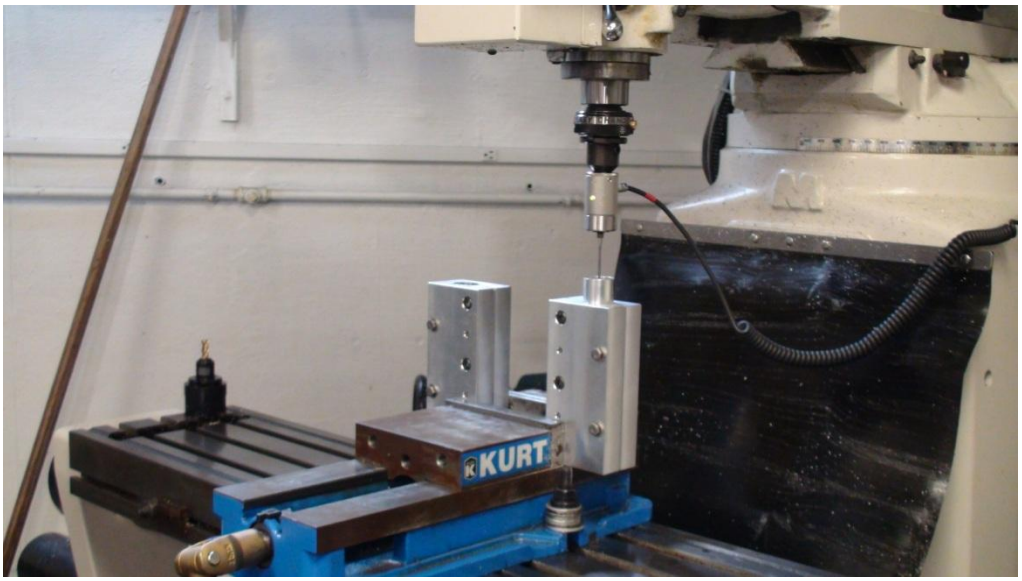

Fig. 4-10. The CNC setup.

The computerized numerical control (CNC) machine in Fig. 4-10 measures using a Cartesian coordinate system, with the origin found at the center of the vise that held the tube stationary and vertical. With X and Y data points, the diameter of the tube is easily found using Eq. (4-1).

$$D_{tube} = 2 \cdot \left(\sqrt{X^2 + Y^2} + \frac{D_{probe}}{2} \right) \tag{4-1}$$

To better understand these variables, a schematic has been drawn to illustrate. Please see Fig. 4-11.

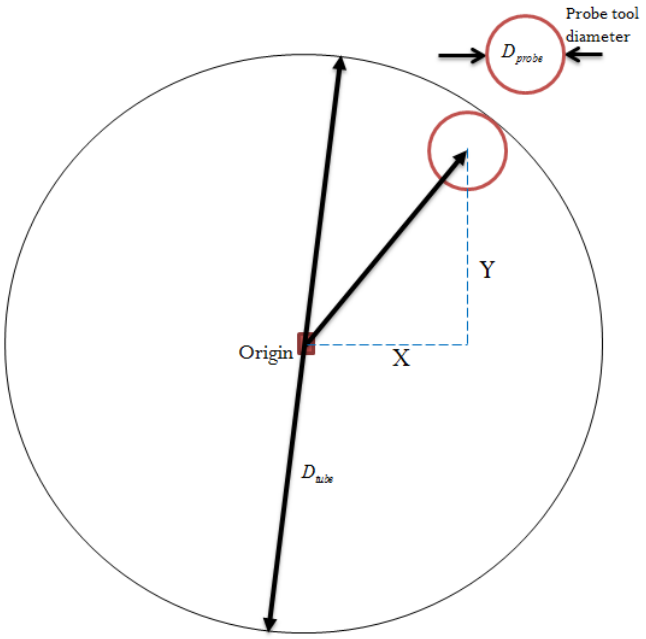

Fig. 4-11. Schematic of dimensions for calculating the inner diameter of tube.

Using the X and Y data points, the diameter at each measurement can be calculated that will be used later to determine roundness overall. The overall depth measured is 0.75 inches measured from top of the tube due to short probe length. Longer probes are estimated to cost approximately $5000 but the accuracy decreases as the probe length increases. Therefore, to save money and obtain good results, both ends were measured and recorded. The probe is placed inside, approximately 0.07 inches down to begin measurements. The CNC machine makes 60 diameter measurements for one circumference, with 15 different circumference levels. The Z step depth is 0.05 inches. The process is repeated on the opposite end of the tube for a total of 2000+ measurements. The process for one tube takes approximately 2 hours to complete. See Fig. 4-12 for a schematic of the dimensions for the tool path.

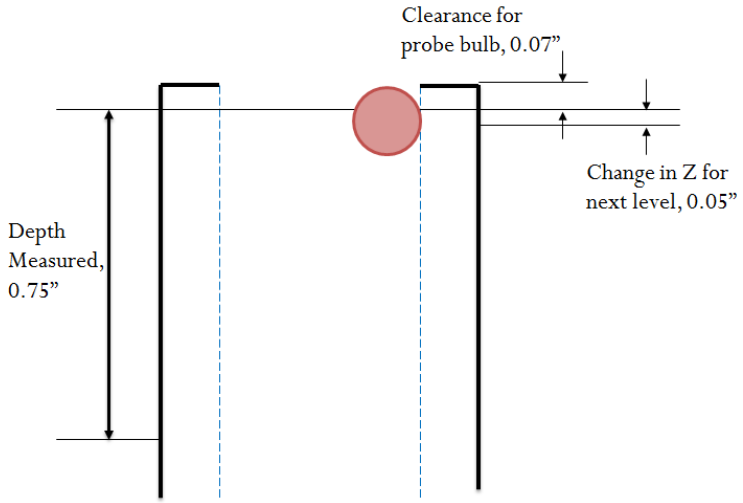

Fig. 4-12. Schematic of dimensions for one end of the tube for overall depth measurements.

Once measurements were taken, the data is imported as a “DIG” file, used by M & G code machines, such as CNC machines. The “DIG” file is opened in Word and through a series of customized macros written in Microsoft Word and Excel, the data is formatted to be opened in Excel. Some of the calculations made include roundness at each level and the diameter standard deviation. Below, Fig. 4-13 shows the probe inside a tube.

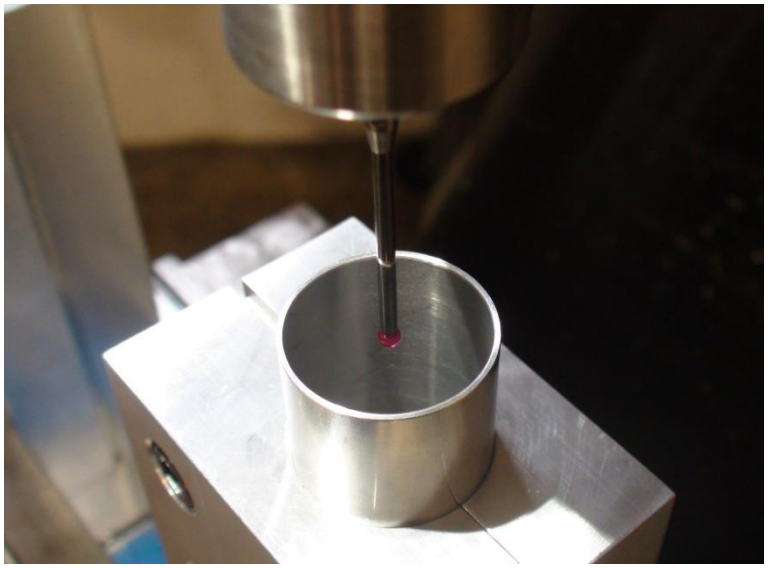

Fig. 4-13. Probe taking measurements.

Table 4-2 is a sample of the data collected as well as calculations. Sum of the squares was used in order to in order to detect differences throughout the data. Roundness is only calculated at one z depth. Roundness at one level may be compared to another level, but never combined.

Table 4-2. Sample data collected for outer tube #3[3].

				Radius	Diameter									
Mean				0.5534	1.1068									
STD Dev				0.00055	0.00109									
Sum of the squared error				0.0003	0.00120									
tool diameter				0.123										
EXP 3	Top Outer													
Axis 1	X	Axis 2	Y	Axis 3	Z	Radius	(yi - ybar)^2	Diameter	(yi - ybar)^2	Nominal	Measure	Average	(yi - yn)^2	Roundness
X	0.4908	Y	0	Z	-0.6048	0.5523	0.00000	1.1046	0.00000	1.107	1	1.1068	0.00001	0.00114116
X	0.4884	Y	0.0499	Z	-0.6048	0.5524	0.00000	1.1049	0.00000	1.107	2	1.1068	0.00000	
X	0.481	Y	0.0994	Z	-0.6048	0.5527	0.00000	1.1053	0.00000	1.107	3	1.1068	0.00000	
X	0.4686	Y	0.1478	Z	-0.6048	0.5529	0.00000	1.1057	0.00000	1.107	4	1.1068	0.00000	
X	0.4514	Y	0.1947	Z	-0.6048	0.5531	0.00000	1.1062	0.00000	1.107	5	1.1068	0.00000	
X	0.4295	Y	0.2397	Z	-0.6048	0.5534	0.00000	1.1067	0.00000	1.107	6	1.1068	0.00000	
X	0.4031	Y	0.2821	Z	-0.6048	0.5535	0.00000	1.1070	0.00000	1.107	7	1.1068	0.00000	0.001133971
X	0.3726	Y	0.3217	Z	-0.6048	0.5538	0.00000	1.1075	0.00000	1.107	8	1.1068	0.00000	
X	0.3381	Y	0.3579	Z	-0.6048	0.5538	0.00000	1.1077	0.00000	1.107	9	1.1068	0.00000	

[3] Note: Data can be compared to static measurements in Table 4-1, see pink highlighted cells.

From Table 4-2, the roundness of the outer tube used in experiment three (smallest plug size, maximum relief depth, smallest foil gap, and smallest distance to relief area) has a roundness average of approximately 0.0011 inches, with an average diameter of 1.1068 inches to the nominal 1.107 inches and a standard deviation of 0.001 inches. From the static measurements, the three diameter results were found to be 1.104 inches, 1.104 inches and 1.105 inches. The initial measurements are not as accurate as the CNC measurements and therefore should only be used to determine if the tubes are merely within the appropriate tolerance range. The second set of data (opposite end) for tube #3 used in Table 4-2 showed even better results: roundness was 0.0007 inches, but a higher standard deviation of all measured diameters at 0.0045 inches. Combining these efforts for every tube made for the first set of experiments, Table 4-3 shows the results for selected roundness measurements and their averages.

Table 4-3. Roundness tolerance results.

		INNER 1	INNER 2	INNER 3	INNER 4	INNER 5	INNER 6	INNER 7	INNER 8	INNER 9	
EXP #1	Roundness	0.000991	0.000909	0.000544	0.002681	0.000637	0.00097	0.001553	0.001282	0.000763	
EXP #1	Roundness	0.000986	0.000922	0.00049	0.002485	0.000915	0.001505	0.001278	0.000951	0.00085	
EXP #1	Roundness	0.001023	0.000489	0.000559	0.000516	0.001156	0.001511	0.00165	0.00115	0.001506	
EXP #1	Roundness	0.000827	0.000845	0.001	0.000454	0.001522	0.000906	0.000673	0.008356	0.000936	
	AVERAGE	0.000957	0.000791	0.000648	0.001534	0.001057	0.001223	0.001288	0.002935	0.001014	0.001272

		OUTER 1	OUTER 2	OUTER 3	OUTER 4	OUTER 5	OUTER 6	OUTER 7	OUTER 8	OUTER 9	
EXP #1	Roundness	0.000767	0.000647	0.001141	0.000614	0.000762	0.001705	0.000426	0.001057	0.001461	
EXP #1	Roundness	0.000853	0.000726	0.001134	0.001184	0.001298	0.007974	0.004124	0.000809	0.003878	
EXP #1	Roundness	0.001037	0.002315	0.000656	0.00128	0.001278	0.000627	0.001402	0.001072	0.001016	
EXP #1	Roundness	0.000963	0.003044	0.007585	0.001554	0.001688	0.009801	0.004146	0.001053	0.003628	
	AVERAGE	0.000905	0.001683	0.002629	0.001158	0.001256	0.005027	0.002525	0.000998	0.002496	0.002075

From this table, an appropriate tolerance may be applied to the targets for future machining purposes. Consequentially, the inner tube was found to have better roundness results while the

outer tube was double. Therefore, a roundness tolerance of 0.002 inches for the surfaces in contact is a reasonable classification.

Out of curiosity, the diameters calculated from the X and Y data points were plotted in Fig. 4-14. An interesting phenomenon was found: the results exhibited a sinusoidal response. Some responses were consistent as shown in Fig. 4-14, while others grew exponentially larger.

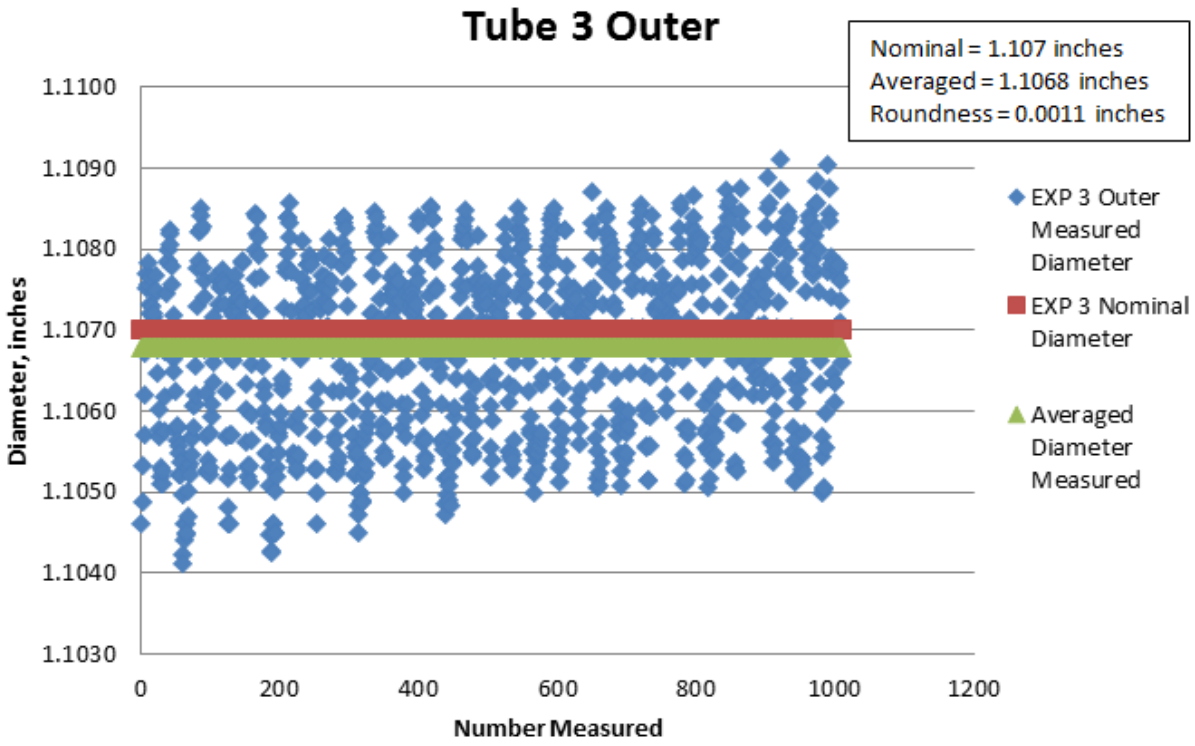

Fig. 4-14. Plots of the measured diameter vs. measurement number.

The nominal diameter is 1.107 inches, while the averaged diameter is 1.1068 inches. However, from Fig. 4-14, the sinusoidal curve is very consistent. The initial explanations for sinusoidal were attributed to machine hysteresis and overshoot. As the machine automatically measures points, the table moves. The machine movements are tracked by the amount of revolutions made by a stepper motor. The sum of both the machine error and overshoot error could cause the

phenomena seen in the plots. With high feed-rates, it could be possible that the peaks move farther apart for larger standard deviations in the diameter measurements.

More tubes were tested under extremely slow feed rates in order to hopefully eliminate the sinusoidal effect; however, additional plots were more distinctive sinusoidal. The final explanation was that the machining effects were being picked up rather than CNC errors. The targets are machined on the lathe, which could account for the consistency of the peaks.

The roundness for the tube used in was found to be 0.0011 inches, just slightly larger than expected at 0.0010 inches. However, the inner diameter of the outer tube is of much consequence to the assembly of the tubes. The relaxed roundness tolerance applies mainly to the inner diameter of the inner tube and with stricter tolerances used for the outer diameter of the inner tube. Currently, the CNC machine only measures inner diameter of both tubes. Roundness for the inner diameter of the inner tube may have a larger impact if needed for the disassembly device that may have the option to use a mandrel.

Optimal Condition

The optimal result is suggested that outer surface of the outer tube and the inner surface of the inner tube have a roundness tolerance of 0.002 inches. The inner surface of the outer tube and outer surface of the inner tube should have a roundness tolerance of 0.001 inches.

OUTPUT 3 – RESIDUAL STRESS

The third output is residual stress. Residual stress is the amount of built in stresses that exists after deformation. Once welded, some of those stresses relax in the targets because of the presence of heat. Residual stress is difficult to model both numerically or analytically. After welding, the samples undergo x-ray diffraction testing. Initially, only one measurement was

made per target at the middle of the foil area. The results were found to be somewhat unexpected and unusual. To show more test results, the number of measurements were increased to seven measurements per target in order to get an average of the residual stress. For each target, two different types of measurements were made: hoop stress and longitudinal stress.

Experimental Results

Using the equations mentioned in the previous section, the hoop and longitudinal stresses may be found experimentally. The following table provides the results gathered, measurements are made in MPa. Some of the results were unexpected; for instances, the hoop stress recording of point 7 for sample 7 is -119.54, which is 111.64 MPa larger than the previous measurement, at point 6 of the same sample. These anomalies may be attributed to the foil not perfectly within the relief area and perhaps wrapping around the lip of the material step. This would make sense because deformation here would be higher because of the extra thickness and therefore leaving more built in stress. Results for one matrix set of experiments are shown in Table 4-4.

Table 4-4. Residual stress measurements for hoop and longitudinal.

ASSEMBLY Comments		XRD RESULTS (BEFORE HEATING)							
Tubes are marked via sample number as well as hash marks (# sample)		**OUTER TUBE SURFACE PT1**	**OUTER TUBE SURFACE PT2**	**OUTER TUBE SURFACE PT3**	**OUTER TUBE SURFACE PT4**	**OUTER TUBE SURFACE PT5**	**OUTER TUBE SURFACE PT6**	**OUTER TUBE SURFACE PT7**	**COMMENTS**
Marking: 1 Incorrectly dimensioned	HOOP	8.240	32.500	9.700	1.620	9.780	43.540	36.010	
	LONG	-2.510	11.340	6.630	2.650	6.770	9.090	-7.99	
Marking: 2L	HOOP	-31.49	2.510	33.970	-23.61	-43.29	-22.66	-72.16	
	LONG	-7.98	14.500	-16.36	-51.17	-75.18	3.140	-64.59	
Marking: 3L	HOOP	-55.50	-21.91	-9.81	-20.7	-41.53	6.640	-73.10	
	LONG	-92.30	-75.28	-118.28	-56.56	-88.92	-110.90	-87.16	
Marking: 4L	HOOP	14.06	-19.95	9.83	-28.12	-33.58	61.67	-31.09	
	LONG	-37.70	-43.26	-15.93	-90.46	-57.82	-104.36	-58.08	
Marking: 5	HOOP	-43.63	-7.29	-3.29	1.23	2.99	-6.26	8.28	
	LONG	-21.70	-7.49	-43.54	-26.21	-1.82	9.59	-46.32	
Marking: 6L	HOOP	11.56	22.72	-37.58	-11.59	8.54	38.62	22.32	Initial Test -25.40 (axial) -0.54 (hoop)
	LONG	-11.34	-17.94	-34.22	33.32	-39.23	26.52	-54.84	
Marking: 7L	HOOP	57.48	51.17	6.71	-14.44	16.92	-7.90	-119.34	
	LONG	-85.14	-98.84	-46.50	-53.06	-112.03	-89.82	-119.54	
Marking: 8L	HOOP	48.82	12.040	11.180	20.290	1.370	12.300	-19.11	
	LONG	-57.20	-51.67	-60.98	-56.91	-63.74	-45.74	-78.37	
Marking: 9	HOOP	-42.50	-59.69	0.73	16.67	39.53	-16.06	12.64	
	LONG	-61.88	39.32	-14.93	18.51	5.40	-17.57	35.42	
Marking: 1R Correct dimensions	HOOP	-56.43	-43.53	-30.34	-30.69	-11.42	-0.14	-34.30	
	LONG	-32.05	-13.99	-84.16	-24.70	-52.71	-21.65	-55.46	

Robust Analysis Tables

As stated previously, the ideal target will have some stresses, both hoop and longitudinal. Robust analysis was done both for hoop and longitudinal. A nominal value of 43 MPa, found through computer simulations of the FEA model, was used for the hoop analysis and the longitudinal were minimized. Table 4-5 shows the measurements and signal to noise calculations for only hoop stress. Notice the most hoop stress exists in sample 7 which used the largest draw plug. Contradictorily, the least hoop stress was seen in sample 5. The nominal condition was found in sample 4.

Table 4-5. Signal to Noise calculations for residual hoop stress.

Quality Characteristic: the Nominal the better 43 MPa

Overall Average: -41.62 dB

Experiments/Level: 9

Measurements in MPa

L-9	Factors Tested at Level 1, 2, and 3											
Trial #	Punch Size (A)	Relief Depth (B)	Gap (C)	Distance to Relief (D)	Meas 1	Meas 2	Meas 3	Meas 4	Meas 5	Meas 6	Meas 7	S/N
1	1	1	1	1	-56.43	-43.53	-30.34	-30.69	-11.42	-0.14	-34.3	-42.8955
2	1	2	2	2	-31.49	2.51	33.97	-23.61	-43.29	-22.66	-72.16	-44.8422
3	1	3	3	3	-55.5	-21.91	-9.81	-20.7	-41.53	6.64	-73.1	-44.5317
4	2	1	2	3	14.06	-19.95	9.83	-28.12	-33.58	61.67	-31.09	-42.4560
5	2	2	3	1	-43.63	-7.29	-3.29	1.23	2.99	-6.26	8.28	-39.4037
6	2	3	1	2	11.56	22.72	-37.58	-11.59	8.54	38.62	22.32	-37.5906
7	3	1	3	2	57.48	51.17	6.71	-14.44	16.92	-7.9	-119.34	-45.2051
8	3	2	1	3	48.82	12.04	11.18	20.29	1.37	12.3	-19.11	-38.6542
9	3	3	2	1	-42.5	-59.69	0.73	16.67	39.53	-16.06	12.64	-38.9879
												-41.6186

From the table above, the average signal-to-noise result was found to be -41.62 dB. Next, the mean effect of each factor is found and shown in Table 4-6. Highlighted values are best results and are used again in a later table.

Table 4-6. Mean effect of each factor for residual hoop stress.

	Punch Size (A)	Relief Depth (B)	Gap (C)	Distance to Relief (D)
1	-44.0898	-43.5189	-39.7135	-40.4290
2	-39.8168	-40.9667	-42.0954	-42.5460
3	-40.9491	-40.3701	-43.0469	-41.8806
Diff	4.2731	3.1488	3.3334	2.1169

Once the mean effect of each factor is known, a response graph can be made of the average signal to noise for each factor and their corresponding levels. See Fig. 4-15 for the response graph. To get the nominal-the-better result, the valued point will be a nominal value (43 MPa) in relation to the average signal-to-noise, which is represented as a black horizontal line. In this case, the best result combination will contain either: A_2, B_3, C_1, and/or D_1.

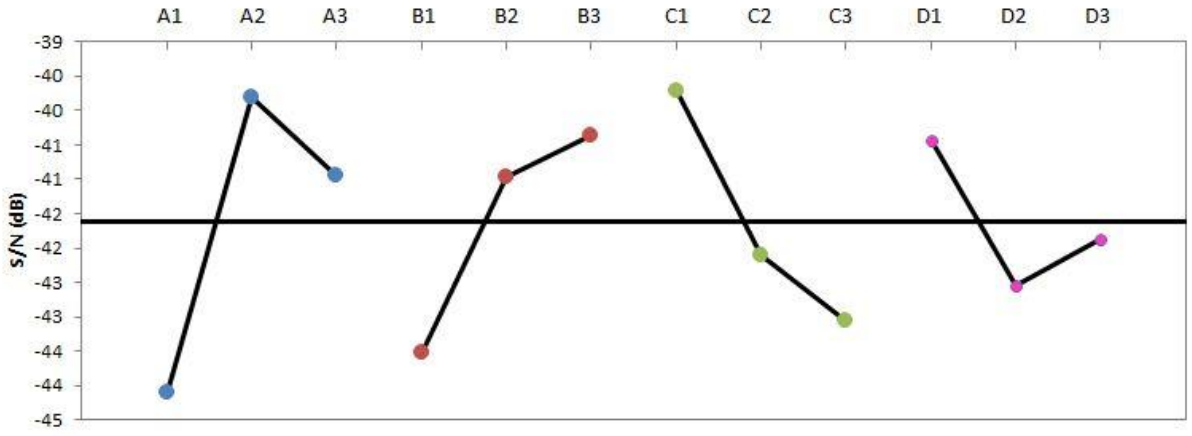

Fig. 4-15. Response graph for residual hoop stress.

Next, using Table 4-6, the analysis of variance table may be completed. The variance of each factor is calculated and then a percentage calculated as well. See Table 4-7 for complete ANOVA results for hoop stress. Here, the column headers are the degrees of freedom (DF), total sum of squares of the deviation from the mean values for all levels of the factor (Sx), the mean square due to factor (Vx), variance ratio used to measure the effect of the factor compared with the random effect due to error (F), and percent contribution to the assembly (ρ).

Table 4-7. ANOVA results for residual hoop stress.

Source	DF	Sx	Vx	F	ρ
Punch Size (A)	2	29.41	14.70	8.36	41.47%
Relief Depth (B)	2	16.78	8.39	4.77	23.67%
Gap (C)	2	17.69	8.85	5.03	24.95%
Distance to Relief (D)	2	7.03	3.52	--	9.92%
TOTAL	8	70.91	8.86	--	100.00%
ERROR	2	7.03	3.52	--	--

From the ANOVA results, the insignificant factor is the Distance to Relief (D); therefore, the most important factors are found to be Punch Size (A), Relief Depth (B), and Gap (C), as can be deduced from the percentage contribution. With that, then the level with the lowest mean effect will be the best condition. For the residual hoop stress study, the optimal solution signal-to-noise is -36.66 dB ± 2.977 dB at 95% confidence. Those conditions are a medium punch size deformation of 0.010 inches (plug size 1.047 inches), level A_2, largest relief depth of 0.008 inches B_3, and biggest foil gap of 0.500 inches C_1. A sample size of 13 will allow a 95% chance of avoiding a type II error.

This study would not be complete without assessing the longitudinal stress as well. The ideal target will have the least residual longitudinal stresses. Table 4-8 shows the measurements and signal to noise calculations for only longitudinal stress. Notice the most axial stress exists in sample 7 again which used the largest draw plug, but assembly issues could affect higher residual stress measurements (i.e. foil edges near tube lip). Contradictorily, the least axial stress was seen in sample 9, which was also found to be closest to the nominal condition.

Table 4-8. Signal to Noise calculations for residual longitudinal stress.

Quality Characteristic: the SMALLER the better

Overall Average: -33.99 dB

Experiments/Level: 9

Measurements in MPa

L-9	Factors Tested at Level 1, 2, and 3											
Trial #	**Punch Size (A)**	**Relief Depth (B)**	**Gap (C)**	**Distance to Relief (D)**	**Meas 1**	**Meas 2**	**Meas 3**	**Meas 4**	**Meas 5**	**Meas 6**	**Meas 7**	**S/N**
1	1	1	1	1	-32.05	-13.99	-84.16	-24.70	-52.71	-21.65	-55.46	-33.3785
2	1	2	2	2	-7.98	14.5	-16.36	-51.17	-75.18	3.14	-64.59	-32.6864
3	1	3	3	3	-92.3	-75.28	-118.28	-56.56	-88.92	-110.9	-87.16	-39.2706
4	2	1	2	3	-37.7	-43.26	-15.93	-90.46	-57.82	-104.36	-58.08	-36.2232
5	2	2	3	1	-21.70	-7.49	-43.54	-26.21	-1.82	9.59	-46.32	-28.8330
6	2	3	1	2	-11.34	-17.94	-34.22	33.32	-39.23	26.52	-54.84	-30.5698
7	3	1	3	2	-85.14	-98.84	-46.50	-53.06	-112.03	-89.82	-119.54	-39.1004
8	3	2	1	3	-57.2	-51.67	-60.98	-56.91	-63.74	-45.74	-78.37	-35.5623
9	3	3	2	1	-61.88	39.32	-14.93	18.51	5.40	-17.57	35.42	-30.3188
												-33.9937

From the table above, the average signal-to-noise result was found to be –33.99 dB. Next, the mean effect of each factor is found and shown in Table 4-9. Highlighted values are best results for a later table.

Table 4-9. Mean effect of each factor for residual longitudinal stress.

	Punch Size (A)	**Relief Depth (B)**	**Gap (C)**	**Distance to Relief (D)**
1	-35.1118	-36.2340	-33.1702	-30.8434
2	-31.8753	-32.3605	-33.0761	-34.1189
3	-34.9938	-33.3864	-35.7347	-37.0187
Diff	3.2365	3.8735	2.6586	6.1753

Once the mean effect of each factor is known, a response graph can be made of the average signal to noise for each factor and their corresponding levels. See Fig. 4-16 for the response

graph. To get the smaller-the-better result, the valued point will be smallest value in relation to the average signal-to-noise, which is represented as a black horizontal line. In this case, the best result combination will contain either: A_2, B_2, C_2, and/or D_1.

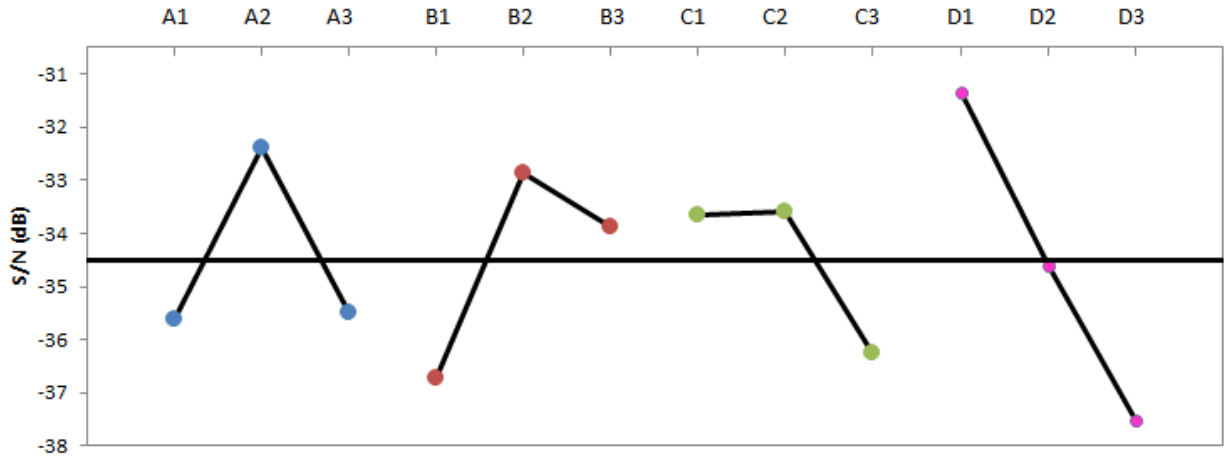

Fig. 4-16. Response graph for residual longitudinal stress.

Next, using Table 4-9, the analysis of variance table may be completed. The variance of each factor is calculated and then a percentage calculated as well. See Table 4-10 for complete ANOVA results for hoop stress. Here, the column headers are the degrees of freedom (DF), total sum of squares of the deviation from the mean values for all levels of the factor (Sx), the mean square due to factor (Vx), variance ratio used to measure the effect of the factor compared with the random effect due to error (F), and percent contribution to the assembly (ρ).

Table 4-10. ANOVA results for residual longitudinal stress.

Source	DF	Sx	Vx	F	ρ
Punch Size (A)	2	20.21	10.11	2.96	17.53%
Relief Depth (B)	2	24.17	12.08	3.54	20.96%
Gap (C)	2	13.65	6.83	--	11.84%
Distance to Relief (D)	2	57.27	28.64	8.39	49.67%
TOTAL	8	115.30	14.41	--	100.00%
ERROR	2	13.65	6.83	--	--

From the ANOVA results, the insignificant factor is Gap (C); therefore, the most important factors found to be Punch Size (A), Relief Depth (B), and the Distance to Relief (D), as can be deduced from the percentage contribution of 17.53%, 20.96% and 49.67%, respectively. With that, then the level with the lowest mean effect will be the best condition. For the residual longitudinal stress study, the optimal solution signal-to-noise is -27.09 dB ± 3.796 dB at 95% confidence. Those optimal conditions are the medium punch size deformation of 0.010 inches (plug size 1.047 inches), level A_2, medium relief depth of 0.007 inches B_2, and largest relief to distance (relief distance of 1.372 inches) at level D_1. A sample size of 13 will allow a 95% chance of avoiding a type II error.

Optimal Condition

From the robust analysis, the best condition for residual stresses was found to be with the medium plug, medium relief depth and largest distance to relief, levels A_2, B_2, and D_1. Sample 5 is the only sample that fits these requirements and was found to fulfill the optimal condition.

OUTPUT 4 – PRESENCE OF AIR GAPS

The fourth output is the presence of air gaps, also defined as one of the negative defects. The main defects that were found were weld cracks and air gaps due to improper deformation. Weld cracks are discussed in the weld study section.

AIR GAPS

If the deformation is too small, air gaps are visible on the cross-section of the foil area. Too large of an air gap will prevent good thermal contact, but very small gaps are necessary for fission gas expansion. Samples were assembled and deformed. After sanding and polishing the

cross-section area, samples were checked under the SEM and ImageJ used to quantify the air gaps.

SEM Results

The following figures are results from viewing the cross-section of the foil area under the SEM. Due to the nature of the metallic material, the SEM provided the best views of the targets. The large dark gaps are air gaps.

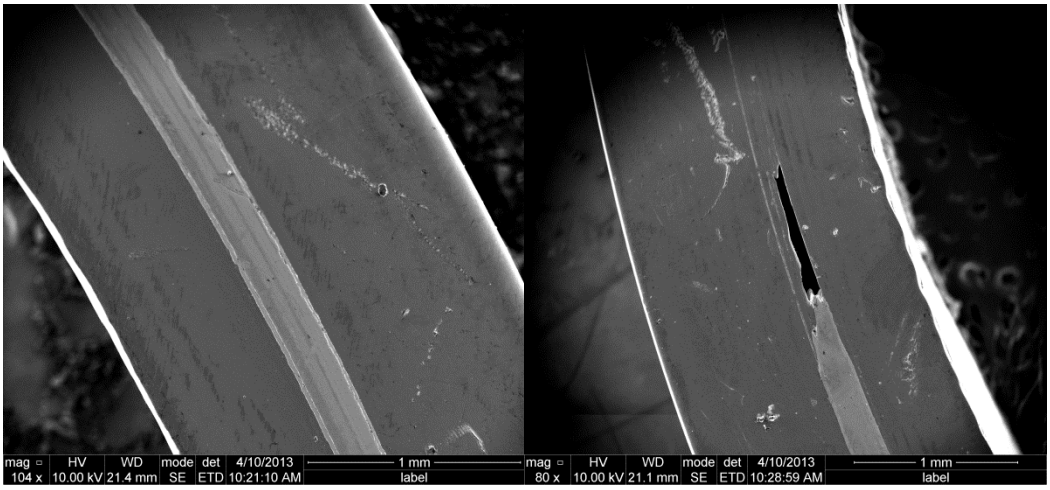

(a) (b)

Fig. 4-17. SEM review of sample 1 (smallest deformation, smallest relief depth, largest foil gap, largest distance to relief area).

Clearly, many gaps can be seen in the samples that used the smallest plug (Fig. 4-17, Fig. 4-18, and Fig. 4-19). It was quickly determined that the smallest amount of deformation was not enough to fully seal the foil between the target tubes.

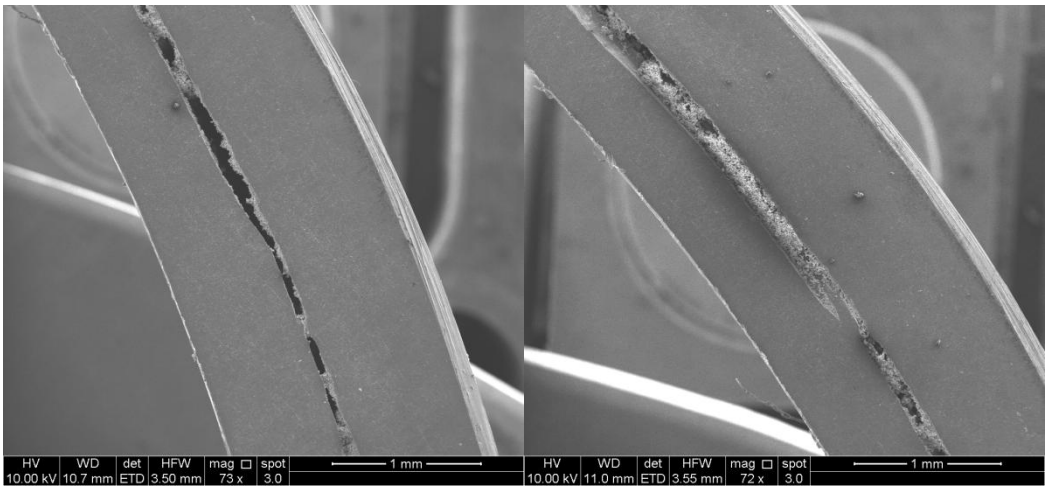

(a) (b)

Fig. 4-18. SEM review of sample 2 (smallest deformation, middle relief depth, middle foil gap, middle distance to relief area).

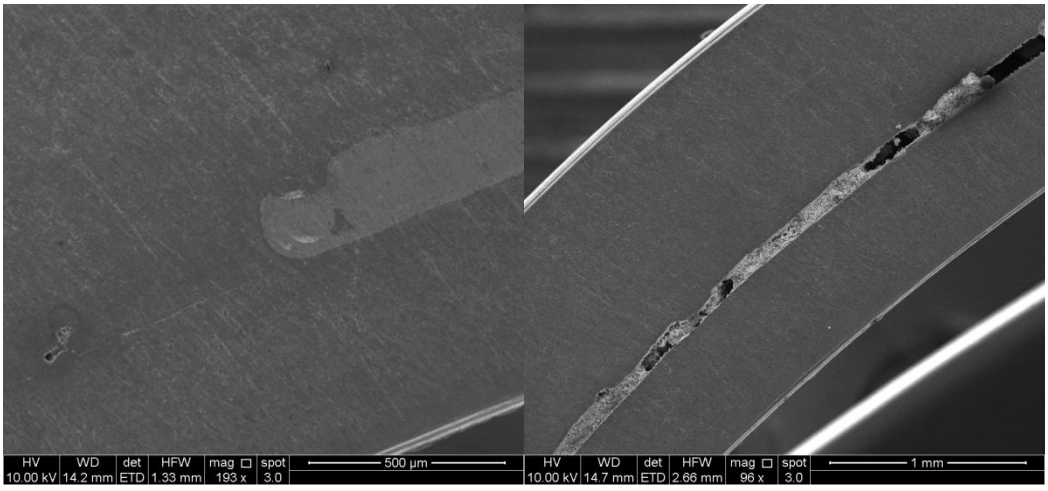

(a) (b)

Fig. 4-19. SEM review of sample 3 (smallest deformation, largest relief depth, smallest foil gap, smallest distance to relief area).

Sample 3 showed one foil end closing well but issues around the opposite foil end, as seen in Fig. 4-19a and Fig. 4-19b.

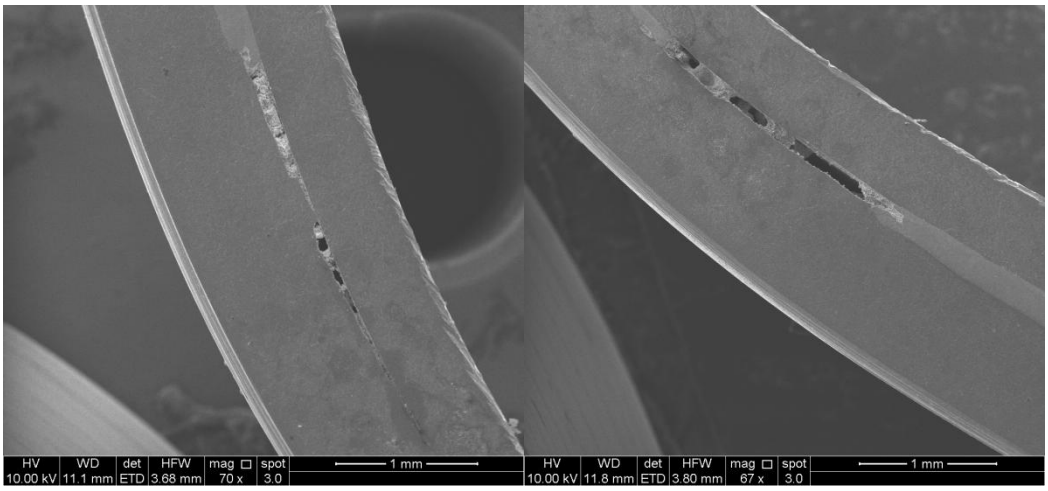

(a) (b)

Fig. 4-20. SEM review of sample 4 (middle deformation, smallest relief depth, middle foil gap, smallest distance to relief area).

Good results are evident in Fig. 4-20a with fairly good closure around the foil ends; however, the opposite ends has a large gap, in Fig. 4-20b.

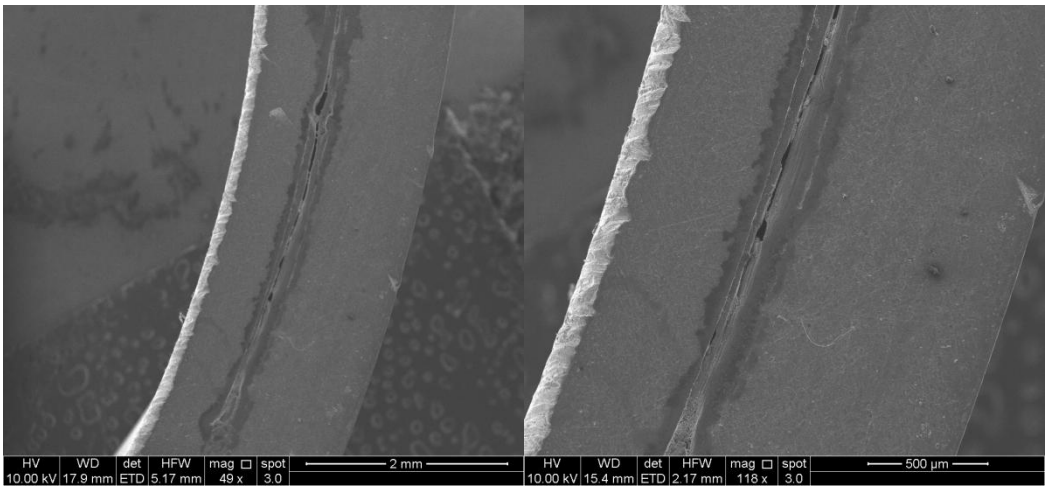

(a) (b)

Fig. 4-21. SEM review of sample 5 (middle deformation, middle relief depth, smallest foil gap, largest distance to relief area).

Sample 5 in Fig. 4-21a and Fig. 4-21b have very small gaps and is consider a good result in terms of the air gaps.

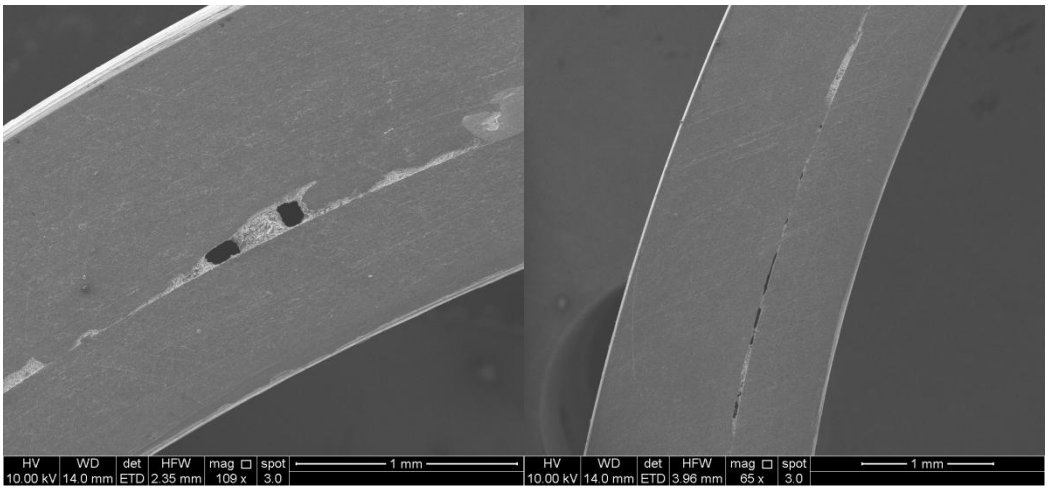

(a) (b)

Fig. 4-22. SEM review of sample 6 (middle deformation, largest relief depth, largest foil gap, middle distance to relief area).

Large gaps can be seen in Fig. 4-22a but fairly good closure throughout the rest of the target is shown in Fig. 4-22b.

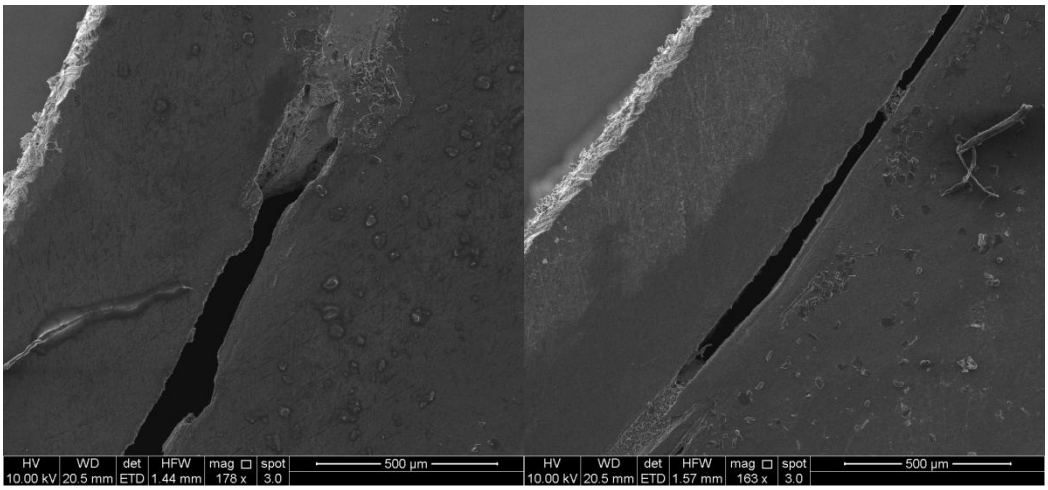

(a) (b)

Fig. 4-23. SEM review of sample 7 (largest deformation, smallest relief depth, smallest foil gap, middle distance to relief area).

In Fig. 4-23a and Fig. 4-23b have moderately large gaps and again are prominent around the foil edge.

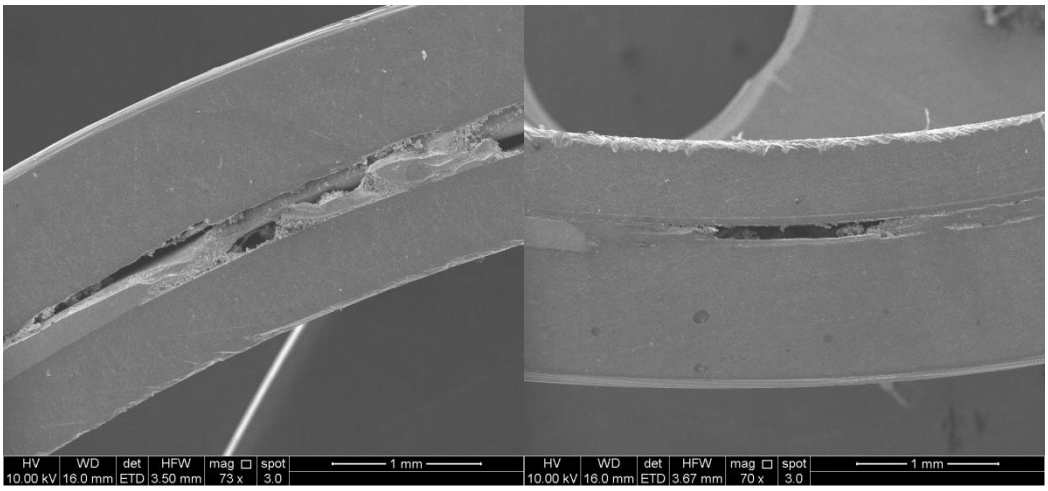

(a) (b)

Fig. 4-24. SEM review of sample 8 (largest deformation, middle relief depth, largest foil gap, smallest distance to relief area).

Poor contact is evident in Fig. 4-24a and the foil ends are not closing properly either in Fig. 4-24b.

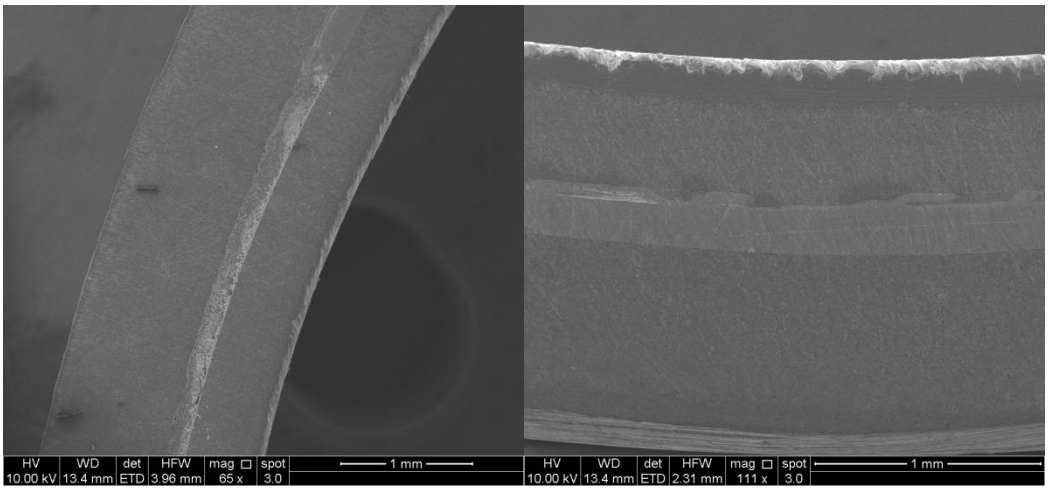

(a) (b)

Fig. 4-25. SEM review of sample 9 (largest deformation, largest relief depth, middle foil gap, largest distance to relief area).

Sample 9 in Fig. 4-25a and Fig. 4-25b show no gaps at all. However, review without the SEM of the back side of the cross section revealed very small gaps; therefore, no sample was perfectly without air gaps. Thus, the robust analysis should find the smallest gap of all nine experiments.

Why Defects?

Air gaps are considered defects because the gaps prevent good thermal contact. However, a few gaps are necessary for fission gas expansion. These air gaps are the result of poor deformation. Preliminary results show that the largest deformations seal the foil area better than the smallest and medium deformation targets.

Robust Analysis Tables

The ideal target has very little air gaps after deformation. The robust analysis tables below will show the condition of the best target. The analysis done here was to discover which targets had the best combination that resulted with the fewest air gaps. Therefore, the quality characteristic will be "the smaller, the better." Table 4-11 provides the measurements made with ImageJ and converted to micrometers. Similar to the weld pores, if the measurements are too small, the calculations will not be accurate; therefore, large values were used for calculations. Please note that while sample 9 in Fig. 4-25 had no gaps, the robust analysis cannot have a zero factor or a very small number. Therefore, a floor average was found to substitute.

Table 4-11. Signal to Noise calculations for air gaps.

Quality Characteristic: the smaller the better
Overall Average: -39.17 dB
Experiments/Level: 9

Measurements in μm

L-9	Factors Tested at Level 1, 2, and 3				Meas 1	Meas 2	Meas 3	S/N
Trial #	**Punch Size (A)**	**Relief Depth (B)**	**Gap (C)**	**Distance to Relief (D)**				
1	1	1	1	1	94	80	26	-37.2261
2	1	2	2	2	143	107	125	-41.9978
3	1	3	3	3	94	25	60	-36.3928
4	2	1	2	3	87	65	76	-37.6765
5	2	2	3	1	63	33	48	-33.9270
6	2	3	1	2	109	26	68	-37.5659
7	3	1	3	2	138	65	101	-40.4799
8	3	2	1	3	318	115	216	-47.2887
9	3	3	2	1	100	100	100	-40.0000
								-39.1727

From the table above, the average signal-to-noise result was found to be -39.08 dB. Next, the mean effect of each factor is found and shown in Table 4-12. Highlighted values are best results for a later table.

Table 4-12. Mean effect of each factor for air gaps.

	Punch Size (A)	**Relief Depth (B)**	**Gap (C)**	**Distance to Relief (D)**
1	-38.5389	-38.4608	-40.6936	-37.0510
2	-36.3898	-41.0712	-39.8914	-40.0145
3	-42.5895	-37.9862	-36.9332	-40.4526
Diff	6.1997	3.0850	3.7604	3.4016

Once the mean effect of each factor is known, a response graph can be made of the average signal to noise for each factor and their corresponding levels. See Fig. 4-26 for the response

graph. To get the smaller-the-better result, the valued point will be smallest value in relation to the average signal-to-noise, which is represented as a black horizontal line. In this case, the best result combination will contain either: A_2, B_3, C_3, and/or D_1.

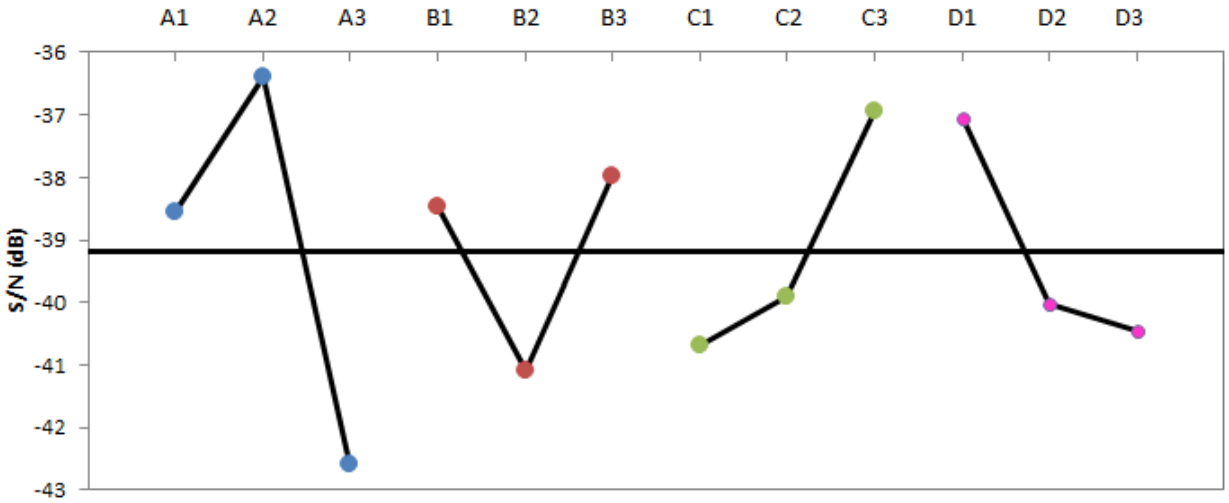

Fig. 4-26. Response graph for air gaps.

Next, using Table 4-12, the analysis of variance table may be completed. The variance of each factor is calculated and then a percentage calculated as well. See Table 4-13 for complete ANOVA results. Here, the column headers are the degrees of freedom (DF), total sum of squares of the deviation from the mean values for all levels of the factor (Sx), the mean square due to factor (Vx), variance ratio used to measure the effect of the factor compared with the random effect due to error (F), and percent contribution to the assembly (ρ).

Table 4-13. ANOVA results for air gaps.

Source	DF	Sx	Vx	F	ρ
Punch Size (A)	2	59.46	29.73	6.411	49.51%
Relief Depth (B)	2	16.56	8.28	0.892	13.79%
Gap (C)	2	23.53	11.77	2.537	19.60%
Distance to Relief (D)	2	20.55	10.27	1.108	17.11%
TOTAL	8	120.10	15.01	--	100.00%
ERROR	4	37.10	9.28	--	--

From the ANOVA results, the insignificant factors are the Relief Depth (B) and Distance to Relief (D); therefore, the most important factors found to be Punch Size (A) and Gap (C), as can be deduced from the percentage contribution. With that, then the level with the lowest mean effect will be the best condition. To minimize air gaps, the optimal solution signal-to-noise is -34.15 dB ± 3.875 dB with 95% confidence. Those optimal conditions are the medium punch size deformation of 0.010 (plug size 1.047 inches) and smallest gap distance of 0.150 inches, levels A_2 and C_3. A sample size of 13 will allow a 95% chance of avoiding a type II error.

Optimal Condition

From the robust analysis, the best condition was found to be a medium plug with the smallest foil gap. Therefore, based on these results, sample 5 is once again proves to be closest to the optimal condition.

OUTPUT 5 – FOIL VOLUME

One of the key components to this project is to maximize the amount of uranium foil volume. Because LEU foil is not as enriched as HEU, the amount of LEU foil necessary to produce the same amount of molybdenum – 99 using HEU foil will be greater. Therefore, the necessity of maximizing the amount of foil is an important factor to review.

Robust Analysis Tables

The ideal target has the largest possible foil volume. The robust analysis tables below will show the optimal condition of the best target having the most foil. The analysis done here was to discover which targets had the best combination that resulted with the maximum foil volume.

Therefore, the quality characteristic will be "the larger, the better." Table 4-14 provides the volume calculations made based on the foil width, length and thickness (0.150 mm).

Table 4-14. Signal to Noise calculations for foil volume.

Quality Characteristic: the LARGER the better
Overall Average: -21.77 dB
Experiments/Level: 9

Measurements in in³

L-9	Factors Tested at Level 1, 2, and 3					
Trial #	**Punch Size (A)**	**Relief Depth (B)**	**Gap (C)**	**Distance to Relief (D)**	**Meas 1**	**S/N**
1	1	1	1	1	0.05797736	-24.7348
2	1	2	2	2	0.0862885	-21.2809
3	1	3	3	3	0.09981149	-20.0164
4	2	1	2	3	0.09559977	-20.3909
5	2	2	3	1	0.06676181	-23.5094
6	2	3	1	2	0.08051726	-21.8822
7	3	1	3	2	0.10980312	-19.1877
8	3	2	1	3	0.08918929	-20.9937
9	3	3	2	1	0.0635374	-23.9394
						-21.7706

From the table above, the average signal-to-noise result was found to be -21.77 dB. Next, the mean effect of each factor is found and shown in Table 4-15. Highlighted values are best results for a later table.

Table 4-15. Mean effect of each factor for foil volume.

	Punch Size (A)	**Relief Depth (B)**	**Gap (C)**	**Distance to Relief (D)**
1	-22.0107	-21.4378	-22.5369	-24.0612
2	-21.9275	-21.9280	-21.8704	-20.7836
3	-21.3736	-21.9460	-20.9045	-20.4670
Diff	0.6371	0.5082	1.6324	3.5942

Once the mean effect of each factor is known, a response graph can be made of the average signal to noise for each factor and their corresponding levels. See Fig. 4-27 for the response graph. To get the larger-the-better result, the valued point will be smallest value in relation to the average signal-to-noise, which is represented as a black horizontal line. In this case, the best result combination will contain either: A_3, B_1, C_3, and/or D_3.

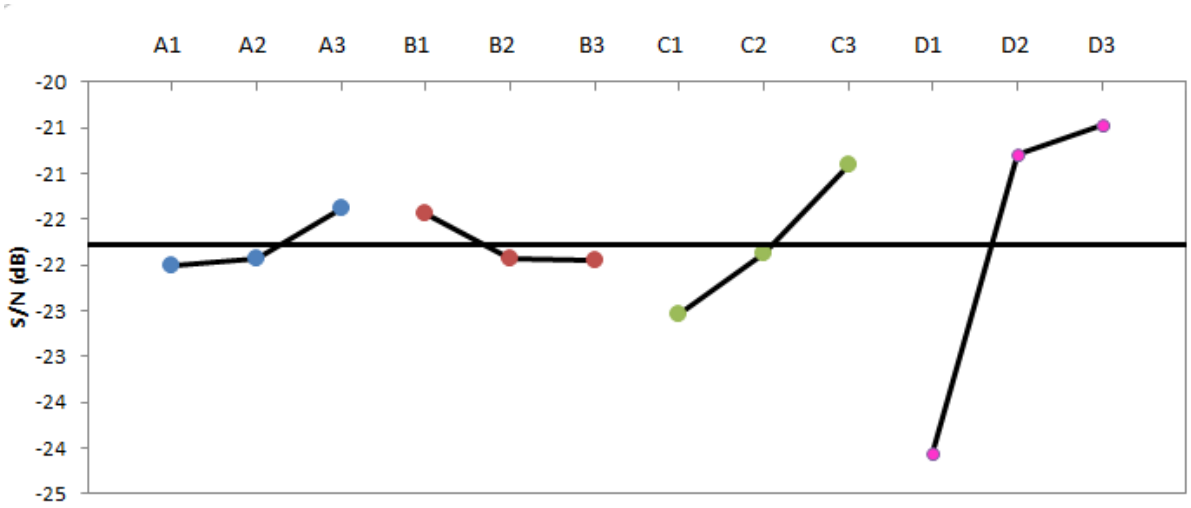

Fig. 4-27. Response graph for foil volume.

Next, using Table 4-15, the analysis of variance table may be completed. The variance of each factor is calculated and then a percentage calculated as well. See Table 4-16 for complete ANOVA results. Here, the column headers are the degrees of freedom (DF), total sum of squares of the deviation from the mean values for all levels of the factor (Sx), the mean square due to factor (Vx), variance ratio used to measure the effect of the factor compared with the random effect due to error (F), and percent contribution to the assembly (ρ).

Table 4-16. ANOVA results for foil volume.

Source	DF	Sx	Vx	F	ρ
Punch Size (A)	2	0.72	0.36	1.18	2.48%
Relief Depth (B)	2	0.50	0.25	0.82	1.72%
Gap (C)	2	4.04	2.02	53.07	13.93%
Distance to Relief (D)	2	23.76	11.88	39.00	81.87%
TOTAL	8	29.02	3.63	--	100.00%
ERROR	4	1.22	0.30	--	--

From the ANOVA results, the insignificant factors are the Punch Size (A) and the Relief Depth (B); therefore, the most important factors found to be and Gap (C) and Distance to Relief (D), as can be deduced from the percentage contribution. With that, then the level with the lowest mean effect will be the best condition. To minimize air gaps, the optimal solution signal-to-noise is -19.60 dB ± 1.905 dB at 95% confidence. Those optimal conditions are the smallest gap distance of 0.150 inches and the smallest relief distance of 0.50 inches, levels C_3 and D_3. This new volume is found to be 225 % larger than the original foil volume of 0.0442 in^3. A sample size of 13 will allow a 95% chance of avoiding a type II error.

Optimal Condition

From the robust analysis, the best condition was found to be a medium plug with the smallest foil gap. Therefore, based on these results, sample 3 illustrates the optimal condition for the two factors found to affect the foil volume the most.

OUTPUT 6 – WELD STUDY

One of fundamental components to the annular target study is to ensure that the target ends are sealed and can withstand fission gas pressures. There were sets of targets that were TIG welded

and EB welded and then a comparison of the two processes was done as well. The difference will be in the amount of defects.

TIG WELD CRACKS

The weld cracks were found by assembling the target and TIG welding the end. Afterwards, the samples were then split along the longitudinal axis. The weld ends were etched, according to the process outlined in Chapter 3. The samples were then reviewed under the optical microscope for gaps and cracks.

Optical Microscope Results

The following figures are results from the welds. The coloring is a result from the etching to better show the surface of the material.

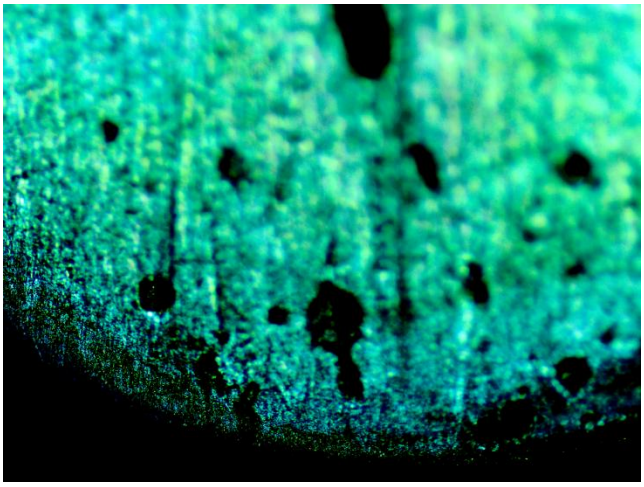

Fig. 4-28. Optical microscope review of sample 1 (smallest deformation, smallest relief depth, largest foil gap, largest distance to relief area).

The holes seen in Fig. 4-28 can be common with welds that have too much residual stress built up in the material or can be the result of the formation of gas pockets in the weld metal as a result from too much heat.

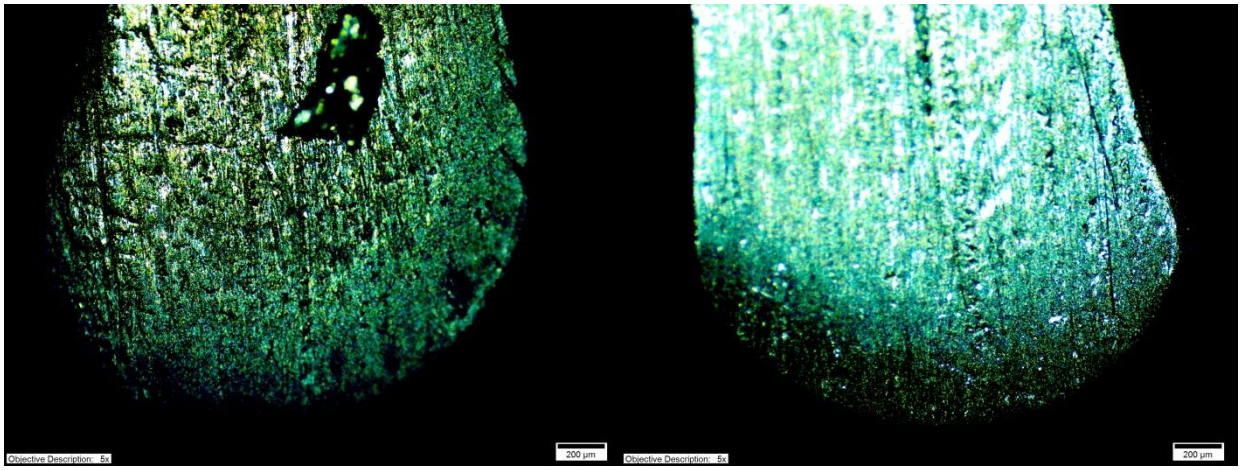

(a) (b)

Fig. 4-29. Optical microscope review of sample 2 (smallest deformation, middle relief depth, middle foil gap, middle distance to relief area).

In Fig. 4-29a, the big spot towards the top of the photo is result of the deionized water rinse, not cracks or gaps. Also, Fig. 4-29b shows a slight crack to the right of the weld.

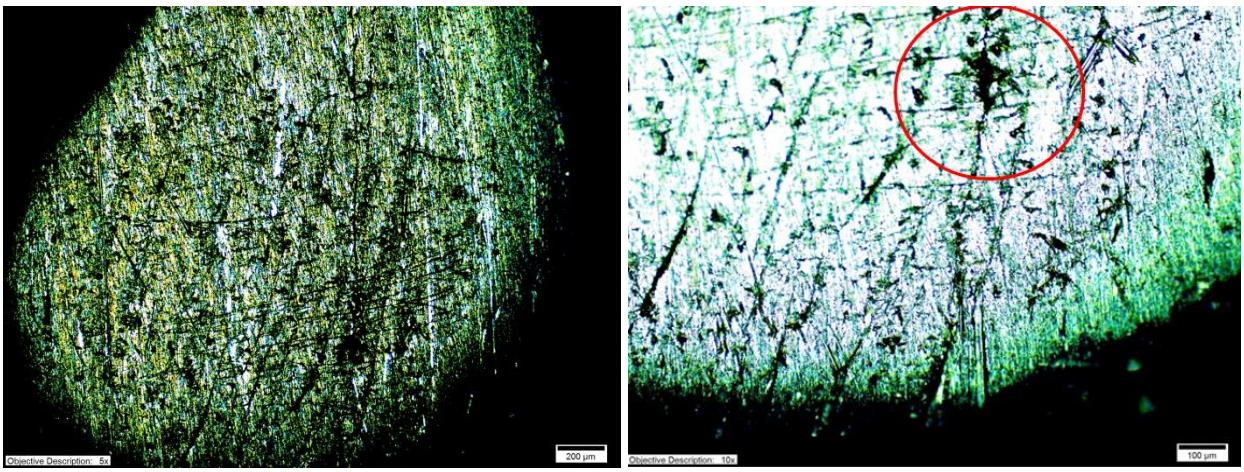

(a) (b)

Fig. 4-30. Optical microscope review of sample 3 (smallest deformation, largest relief depth, smallest foil gap, smallest distance to relief area).

The striations in Fig. 4-30a and Fig. 4-30b are from polishing and are most evident in this sample. However, with greater magnification, weld cracks become more visible; see Fig. 4-30b, towards top of picture.

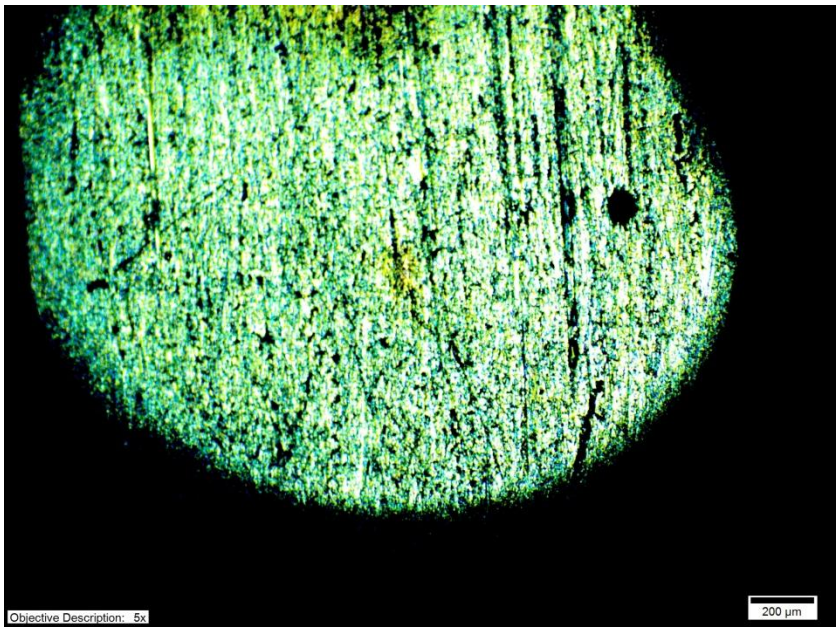

Fig. 4-31. Optical microscope review of sample 4 (middle deformation, smallest relief depth, middle foil gap, smallest distance to relief area).

In Fig. 4-31, there is one gas pore; otherwise, this was a good sample.

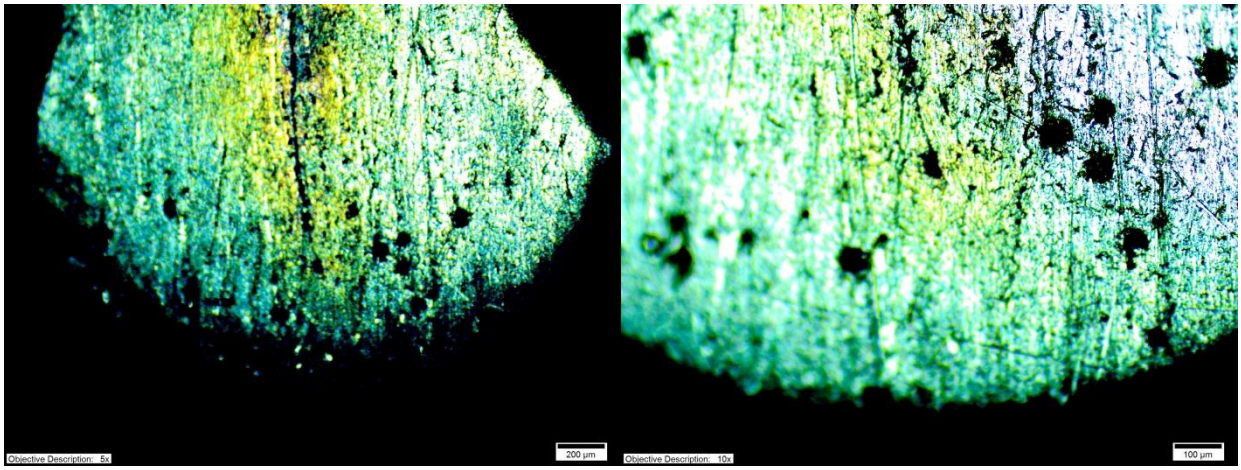

(a) (b)

Fig. 4-32. Optical microscope review of sample 5 (middle deformation, middle relief depth, smallest foil gap, largest distance to relief area).

Above, Fig. 4-32b is a magnified version of Fig. 4-32a. It is important to notice many weld pores that were most likely caused by too much heat.

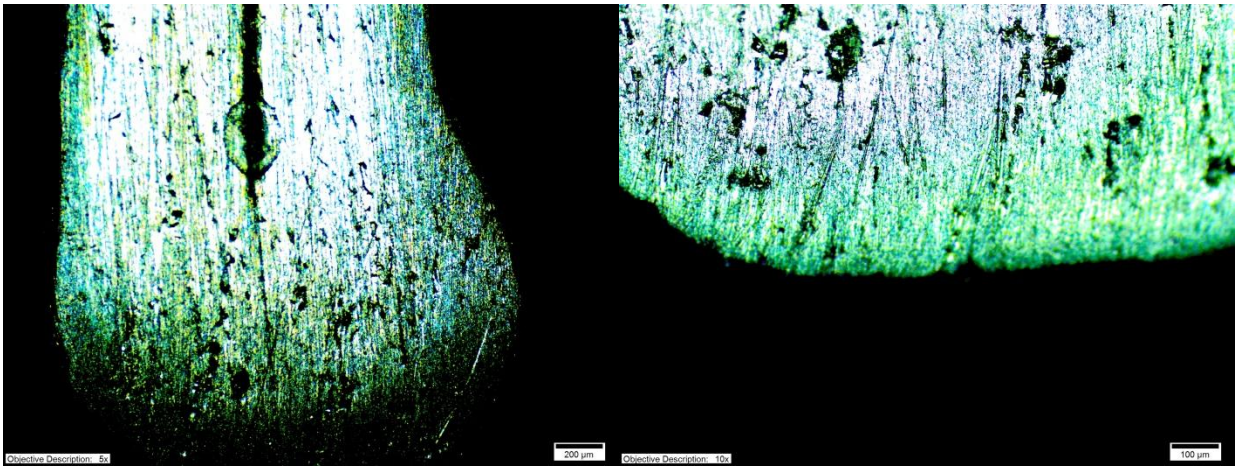

(a) (b)

Fig. 4-33. Optical microscope review of sample 6 (middle deformation, largest relief depth, largest foil gap, middle distance to relief area).

The results from sample 6 are shown in Fig. 4-33a and b. The large gap shown in Fig. 4-33a is the result of no foil. This particular sample had a longer foil to be used, but in order to cut assembly time and reduce costs, the short foil option was used instead (3.5 inches rather 5.244 inches). Again, many pores are shown in Fig. 4-33b, but the pores are much smaller and not so deep as previous experiments.

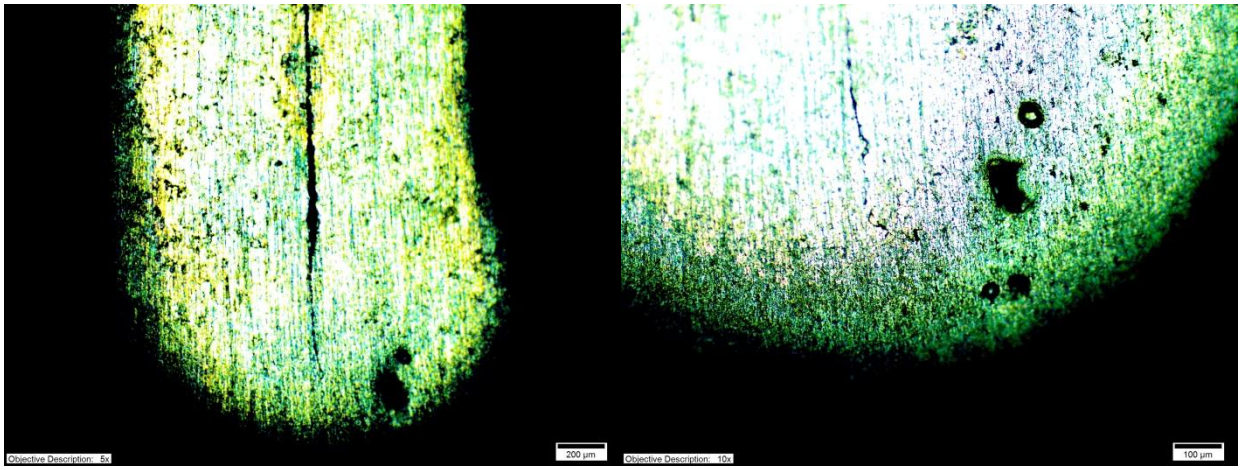

(a) (b)

Fig. 4-34. Optical microscope review of sample 7 (largest deformation, smallest relief depth, smallest foil gap, middle distance to relief area).

Sample 7 in Fig. 4-34a and b has one large gas pore, which is not an improvement to sample 6, Fig. 4-33a. However, the gap being most visible could be attributed to not enough filler material during welding.

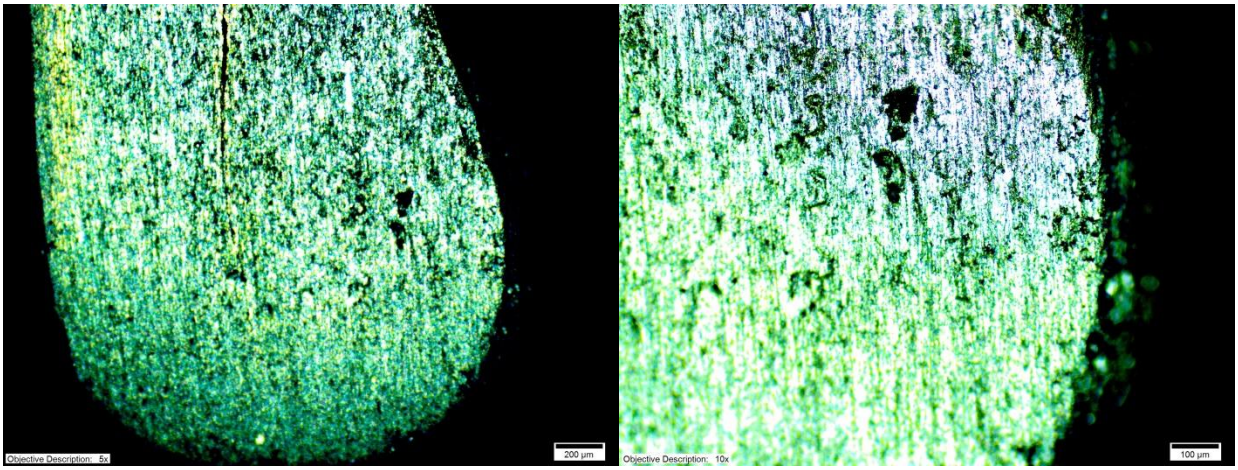

(a) (b)

Fig. 4-35. Optical microscope review of sample 8 (largest deformation, middle relief depth, largest foil gap, smallest distance to relief area).

Sample 8 was a good result but under the conditions as outlined in the robust analysis, the largest plug deformation overall did not have good results. Above, Fig. 4-35a and b show a good result.

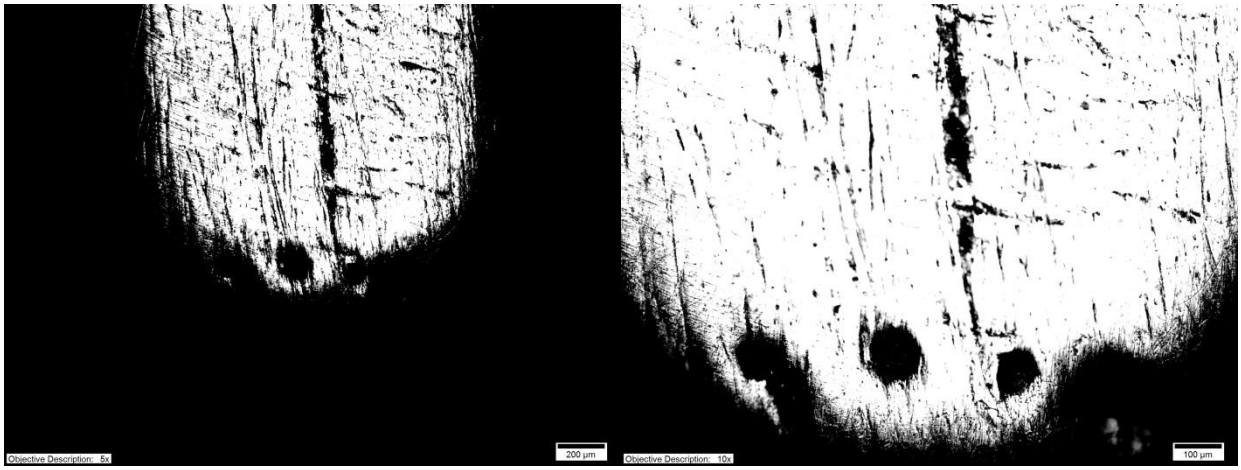

(a) (b)

Fig. 4-36. Optical microscope review of sample 9 (largest deformation, largest relief depth, middle foil gap, largest distance to relief area).

As seen before, large pores make sample 9 a poor example of welding. Above Fig. 4-36b really makes those defects visible.

Why Defects?

The main defects found with the welds were material cracks and minute weld gaps which could result from too much heat, too much residual stress from deformation, or not enough filler material during TIG welding. From the figure, ImageJ quantified the gap distance to use in the robust analysis calculations. Once heat is applied to the target, the material reacts by expanding and the crystal structure changes as well. As the material cools, cracks can appear on the surfaces, such as those near the foil. If the foil is not sealed properly, the target has failed. Material that has built up residual stresses will eventually lead to cracking once succumbed to heat.

Robust Analysis Tables

The analysis done here was to discover which targets had the best welds with the fewest gaps and cracks. Therefore, the quality characteristic will be "the smaller, the better." Table 4-17 provides the measurements made with ImageJ and converted to micrometers. If the measurements are too small, those will not be suitable and the calculations will not be accurate. Therefore, large values were used for calculations.

Table 4-17. Signal to Noise calculations for weld pores.

Quality Characteristic: the SMALLER the better
Overall Average: -41.96 dB
Experiments/Level: 9

Measurements in μm

L-9	Factors Tested at Level 1, 2, and 3								
Trial #	**Punch Size (A)**	**Relief Depth (B)**	**Gap (C)**	**Distance to Relief (D)**	**Meas 1**	**Meas 2**	**Meas 3**	**Meas 4**	**S/N**
1	1	1	1	1	189.024	141.51	124.888	151.8073	-43.7290
2	1	2	2	2	200.959	147.672	174.3155	160.9938	-44.7165
3	1	3	3	3	85.959	85.959	85.959	85.959	-38.6858
4	2	1	2	3	66.408	66.408	66.408	66.408	-36.4444
5	2	2	3	1	59.548	66.068	75.24	55.154	-36.1841
6	2	3	1	2	120.219	120.219	120.219	120.219	-41.5995
7	3	1	3	2	148.219	103.966	126.0925	126.0925	-42.0801
8	3	2	1	3	127.84	84.145	105.9925	105.9925	-40.5968
9	3	3	2	1	540.3	416.395	478.3475	478.3475	-53.6311
									-41.9630

From the table above, the average signal-to-noise result was found to be -41.96 dB. Next, the mean effect of each factor is found and shown in Table 4-18. Highlighted values are best results for a later table.

Table 4-18. Mean effect of each factor for weld pores.

	Punch Size (A)	Relief Depth (B)	Gap (C)	Distance to Relief (D)
1	-42.3771	-40.7512	-41.9751	-44.5148
2	-38.0760	-40.4991	-44.9307	-42.7987
3	-45.4360	-44.6388	-38.9834	-38.5757
Diff	7.3600	4.1397	5.9473	5.9391

Once the mean effect of each factor is known, a response graph can be made of the average signal to noise for each factor and their corresponding levels. See Fig. 4-37 for the response graph. To get the smaller-the-better result, the valued point will be smallest value in relation to the average signal-to-noise, which is represented as a black horizontal line. In this case, the best result combination will contain either: A_2, B_2, C_3, and/or D_3.

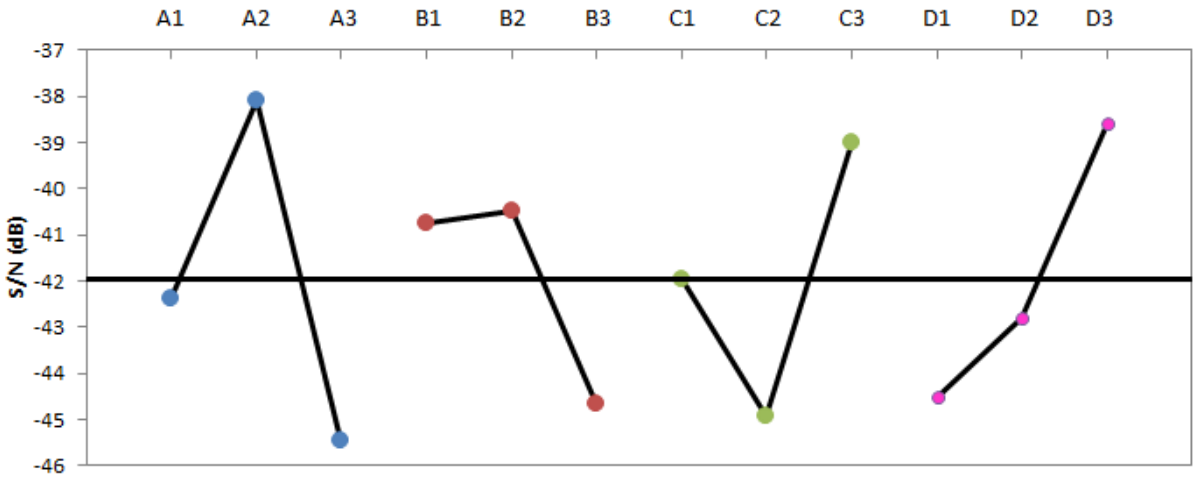

Fig. 4-37. Response graph for weld pores.

Next, using Table 4-18, the analysis of variance table may be completed. The variance of each factor is calculated and then a percentage calculated as well. See Table 4-19 for complete ANOVA results. Here, the column headers are the degrees of freedom (DF), total sum of squares of the deviation from the mean values for all levels of the factor (Sx), the mean square

due to factor (Vx), variance ratio used to measure the effect of the factor compared with the random effect due to error (F), and percent contribution to the assembly (ρ).

Table 4-19. ANOVA results for weld pores.

Source	DF	Sx	Vx	F	ρ
Punch Size (A)	2	82.03	41.01	5.08	36.71%
Relief Depth (B)	2	32.31	16.16	1.00	14.46%
Gap (C)	2	53.06	26.53	3.28	23.74%
Distance to Relief (D)	2	56.05	28.03	3.47	25.08%
TOTAL	8	223.45	27.93	--	100.00%
ERROR	2	32.31	16.16	--	--

From the ANOVA results, the insignificant factor is the Relief Depth (B); therefore, the most important factors found to be Punch Size (A), Gap (C) and Distance to Relief (D), as can be deduced from the percentage contribution. With that, then the level with the lowest mean effect will be the best condition. For the weld cracks and pores, the optimal solution signal-to-noise is -31.71 dB ± 5.285 dB at 95% confidence. Those optimal conditions are the medium punch size deformation of 0.010 (plug size 1.047 inches), the smallest gap size at 0.150 inches and the smallest distance to the relief area of 0.500 inches, levels A_2, B_3 and D_3. A sample size of 13 will allow a 95% chance of avoiding a type II error.

Optimal Condition

The best condition for welds was found at a medium plug size of 1.047 inches, smallest gap size of 0.150 inches and the smallest distance to the relief area of 0.500 inches.

EB WELD STUDY

Sealing the target ends is crucial so that the uranium foil is contained during irradiation; thus, preventing leakage or even contamination of the radioisotopes. TIG welding is acceptable if

producing fewer than 1000 targets per year. However, for high scale production, a more precise method may be warranted in order to produce more targets faster. Electron Beam welding (EBW) is a fusion welding process in which a beam of high-velocity electrons is applied to two materials to be joined. Often, the weld is performed under vacuum conditions to prevent dissipation of the electron beam. With the target under vacuum, weld flaws are less likely to appear compared to contaminants affecting TIG welding. Shown previously, Fig. 3-10a and Fig. 3-10b show a representation of the weld itself as well as a target end sample that was EB welded. The weld is clean, precise and does not leave a mound of welded material, known as a hump, around the edges that is visible with the TIG welded targets. All samples were examined using a Nikon SMZ-10 stereomicroscope with a 115 V AC Fiber Optic Light source. The sample photos were taken with a Polaroid digital microscope camera with a HRD-100-CMT lens.

Like the TIG welded samples, the EB targets were difficult to weld due to contaminants between the tubes. Contaminants were but not limited to paper particles, dust, oxide layers, leftover lubricant, leftover cleaning substance, etc. However, also like the TIG welded study, a neutral pH fluid can be used to clean the targets and a volatile liquid chosen to effectively evaporate all traces. Acetone is a widely used laboratory cleaner and can ideal for this situation. Contaminants were also somewhat a problem for EB welding, even though the target was under a vacuum during the weld process. However, the targets still sealed after three passes on each end. A possible explanation might be that the trapped air expands under extreme temperatures and is forced to escape out the second weld end. From the original 9 target matrix set, all targets were welded and sectioned as shown below.

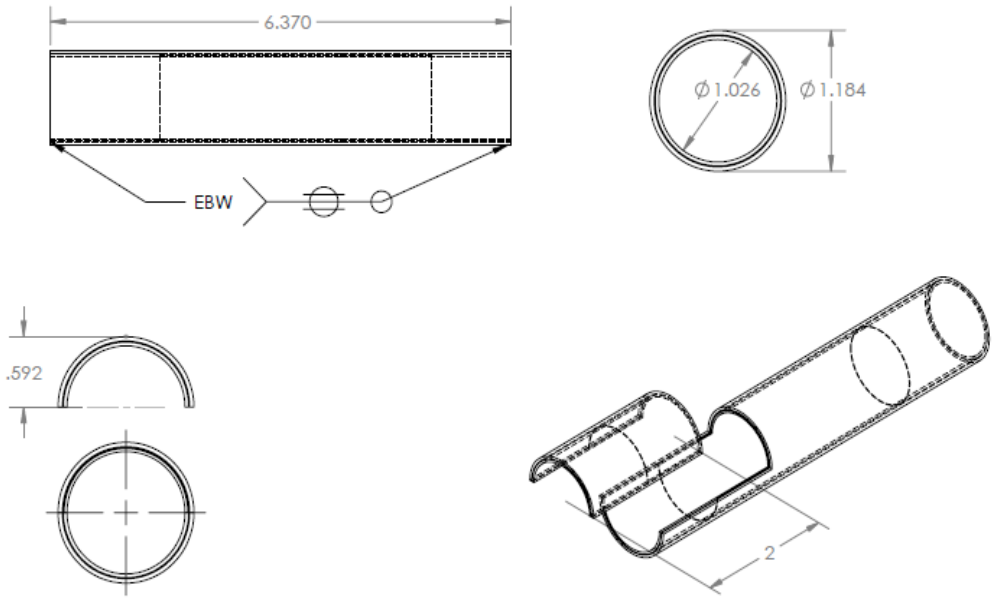

Fig. 4-38. Weld study sectioning.

Preliminary Results

Before the entire matrix set was welded, a preliminary check was done to see how the targets would handle sectioning as well as how thick the weld was. The first target (sample 6) was EB welded at Y-12 by their technician. A very interesting phenomena was seen – one end showed a perfect gap that rose the weld up. This gap was only seen on one end, probably the last end welded. This caused the weld to extend past the thickness of the target and overhand off the side.

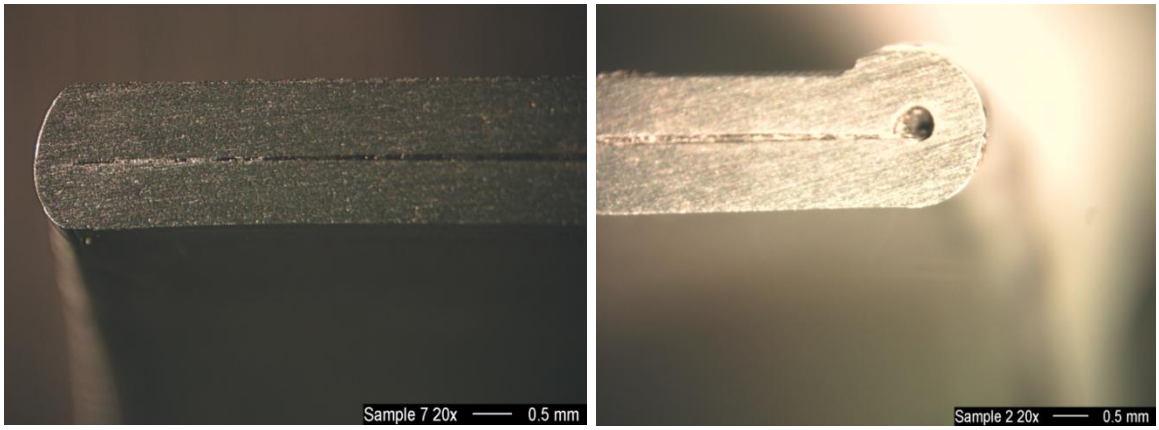

(a) First end welded (b) Second end welded.

Fig. 4-39. Sample 6 (a) EB welded at Y-12, notice the large air gap in (b).

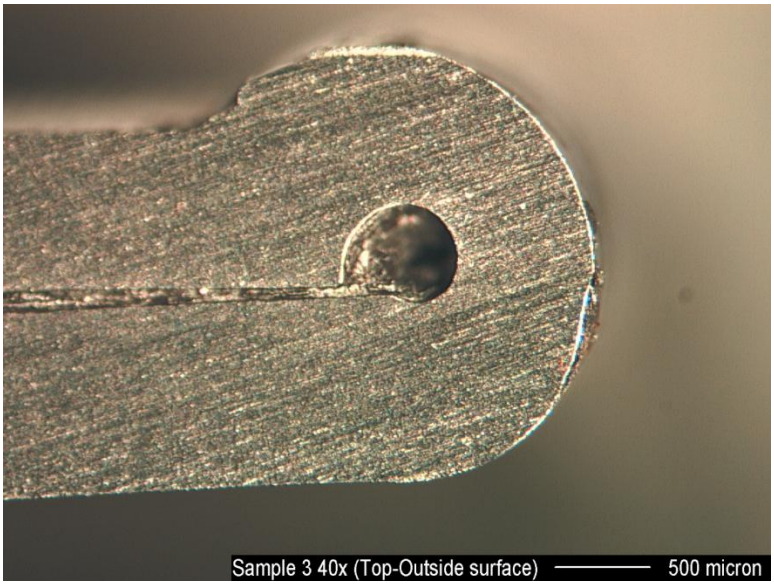

Fig. 4-40. Zoomed shot of Fig. 4-39 (b) of the air gap.

Experimental Results

Initially, it was not determined if the air gap would be prevalent in every target. The weld bead for this particular target was quite wide; and perhaps, the wide bead would encouraged the trapped air to rise towards the surface.

It is important to note that the samples may look as if the tubes are beginning to separate. This is normal due to the sectioning. Due to the elastic/plastic design scenario, the tubes are naturally supposed to separate as the target is disassembled.

Samples without air gaps included samples 1, 2, and 7. All other samples had one very small air gaps. Unlike TIG welded, there were no multiple gaps throughout the welds. The air gap here only existed where the weld and tubes come into contact. Below, Fig. 4-41 through Fig. 4-51 are the results from the EB welds. Pictures were taken on a Nikon stereomicroscope, courtesy of Oak Ridge National Laboratory.

Sample 1

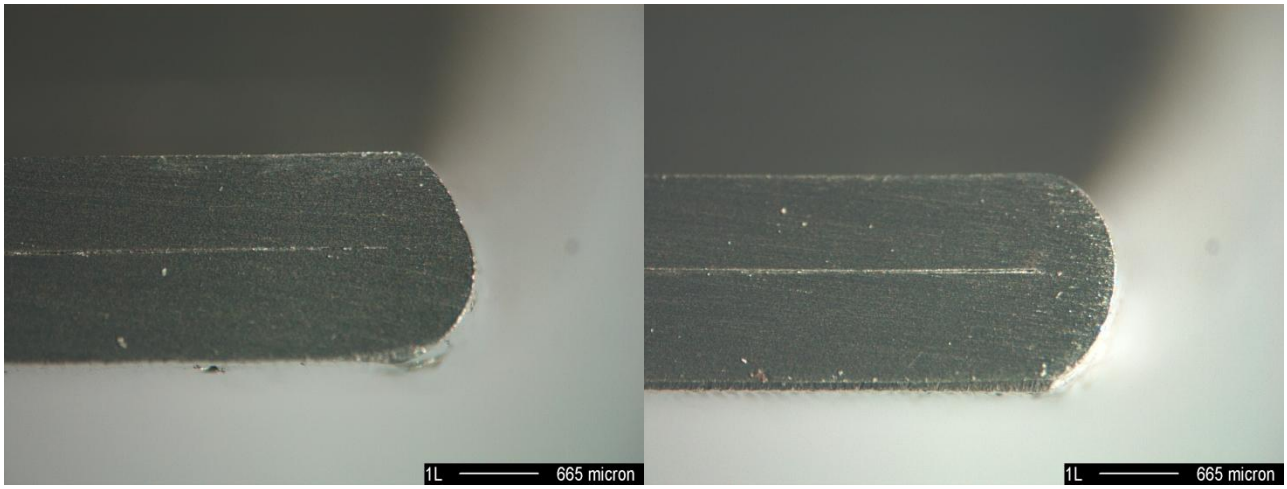

(a) (b)

Fig. 4-41. Sample 1 with shots of both welded ends, (a) and (b).

Sample 2

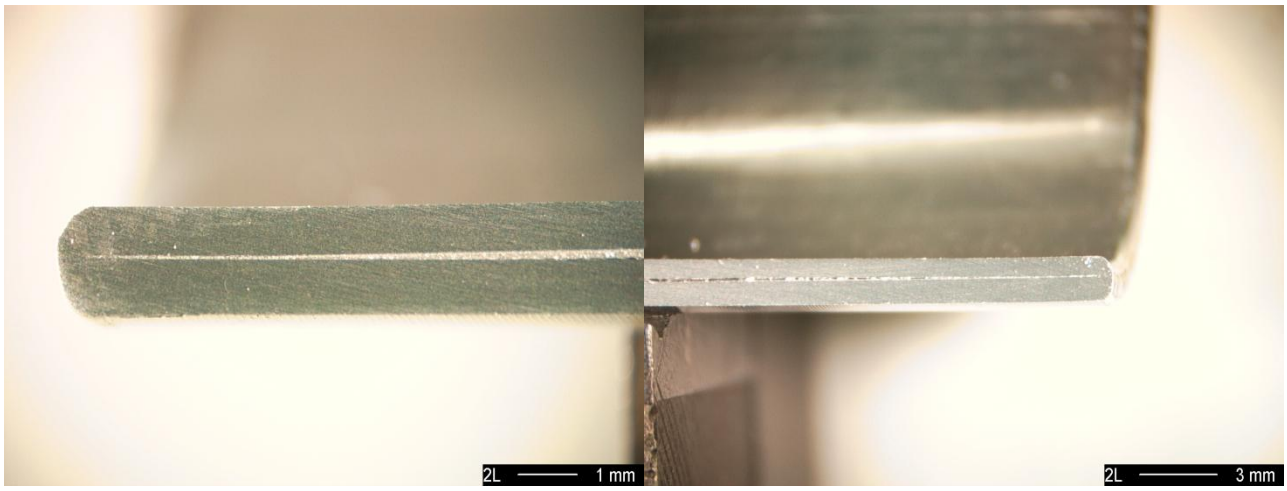

(a) (b)

Fig. 4-42. Sample 2, shots from both welded ends, (a) and (b).

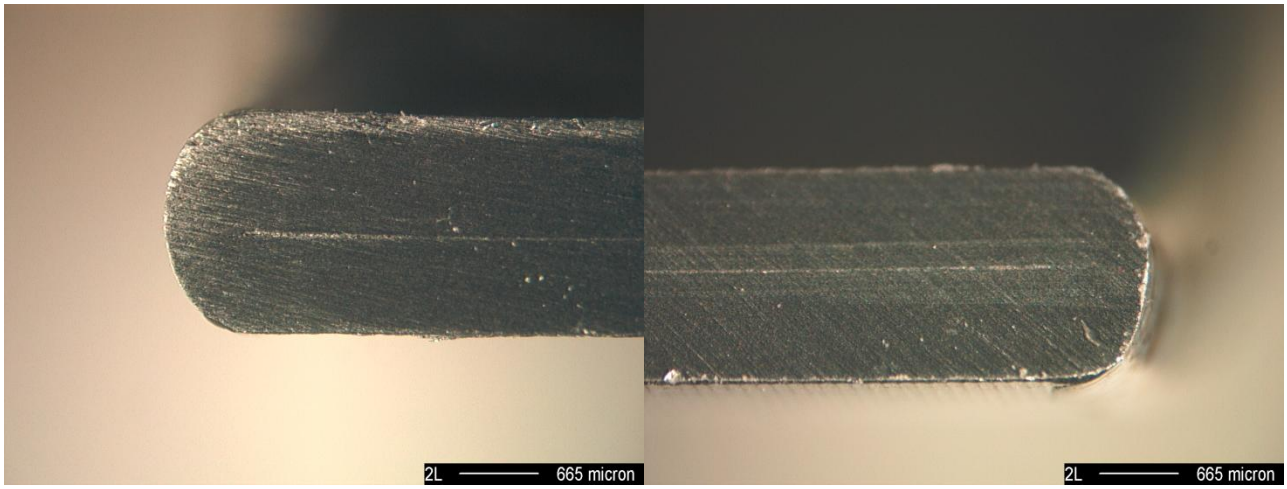

(a) (b)

Fig. 4-43. Sample 2, zoomed shots from Fig. 4-42 (a) and Fig. 4-42 (b).

Sample 3

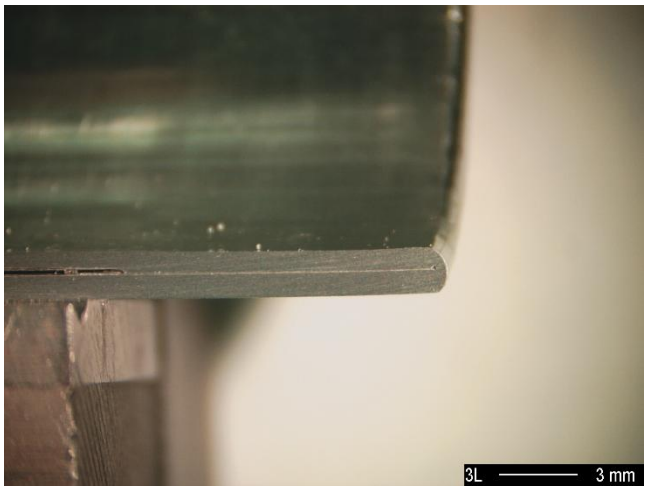

(a)

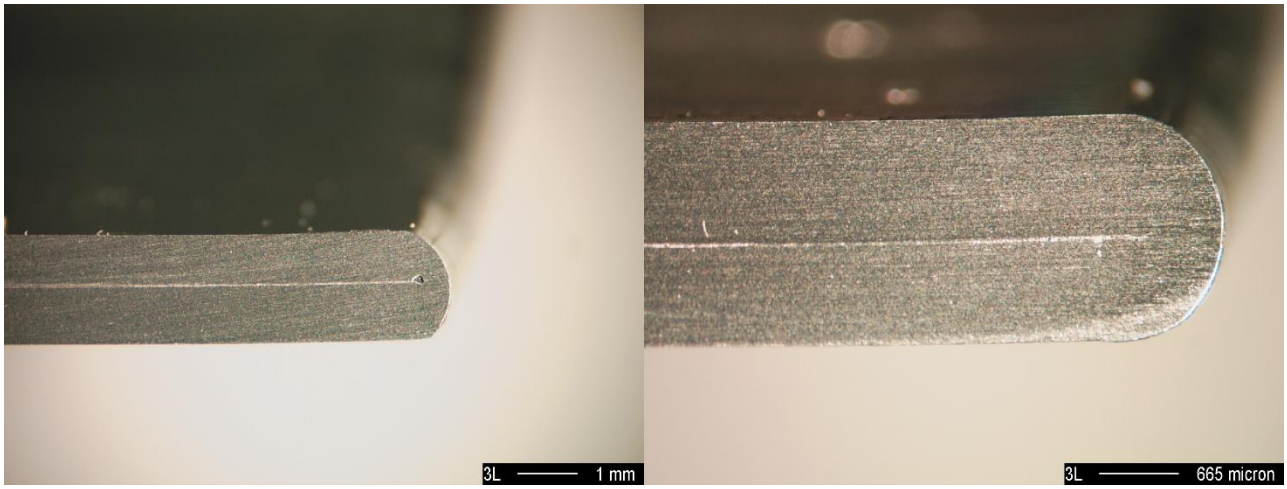

(a) (b)

Fig. 4-44. Sample 3 (a), welded ends, (b) and (c). Notice the small air gap (b).

Sample 4

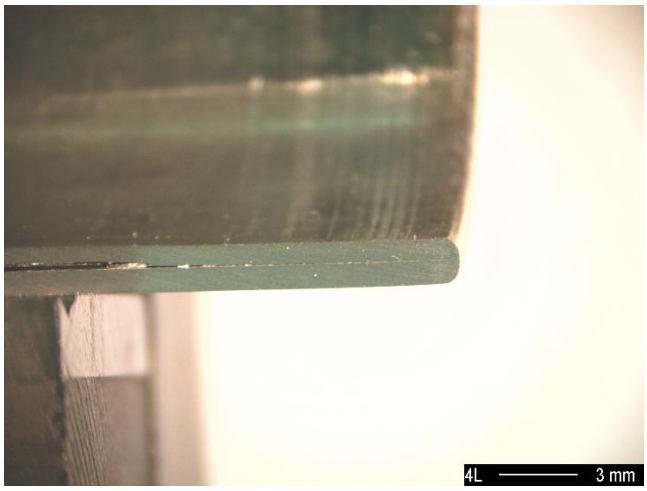

(a)

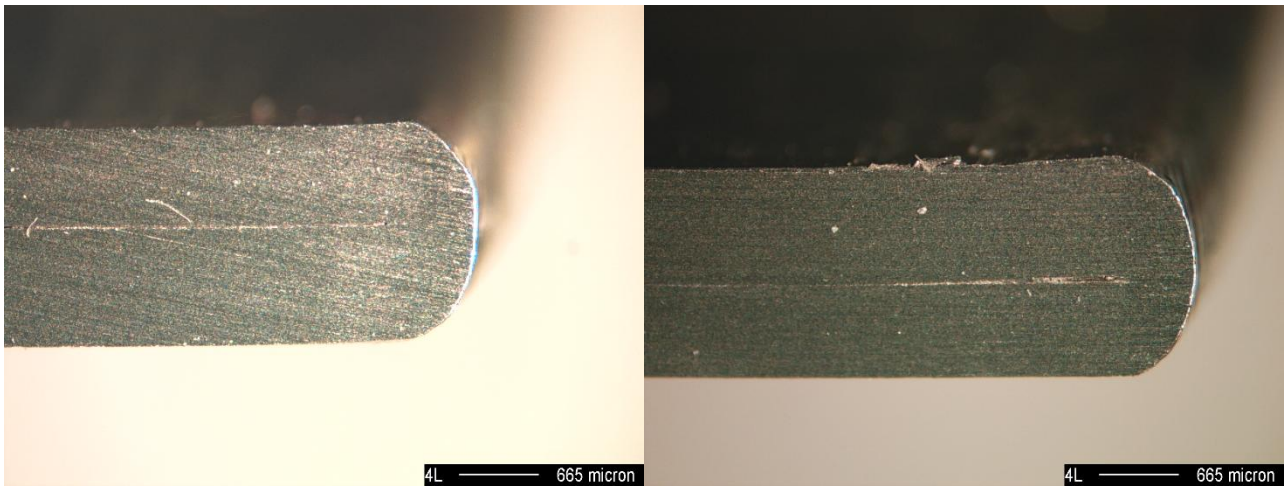

(a) (b)

Fig. 4-45. Sample 4 (a) with zoomed shots of the EB welds of both ends, (b) and (c). No air gaps present.

Sample 5

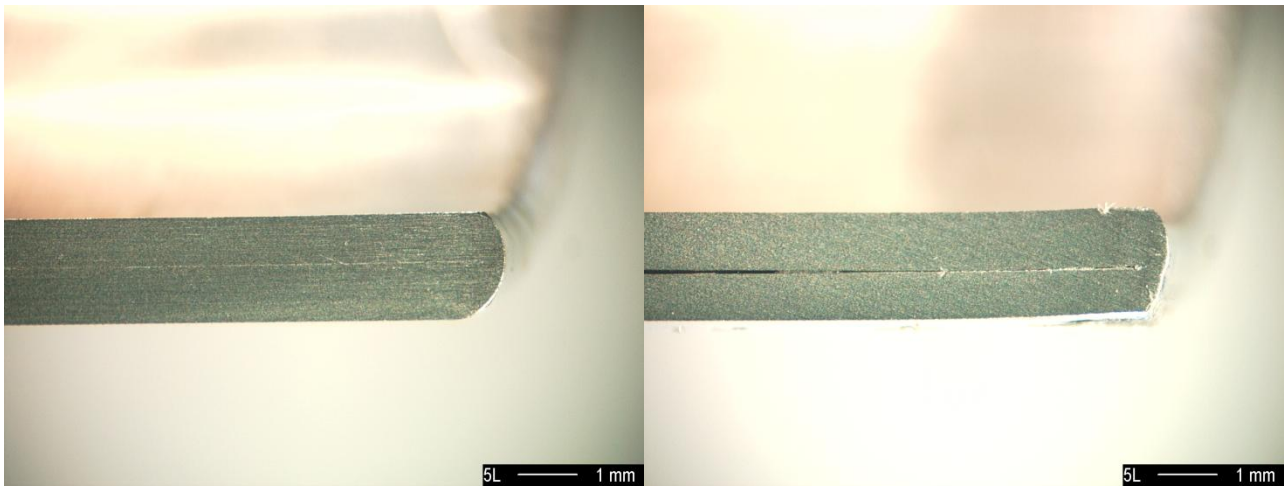

(a) (b)

Fig. 4-46. Sample 5, with shots from both ends of welded target, (a) and (b).

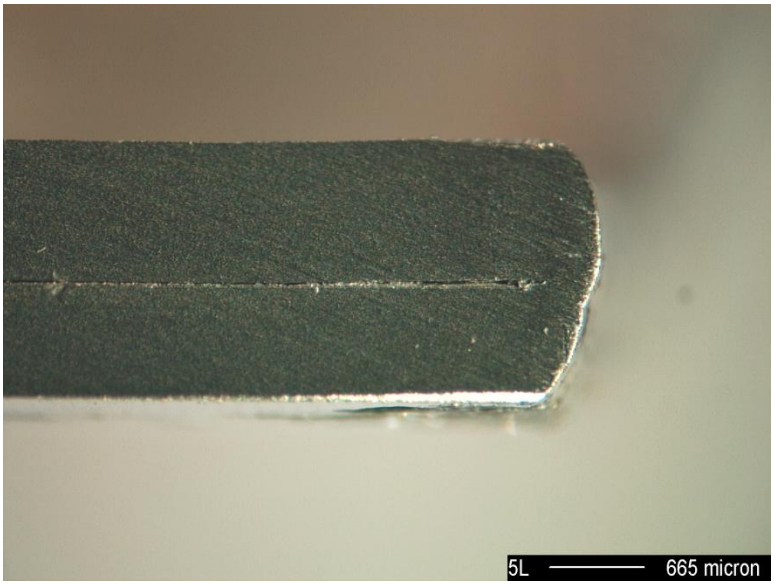

Fig. 4-47. Sample 5, zoomed shot of Fig. 4-46 (b).

Sample 7

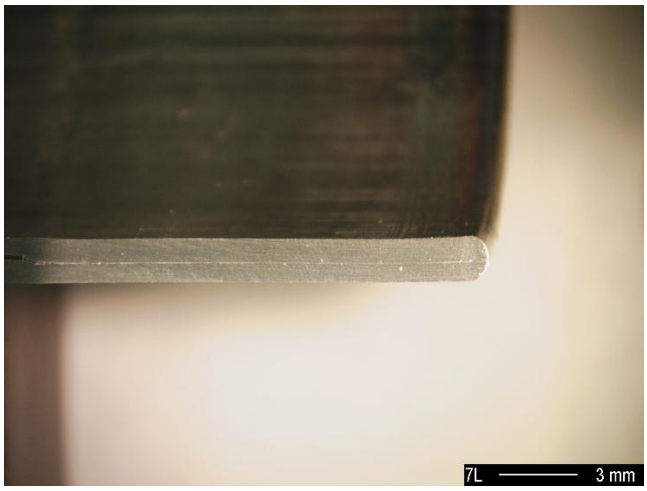

(a)

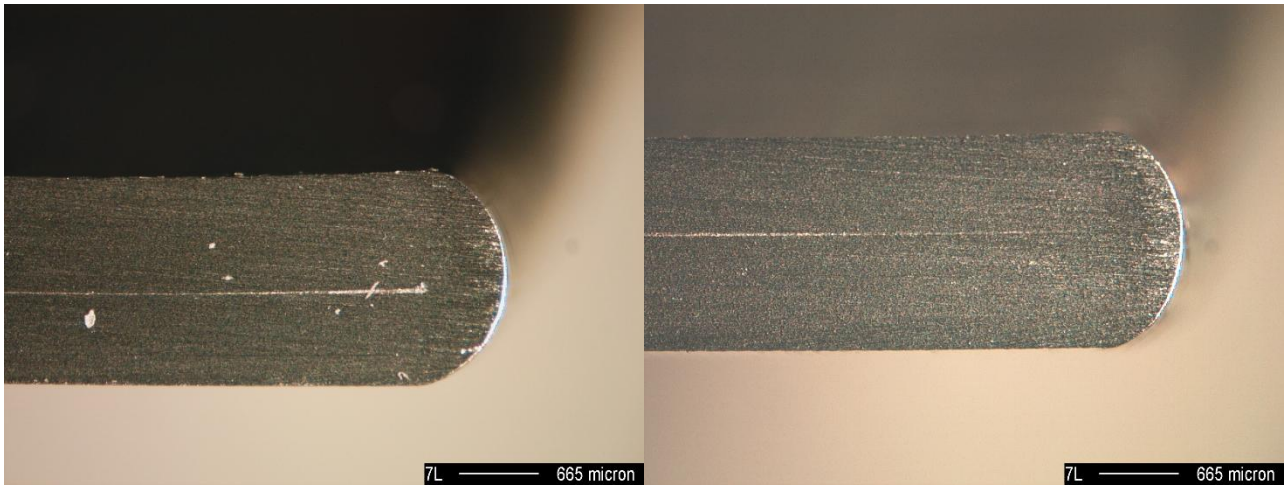

(b) (c)

Fig. 4-48. Sample 7 (a), with zoomed shots of the EB welds of both ends, (b) and (c). No air gaps.

Sample 8

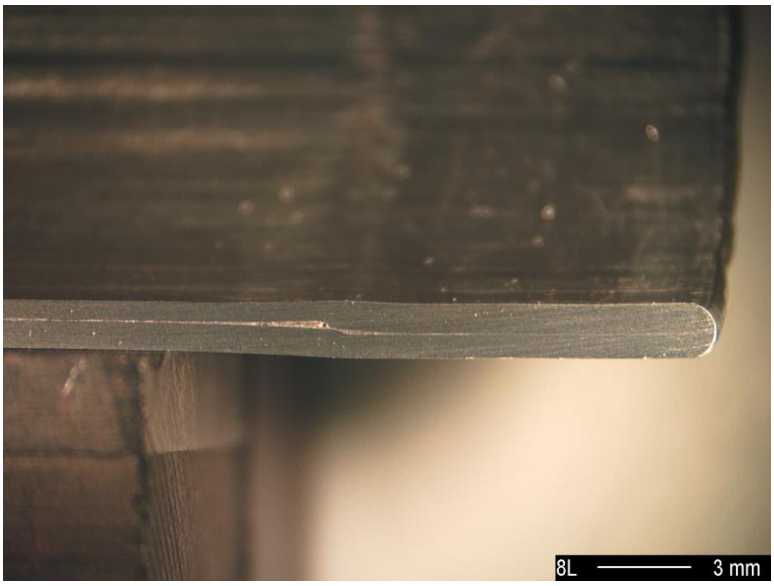

(a)

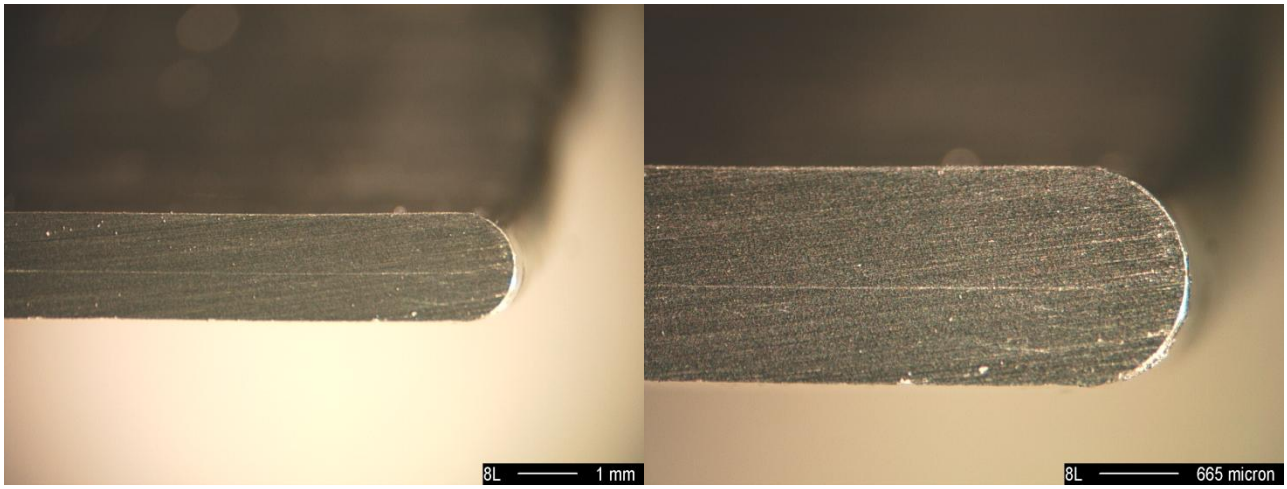

(b) (c)

Fig. 4-49. Sample 8 (a) with zoomed shots of EB welds, (b) and (c).

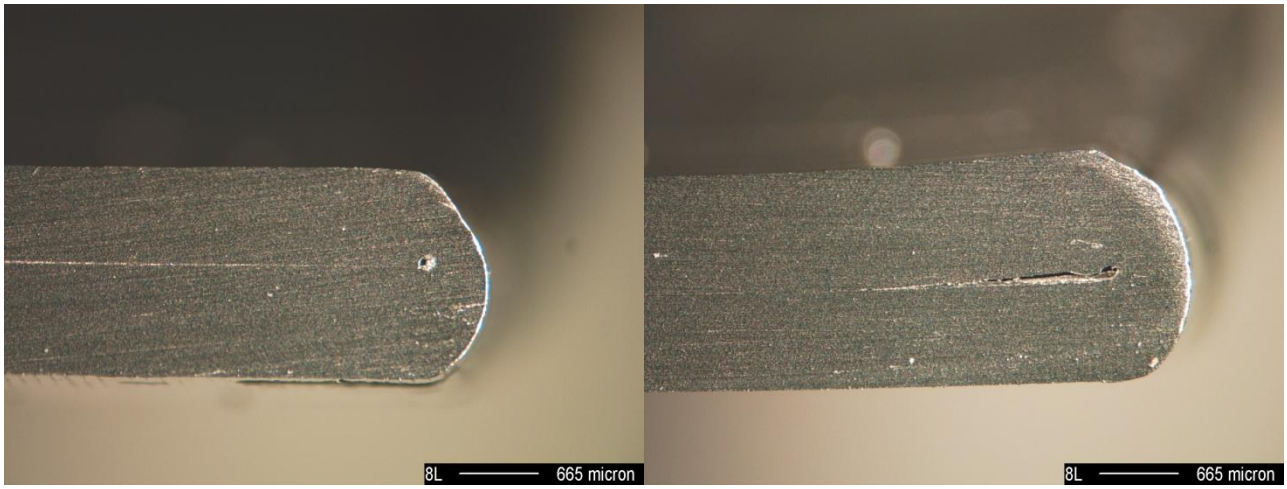

(a) (b)

Fig. 4-50. Sample 8, additional shots of EB welded ends, (a) and (b).

Sample 9

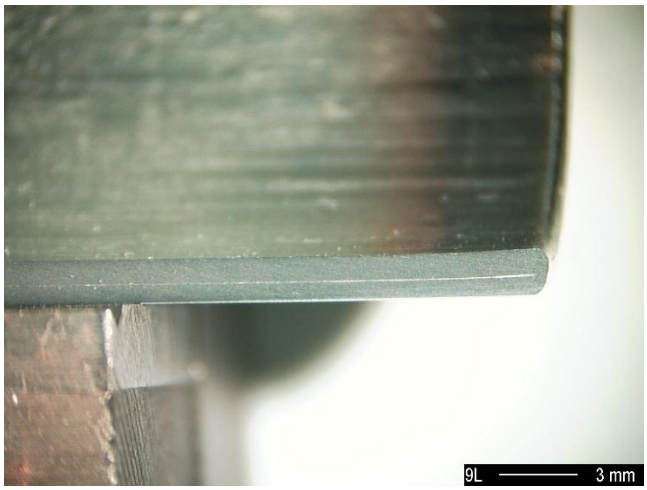

(a)

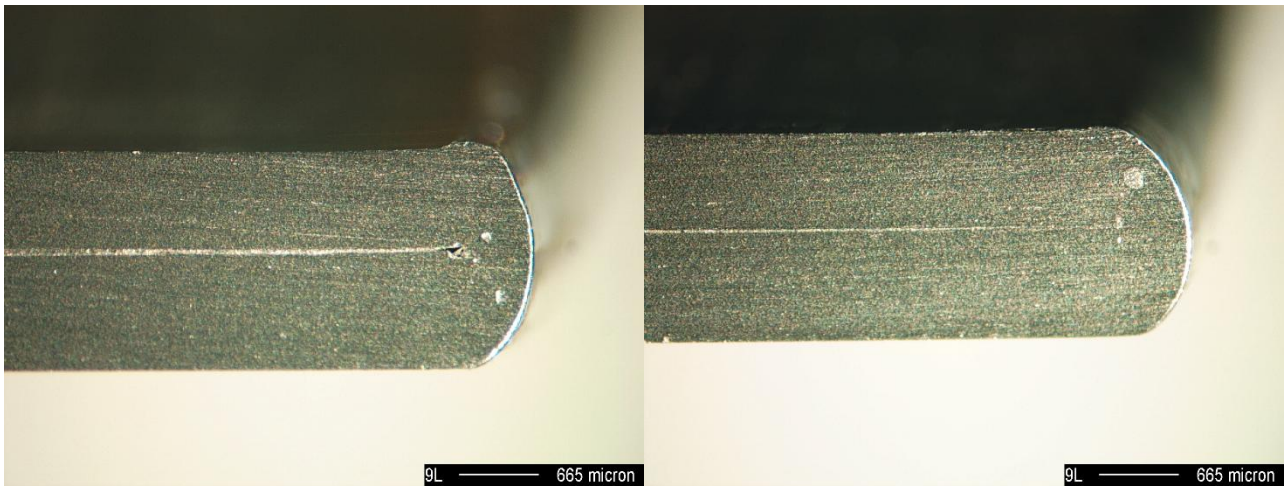

(b) (c)

Fig. 4-51. Sample 9 (a), with welded ends, (b) and (c). Note the small air gap (b).

Clearly, the targets welded at ORNL were of much better quality than the one welded at Y-12. With only one very small gap, it is speculated that this gap may not be attributed to the welds, but rather to the distance already present from the deformation of the tubes. These available spaces could be room for the fission gas expansion and may be found to be favorable. Every weld carefully checked visually from ORNL was clean and sealed the ends. The only concern that might be an issue is the EB welds strength or rather, the thinness – are the welds strong enough to within the fission gas pressure? This is where the TIG welded samples showed large weld thickness.

CONCLUSION OF ROBUST ANALYSIS

Using the results from each output, the summary of the outputs is shown in the following table, Table 4-20.

Table 4-20. Summary of outputs.

Gap Defects	A_2 C_3
Weld cracks/gaps	A_2 C_3 D_3
Forming pressure	A_2
Hoop stress	A_2 B_3 C_1
Longitudinal stress	A_2 B_2 D_1
Foil Volume	C_3 D_3

It can be assumed that the following conditions will produce the best target at the optimal condition: A_2 (1.047 inches deformation), B_2 (0.007 inches relief depth), C_3 (0.150 inches foil gap) and D_3 (0.500 inches distance to relief area). The sample that carries these four conditions was not part of the original L-9 experimental samples, but was machined and assembled. The drawings for the optimal solution match those of sample 8. The drawings for the inner and outer tubes are provided in Fig. 4-52 and Fig. 4-53. For best results, EB weld target ends.

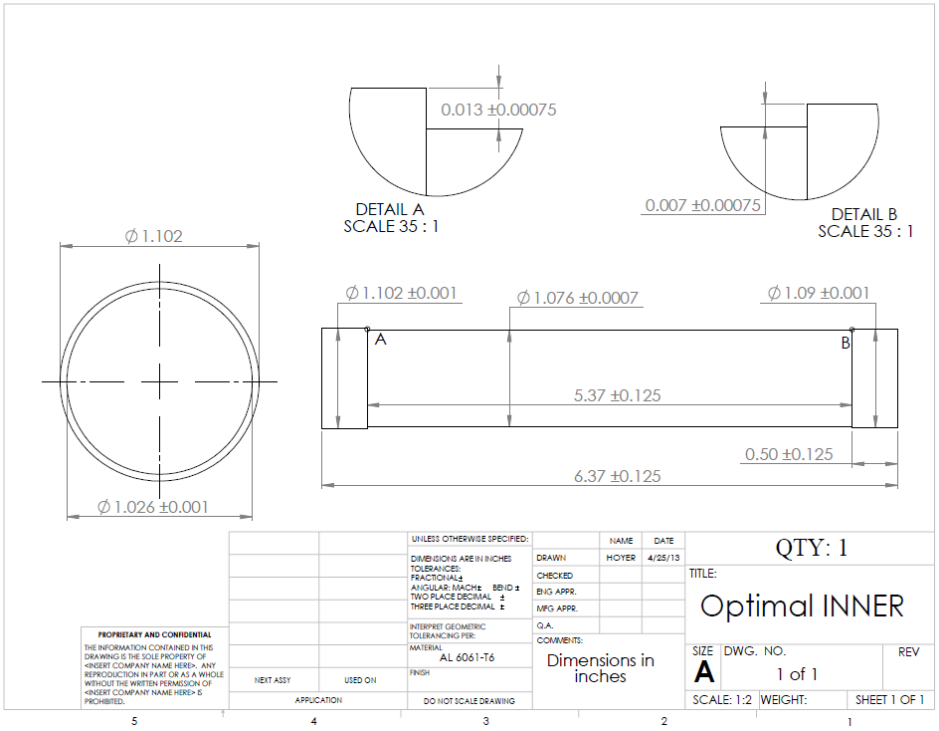

Fig. 4-52. Detail part drawing of optimal inner tube for target assembly.

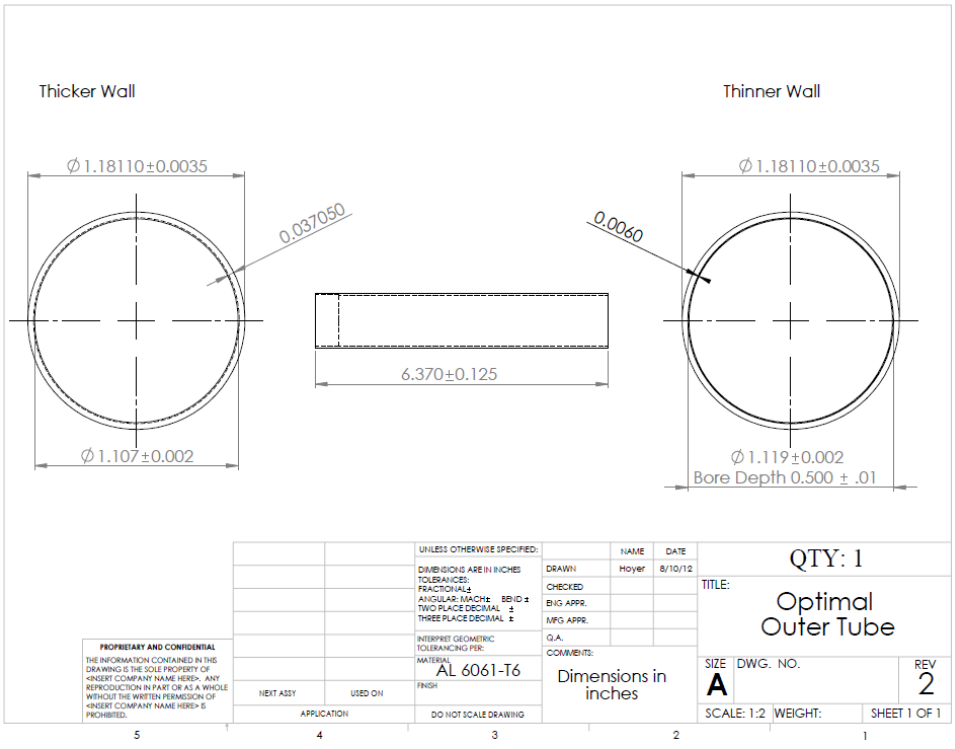

Fig. 4-53. Detail part drawing of optimal outer tube for target assembly.

RELIABILITY ANALYSIS

Once the optimal conditions are found, how reliable will this design be? The machining tolerances were added with diameter tolerances at 0.001 inches. However, are diameter tolerances of 0.001 reasonable? Using Monte Carlo simulation, the number of samples and range of diameters may be varied to find failure rate of target deformation based on drawing pressure equations used in Eq. (2-1). The main goal for reliability analysis is to determine the failure rate of the targets from the tolerances, as well as determining the reliability of the process during any point during its operational lifecycle.

Accelerated Testing

The goal for Monte Carlo simulations is to simply find the acceptable diameter tolerances that prevented target rupture as well as no deformation at all due to large tube diameters. The optimization code was designed to vary the range of tolerances in order to find zero failure rates. Table 4-21 provides the results found through this process. Computational time was insignificant. The results will help validate the deformation process for elastically deformed outer tubes. As part of the robust analysis, strict reliability exploration is applied in order to determine the most realistic estimate.

Table 4-21. Accelerated test results with failure rates and acceptable target tolerances.

Distribution	Plugs Size	Number of Samples	Failure Rate (%)	Average Pressure (MPa)	Std Pressure (MPa)	Tolerance Inner Tube (inches)	Tolerance Outer Tube (inches)
NORMAL	1.046	10,000	0.00%	93.50	18.72	+0.042/-0.036	+0.042/-0.045
	1.047	10,000	0.00%	96.02	19.77	+0.042/-0.042	+0.048/-0.050
	1.048	10,000	0.00%	98.44	21.97	+0.043/-0.043	+0.051/-0.055
EXPONENTIAL	1.046	10,000	0.00%	82.78	8.00	+0.040	+0.056
	1.047	10,000	0.00%	84.89	8.27	+0.036	+0.067
	1.048	10,000	0.00%	87.25	8.26	+0.041	+0.053
LOGNORMAL	1.046	10,000	0.00%	108.85	20.07	+0.013/-0.089	+0.015/-0.085
	1.047	10,000	0.00%	106.28	13.00	+0.008/-0.053	+0.010/-0.060
	1.048	10,000	0.00%	114.34	21.13	+0.016/-0.092	+0.016/-0.096

Each accelerated test produces a histogram plot of the samples. Below, Fig. 4-54a, b and c show the histogram plots for the three different plug sizes that were used during the robust analysis testing. The distribution used first was the Normal distribution.

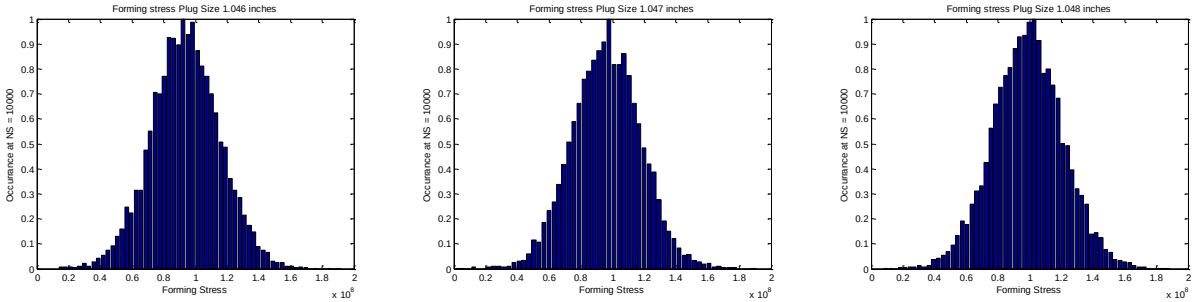

(a) (b) (c)

Fig. 4-54. Histograms of target forming pressure, using plug size 1.046(a), 1.047(b) and 1.048(c) inches and Normal distribution.

From both the histogram plots and the reliability table above, the deformation pressure tends to average near 96.0 MPa, with best tolerance results matching results from the plug size 1.046 inches. Next, the test was iterated again using the Exponential distribution. Below, Fig. 4-55a, b

and c show the histogram plots for the three different plug sizes that were used during the robust analysis testing.

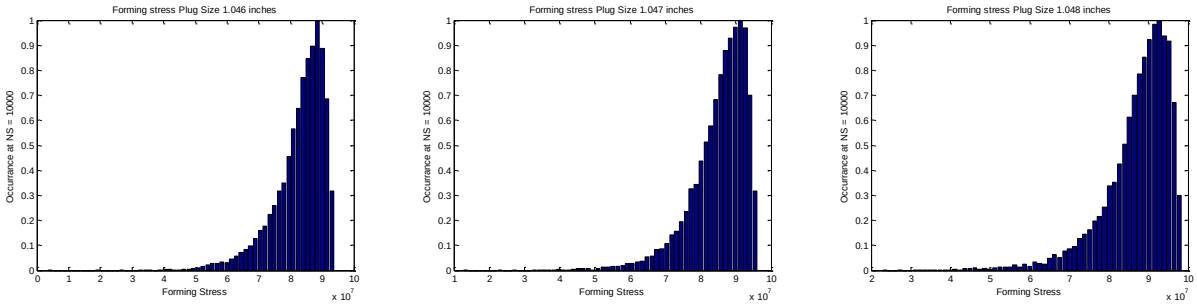

(a) (b) (c)

Fig. 4-55. Histograms of target forming pressure, using plug size 1.046(a), 1.047(b) and 1.048(c) inches and Exponential distribution.

From both the histogram plots and the reliability table above, the deformation pressure averaged near 84.97 MPa which was lower than the Normal distribution results. Best tolerance results matched those results from the plug size 1.048 inches. Next, the test was iterated once again using the Lognormal distribution. Below, Fig. 4-56a, b and c show the histogram plots for the three different plug sizes that were used during the robust analysis testing.

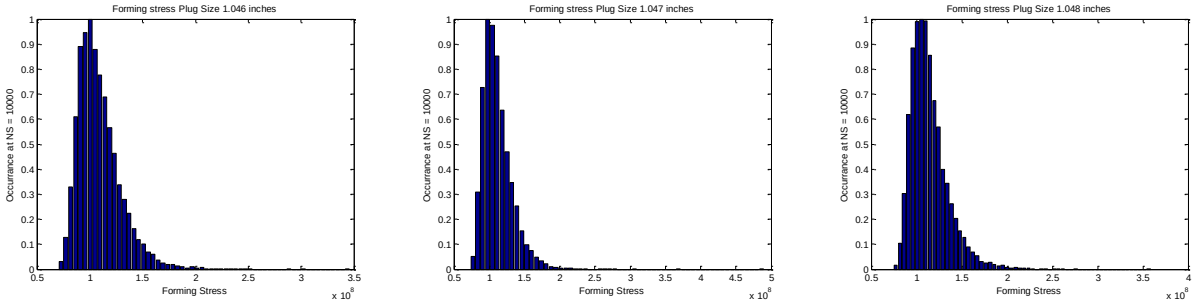

(a) (b) (c)

Fig. 4-56. Histograms of target forming pressure, using plug size 1.046(a), 1.047(b) and 1.048(c) inches and Lognormal distribution.

From both the histogram plots and the reliability table above, the deformation pressure averaged near 109.82 MPa which was highest of the three distribution results. Best tolerance results matched those results from the plug size 1.047 inches.

Note that the exponential distribution found only unilateral tolerances whereas both normal and lognormal distributions found bilateral tolerances. The exponential distribution finds values that are above the expected values; therefore, there exist very few samples around the nominal value results. From these three distributions, the lognormal was found to have the most conservative results; therefore, better tolerance results. Perhaps a diameter tolerance of 0.001 inches is somewhat extreme based on the results. A better solution would to adjust the diameter tolerances to 0.005 inches. The tolerances may be loosened but still ensure no failure during deformation. The drawing pressure range was designated as based on the outer tube deformation requirements at a maximum pressure at yield strength (310 MPa) to 10 MPa, to guarantee some substantial deformation. The nominal values were listed as the following: 1.026 inches inner tube internal diameter and 1.181 inches outer tube external diameter.

These results are merely estimates. The drawing pressure equations used are for single walled tubes, not accurate for two nested tubes. Based on necessary deformation in order to disassembly, the inner tube must be plastically deformed and this phenomenon is not evident through accelerated testing. The MATLAB code for the reliability testing is available in Appendix J: Reliability Testing.

FMEA Results

In addition to accelerated testing, failure mode and effect analysis (FMEA) was also used in determining a subjective reliability for the assembly rig. Obviously, the process must be safe for the operator and environment. Also, the process must correctly deform the targets and not destroy the target. Some of the topics that were addressed in the FMEA analysis were the pump itself, plastic parts, the targets and lastly the draw plugs. Typically, there will not be catastrophic

failure during this process, but reoccurring issues may become frustrating and should be addressed if those issues should exist. Table 4-22 below shows the possible failure modes due to one piece of equipment. Notice that the highest risk level exist with the pump low on fluid and possible surface galling due to lack of lubrication – both of which may be prevented with proper maintenance. Most features were found to have low severity as well as low frequencies.

Table 4-22. Failure modes and effect analysis for assembly rig.

1. Functional or Equipment Identification	2. Functional or Equipment Purpose	3. Failure Modes	4. Failure Mechanism	5. Failure Detection	6. Failure Compensation	7. Failure Effects	8. Severity	9. Frequency	10. Risk Level	11. Preventive Measures
1.0 Pump	Drives plug during deformation	1.1 Pressure Leak	Inadequate prop size	Inspection	None.	No deformation	1	3	3	Check for leaks
		1.2 Low on Fluid	Operator Error	Screeching noise	None.	Little or no deformation	2	4	8	Pump maintenance
2.0 FDM Parts	Hold die in place during deformation	1.1 Failure to hold die	Broken parts due to spring force	Inspection	None.	No deformation	1	2	2	Use AL material or Ultem
		1.2 Failure to be inline	Deformation is inconsistent with smearing	Inspection	None.	Incorrect deformation	1	2	2	Check that the die is locked in
3.0 Targets	Carry LEU foil	1.1 Surface galling	Deformation is inconsistent with galling	Inspection or observed by operator	Lubricate inner tube	Inconvenience to operator	2	3	6	Lubricate inner surface of target
4.0 Plugs	Source of deformation	1.1 Surface galling	Structure not aligned correctly	Visual Inspection	None.	Incorrect deformation	2	1	2	Check alignment prior to use
		1.2 Too much/too little deformation	Wrong size	Caliper Inspection	None.	Incorrect deformation	1	2	2	Verify plug size prior to use

From the above table, the severity and frequency values are plotted graphically to point out any borderline issues. With the use of FMEA, the assembly rig was found to be quite sturdy. The main parts that had high risk levels were the pump and target due to low fluid and no lubrication.

Ultimately, failure was not catastrophic which is fortunate. Below, Fig. 4-57 provides a more visual look at the FMEA.

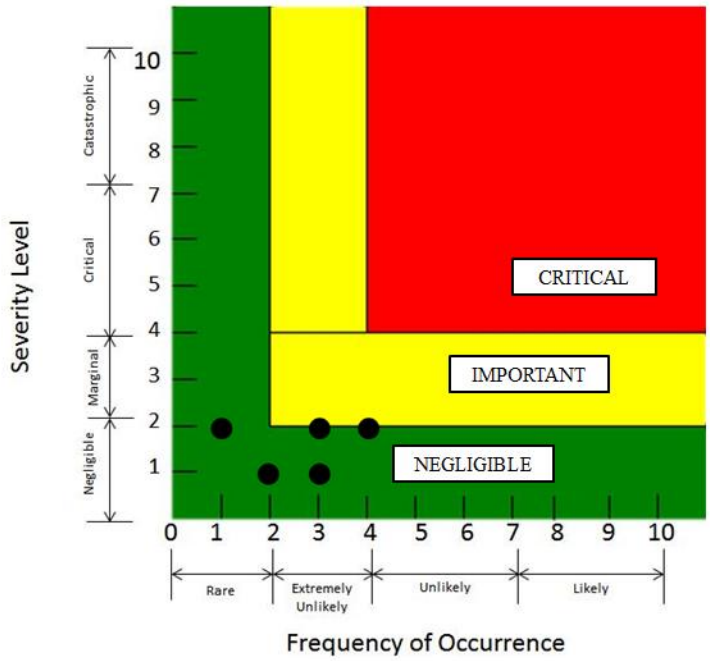

Fig. 4-57. Failure modes, graphically illustrated.

CHAPTER 5

CONCLUSION

SUMMARY

In order to comply with the presidential order of eventually eliminating HEU from any and all processes, a new source must be found suitable to replace. The program to reduce the use of HEU in the civilian sphere was initiated in 1978 and still continues today with efforts focusing on LEU, a lesser enriched uranium. However, HEU has many more uses than producing medical isotopes. This research focused primarily on the target design for the production of molybdenum – 99 in order to create the highly desired medical isotope that is the daughter isotope to molybdenum – 99, Technetium – 99m.

Annular targets have been a proposed idea for the production of molybdenum – 99 since the 1980s. However, few tests have been tried to verify the target dimensions and material type. Evident in the literary research, most testing was done on target material and foil barrier material. While these efforts are important, the containment of the molybdenum – 99 is critical in order for the project to succeed. Annular targets are advantageous because the foil volume can be varied and the cooling of annular targets is much better than the tradition plates, due to cooling of more target surfaces. While the tradition HEU method produces pure molybdenum – 99, the waste content is very high. The new annular design was also chosen with the promise to increase the molybdenum – 99 yield while decreasing the amount of waste. The materials used in this research was aluminum 6061-T6 tube material, 304 stainless steel foil as the uranium substitute, and nickel foil for the fission barrier foil.

This research was done in hopes of finding an optimized quality target design that may have fast assembly time, little or no defects, maximized foil volume, realistic tolerances, and predicted reliability. Through a series of carefully planned tests, the multiple outputs showed very promising results. Each measured output was reviewed in a series of robust analysis studies in order to determine significant factors. Once those optimized factors are known, an optimized target design may be presented.

CONCLUSIONS

A target design has been successfully developed and optimized for the production of molybdenum–99 in a high quality target. The design solution has the following features:

1. Roundness tolerance for inner tube internal diameter at 0.002 inches, inner tube outer diameter at 0.001 inches, outer tube internal diameter at 0.001 inches and outer tube outer diameter at 0.002 inches.
2. The deformation size that gave the best results was 1.047 inches, the medium draw plug.
3. As a result of the medium plug size, the residual stresses were also minimized.
4. The foil volume was maximized to 0.0998 in^3, 225 % larger than suggested volume.
5. Little or no defects (air gaps, weld pores, etc.).
6. Reliable assembly rig assessment.
7. Diameter tolerances were found to be approximately ± 0.005 inches, much looser than initial tolerances of ± 0.001 inches.
8. TIG welding is acceptable, but for high-scale production, EB welding is preferred for precise and small welds.

RECOMMENDATIONS/FUTURE WORK

While this improved design provides an optimized target, there are many factors that affect the assembly process, ranging from type of lubrication to cleaning procedures. In order for these results to be valid, it is necessary that the procedure outlined in this text is used. Additional work will continue such as additional x-ray diffraction testing after targets have undergone simulated irradiation processes. Also, an EB weld study is to be conducted as well to validate that EB welds are more accurate and do not affect the target material as TIG welding does.

REFERENCES

[1] G. W. Bush, "President's Statement on Energy Policy Act of 2005," 2005.

[2] P. Staples, "IAEA Consultancy Meeting on Conversion Planning for Mo-99 Production Facilities from HEU to LEU," 2010.

[3] P. Karamozkos, "Nuclear Terrorism and Nuclear Medicine - Removing weapons grade uranium from the nuclear supply chain," *ANZ Nuclear Medicine,* vol. 40, no. 2, pp. 8-15.

[4] National Research Council of the National Academies, Medical Isotope Production Without Highly Enriched Uranium, Washington, DC: The National Academies Press, 2009.

[5] K. Turner, "Thermal-Mechanical Analysis of Targets for High Volume Production of Molybdenum-99 Using Low-Enriched Uranium," 2009.

[6] S. G. Govindarajan, "Thermal-Mechanical Analysis of a Low-Enriched Uranium Foil Based Annular Target For the Production of Molybdenum-99," 2011.

[7] J. Ballinger, "Short- and Long- Term Responses to Molybdenum-99 Shortages in Nuclear Medicine," *The Brtish Journal of Radiology,* vol. 83, pp. 899-901, November 2010.

[8] R. Barnowski, "OP-ED: INSOURCING NUCLEAR MEDICINE," *The Journal of Science Policy & Governance,* vol. 1, no. 1.

[9] C. Hansell, "Nuclear Medicine's Double Hazard: Imperiled Treatment and the Risk of Terrorism," *Nonproliferation Review,* vol. 15, no. 2, pp. 185-208, 2008.

[10] G. S. Thomas and J. Maddahi, "The Technetium Shortage," *Journal of Nuclear Cardiology,* vol. 17, no. 6, pp. 993-998, 2010.

[11] J. Whitlock, "Research Reactors," 16 January 2013. [Online]. Available: nuclearfaq.ca/cnf_sectionH.htm#g2. [Accessed 3 April 2013].

[12] P. Staples, "GTRI's Domestic & International Mo-99 Efforts: The Influence of Politics on Medical Isotopes Production," 2011.

[13] B. Budi Briyatmoko, S. Guswardani, S. P. Purwanta, B. Dadang and M. Kartaman, "Indonesia's Current Status for Conversion of Mo-99 Production to LEU Tission," Serpong, 2006.

[14] P. Staples, "GTRI's Mo-99 Program," 2011.

[15] National Nuclear Security Administration, "United States, Belgium, France, and The Netherlands Announce Joint Statement on HEU Minimization and the Reliable Supply of Medical Isotopes," 2012.

[16] "Iran's Nuclear Program (Nuclear Talks, 2012)," *The New York Times,* 16 November 2012.

[17] J. L. Snelgrove, G. F. Vandegrift and G. L. Hofman, "Development and Processing of LEU Targets for Mo-99 Production," in *Research Reactor Fuel Management (RRFM)*, Bruges, 1997.

[18] H. Arino, H. H. Kramer, J. J. McGovern and A. K. Thornton, "Production of High Purity Fission Product Molybdenum-99". U.S. Patent 3,799,883, 30 June 1971.

[19] A. Mutalib, B. Purwadi, Adang H.G., Hotman L., Moeridoen, Kadarisman, A. Sukmana, Sriyono, A. Suripto, H. Nasution, D. Amin, A. Basiran, A. Gogo, D. Sunaryadi, T. Taryo, G. F. Vandegrift, G. Hofman, C. Conner, J. Sedlet, D. Walker, R. Leonard, E. Wood, T. Wiencek and J. Snelgrove, "Full-Scale Demonstration of the Cintichem Process for the

Production of Mo-99 Using a Low-Enriched Target," in *Reduced Enrichment for Research and Test Reactors*, Sao Paulo, 1998.

[20] K. K. Turner, G. L. Solbrekken and C. W. Allen, "Thermal-Mechanical Analysis of Annular Target Design for High Volume Production of Molybdenum-99 Using Low-Enriched Uranium," in *Proceedings of the ASME 2009 International Mechanical Engineering Congress & Exposition*, Lake Buena Vista, 2009.

[21] "The Whole Weld World!," [Online]. Available: http://www.weldguru.com/tig-welding.html. [Accessed 14 January 2013].

[22] Nuclear Energy Agency, "The Supply of Medical Raioisotopes: An Assessment of Long-term Global Demand for Technetium-99m," Organization for Economic Co-operation and Development, 2011.

[23] A. S. El-Gizawy, "Plastic Deformation Analysis During Target Assembly for Production of Mo-99 Isotopes," Columbia, 2010.

[24] J. A. Schey, Introduction to Manufacturing Processes, McGraw-Hill Companies, Inc., 1999, pp. 358-362.

[25] R. G. Budynas, Advanced Strength and Applied Stress Analysis, McGraw-Hill Companies, Inc., 1999, pp. 568-571.

[26] D. C. Montgomery, Introduction to Statistical Quality Control, John Wiley & Sons, Inc., 1996, pp. 589-601.

[27] tutornik, "Pressure Vessel," tutornik, 2013. [Online]. Available: http://tutornik.com/assignment-homework-problem-question-help/engineering/strength-of-materials/pressure-vessel/. [Accessed 6 April 2013].

[28] PROTO iXRD, Oldcastle.

[29] I. C. Noyan and J. B. Cohen, Residual Stress: Measurement by Diffraction and Interpretation, New York: Spring-Verlag, 1987, pp. pp 101 - 130.

[30] *XrdWin 2.0.87.14553,* Oldcastle, Ontario: PROTO Manufacturing, Ltd..

[31] G. F. Vander Voort, Metallography: Principles and Practice, New York: McGraw-Hill Book Company, 1984.

[32] D. S. S. Corp, *SolidWorks 2013 SP0.0,* 2013.

[33] MathWorks, *MATLAB 2013a,* 2013.

[34] Wikipedia, the free encyclopedia, "Autofrettage," [Online]. Available: en.wikipedia.org/wiki/autofrettage. [Accessed 3 April 2013].

[35] Argonne National Laboratory, *Indonesian Annular Mo-99 Targets,* Argonne National Laboratory, 1999.

APPENDIX A

IMAGEJ INSTRUCTIONS

1. Draw line that matches the scale from picture
2. Analyze – set scale

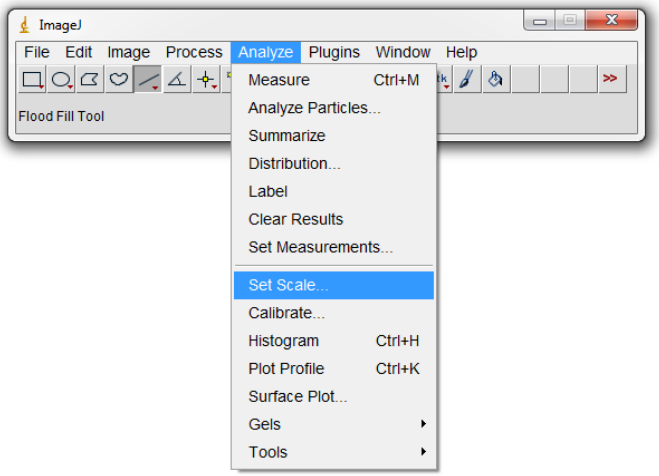

3. Set units and scaling length

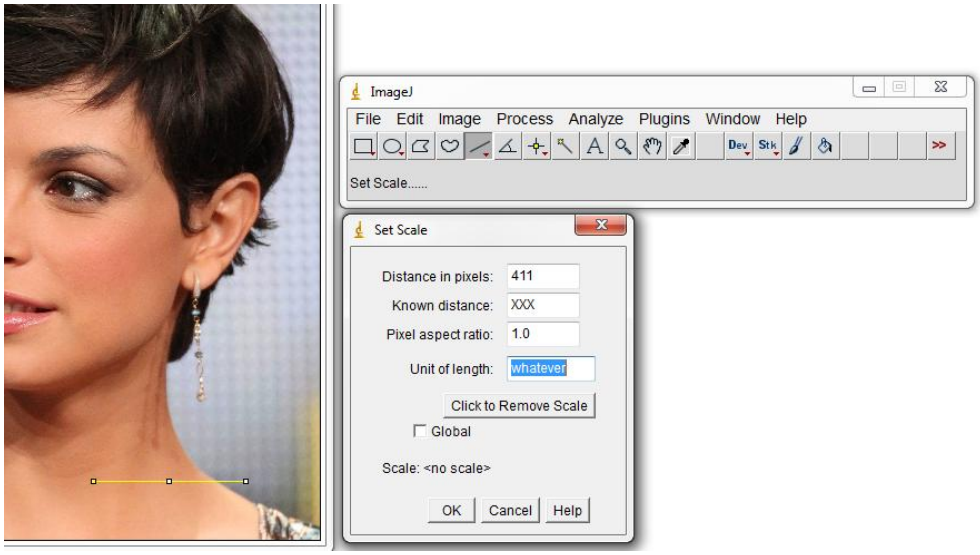

4. Now, draw a new line and measure.

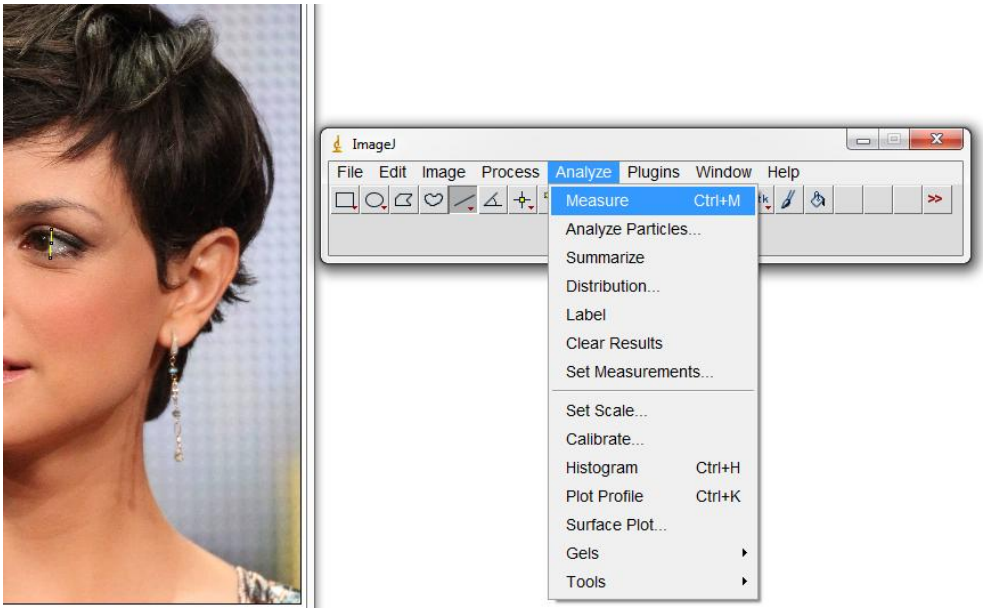

5. Results pop up automatically. Go to length to get overall magnitude:

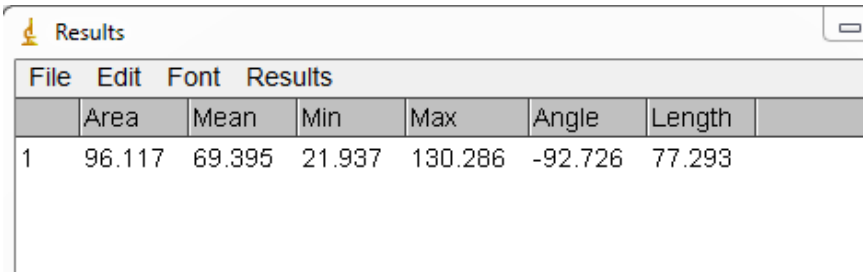

	Area	Mean	Min	Max	Angle	Length
1	96.117	69.395	21.937	130.286	-92.726	77.293

APPENDIX B

ETCHING FORMULA

Aluminum Tubing, Stainless Steel Foil with Nickel Foil Barrier Etching

Etch for pure AL, reveals grain structure. Immerse sample at room temperature for 60 s.

2 g Na OH (Sodium Hydroxide)

4 g Na_2CO_3 (Sodium Carbonate)

94 mL Deionized Water

Mix until solution is clear, immerse sample at room temperature for 60 s.

Note: *Always add NaOH to water – NEVER add water to NaOH*. Refresh solution every other sample.

APPENDIX C

TUBE DRAWINGS

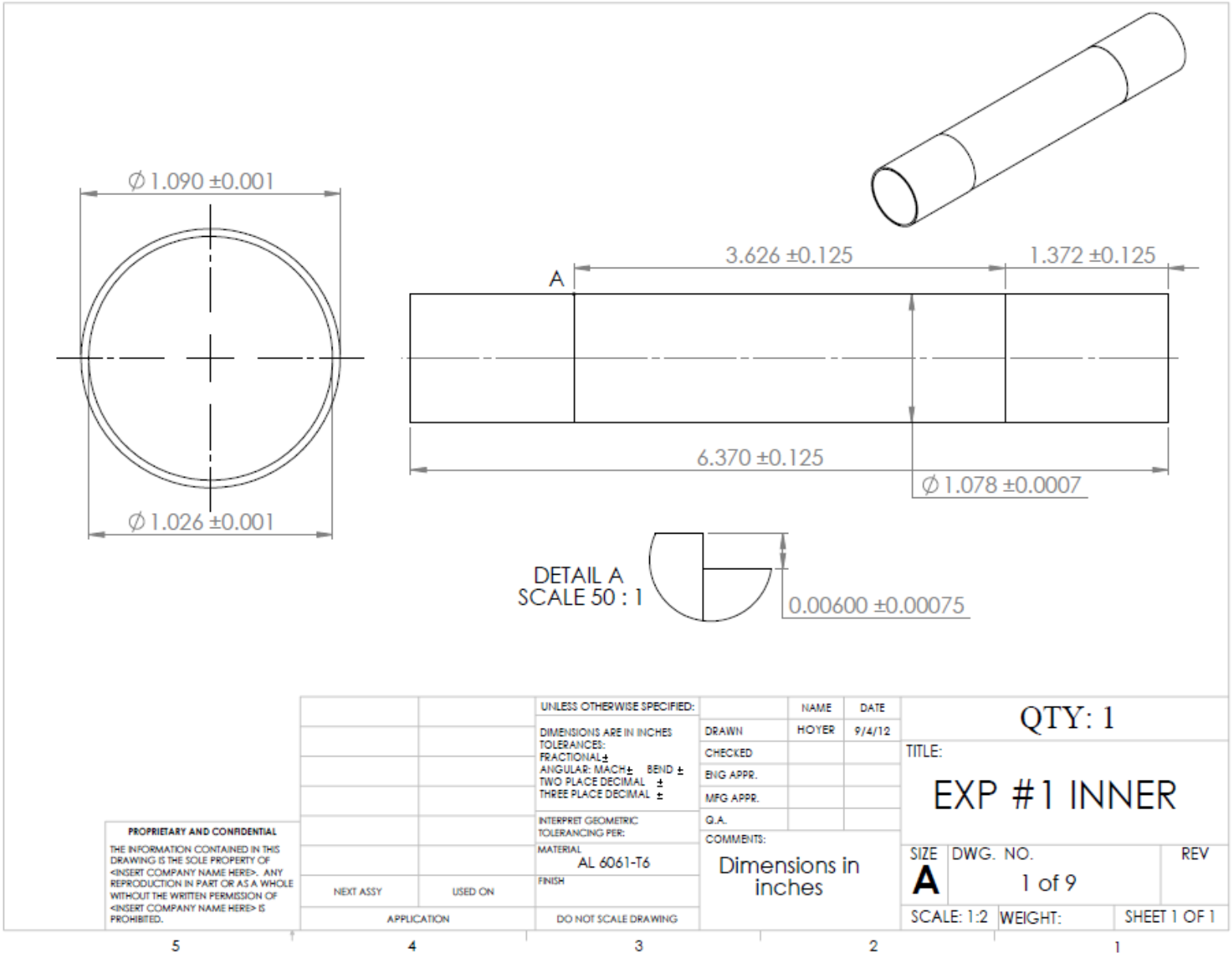
Ø 1.090 ±0.001
Ø 1.026 ±0.001
A
3.626 ±0.125
1.372 ±0.125
6.370 ±0.125
Ø 1.078 ±0.0007
DETAIL A
SCALE 50 : 1
0.00600 ±0.00075
UNLESS OTHERWISE SPECIFIED:
DIMENSIONS ARE IN INCHES
TOLERANCES:
FRACTIONAL ±
ANGULAR: MACH ± BEND ±
TWO PLACE DECIMAL ±
THREE PLACE DECIMAL ±
INTERPRET GEOMETRIC TOLERANCING PER:
MATERIAL
AL 6061-T6
FINISH
NEXT ASSY
USED ON
APPLICATION
DO NOT SCALE DRAWING
NAME
DATE
DRAWN
HOYER
9/4/12
CHECKED
ENG APPR.
MFG APPR.
Q.A.
COMMENTS:
Dimensions in inches
QTY: 1
TITLE:
EXP #1 INNER
SIZE
A
DWG. NO.
1 of 9
REV
SCALE: 1:2
WEIGHT:
SHEET 1 OF 1
PROPRIETARY AND CONFIDENTIAL
THE INFORMATION CONTAINED IN THIS DRAWING IS THE SOLE PROPERTY OF <INSERT COMPANY NAME HERE>. ANY REPRODUCTION IN PART OR AS A WHOLE WITHOUT THE WRITTEN PERMISSION OF <INSERT COMPANY NAME HERE> IS PROHIBITED.
5
4
3
2
1

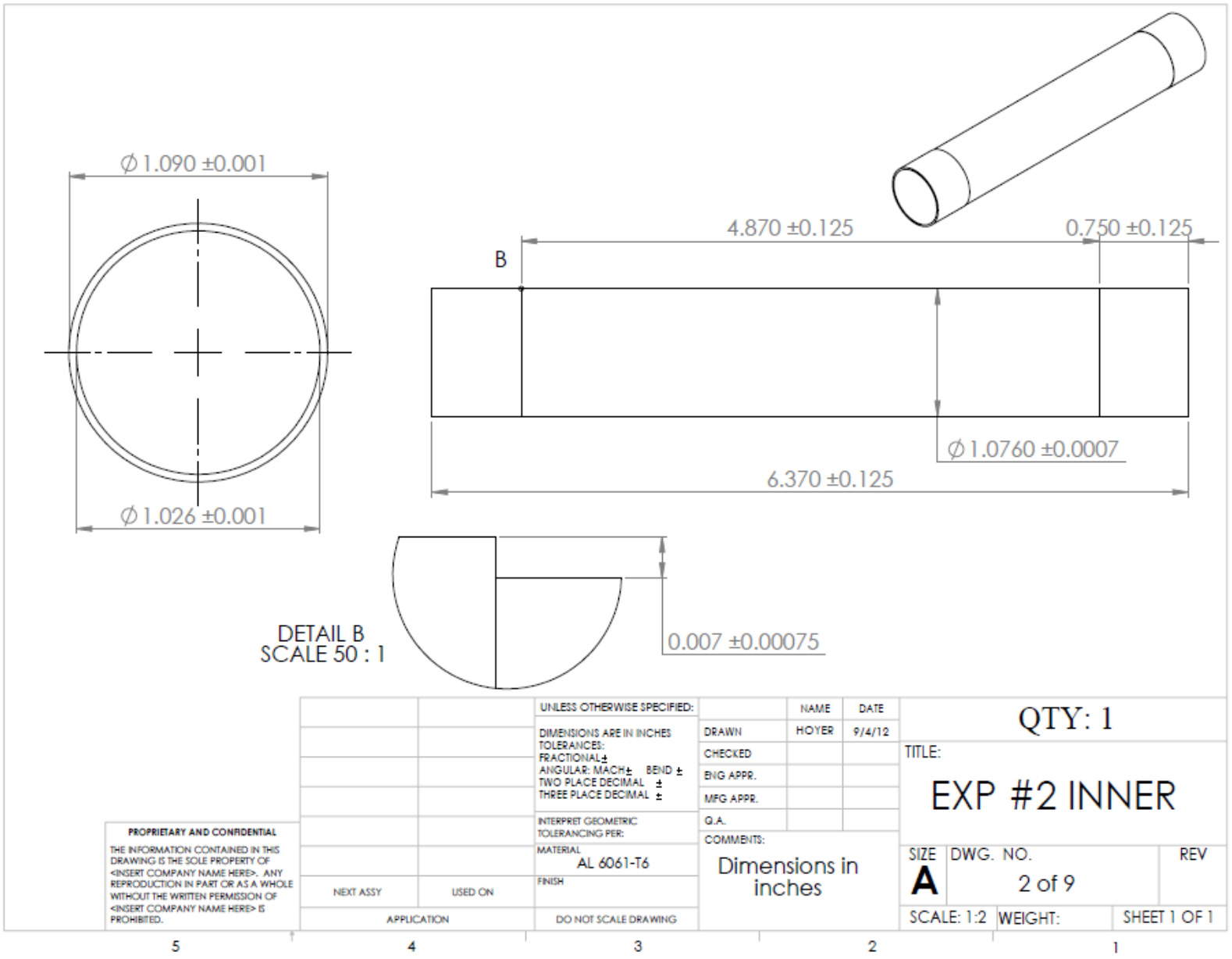
∅1.090 ±0.001
∅1.026 ±0.001
4.870 ±0.125
0.750 ±0.125
B
∅1.0760 ±0.0007
6.370 ±0.125
DETAIL B
SCALE 50 : 1
0.007 ±0.00075
UNLESS OTHERWISE SPECIFIED:
DIMENSIONS ARE IN INCHES
TOLERANCES:
FRACTIONAL ±
ANGULAR: MACH ± BEND ±
TWO PLACE DECIMAL ±
THREE PLACE DECIMAL ±
INTERPRET GEOMETRIC TOLERANCING PER:
MATERIAL
AL 6061-T6
FINISH
DO NOT SCALE DRAWING
NAME
DATE
DRAWN
HOYER
9/4/12
CHECKED
ENG APPR.
MFG APPR.
Q.A.
COMMENTS:
Dimensions in inches
QTY: 1
TITLE:
EXP #2 INNER
SIZE
A
DWG. NO.
2 of 9
REV
SCALE: 1:2
WEIGHT:
SHEET 1 OF 1
NEXT ASSY
USED ON
APPLICATION
PROPRIETARY AND CONFIDENTIAL
THE INFORMATION CONTAINED IN THIS DRAWING IS THE SOLE PROPERTY OF <INSERT COMPANY NAME HERE>. ANY REPRODUCTION IN PART OR AS A WHOLE WITHOUT THE WRITTEN PERMISSION OF <INSERT COMPANY NAME HERE> IS PROHIBITED.
5
4
3
2
1

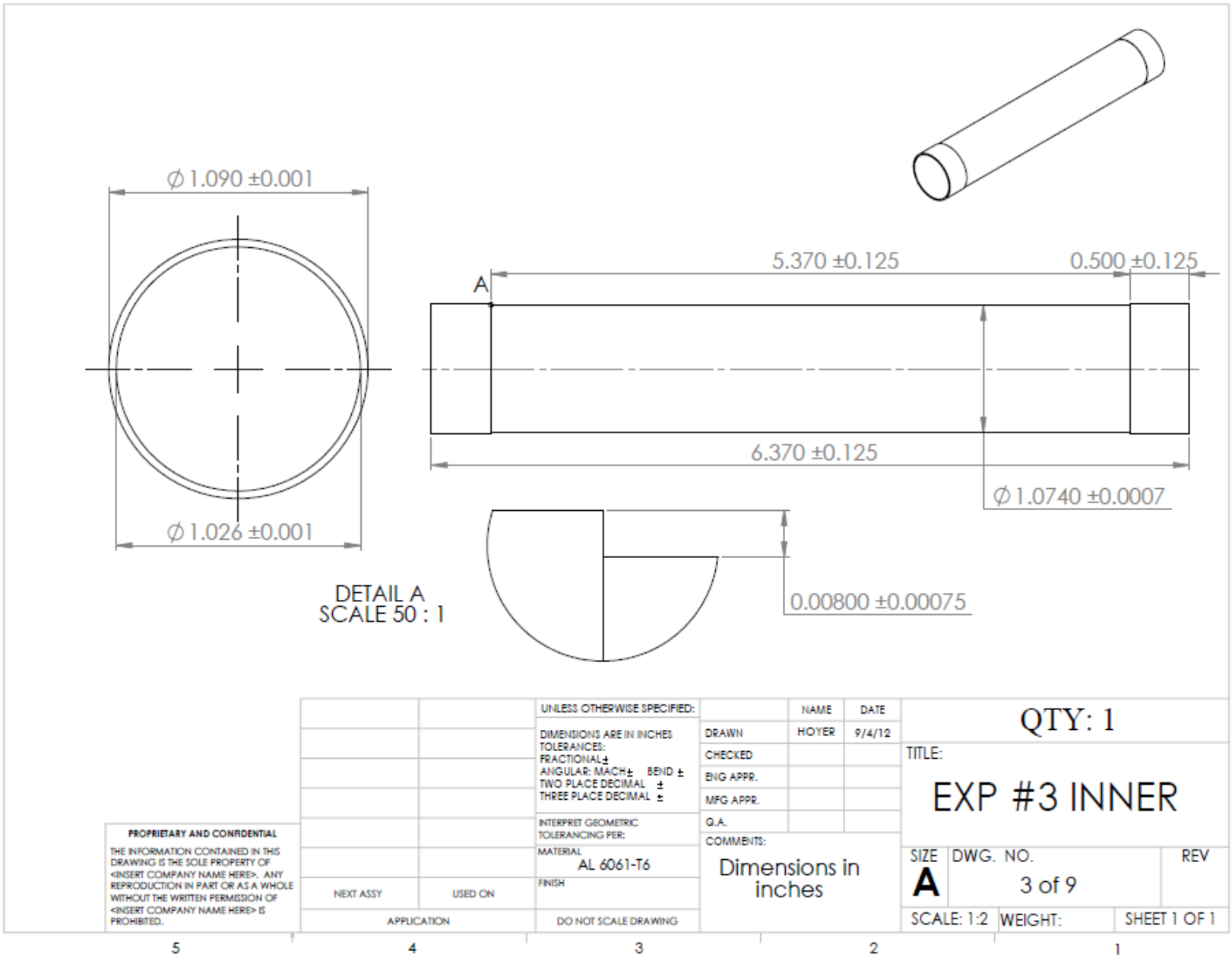
∅ 1.090 ±0.001
∅ 1.026 ±0.001
A
5.370 ±0.125
0.500 ±0.125
6.370 ±0.125
∅ 1.0740 ±0.0007
DETAIL A
SCALE 50 : 1
0.00800 ±0.00075
UNLESS OTHERWISE SPECIFIED:
DIMENSIONS ARE IN INCHES
TOLERANCES:
FRACTIONAL ±
ANGULAR: MACH ± BEND ±
TWO PLACE DECIMAL ±
THREE PLACE DECIMAL ±
INTERPRET GEOMETRIC TOLERANCING PER:
MATERIAL
AL 6061-T6
FINISH
DO NOT SCALE DRAWING
NEXT ASSY
USED ON
APPLICATION
NAME
DATE
DRAWN
HOYER
9/4/12
CHECKED
ENG APPR.
MFG APPR.
Q.A.
COMMENTS:
Dimensions in inches
QTY: 1
TITLE:
EXP #3 INNER
SIZE
A
DWG. NO.
3 of 9
REV
SCALE: 1:2
WEIGHT:
SHEET 1 OF 1
PROPRIETARY AND CONFIDENTIAL
THE INFORMATION CONTAINED IN THIS DRAWING IS THE SOLE PROPERTY OF <INSERT COMPANY NAME HERE>. ANY REPRODUCTION IN PART OR AS A WHOLE WITHOUT THE WRITTEN PERMISSION OF <INSERT COMPANY NAME HERE> IS PROHIBITED.
5
4
3
2
1

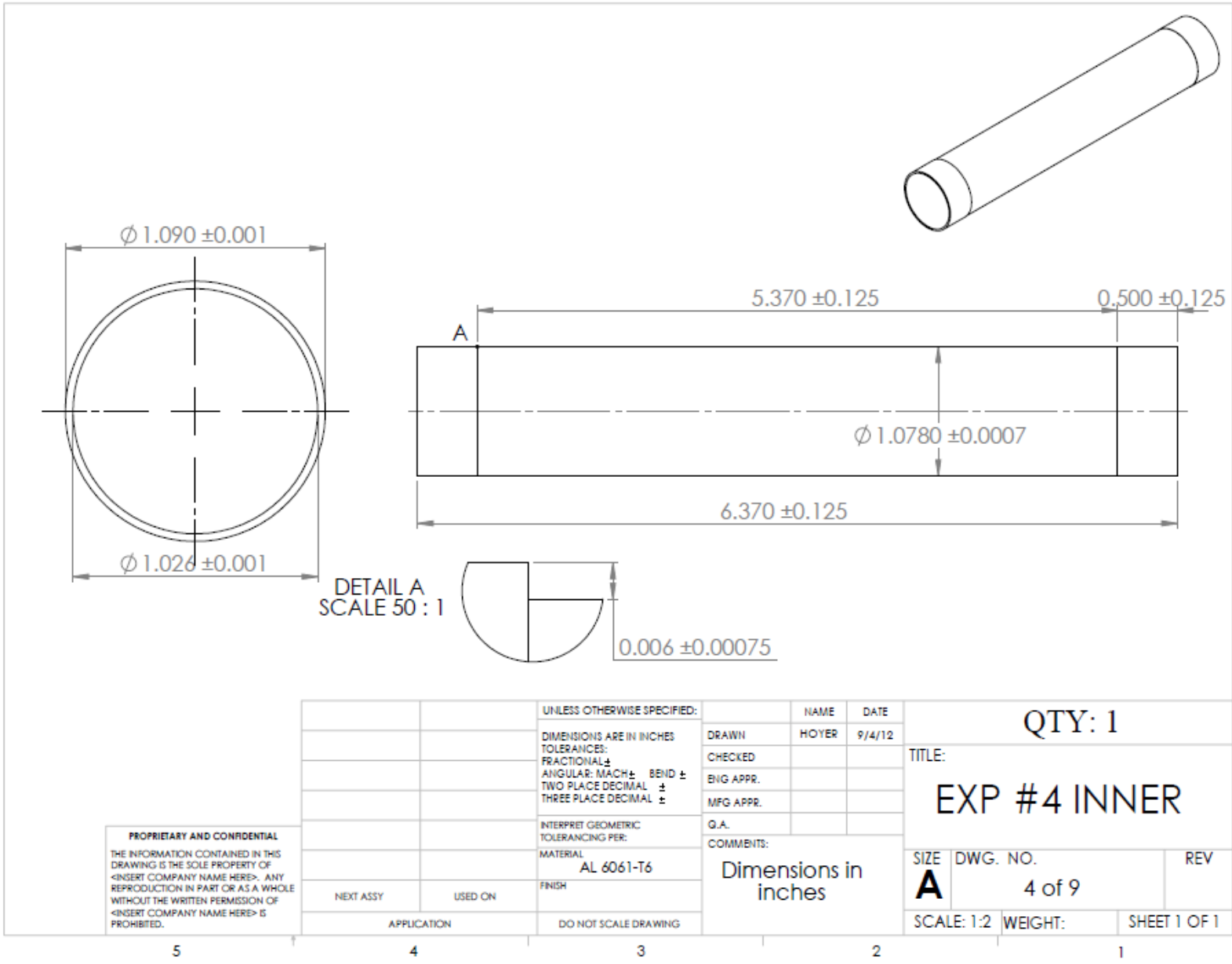
∅1.090 ±0.001
∅1.026 ±0.001
5.370 ±0.125
0.500 ±0.125
A
∅1.0780 ±0.0007
6.370 ±0.125
DETAIL A
SCALE 50 : 1
0.006 ±0.00075
PROPRIETARY AND CONFIDENTIAL
THE INFORMATION CONTAINED IN THIS DRAWING IS THE SOLE PROPERTY OF <INSERT COMPANY NAME HERE>. ANY REPRODUCTION IN PART OR AS A WHOLE WITHOUT THE WRITTEN PERMISSION OF <INSERT COMPANY NAME HERE> IS PROHIBITED.
NEXT ASSY
USED ON
APPLICATION
UNLESS OTHERWISE SPECIFIED:
DIMENSIONS ARE IN INCHES
TOLERANCES:
FRACTIONAL ±
ANGULAR: MACH ± BEND ±
TWO PLACE DECIMAL ±
THREE PLACE DECIMAL ±
INTERPRET GEOMETRIC TOLERANCING PER:
MATERIAL
AL 6061-T6
FINISH
DO NOT SCALE DRAWING
NAME
DATE
DRAWN
HOYER
9/4/12
CHECKED
ENG APPR.
MFG APPR.
Q.A.
COMMENTS:
Dimensions in inches
QTY: 1
TITLE:
EXP #4 INNER
SIZE
A
DWG. NO.
4 of 9
REV
SCALE: 1:2
WEIGHT:
SHEET 1 OF 1
5
4
3
2
1

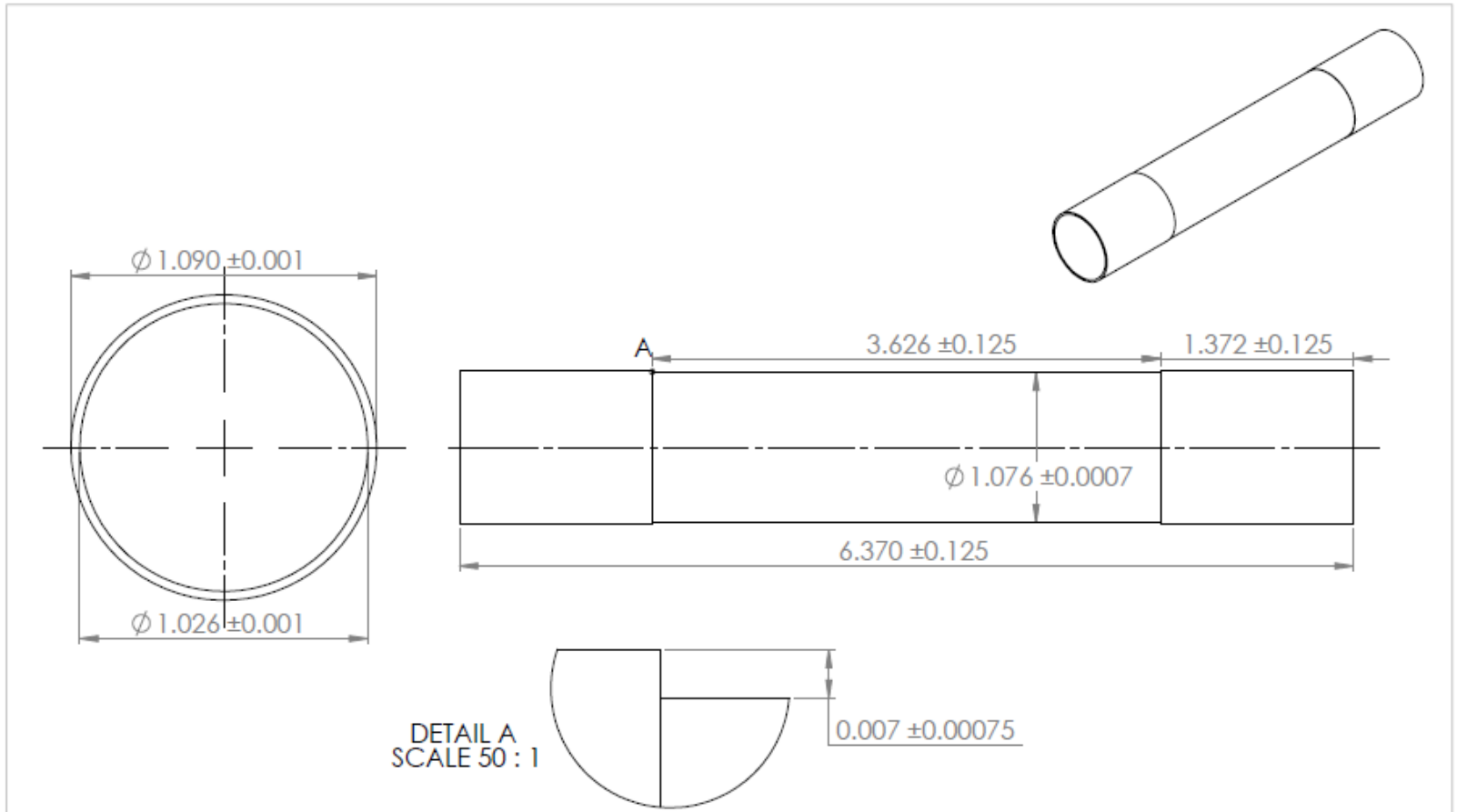

		UNLESS OTHERWISE SPECIFIED:		NAME	DATE
		DIMENSIONS ARE IN INCHES TOLERANCES: FRACTIONAL ± ANGULAR: MACH ± BEND ± TWO PLACE DECIMAL ± THREE PLACE DECIMAL ±	DRAWN	HOYER	9/4/12
			CHECKED		
			ENG APPR.		
			MFG APPR.		
		INTERPRET GEOMETRIC TOLERANCING PER:	Q.A.		
		MATERIAL AL 6061-T6	COMMENTS: Dimensions in inches		
NEXT ASSY	USED ON	FINISH			
APPLICATION		DO NOT SCALE DRAWING			

QTY: 1

TITLE:

EXP #5 INNER

SIZE	DWG. NO.	REV
A	5 of 9	
SCALE: 1:2	WEIGHT:	SHEET 1 OF 1

5 4 3 2 1

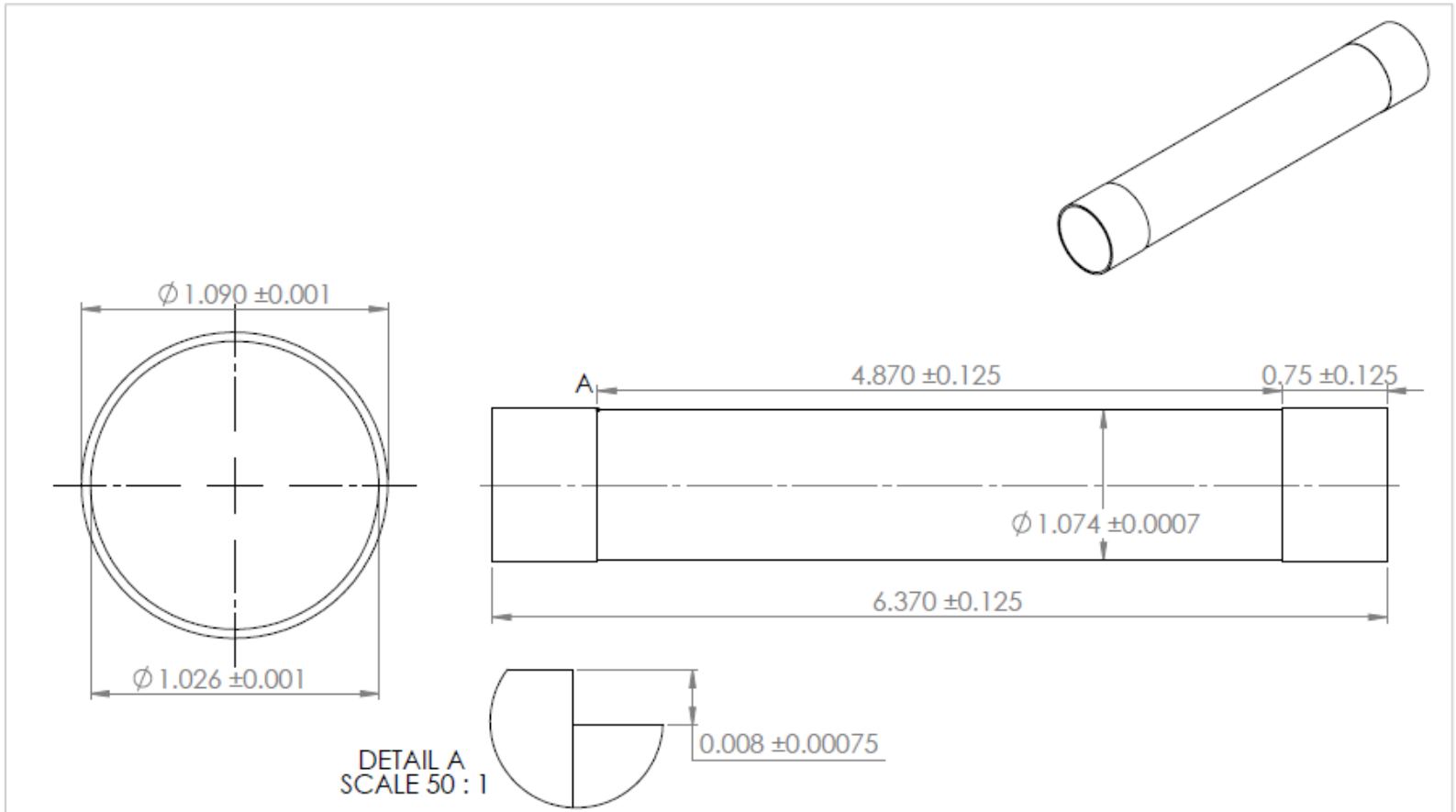

		UNLESS OTHERWISE SPECIFIED:		NAME	DATE
		DIMENSIONS ARE IN INCHES TOLERANCES: FRACTIONAL ± ANGULAR: MACH ± BEND ± TWO PLACE DECIMAL ± THREE PLACE DECIMAL ±	DRAWN	HOYER	9/4/12
			CHECKED		
			ENG APPR.		
			MFG APPR.		
		INTERPRET GEOMETRIC TOLERANCING PER:	Q.A.		
		MATERIAL AL 6061-T6	COMMENTS: Dimensions in inches		
NEXT ASSY	USED ON	FINISH			
APPLICATION		DO NOT SCALE DRAWING			

QTY: 1

TITLE:

EXP #6 INNER

SIZE	DWG. NO.	REV
A	6 of 9	
SCALE: 1:2	WEIGHT:	SHEET 1 OF 1

5 4 3 2 1

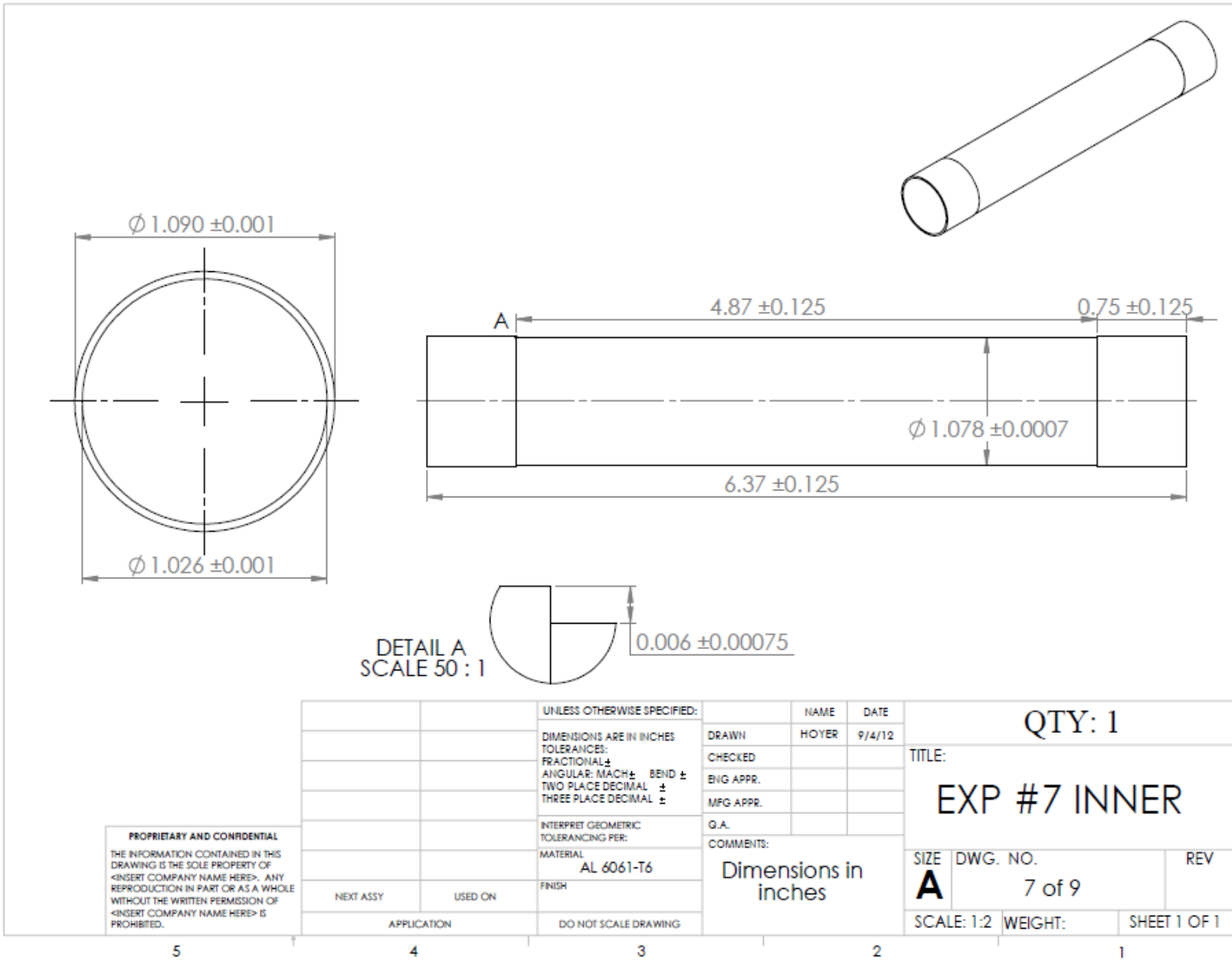
Ø 1.090 ±0.001
Ø 1.026 ±0.001
A
4.87 ±0.125
0.75 ±0.125
Ø 1.078 ±0.0007
6.37 ±0.125
DETAIL A
SCALE 50 : 1
0.006 ±0.00075
UNLESS OTHERWISE SPECIFIED:
DIMENSIONS ARE IN INCHES
TOLERANCES:
FRACTIONAL ±
ANGULAR: MACH ± BEND ±
TWO PLACE DECIMAL ±
THREE PLACE DECIMAL ±
INTERPRET GEOMETRIC TOLERANCING PER:
MATERIAL
AL 6061-T6
FINISH
DO NOT SCALE DRAWING
NAME
DATE
DRAWN
HOYER
9/4/12
CHECKED
ENG APPR.
MFG APPR.
Q.A.
COMMENTS:
Dimensions in inches
QTY: 1
TITLE:
EXP #7 INNER
SIZE
A
DWG. NO.
7 of 9
REV
SCALE: 1:2
WEIGHT:
SHEET 1 OF 1
NEXT ASSY
USED ON
APPLICATION
PROPRIETARY AND CONFIDENTIAL
THE INFORMATION CONTAINED IN THIS DRAWING IS THE SOLE PROPERTY OF <INSERT COMPANY NAME HERE>. ANY REPRODUCTION IN PART OR AS A WHOLE WITHOUT THE WRITTEN PERMISSION OF <INSERT COMPANY NAME HERE> IS PROHIBITED.
5
4
3
2
1

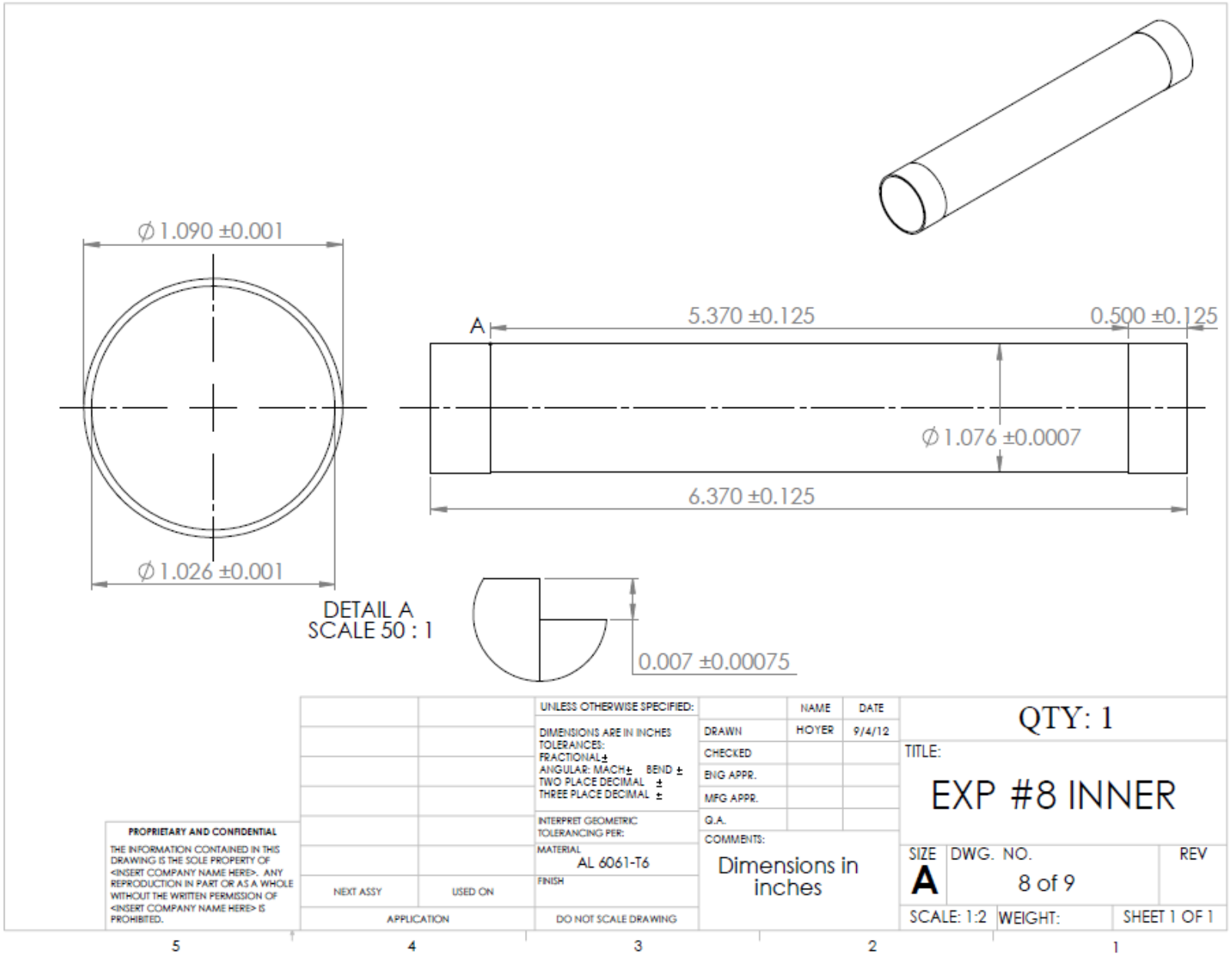
Ø 1.090 ±0.001
Ø 1.026 ±0.001
A
5.370 ±0.125
0.500 ±0.125
Ø 1.076 ±0.0007
6.370 ±0.125
DETAIL A
SCALE 50 : 1
0.007 ±0.00075
UNLESS OTHERWISE SPECIFIED:
DIMENSIONS ARE IN INCHES
TOLERANCES:
FRACTIONAL ±
ANGULAR: MACH ± BEND ±
TWO PLACE DECIMAL ±
THREE PLACE DECIMAL ±
INTERPRET GEOMETRIC TOLERANCING PER:
MATERIAL
AL 6061-T6
FINISH
NEXT ASSY
USED ON
APPLICATION
DO NOT SCALE DRAWING
NAME
DATE
DRAWN
HOYER
9/4/12
CHECKED
ENG APPR.
MFG APPR.
G.A.
COMMENTS:
Dimensions in inches
QTY: 1
TITLE:
EXP #8 INNER
SIZE
A
DWG. NO.
8 of 9
REV
SCALE: 1:2
WEIGHT:
SHEET 1 OF 1
PROPRIETARY AND CONFIDENTIAL
THE INFORMATION CONTAINED IN THIS DRAWING IS THE SOLE PROPERTY OF <INSERT COMPANY NAME HERE>. ANY REPRODUCTION IN PART OR AS A WHOLE WITHOUT THE WRITTEN PERMISSION OF <INSERT COMPANY NAME HERE> IS PROHIBITED.
5
4
3
2
1

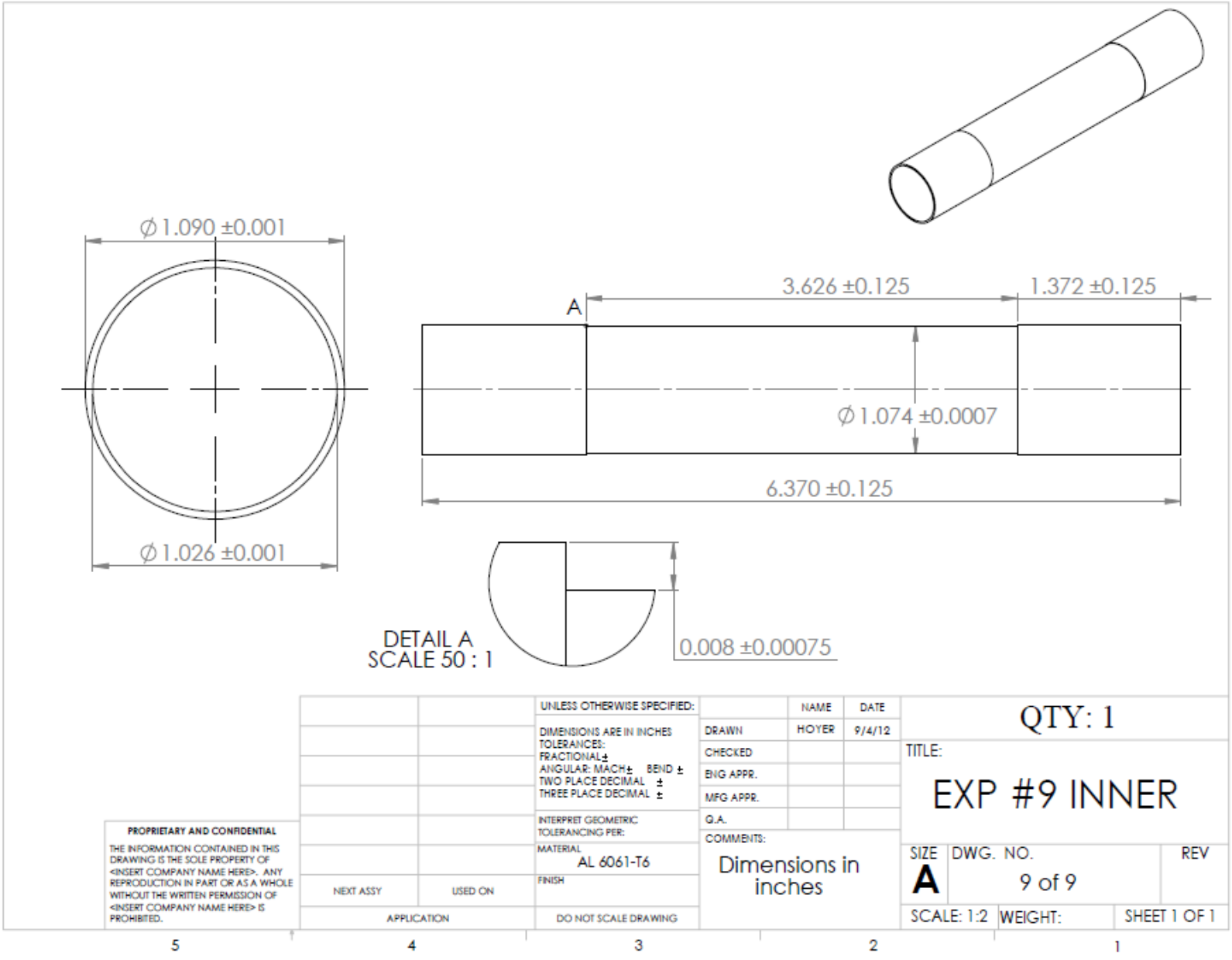
∅1.090 ±0.001
∅1.026 ±0.001
A
3.626 ±0.125
1.372 ±0.125
∅1.074 ±0.0007
6.370 ±0.125
DETAIL A
SCALE 50 : 1
0.008 ±0.00075
UNLESS OTHERWISE SPECIFIED:
DIMENSIONS ARE IN INCHES
TOLERANCES:
FRACTIONAL ±
ANGULAR: MACH ± BEND ±
TWO PLACE DECIMAL ±
THREE PLACE DECIMAL ±
INTERPRET GEOMETRIC TOLERANCING PER:
MATERIAL
AL 6061-T6
FINISH
DO NOT SCALE DRAWING
NAME
DATE
DRAWN
HOYER
9/4/12
CHECKED
ENG APPR.
MFG APPR.
Q.A.
COMMENTS:
Dimensions in inches
QTY: 1
TITLE:
EXP #9 INNER
SIZE
A
DWG. NO.
9 of 9
REV
SCALE: 1:2
WEIGHT:
SHEET 1 OF 1
NEXT ASSY
USED ON
APPLICATION
PROPRIETARY AND CONFIDENTIAL
THE INFORMATION CONTAINED IN THIS DRAWING IS THE SOLE PROPERTY OF <INSERT COMPANY NAME HERE>. ANY REPRODUCTION IN PART OR AS A WHOLE WITHOUT THE WRITTEN PERMISSION OF <INSERT COMPANY NAME HERE> IS PROHIBITED.
5
4
3
2
1

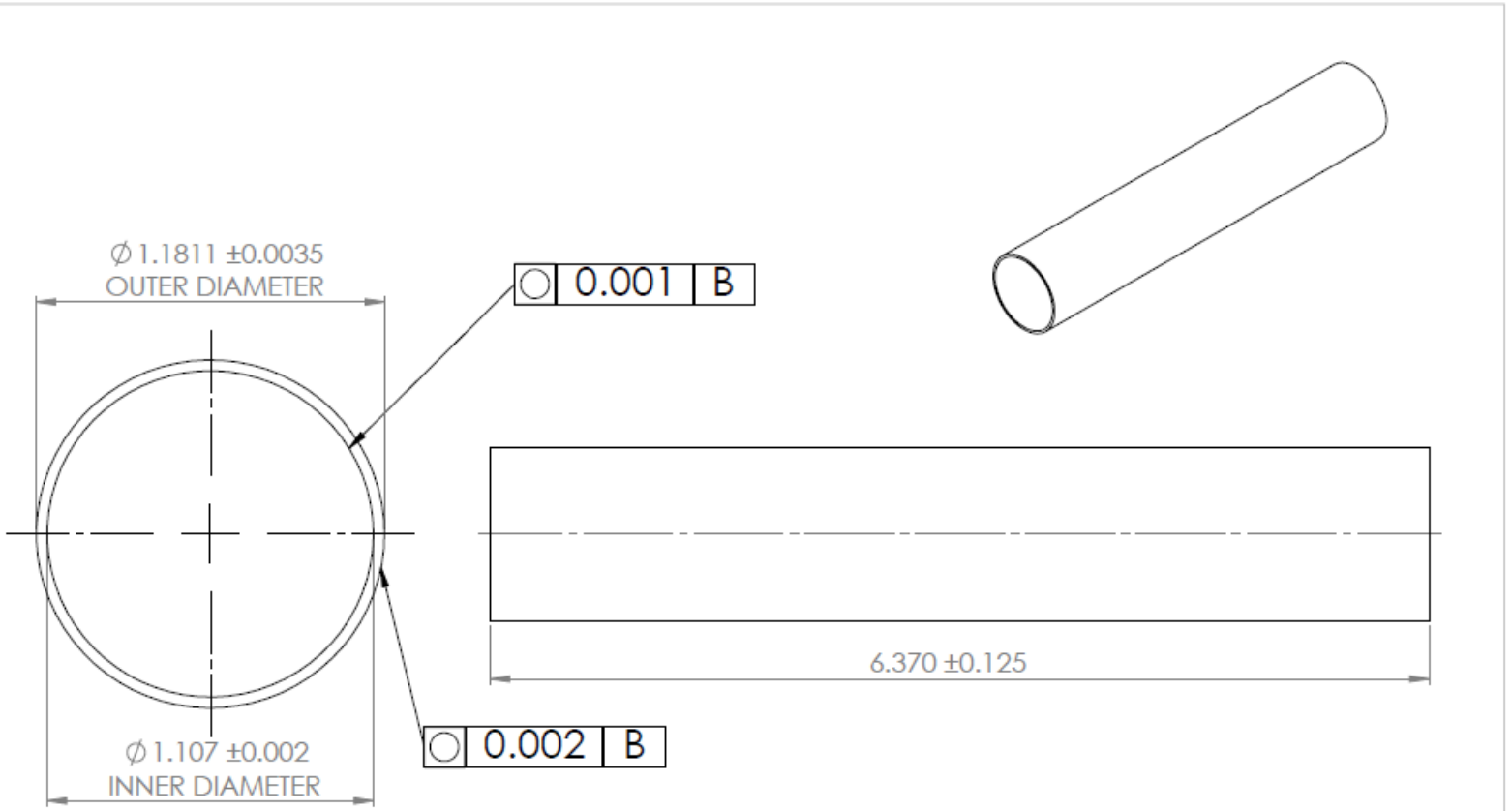

		UNLESS OTHERWISE SPECIFIED:		NAME	DATE
		DIMENSIONS ARE IN INCHES TOLERANCES: FRACTIONAL ± ANGULAR: MACH ± BEND ± TWO PLACE DECIMAL ± THREE PLACE DECIMAL ±	DRAWN	Hoyer	8/10/12
			CHECKED		
			ENG APPR.		
			MFG APPR.		
			Q.A.		
		INTERPRET GEOMETRIC TOLERANCING PER:	COMMENTS:		
		MATERIAL AL 6061-T6	Dimensions in inches		
NEXT ASSY	USED ON	FINISH			
APPLICATION		DO NOT SCALE DRAWING			

QTY: 9

TITLE: Outer Tube MU Design

SIZE	DWG. NO.	REV
A		

SCALE: 1:2	WEIGHT:	SHEET 1 OF 1

5 4 3 2 1

Longer Foil Options

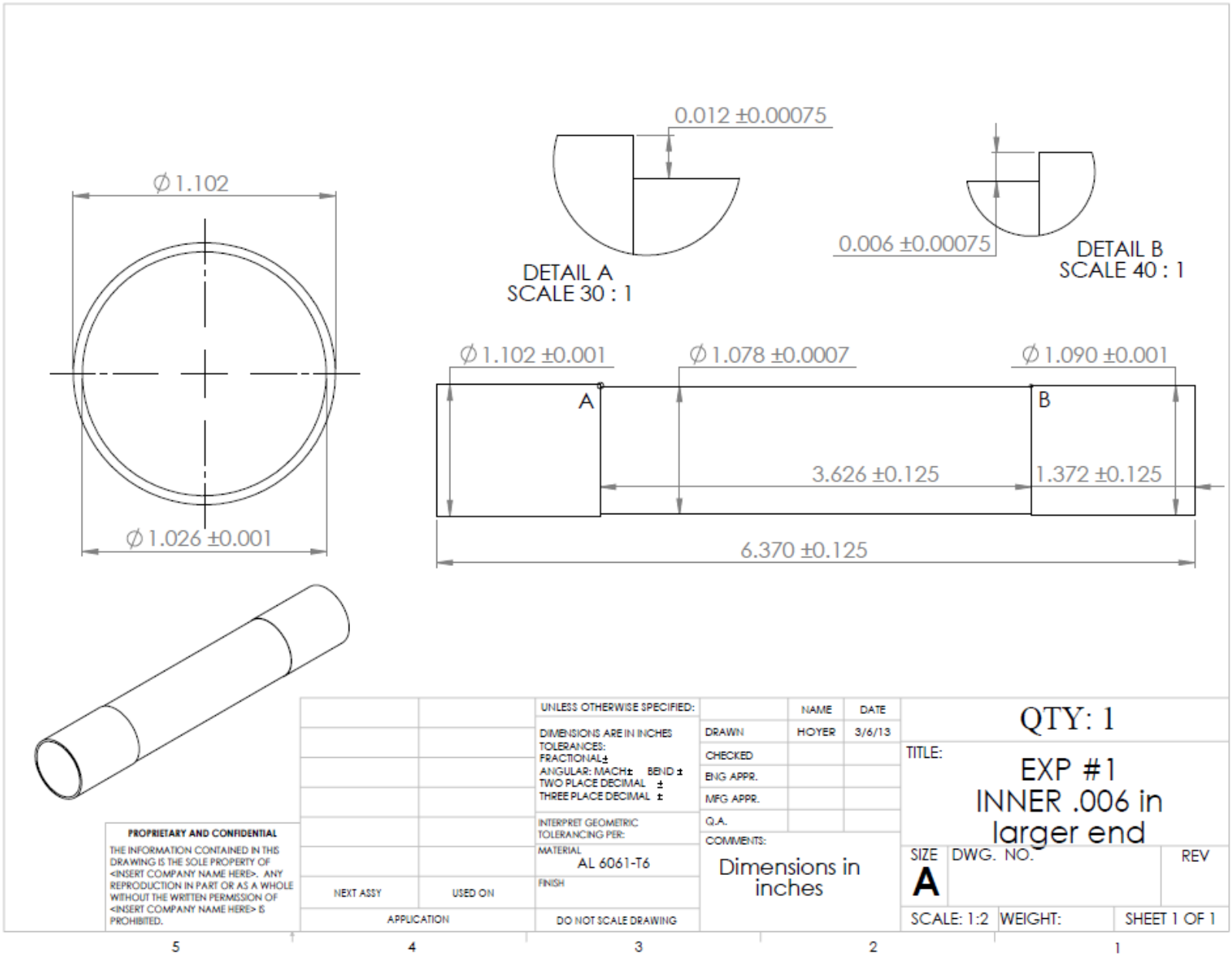
0.012 ±0.00075
DETAIL A
SCALE 30 : 1
0.006 ±0.00075
DETAIL B
SCALE 40 : 1
∅ 1.102
∅ 1.026 ±0.001
∅ 1.102 ±0.001
∅ 1.078 ±0.0007
∅ 1.090 ±0.001
A
B
3.626 ±0.125
1.372 ±0.125
6.370 ±0.125
PROPRIETARY AND CONFIDENTIAL
THE INFORMATION CONTAINED IN THIS DRAWING IS THE SOLE PROPERTY OF <INSERT COMPANY NAME HERE>. ANY REPRODUCTION IN PART OR AS A WHOLE WITHOUT THE WRITTEN PERMISSION OF <INSERT COMPANY NAME HERE> IS PROHIBITED.
NEXT ASSY
USED ON
APPLICATION
UNLESS OTHERWISE SPECIFIED:
DIMENSIONS ARE IN INCHES
TOLERANCES:
FRACTIONAL ±
ANGULAR: MACH ± BEND ±
TWO PLACE DECIMAL ±
THREE PLACE DECIMAL ±
INTERPRET GEOMETRIC TOLERANCING PER:
MATERIAL
AL 6061-T6
FINISH
DO NOT SCALE DRAWING
NAME
DATE
DRAWN
HOYER
3/6/13
CHECKED
ENG APPR.
MFG APPR.
Q.A.
COMMENTS:
Dimensions in inches
QTY: 1
TITLE:
EXP #1
INNER .006 in larger end
SIZE
A
DWG. NO.
REV
SCALE: 1:2
WEIGHT:
SHEET 1 OF 1
5
4
3
2
1

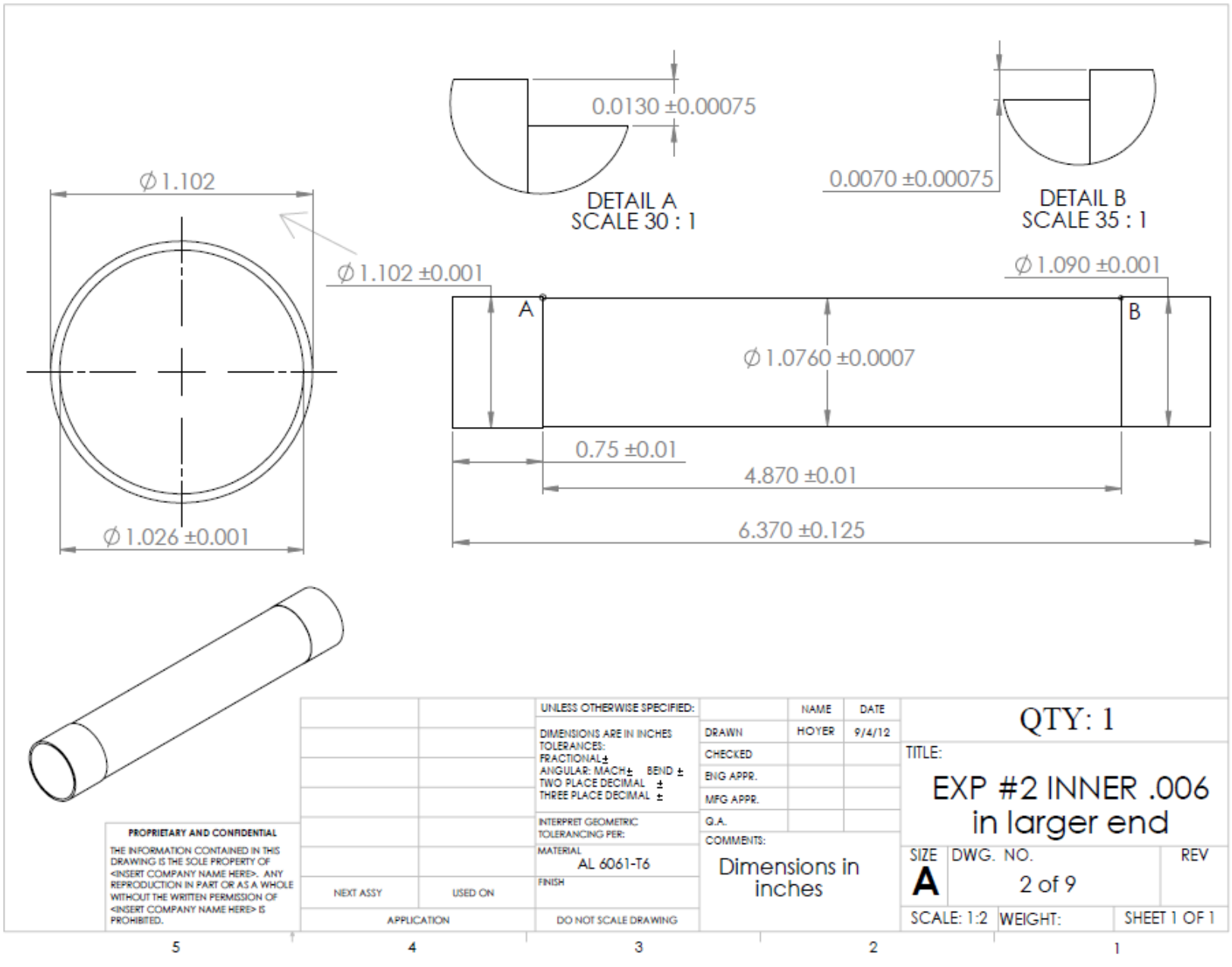
0.0130 ±0.00075
DETAIL A
SCALE 30 : 1
0.0070 ±0.00075
DETAIL B
SCALE 35 : 1
∅1.102
∅1.102 ±0.001
∅1.090 ±0.001
A
B
∅1.0760 ±0.0007
0.75 ±0.01
4.870 ±0.01
6.370 ±0.125
∅1.026 ±0.001
PROPRIETARY AND CONFIDENTIAL
THE INFORMATION CONTAINED IN THIS DRAWING IS THE SOLE PROPERTY OF <INSERT COMPANY NAME HERE>. ANY REPRODUCTION IN PART OR AS A WHOLE WITHOUT THE WRITTEN PERMISSION OF <INSERT COMPANY NAME HERE> IS PROHIBITED.
UNLESS OTHERWISE SPECIFIED:
DIMENSIONS ARE IN INCHES
TOLERANCES:
FRACTIONAL ±
ANGULAR: MACH ± BEND ±
TWO PLACE DECIMAL ±
THREE PLACE DECIMAL ±
INTERPRET GEOMETRIC TOLERANCING PER:
MATERIAL
AL 6061-T6
FINISH
DO NOT SCALE DRAWING
NEXT ASSY
USED ON
APPLICATION
NAME
DATE
DRAWN
HOYER
9/4/12
CHECKED
ENG APPR.
MFG APPR.
G.A.
COMMENTS:
Dimensions in inches
QTY: 1
TITLE:
EXP #2 INNER .006 in larger end
SIZE
A
DWG. NO.
2 of 9
REV
SCALE: 1:2
WEIGHT:
SHEET 1 OF 1
5
4
3
2
1

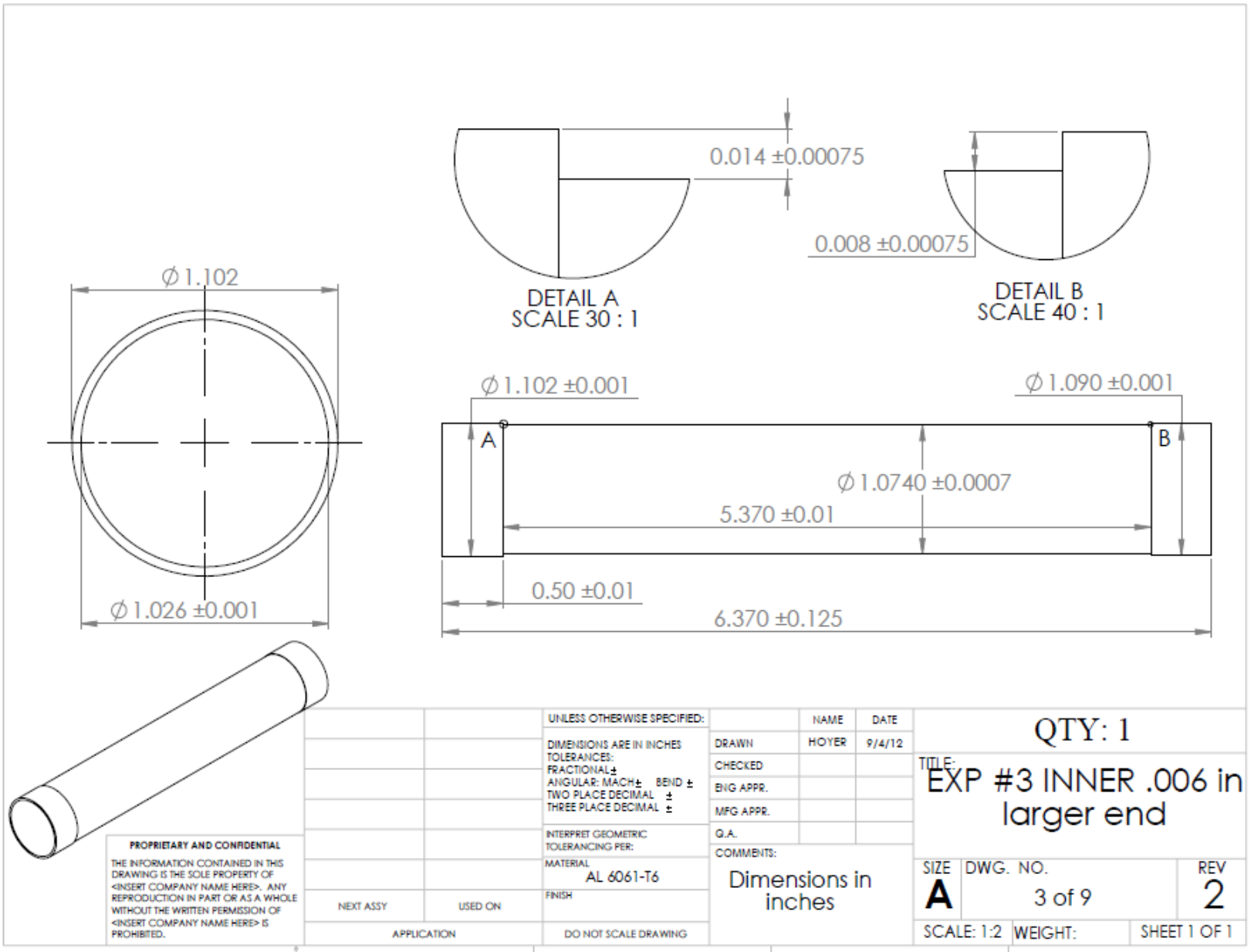
0.014 ±0.00075
0.008 ±0.00075
DETAIL A
SCALE 30 : 1
DETAIL B
SCALE 40 : 1
∅1.102
∅1.026 ±0.001
∅1.102 ±0.001
∅1.090 ±0.001
A
B
∅1.0740 ±0.0007
5.370 ±0.01
0.50 ±0.01
6.370 ±0.125
PROPRIETARY AND CONFIDENTIAL
THE INFORMATION CONTAINED IN THIS DRAWING IS THE SOLE PROPERTY OF <INSERT COMPANY NAME HERE>. ANY REPRODUCTION IN PART OR AS A WHOLE WITHOUT THE WRITTEN PERMISSION OF <INSERT COMPANY NAME HERE> IS PROHIBITED.
NEXT ASSY
USED ON
APPLICATION
UNLESS OTHERWISE SPECIFIED:
DIMENSIONS ARE IN INCHES
TOLERANCES:
FRACTIONAL ±
ANGULAR: MACH ± BEND ±
TWO PLACE DECIMAL ±
THREE PLACE DECIMAL ±
INTERPRET GEOMETRIC TOLERANCING PER:
MATERIAL
AL 6061-T6
FINISH
DO NOT SCALE DRAWING
NAME
DATE
DRAWN
HOYER
9/4/12
CHECKED
ENG APPR.
MFG APPR.
Q.A.
COMMENTS:
Dimensions in inches
QTY: 1
TITLE:
EXP #3 INNER .006 in larger end
SIZE
A
DWG. NO.
3 of 9
REV
2
SCALE: 1:2
WEIGHT:
SHEET 1 OF 1
5
4
3
2
1

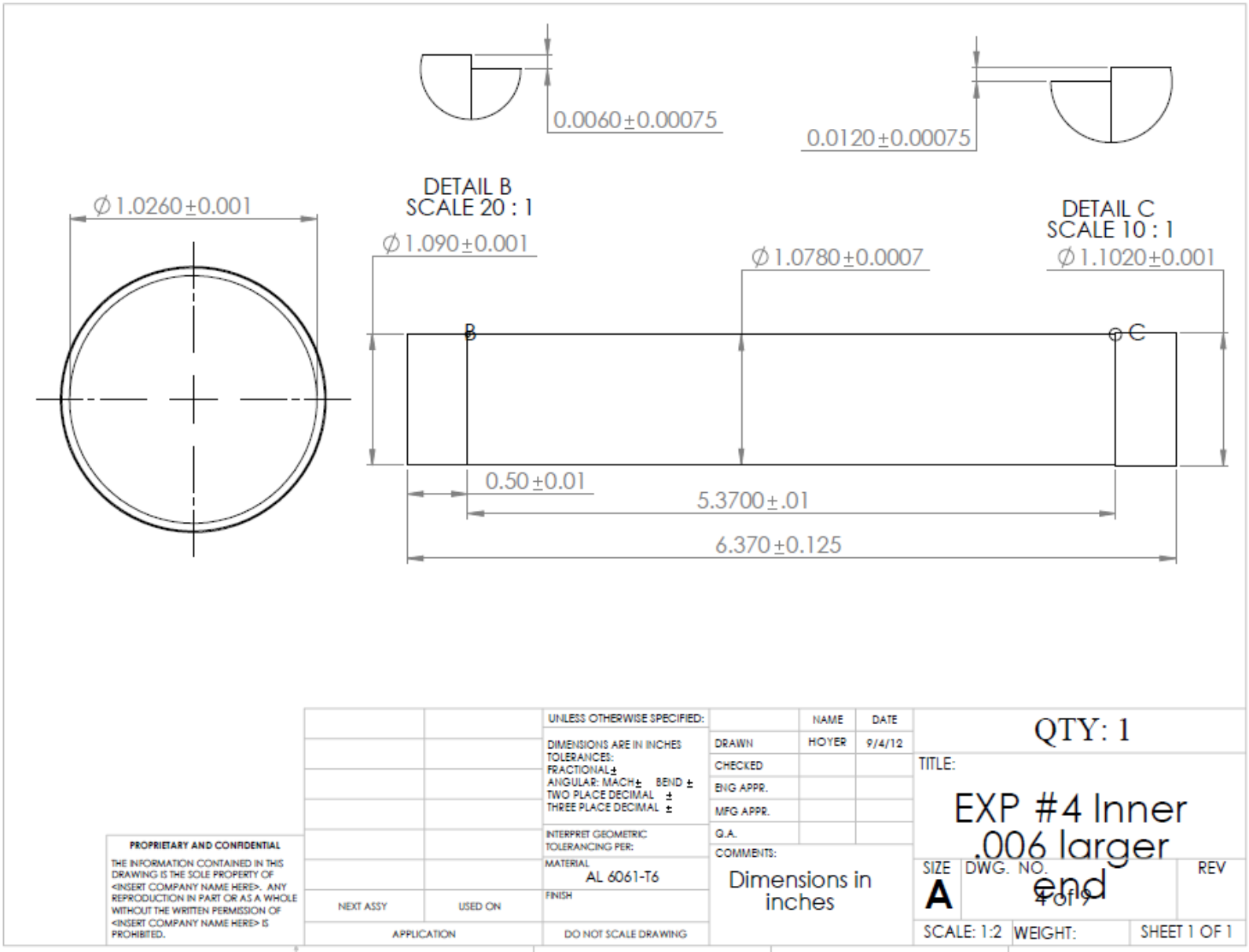
0.0060±0.00075
0.0120±0.00075
DETAIL B
SCALE 20 : 1
DETAIL C
SCALE 10 : 1
Ø1.0260±0.001
Ø1.090±0.001
Ø1.0780±0.0007
Ø1.1020±0.001
B
C
0.50±0.01
5.3700±.01
6.370±0.125
PROPRIETARY AND CONFIDENTIAL
THE INFORMATION CONTAINED IN THIS DRAWING IS THE SOLE PROPERTY OF <INSERT COMPANY NAME HERE>. ANY REPRODUCTION IN PART OR AS A WHOLE WITHOUT THE WRITTEN PERMISSION OF <INSERT COMPANY NAME HERE> IS PROHIBITED.
UNLESS OTHERWISE SPECIFIED:
DIMENSIONS ARE IN INCHES
TOLERANCES:
FRACTIONAL±
ANGULAR: MACH± BEND ±
TWO PLACE DECIMAL ±
THREE PLACE DECIMAL ±
INTERPRET GEOMETRIC TOLERANCING PER:
MATERIAL
AL 6061-T6
FINISH
NEXT ASSY
USED ON
APPLICATION
DO NOT SCALE DRAWING
NAME
DATE
DRAWN
HOYER
9/4/12
CHECKED
ENG APPR.
MFG APPR.
Q.A.
COMMENTS:
Dimensions in inches
QTY: 1
TITLE:
EXP #4 Inner .006 larger end
SIZE
A
DWG. NO.
4 of 9
REV
SCALE: 1:2
WEIGHT:
SHEET 1 OF 1
5
4
3
2
1

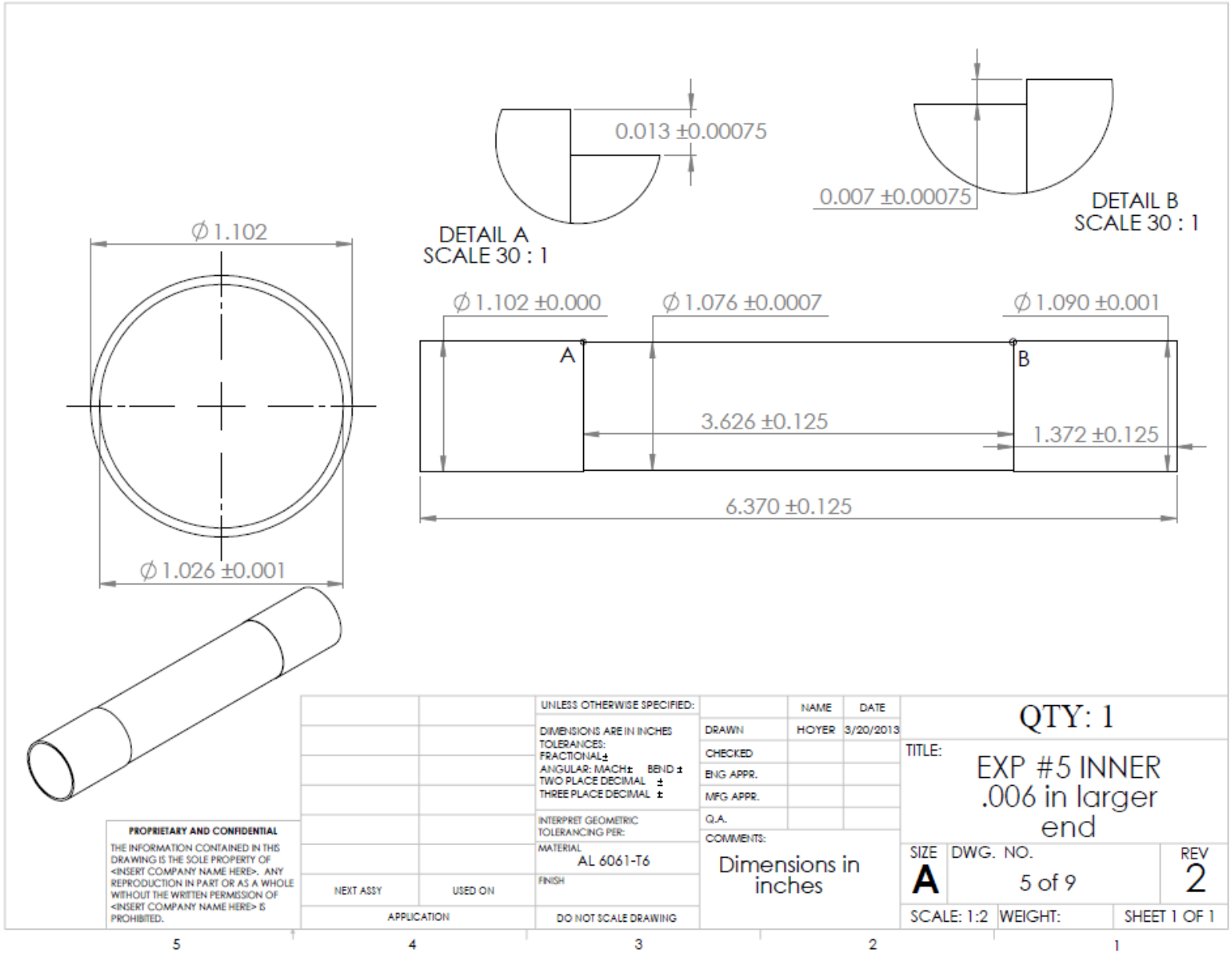
0.013 ±0.00075
DETAIL A
SCALE 30 : 1
0.007 ±0.00075
DETAIL B
SCALE 30 : 1
∅1.102
∅1.026 ±0.001
∅1.102 ±0.000
∅1.076 ±0.0007
∅1.090 ±0.001
A
B
3.626 ±0.125
1.372 ±0.125
6.370 ±0.125
PROPRIETARY AND CONFIDENTIAL
THE INFORMATION CONTAINED IN THIS DRAWING IS THE SOLE PROPERTY OF <INSERT COMPANY NAME HERE>. ANY REPRODUCTION IN PART OR AS A WHOLE WITHOUT THE WRITTEN PERMISSION OF <INSERT COMPANY NAME HERE> IS PROHIBITED.
UNLESS OTHERWISE SPECIFIED:
DIMENSIONS ARE IN INCHES
TOLERANCES:
FRACTIONAL ±
ANGULAR: MACH ± BEND ±
TWO PLACE DECIMAL ±
THREE PLACE DECIMAL ±
INTERPRET GEOMETRIC TOLERANCING PER:
MATERIAL
AL 6061-T6
FINISH
NEXT ASSY
USED ON
APPLICATION
DO NOT SCALE DRAWING
NAME
DATE
DRAWN
HOYER
3/20/2013
CHECKED
ENG APPR.
MFG APPR.
Q.A.
COMMENTS:
Dimensions in inches
QTY: 1
TITLE:
EXP #5 INNER .006 in larger end
SIZE
A
DWG. NO.
5 of 9
REV
2
SCALE: 1:2
WEIGHT:
SHEET 1 OF 1
5
4
3
2
1

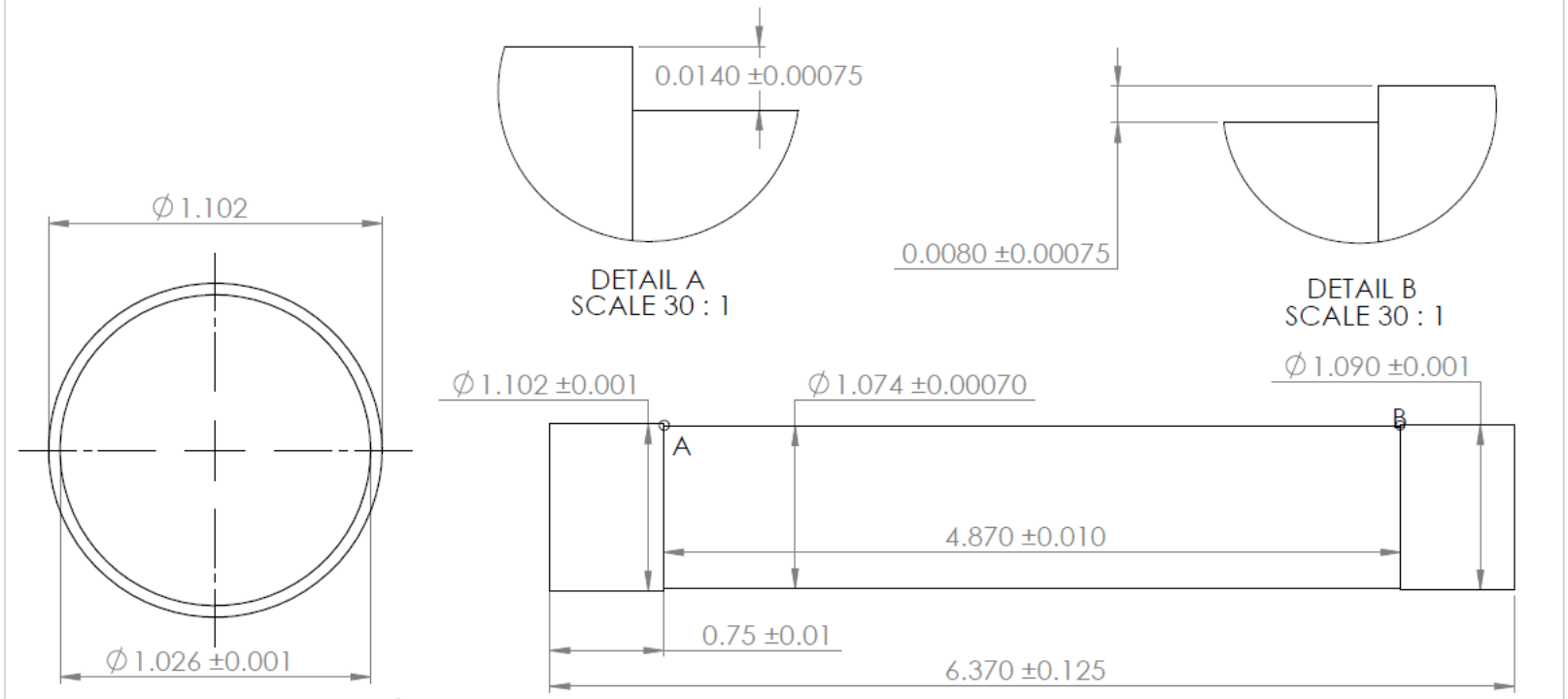

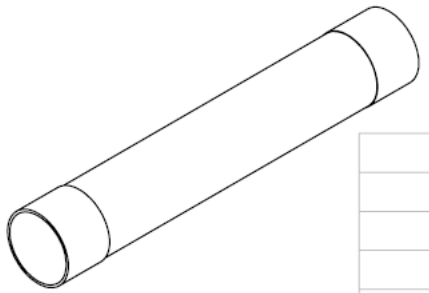

NEXT ASSY	USED ON	
APPLICATION		

UNLESS OTHERWISE SPECIFIED:

DIMENSIONS ARE IN INCHES
TOLERANCES:
FRACTIONAL ±
ANGULAR: MACH ± BEND ±
TWO PLACE DECIMAL ±
THREE PLACE DECIMAL ±

INTERPRET GEOMETRIC TOLERANCING PER:

MATERIAL
AL 6061-T6

FINISH

DO NOT SCALE DRAWING

	NAME	DATE
DRAWN	HOYER	9/4/12
CHECKED		
ENG APPR.		
MFG APPR.		
Q.A.		

COMMENTS:
Dimensions in inches

QTY: 1

TITLE:
EXP #6 INNER .006 in larger end

SIZE	DWG. NO.	REV
A	6 of 9	2

SCALE: 1:2 | WEIGHT: | SHEET 1 OF 1

5 4 3 2 1

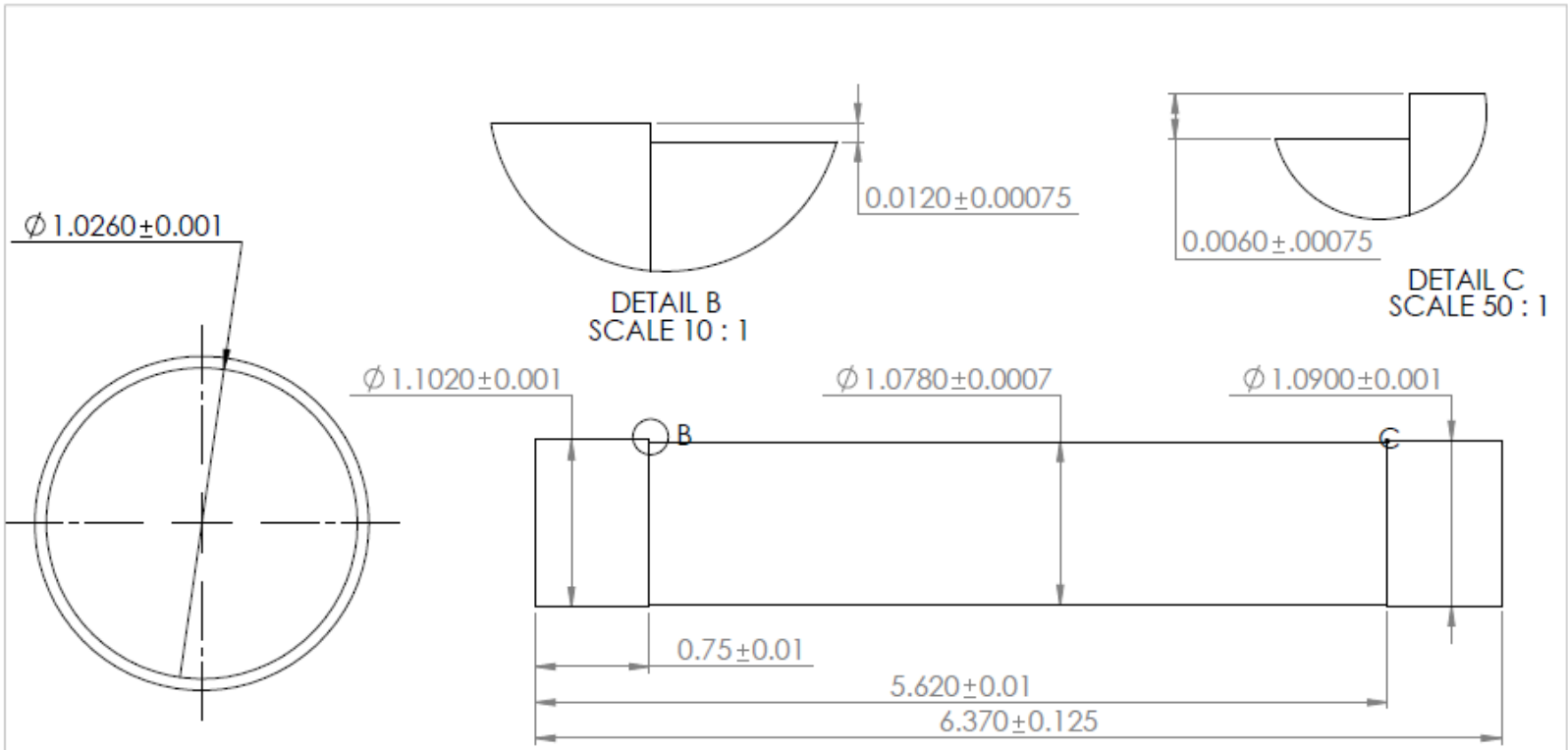

		UNLESS OTHERWISE SPECIFIED:		NAME	DATE
		DIMENSIONS ARE IN INCHES TOLERANCES: FRACTIONAL ± ANGULAR: MACH ± BEND ± TWO PLACE DECIMAL ± THREE PLACE DECIMAL ±	DRAWN	HOYER	9/4/12
			CHECKED		
			ENG APPR.		
			MFG APPR.		
		INTERPRET GEOMETRIC TOLERANCING PER:	Q.A.		
		MATERIAL AL 6061-T6	COMMENTS: Dimensions in inches		
NEXT ASSY	USED ON	FINISH			
APPLICATION		DO NOT SCALE DRAWING			

QTY: 1

TITLE: EXP #7 Inner .006 in larger end

SIZE	DWG. NO.	REV
A	4 of 9	

SCALE: 1:2 | WEIGHT: | SHEET 1 OF 1

5 4 3 2 1

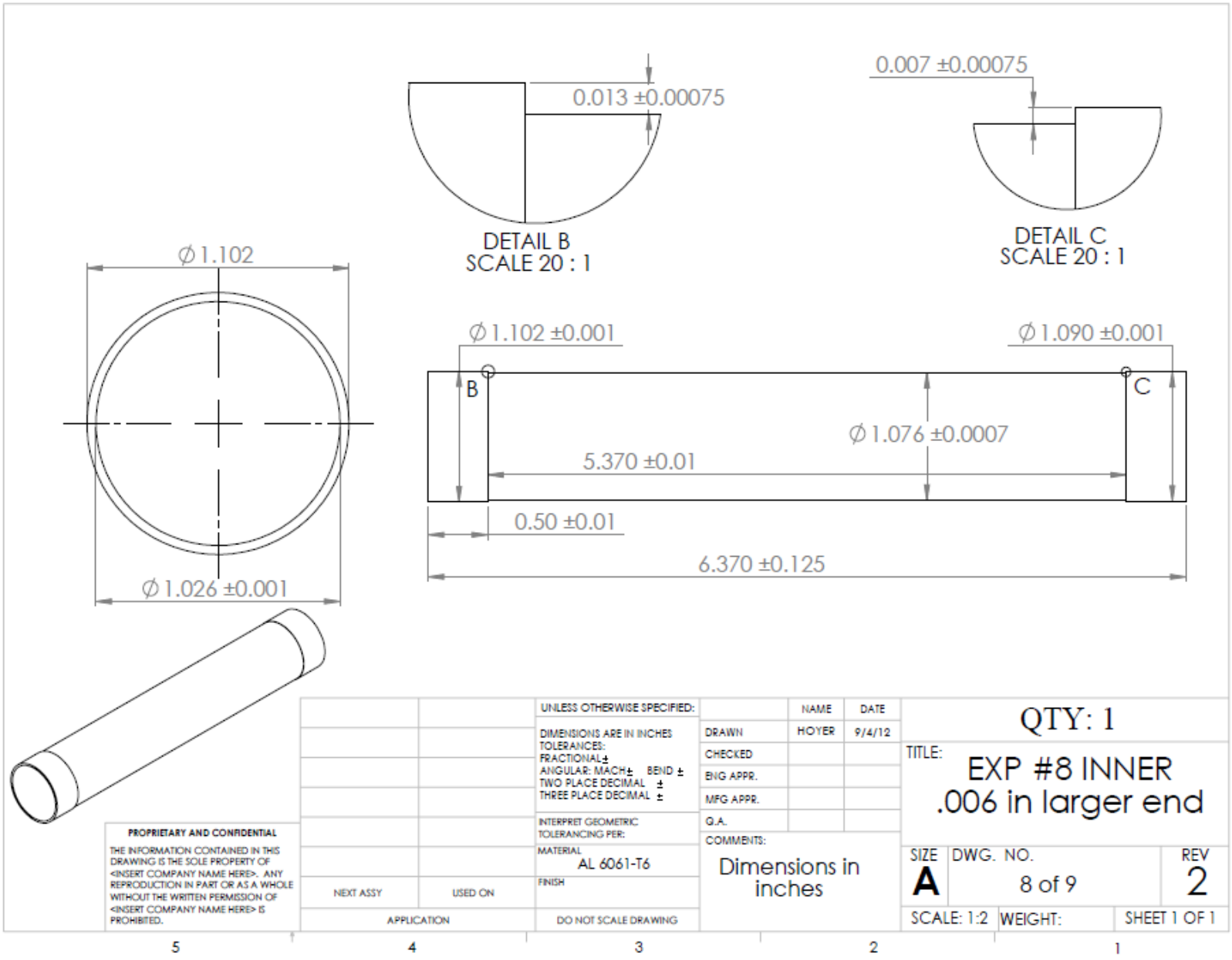
0.013 ±0.00075
DETAIL B
SCALE 20 : 1
0.007 ±0.00075
DETAIL C
SCALE 20 : 1
∅1.102
∅1.026 ±0.001
∅1.102 ±0.001
∅1.090 ±0.001
B
C
∅1.076 ±0.0007
5.370 ±0.01
0.50 ±0.01
6.370 ±0.125
PROPRIETARY AND CONFIDENTIAL
THE INFORMATION CONTAINED IN THIS DRAWING IS THE SOLE PROPERTY OF <INSERT COMPANY NAME HERE>. ANY REPRODUCTION IN PART OR AS A WHOLE WITHOUT THE WRITTEN PERMISSION OF <INSERT COMPANY NAME HERE> IS PROHIBITED.
UNLESS OTHERWISE SPECIFIED:
DIMENSIONS ARE IN INCHES
TOLERANCES:
FRACTIONAL ±
ANGULAR: MACH ± BEND ±
TWO PLACE DECIMAL ±
THREE PLACE DECIMAL ±
INTERPRET GEOMETRIC TOLERANCING PER:
MATERIAL
AL 6061-T6
FINISH
NEXT ASSY
USED ON
APPLICATION
DO NOT SCALE DRAWING
NAME
DATE
DRAWN
HOYER
9/4/12
CHECKED
ENG APPR.
MFG APPR.
Q.A.
COMMENTS:
Dimensions in inches
QTY: 1
TITLE:
EXP #8 INNER
.006 in larger end
SIZE
A
DWG. NO.
8 of 9
REV
2
SCALE: 1:2
WEIGHT:
SHEET 1 OF 1
5
4
3
2
1

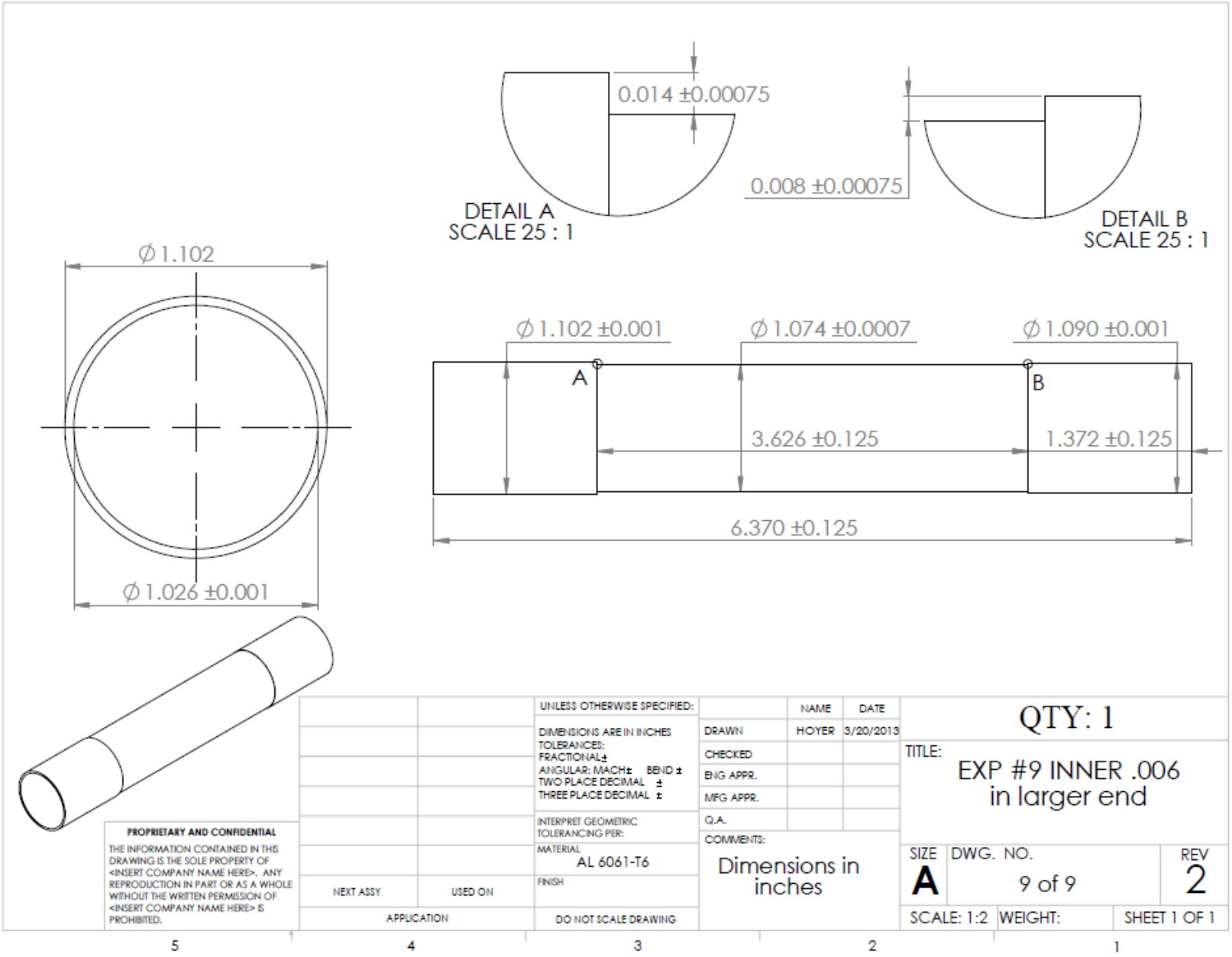
0.014 ±0.00075
DETAIL A
SCALE 25 : 1
0.008 ±0.00075
DETAIL B
SCALE 25 : 1
∅1.102
∅1.026 ±0.001
∅1.102 ±0.001
∅1.074 ±0.0007
∅1.090 ±0.001
A
B
3.626 ±0.125
1.372 ±0.125
6.370 ±0.125
PROPRIETARY AND CONFIDENTIAL
THE INFORMATION CONTAINED IN THIS DRAWING IS THE SOLE PROPERTY OF <INSERT COMPANY NAME HERE>. ANY REPRODUCTION IN PART OR AS A WHOLE WITHOUT THE WRITTEN PERMISSION OF <INSERT COMPANY NAME HERE> IS PROHIBITED.
NEXT ASSY
USED ON
APPLICATION
UNLESS OTHERWISE SPECIFIED:
DIMENSIONS ARE IN INCHES
TOLERANCES:
FRACTIONAL ±
ANGULAR: MACH ± BEND ±
TWO PLACE DECIMAL ±
THREE PLACE DECIMAL ±
INTERPRET GEOMETRIC TOLERANCING PER:
MATERIAL
AL 6061-T6
FINISH
DO NOT SCALE DRAWING
NAME
DATE
DRAWN
HOYER
3/20/2013
CHECKED
ENG APPR.
MFG APPR.
Q.A.
COMMENTS:
Dimensions in inches
QTY: 1
TITLE:
EXP #9 INNER .006 in larger end
SIZE
A
DWG. NO.
9 of 9
REV
2
SCALE: 1:2
WEIGHT:
SHEET 1 OF 1
5
4
3
2
1

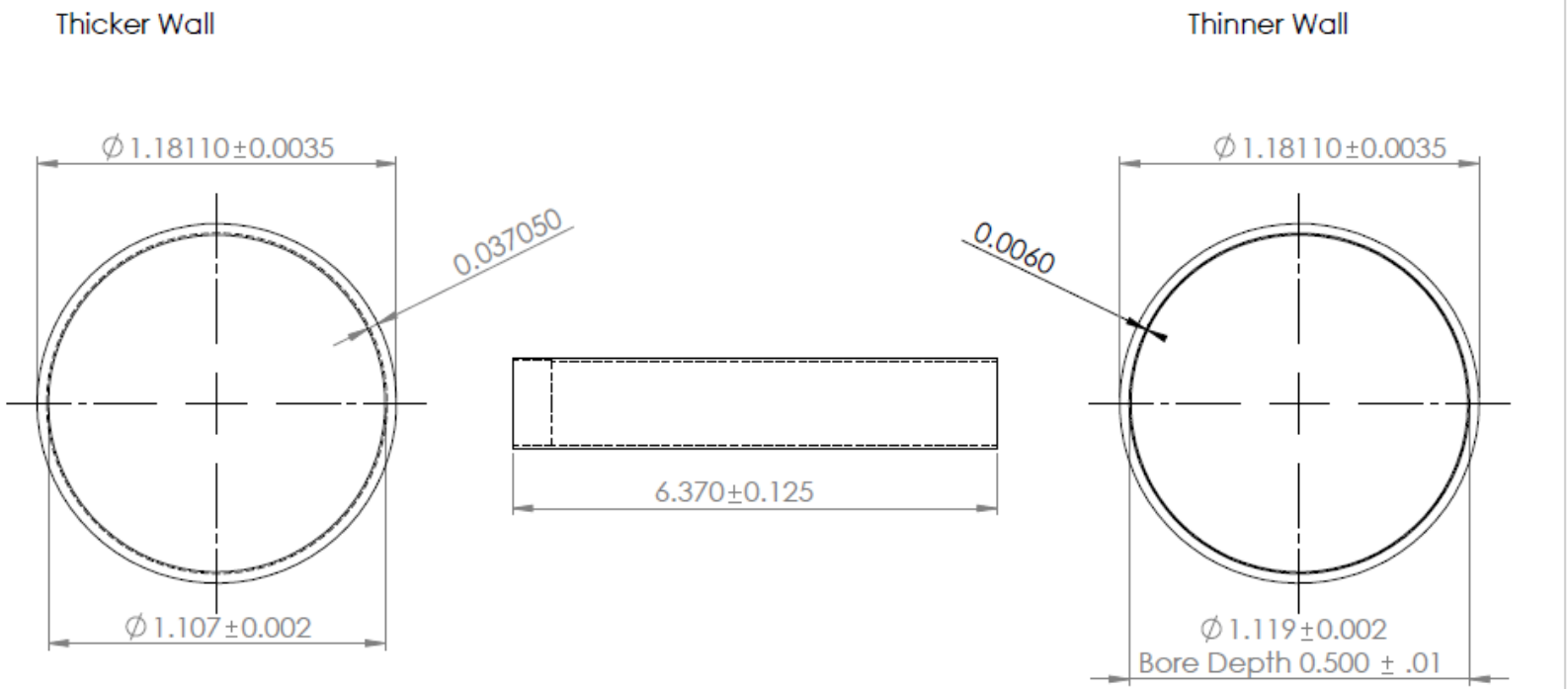

		UNLESS OTHERWISE SPECIFIED:		NAME	DATE
		DIMENSIONS ARE IN INCHES TOLERANCES: FRACTIONAL ± ANGULAR: MACH ± BEND ± TWO PLACE DECIMAL ± THREE PLACE DECIMAL ±	DRAWN	Hoyer	8/10/12
			CHECKED		
			ENG APPR.		
			MFG APPR.		
			Q.A.		
		INTERPRET GEOMETRIC TOLERANCING PER:	COMMENTS:		
		MATERIAL AL 6061-T6	Dimensions in inches		
NEXT ASSY	USED ON	FINISH			
APPLICATION		DO NOT SCALE DRAWING			

QTY: 3

TITLE:
Outer Tube
MU Design .006 in larger end

SIZE	DWG. NO.	REV
A		2

SCALE: 1:2	WEIGHT:	SHEET 1 OF 1

5 4 3 2 1

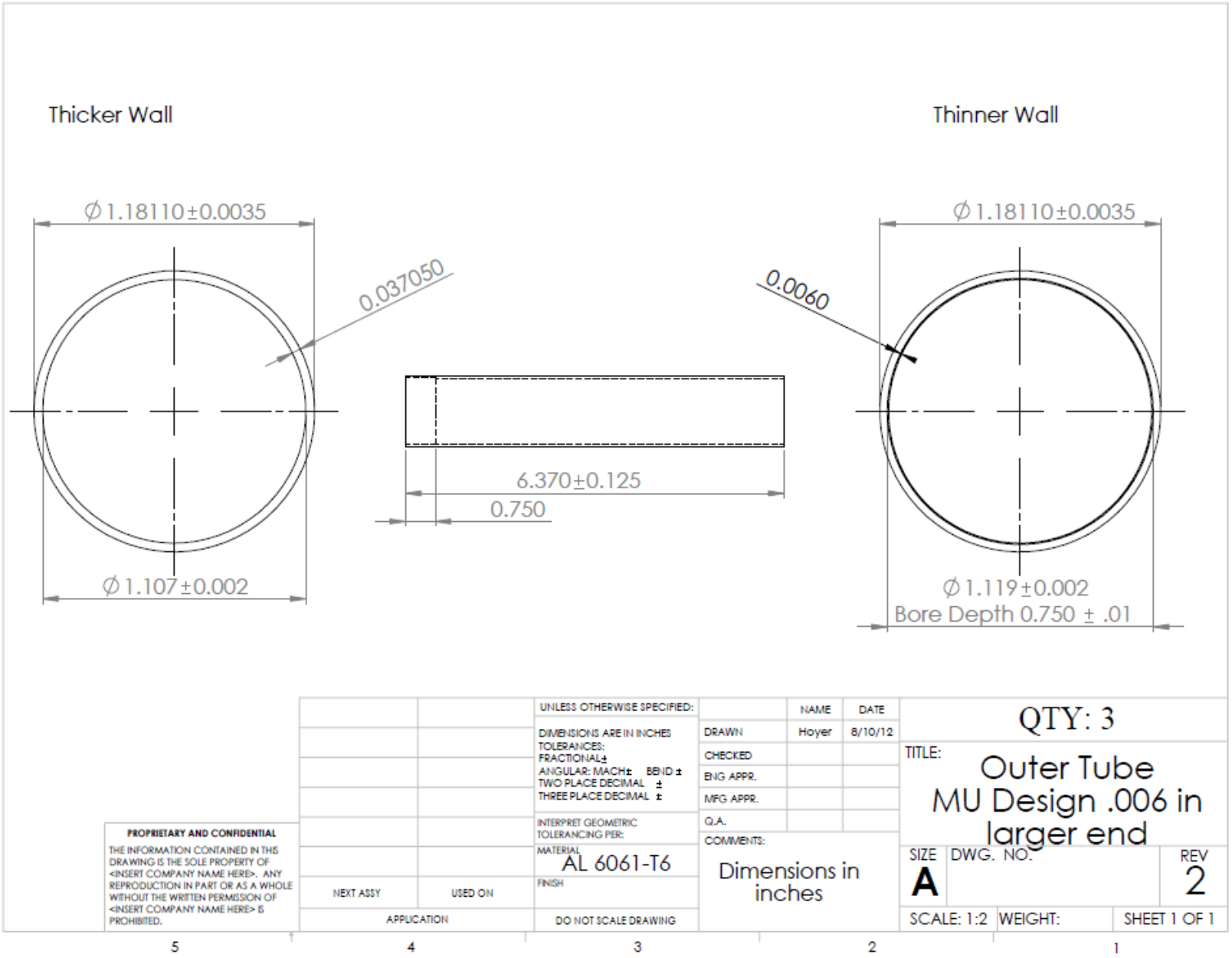
Thicker Wall
Thinner Wall
∅1.18110±0.0035
0.037050
0.0060
∅1.18110±0.0035
6.370±0.125
0.750
∅1.107±0.002
∅1.119±0.002
Bore Depth 0.750 ± .01
UNLESS OTHERWISE SPECIFIED:
DIMENSIONS ARE IN INCHES
TOLERANCES:
FRACTIONAL±
ANGULAR: MACH± BEND ±
TWO PLACE DECIMAL ±
THREE PLACE DECIMAL ±
INTERPRET GEOMETRIC TOLERANCING PER:
MATERIAL
AL 6061-T6
FINISH
DO NOT SCALE DRAWING
NEXT ASSY
USED ON
APPLICATION
NAME
DATE
DRAWN
Hoyer
8/10/12
CHECKED
ENG APPR.
MFG APPR.
Q.A.
COMMENTS:
Dimensions in inches
QTY: 3
TITLE:
Outer Tube
MU Design .006 in larger end
SIZE
A
DWG. NO.
REV
2
SCALE: 1:2
WEIGHT:
SHEET 1 OF 1
PROPRIETARY AND CONFIDENTIAL
THE INFORMATION CONTAINED IN THIS DRAWING IS THE SOLE PROPERTY OF <INSERT COMPANY NAME HERE>. ANY REPRODUCTION IN PART OR AS A WHOLE WITHOUT THE WRITTEN PERMISSION OF <INSERT COMPANY NAME HERE> IS PROHIBITED.
5
4
3
2
1

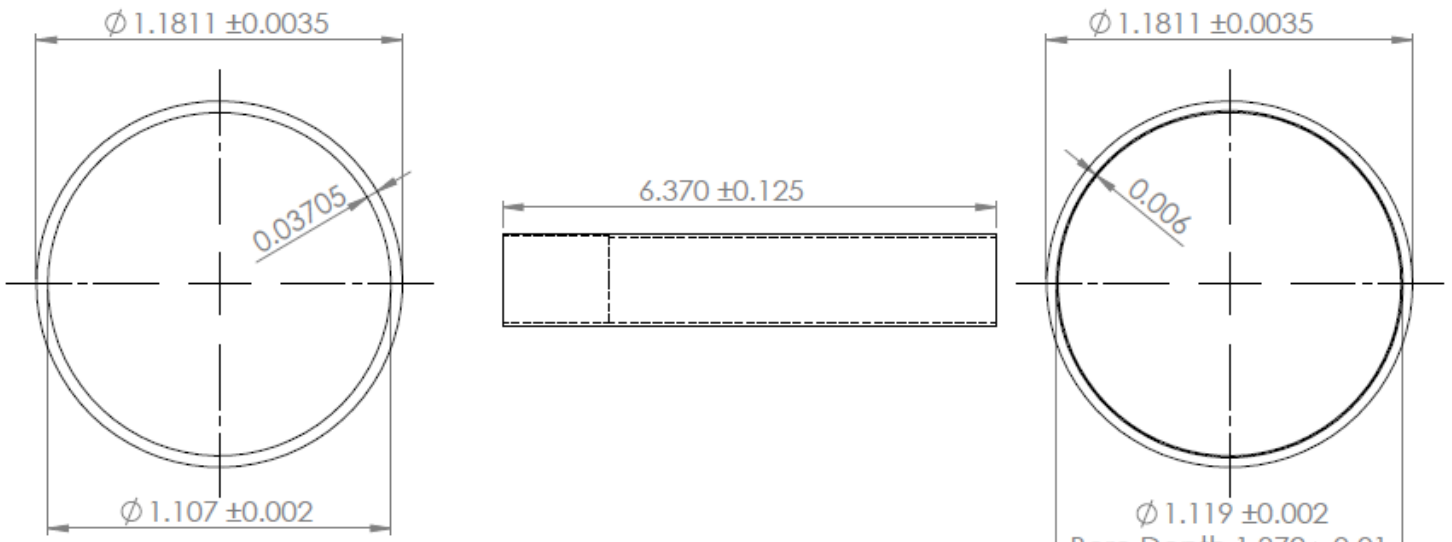

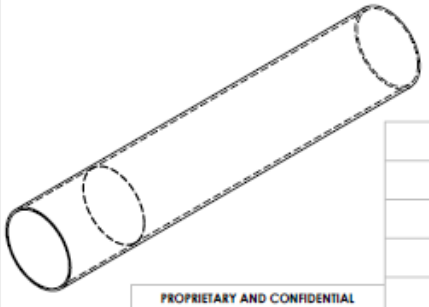

		UNLESS OTHERWISE SPECIFIED:		NAME	DATE
		DIMENSIONS ARE IN INCHES TOLERANCES: FRACTIONAL± ANGULAR: MACH± BEND ± TWO PLACE DECIMAL ± THREE PLACE DECIMAL ±	DRAWN	HOYER	3/6/13
			CHECKED		
			ENG APPR.		
			MFG APPR.		
		INTERPRET GEOMETRIC TOLERANCING PER:	Q.A.		
		MATERIAL AL 6061-T6	COMMENTS: Dimensions in inches		
NEXT ASSY	USED ON	FINISH			
APPLICATION		DO NOT SCALE DRAWING			

QTY: 3

TITLE: Outer Tube MU Design .006 larger end

SIZE	DWG. NO.	REV
A	2 of 2	2

SCALE: 1:2 | WEIGHT: | SHEET 1 OF 1

5 4 3 2 1

APPENDIX D

PLUG DRAWINGS

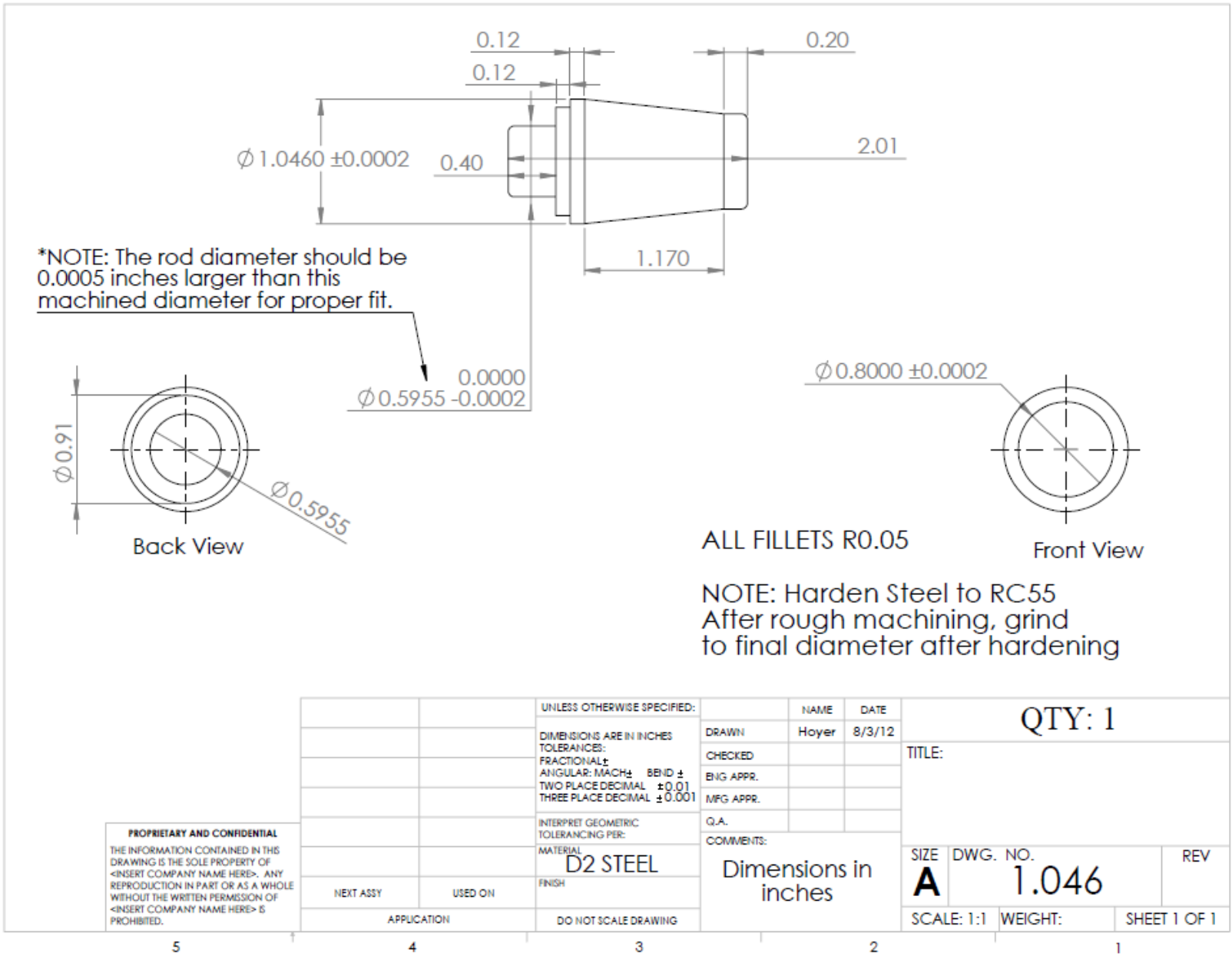
0.12
0.12
0.20
Ø 1.0460 ±0.0002
0.40
2.01
1.170
*NOTE: The rod diameter should be 0.0005 inches larger than this machined diameter for proper fit.
0.0000
Ø 0.5955 -0.0002
Ø 0.91
Ø 0.5955
Back View
Ø 0.8000 ±0.0002
Front View
ALL FILLETS R0.05
NOTE: Harden Steel to RC55
After rough machining, grind
to final diameter after hardening
UNLESS OTHERWISE SPECIFIED:
DIMENSIONS ARE IN INCHES
TOLERANCES:
FRACTIONAL ±
ANGULAR: MACH ± BEND ±
TWO PLACE DECIMAL ±0.01
THREE PLACE DECIMAL ±0.001
INTERPRET GEOMETRIC TOLERANCING PER:
MATERIAL
D2 STEEL
FINISH
NEXT ASSY
USED ON
APPLICATION
DO NOT SCALE DRAWING
NAME
DATE
DRAWN
Hoyer
8/3/12
CHECKED
ENG APPR.
MFG APPR.
Q.A.
COMMENTS:
Dimensions in inches
QTY: 1
TITLE:
SIZE
A
DWG. NO.
1.046
REV
SCALE: 1:1
WEIGHT:
SHEET 1 OF 1
PROPRIETARY AND CONFIDENTIAL
THE INFORMATION CONTAINED IN THIS DRAWING IS THE SOLE PROPERTY OF <INSERT COMPANY NAME HERE>. ANY REPRODUCTION IN PART OR AS A WHOLE WITHOUT THE WRITTEN PERMISSION OF <INSERT COMPANY NAME HERE> IS PROHIBITED.
5
4
3
2
1

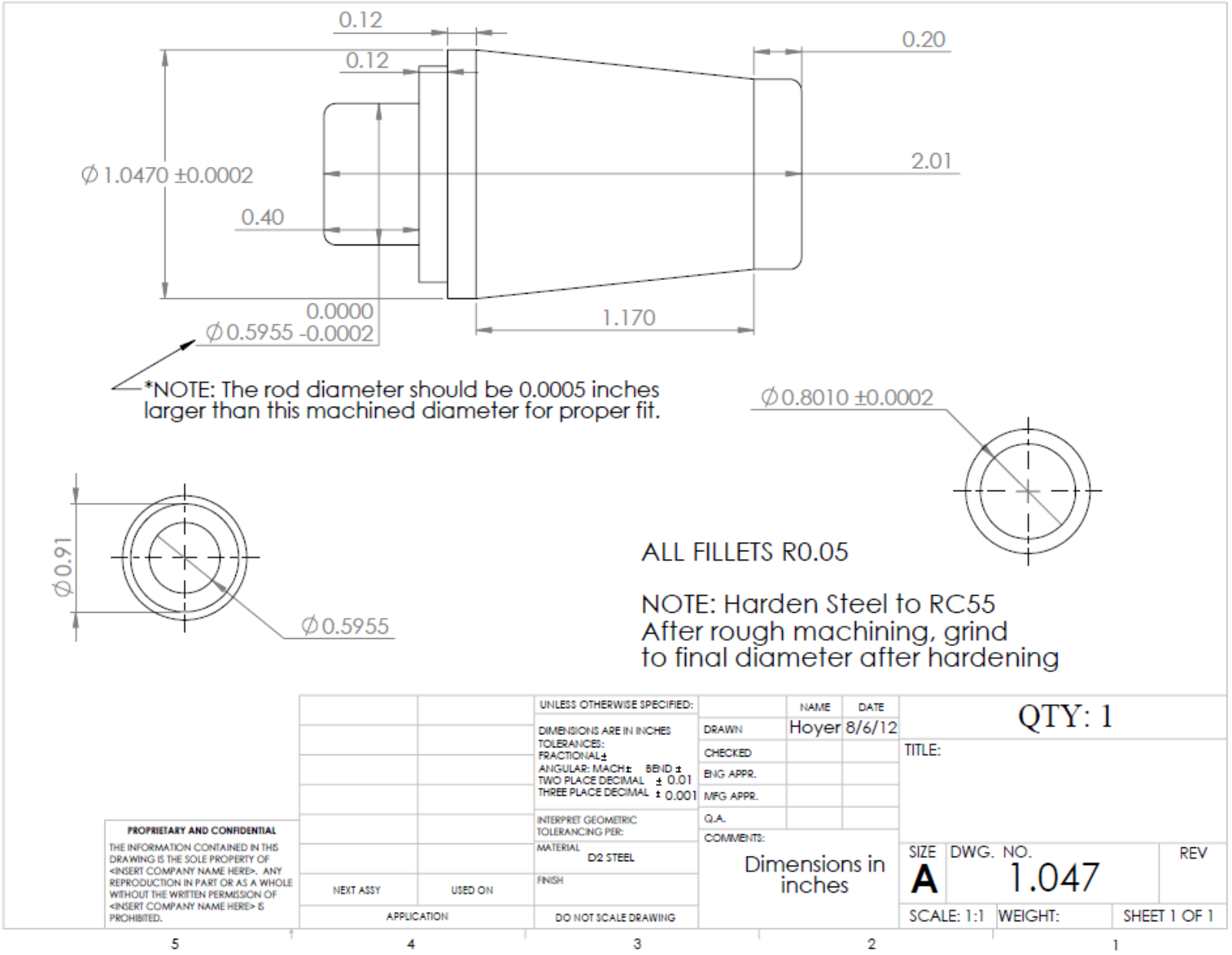
0.12
0.12
0.20
2.01
∅1.0470 ±0.0002
0.40
0.0000
∅0.5955 -0.0002
1.170
*NOTE: The rod diameter should be 0.0005 inches larger than this machined diameter for proper fit.
∅0.8010 ±0.0002
∅0.91
∅0.5955
ALL FILLETS R0.05
NOTE: Harden Steel to RC55
After rough machining, grind
to final diameter after hardening
UNLESS OTHERWISE SPECIFIED:
DIMENSIONS ARE IN INCHES
TOLERANCES:
FRACTIONAL ±
ANGULAR: MACH ± BEND ±
TWO PLACE DECIMAL ± 0.01
THREE PLACE DECIMAL ± 0.001
INTERPRET GEOMETRIC TOLERANCING PER:
MATERIAL
D2 STEEL
FINISH
NEXT ASSY
USED ON
APPLICATION
DO NOT SCALE DRAWING
NAME
DATE
DRAWN
Hoyer
8/6/12
CHECKED
ENG APPR.
MFG APPR.
Q.A.
COMMENTS:
Dimensions in inches
QTY: 1
TITLE:
SIZE
A
DWG. NO.
1.047
REV
SCALE: 1:1
WEIGHT:
SHEET 1 OF 1
PROPRIETARY AND CONFIDENTIAL
THE INFORMATION CONTAINED IN THIS DRAWING IS THE SOLE PROPERTY OF <INSERT COMPANY NAME HERE>. ANY REPRODUCTION IN PART OR AS A WHOLE WITHOUT THE WRITTEN PERMISSION OF <INSERT COMPANY NAME HERE> IS PROHIBITED.
5
4
3
2
1

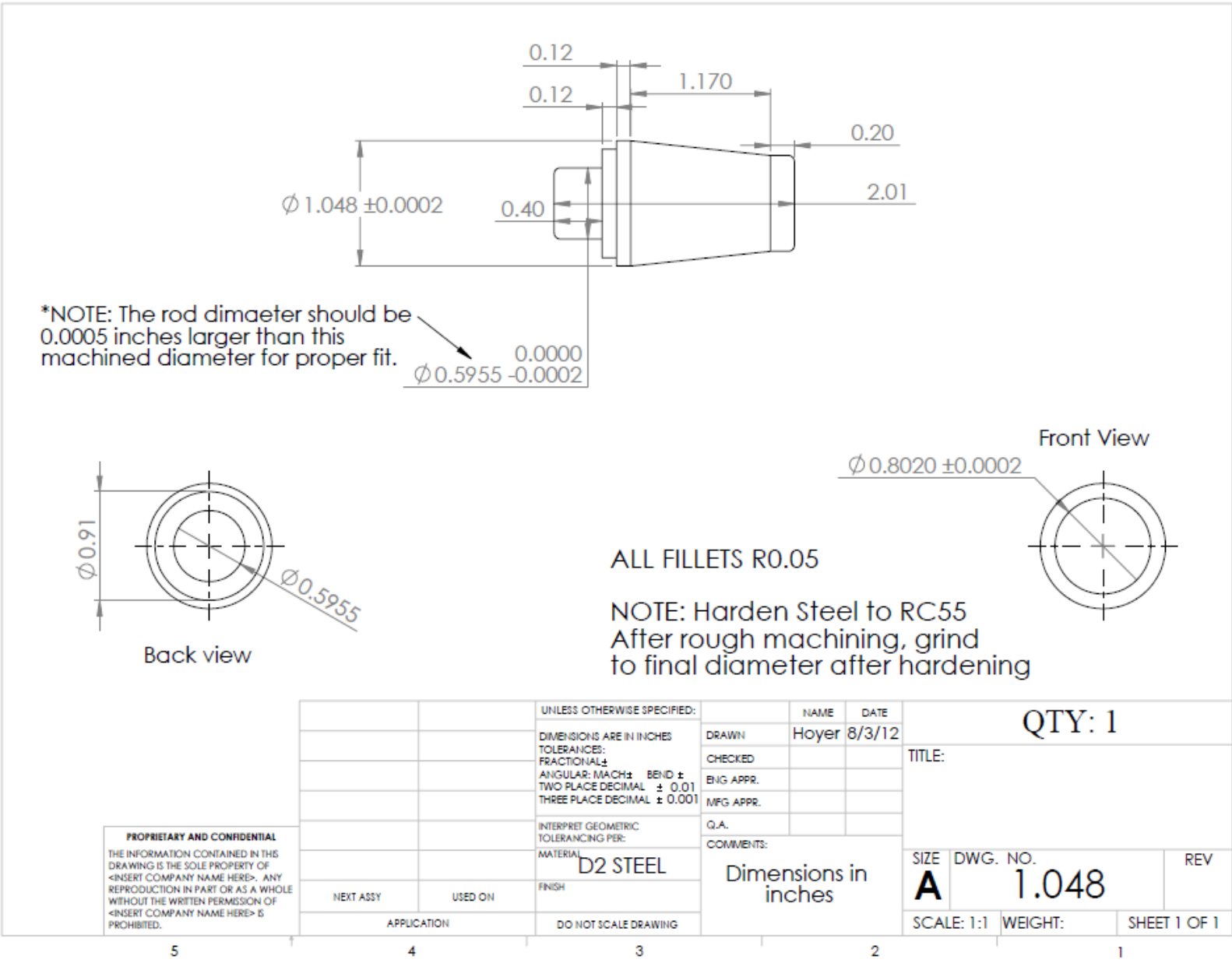
0.12
0.12
1.170
0.20
2.01
∅1.048 ±0.0002
0.40
*NOTE: The rod dimaeter should be 0.0005 inches larger than this machined diameter for proper fit.
0.0000
∅0.5955 -0.0002
Front View
∅0.8020 ±0.0002
∅0.91
∅0.5955
Back view
ALL FILLETS R0.05
NOTE: Harden Steel to RC55
After rough machining, grind to final diameter after hardening
UNLESS OTHERWISE SPECIFIED:
DIMENSIONS ARE IN INCHES
TOLERANCES:
FRACTIONAL ±
ANGULAR: MACH ± BEND ±
TWO PLACE DECIMAL ± 0.01
THREE PLACE DECIMAL ± 0.001
INTERPRET GEOMETRIC TOLERANCING PER:
MATERIAL D2 STEEL
FINISH
NEXT ASSY
USED ON
APPLICATION
DO NOT SCALE DRAWING
NAME
DATE
DRAWN Hoyer 8/3/12
CHECKED
ENG APPR.
MFG APPR.
Q.A.
COMMENTS:
Dimensions in inches
QTY: 1
TITLE:
SIZE A
DWG. NO. 1.048
REV
SCALE: 1:1
WEIGHT:
SHEET 1 OF 1
PROPRIETARY AND CONFIDENTIAL
THE INFORMATION CONTAINED IN THIS DRAWING IS THE SOLE PROPERTY OF <INSERT COMPANY NAME HERE>. ANY REPRODUCTION IN PART OR AS A WHOLE WITHOUT THE WRITTEN PERMISSION OF <INSERT COMPANY NAME HERE> IS PROHIBITED.
5
4
3
2
1

APPENDIX E

ASSEMBLY RIG DRAWINGS

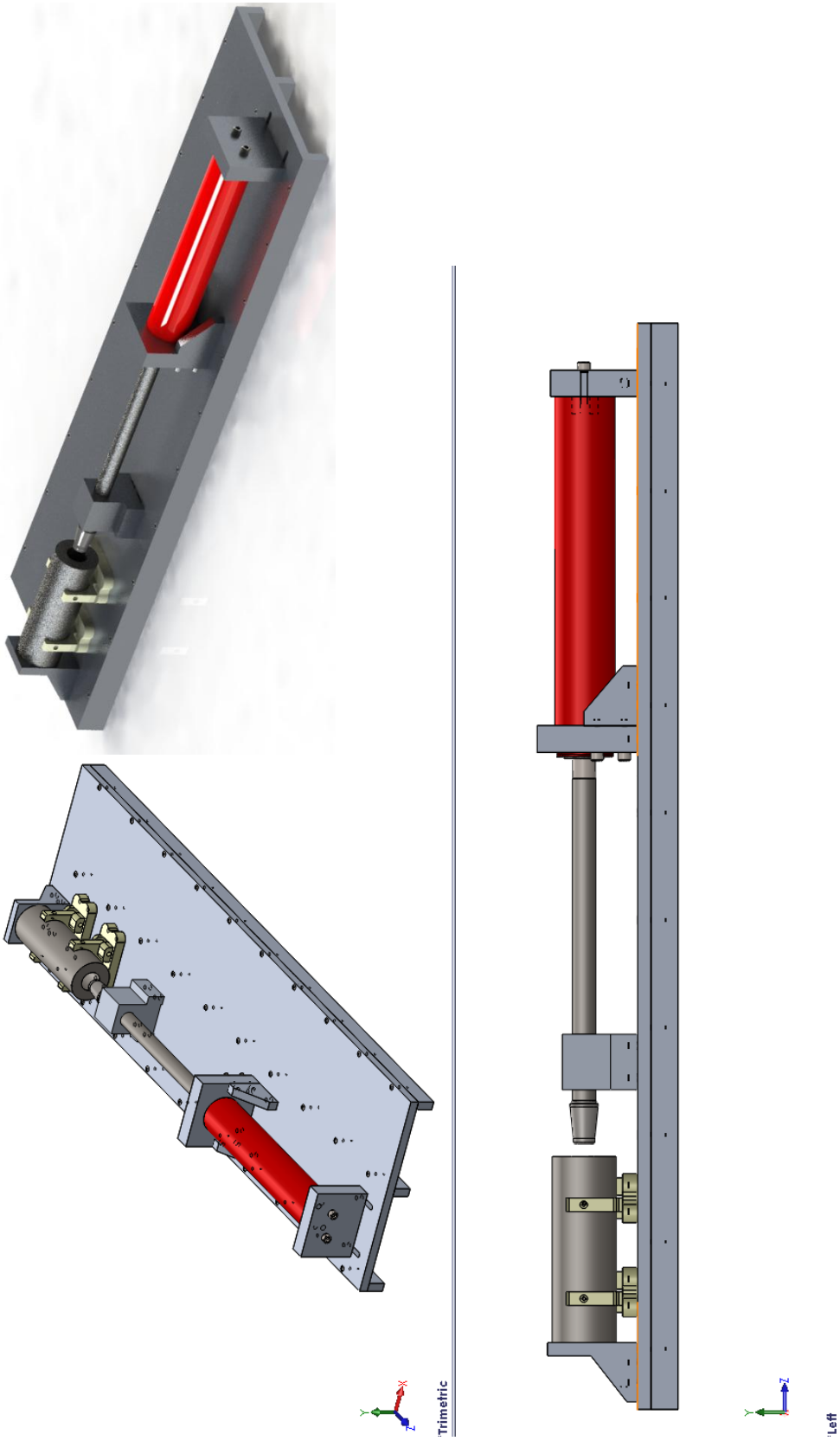
Trimetric
Left

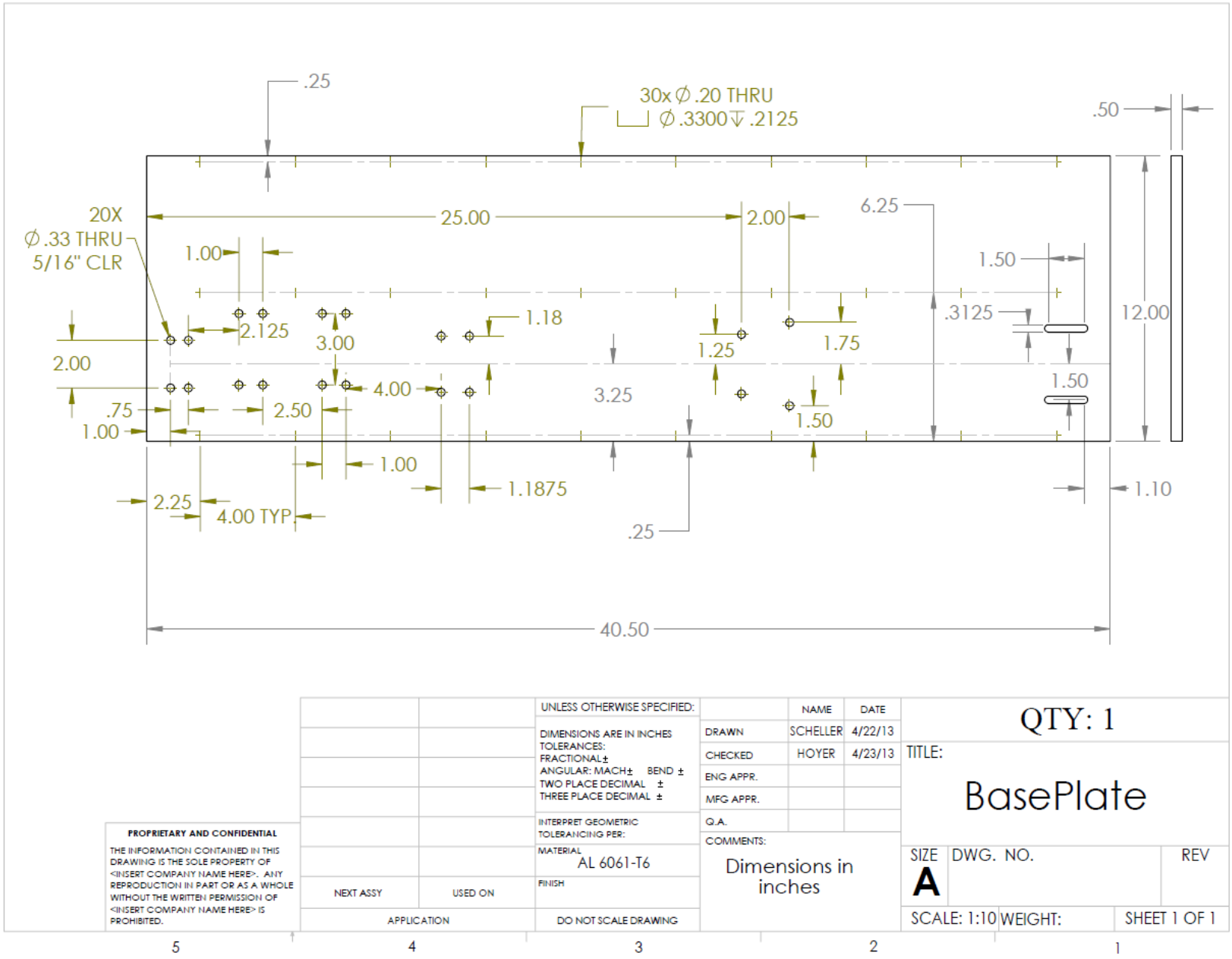
.25
30x ∅ .20 THRU
∅ .3300 ↧ .2125
.50
20X
∅ .33 THRU
5/16" CLR
25.00
2.00
6.25
1.00
1.50
.3125
12.00
2.125
3.00
1.18
1.25
1.75
2.00
4.00
3.25
1.50
.75
2.50
1.50
1.00
1.00
1.1875
1.10
2.25
4.00 TYP.
.25
40.50
PROPRIETARY AND CONFIDENTIAL
THE INFORMATION CONTAINED IN THIS DRAWING IS THE SOLE PROPERTY OF <INSERT COMPANY NAME HERE>. ANY REPRODUCTION IN PART OR AS A WHOLE WITHOUT THE WRITTEN PERMISSION OF <INSERT COMPANY NAME HERE> IS PROHIBITED.
NEXT ASSY
USED ON
APPLICATION
UNLESS OTHERWISE SPECIFIED:
DIMENSIONS ARE IN INCHES
TOLERANCES:
FRACTIONAL ±
ANGULAR: MACH ± BEND ±
TWO PLACE DECIMAL ±
THREE PLACE DECIMAL ±
INTERPRET GEOMETRIC TOLERANCING PER:
MATERIAL
AL 6061-T6
FINISH
DO NOT SCALE DRAWING
NAME
DATE
DRAWN
SCHELLER
4/22/13
CHECKED
HOYER
4/23/13
ENG APPR.
MFG APPR.
Q.A.
COMMENTS:
Dimensions in inches
QTY: 1
TITLE:
BasePlate
SIZE
A
DWG. NO.
REV
SCALE: 1:10
WEIGHT:
SHEET 1 OF 1
5
4
3
2
1

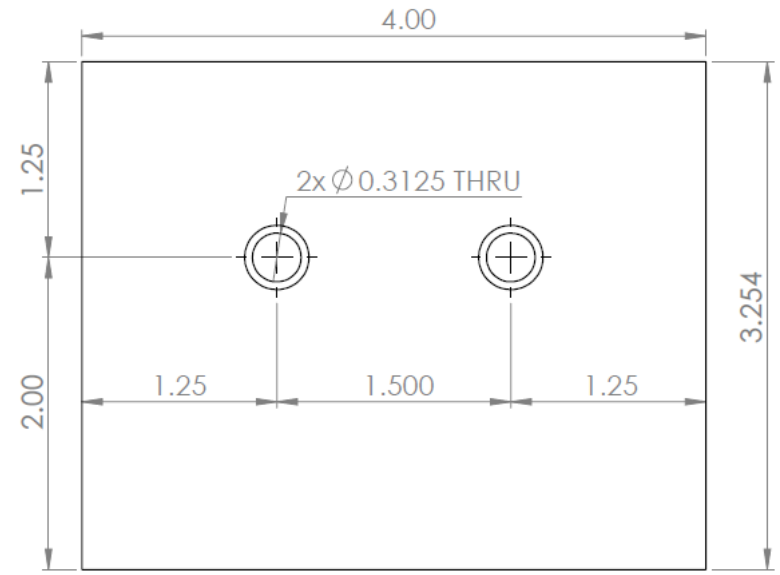

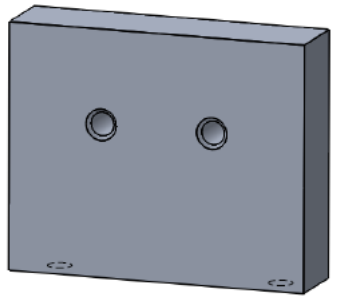

		UNLESS OTHERWISE SPECIFIED:		NAME	DATE
		DIMENSIONS ARE IN INCHES TOLERANCES: FRACTIONAL ± ANGULAR: MACH ± BEND ± TWO PLACE DECIMAL ± THREE PLACE DECIMAL ±	DRAWN	HOYER	4/22/13
			CHECKED		
			ENG APPR.		
			MFG APPR.		
		INTERPRET GEOMETRIC TOLERANCING PER:	Q.A.		
		MATERIAL AL 6061-T6	COMMENTS: Dimensions in inches		
NEXT ASSY	USED ON	FINISH			
APPLICATION		DO NOT SCALE DRAWING			

QTY: 1

TITLE:

CylinderBack

SIZE	DWG. NO.	REV
A		

SCALE: 1:2 | WEIGHT: | SHEET 1 OF 1

5 4 3 2 1

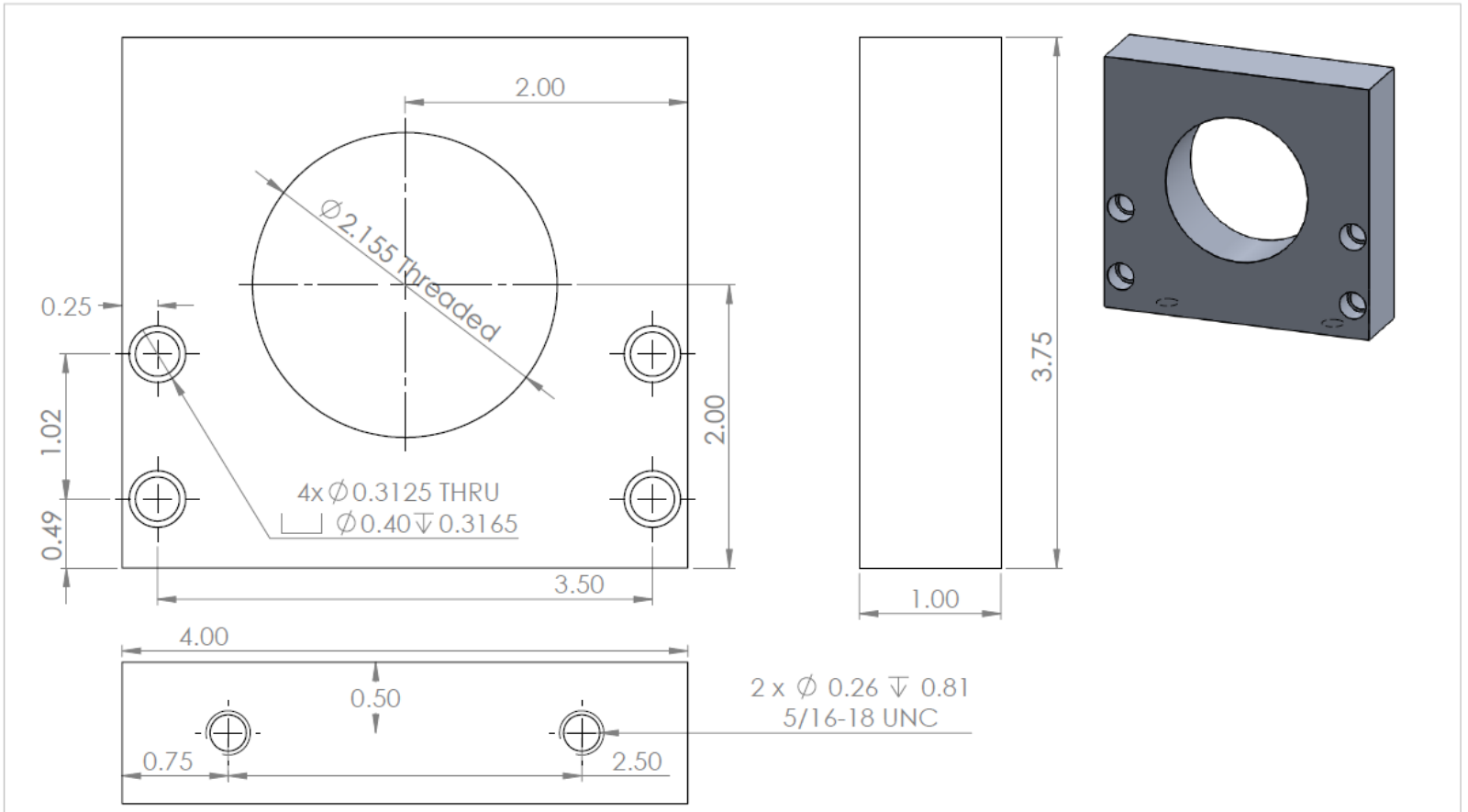

		UNLESS OTHERWISE SPECIFIED:		NAME	DATE
		DIMENSIONS ARE IN INCHES TOLERANCES: FRACTIONAL ± ANGULAR: MACH ± BEND ± TWO PLACE DECIMAL ± THREE PLACE DECIMAL ±	DRAWN	HOYER	4/22/13
			CHECKED		
			ENG APPR.		
			MFG APPR.		
		INTERPRET GEOMETRIC TOLERANCING PER:	Q.A.		
		MATERIAL AL 6061-T6	COMMENTS: Dimensions in inches		
NEXT ASSY	USED ON	FINISH			
APPLICATION		DO NOT SCALE DRAWING			

QTY: 1

TITLE:

CylinderSupport

SIZE	DWG. NO.	REV
A		
SCALE: 1:2	WEIGHT:	SHEET 1 OF 1

5 4 3 2 1

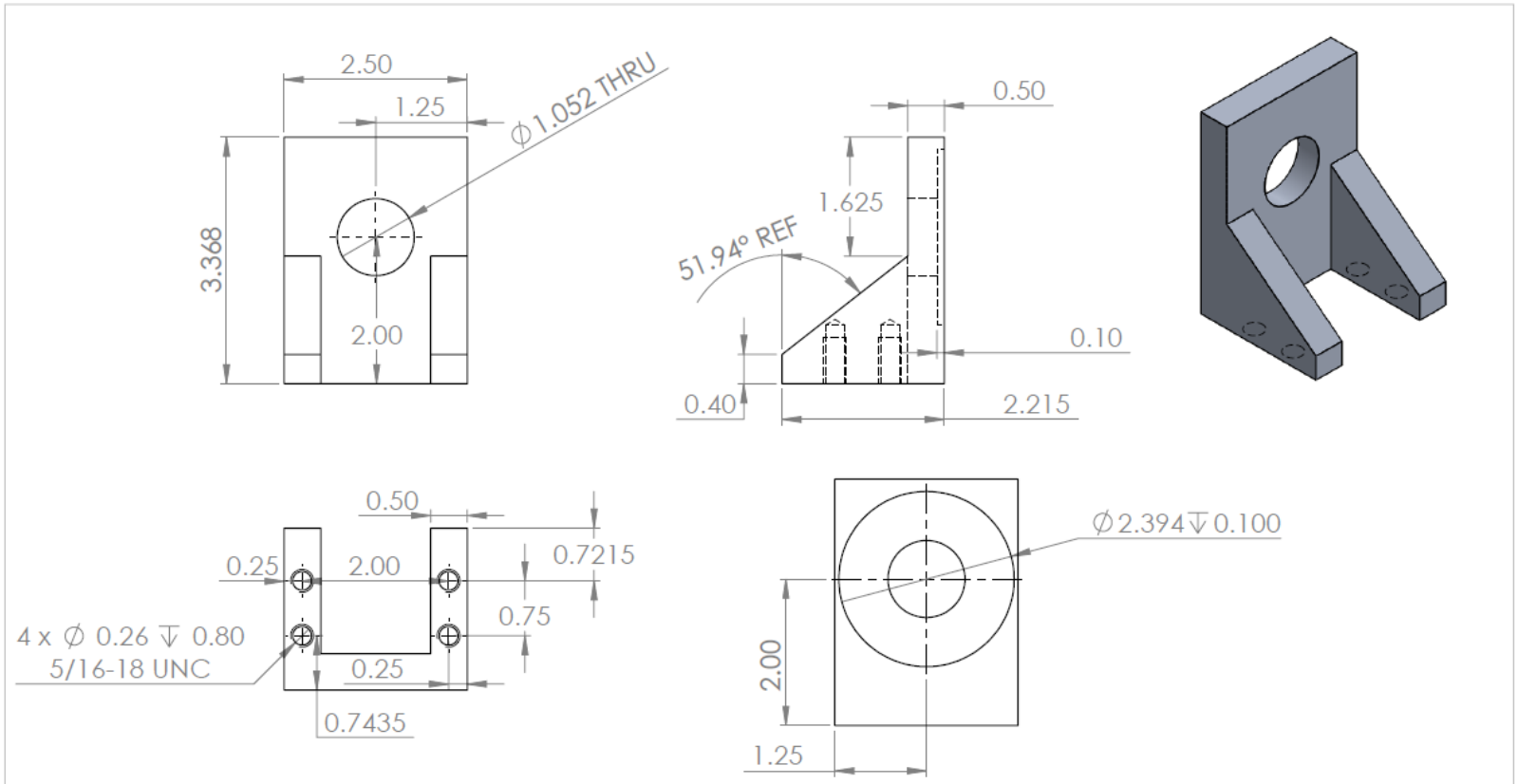

		UNLESS OTHERWISE SPECIFIED:		NAME	DATE
		DIMENSIONS ARE IN INCHES TOLERANCES: FRACTIONAL ± ANGULAR: MACH ± BEND ± TWO PLACE DECIMAL ± THREE PLACE DECIMAL ±	DRAWN	HOYER	4/22/13
			CHECKED		
			ENG APPR.		
			MFG APPR.		
		INTERPRET GEOMETRIC TOLERANCING PER:	Q.A.		
		MATERIAL AL 6061-T6	COMMENTS: Dimensions in inches		
NEXT ASSY	USED ON	FINISH			
APPLICATION		DO NOT SCALE DRAWING			

QTY: 1

TITLE:

DieSupport

SIZE	DWG. NO.	REV
A		
SCALE: 1:2	WEIGHT:	SHEET 1 OF 1

5 4 3 2 1

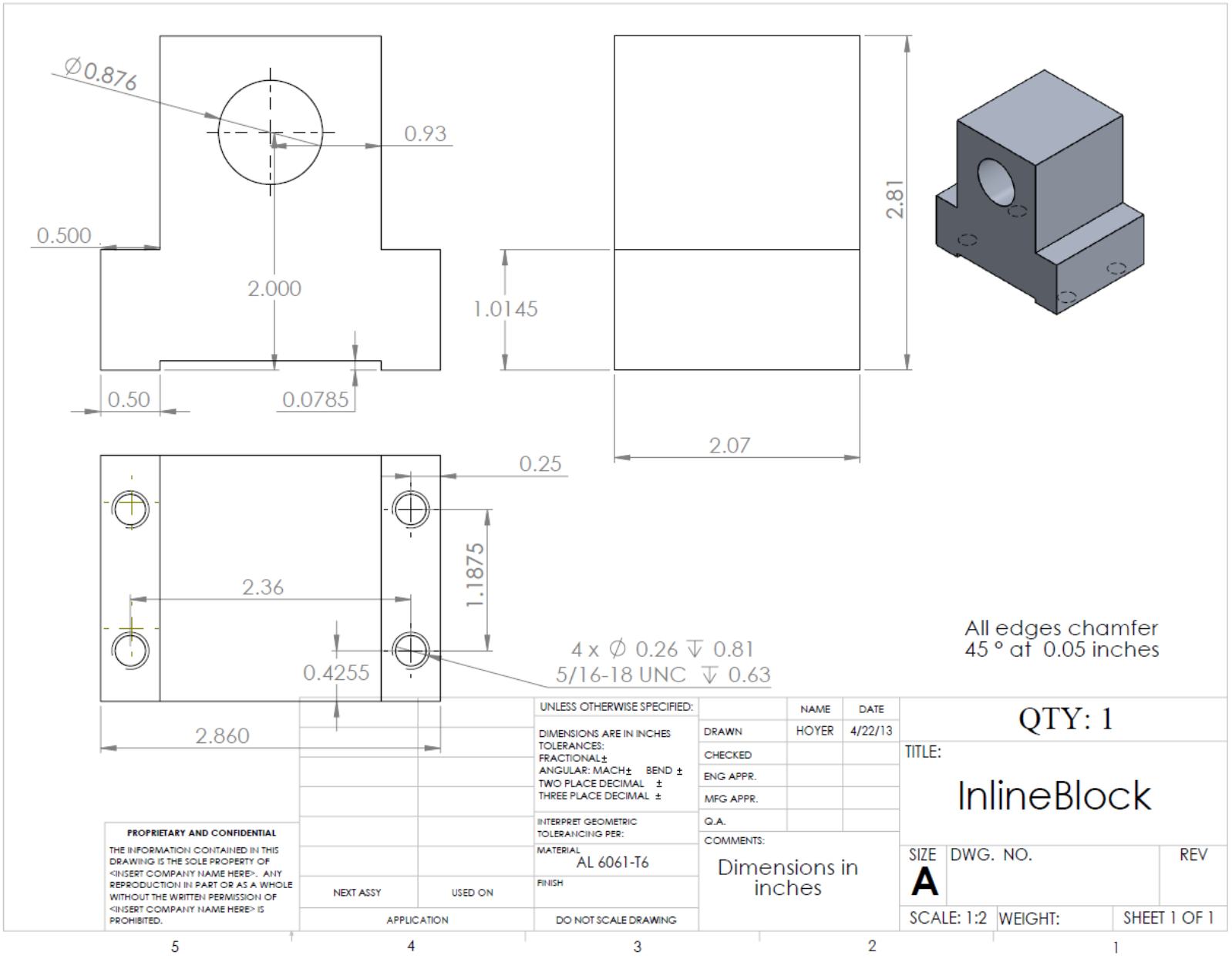
∅0.876
0.93
0.500
2.000
0.50
0.0785
1.0145
2.81
2.07
0.25
1.1875
2.36
0.4255
2.860
4 x ∅ 0.26 ↧ 0.81
5/16-18 UNC ↧ 0.63
All edges chamfer
45 ° at 0.05 inches
UNLESS OTHERWISE SPECIFIED:
DIMENSIONS ARE IN INCHES
TOLERANCES:
FRACTIONAL±
ANGULAR: MACH± BEND ±
TWO PLACE DECIMAL ±
THREE PLACE DECIMAL ±
INTERPRET GEOMETRIC TOLERANCING PER:
MATERIAL
AL 6061-T6
FINISH
NEXT ASSY
USED ON
APPLICATION
DO NOT SCALE DRAWING
NAME
DATE
DRAWN
HOYER
4/22/13
CHECKED
ENG APPR.
MFG APPR.
Q.A.
COMMENTS:
Dimensions in inches
QTY: 1
TITLE:
InlineBlock
SIZE
A
DWG. NO.
REV
SCALE: 1:2
WEIGHT:
SHEET 1 OF 1
PROPRIETARY AND CONFIDENTIAL
THE INFORMATION CONTAINED IN THIS DRAWING IS THE SOLE PROPERTY OF <INSERT COMPANY NAME HERE>. ANY REPRODUCTION IN PART OR AS A WHOLE WITHOUT THE WRITTEN PERMISSION OF <INSERT COMPANY NAME HERE> IS PROHIBITED.
5
4
3
2
1

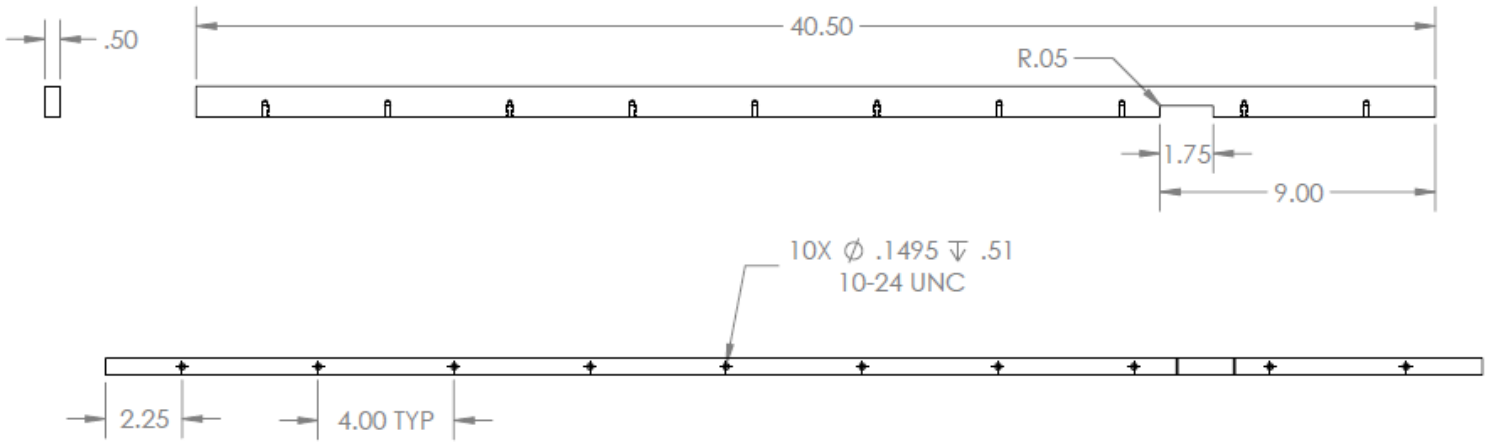

		UNLESS OTHERWISE SPECIFIED:		NAME	DATE	QTY: 1
		DIMENSIONS ARE IN INCHES TOLERANCES: FRACTIONAL ± ANGULAR: MACH ± BEND ± TWO PLACE DECIMAL ± THREE PLACE DECIMAL ±	DRAWN	SCHELLER	4/22/13	TITLE: MiddleFoot
			CHECKED	HOYER	4/23/13	
			ENG APPR.			
			MFG APPR.			
		INTERPRET GEOMETRIC TOLERANCING PER:	Q.A.			
		MATERIAL AL 6061-T6	COMMENTS: Dimensions in inches			SIZE A / DWG. NO. / REV 2
NEXT ASSY	USED ON	FINISH				
APPLICATION		DO NOT SCALE DRAWING				SCALE: 1:20 WEIGHT: / SHEET 1 OF 1

5 4 3 2 1

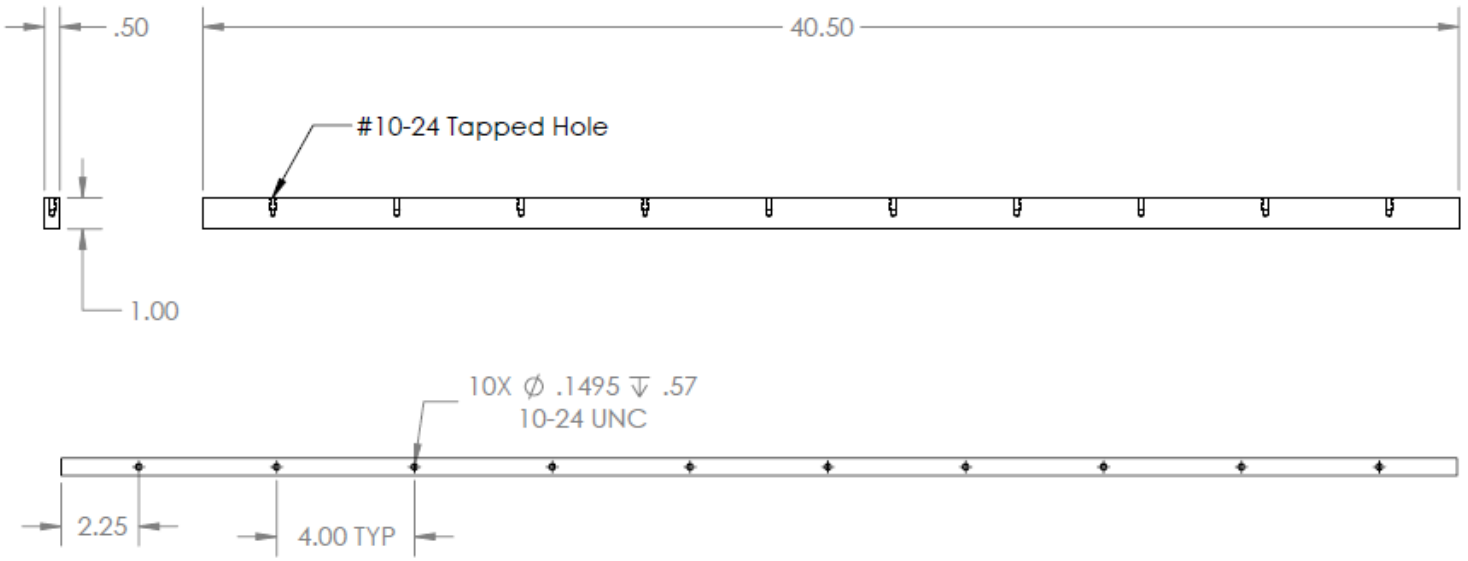

UNLESS OTHERWISE SPECIFIED:		NAME	DATE	QTY: 2	
DIMENSIONS ARE IN INCHES TOLERANCES: FRACTIONAL ± ANGULAR: MACH ± BEND ± TWO PLACE DECIMAL ± THREE PLACE DECIMAL ±	DRAWN	SCHELLER	4/22/13	TITLE: OutsideFoot	
	CHECKED	HOYER	4/23/13		
	ENG APPR.				
	MFG APPR.				
INTERPRET GEOMETRIC TOLERANCING PER:	Q.A.				
MATERIAL: AL 6061-T6	COMMENTS: Dimensions in inches			SIZE: A	DWG. NO. / REV: 2
FINISH				SCALE: 1:1	WEIGHT: / SHEET 1 OF 1
DO NOT SCALE DRAWING					

NEXT ASSY	USED ON
APPLICATION	

5 4 3 2 1

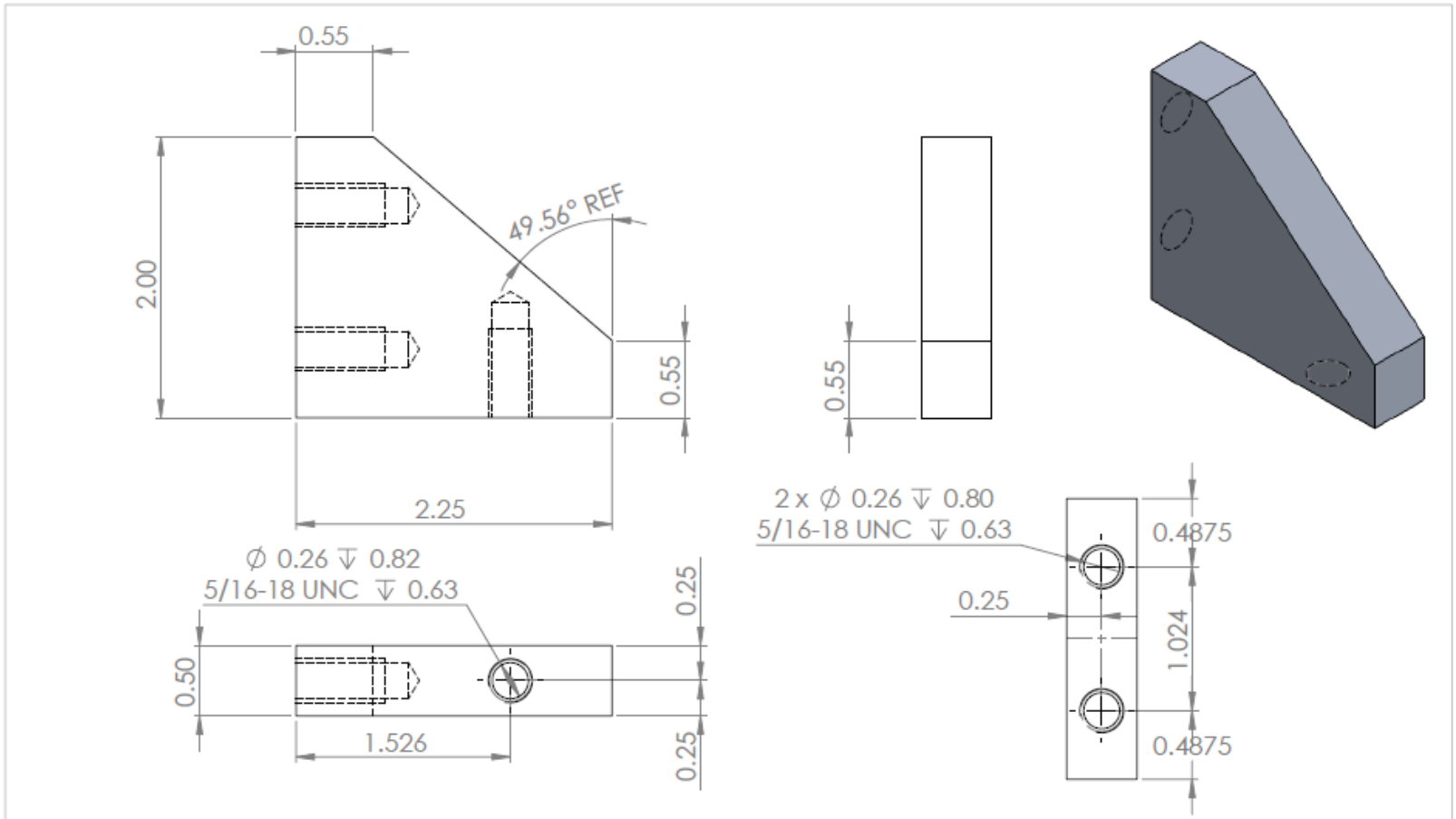

		UNLESS OTHERWISE SPECIFIED:		NAME	DATE
		DIMENSIONS ARE IN INCHES TOLERANCES: FRACTIONAL ± ANGULAR: MACH ± BEND ± TWO PLACE DECIMAL ± THREE PLACE DECIMAL ±	DRAWN	HOYER	4/22/13
			CHECKED		
			ENG APPR.		
			MFG APPR.		
		INTERPRET GEOMETRIC TOLERANCING PER:	Q.A.		
		MATERIAL AL 6061-T6	COMMENTS: Dimensions in inches		
NEXT ASSY	USED ON	FINISH			
APPLICATION		DO NOT SCALE DRAWING			

QTY: 2

TITLE:

Support

SIZE	DWG. NO.	REV
A		

SCALE: 1:1 | WEIGHT: | SHEET 1 OF 1

5 4 3 2 1

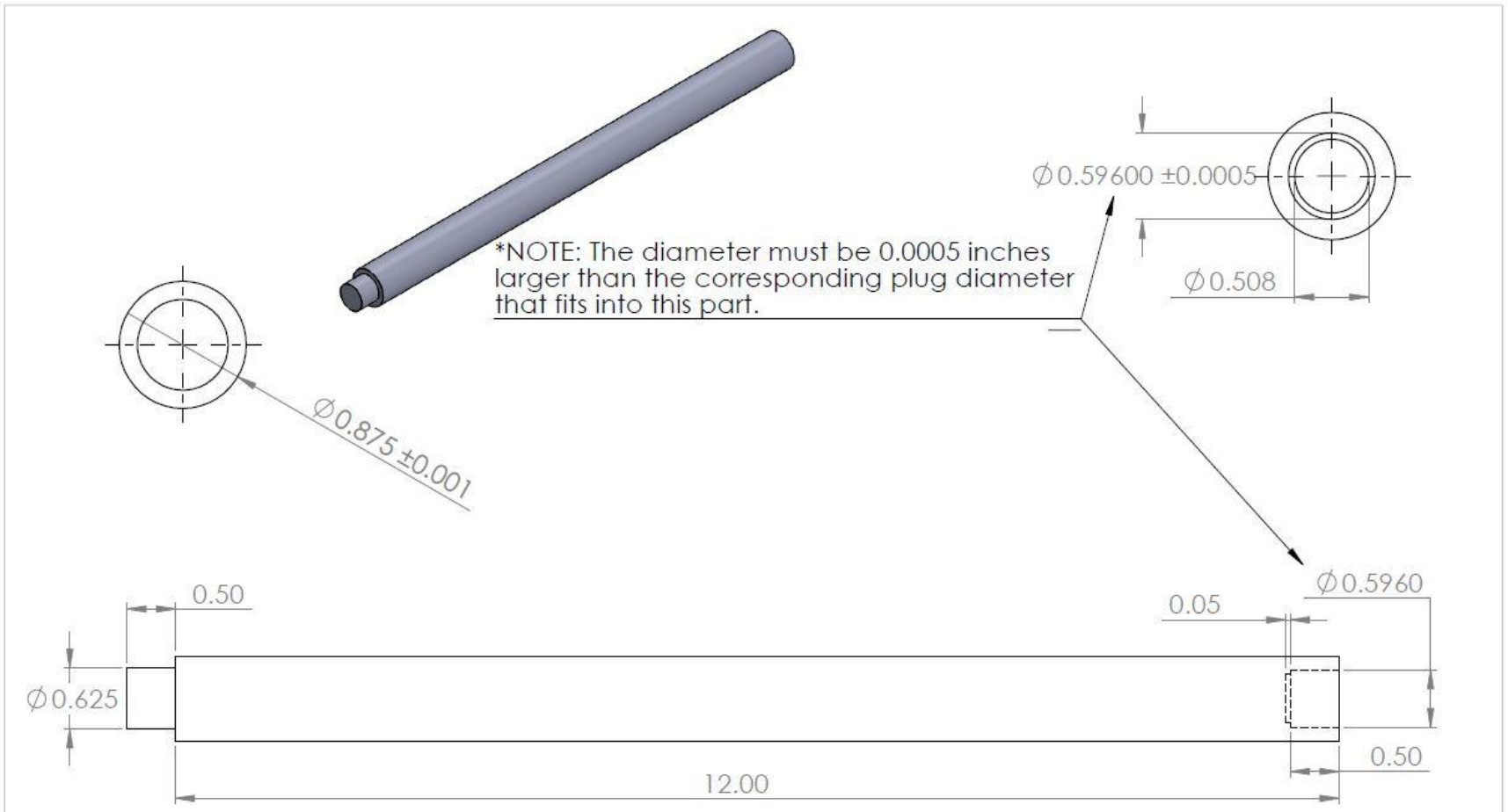

All rounds and edges finished with fillet R0.05

		UNLESS OTHERWISE SPECIFIED:		NAME	DATE
		DIMENSIONS ARE IN INCHES TOLERANCES: FRACTIONAL ± ANGULAR: MACH ± BEND ± TWO PLACE DECIMAL ±0.01 THREE PLACE DECIMAL ±0.001	DRAWN	HOYER	4/23/13
			CHECKED		
			ENG APPR.		
			MFG APPR.		
		INTERPRET GEOMETRIC TOLERANCING PER:	Q.A.		
		MATERIAL Cold Rolled Steel	COMMENTS: Dimensions in inches		
NEXT ASSY	USED ON	FINISH			
APPLICATION		DO NOT SCALE DRAWING			

QTY: 1

TITLE:

Rod

SIZE	DWG. NO.	REV
A		

SCALE: 1:5 | WEIGHT: | SHEET 1 OF 1

5 4 3 2 1

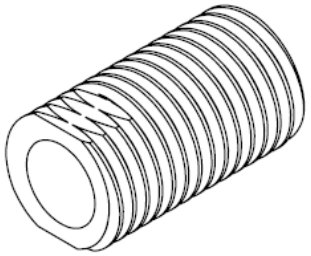

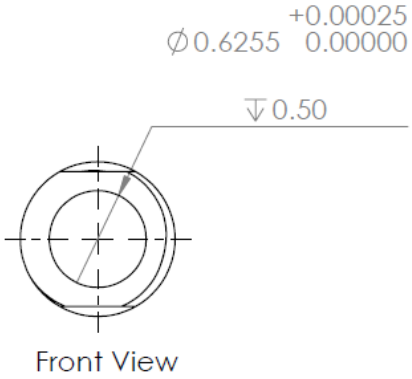

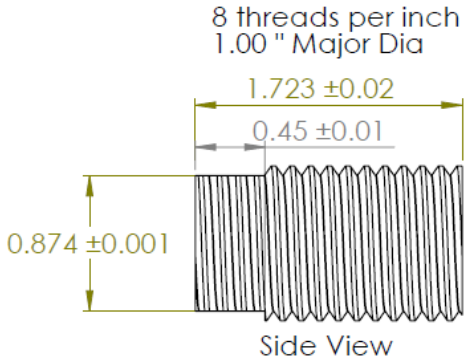

NOTE: The mated rod diameter is to have a clearance of 0.00025 (1/4 thousandths) inches.

UNLESS OTHERWISE SPECIFIED:		NAME	DATE
DIMENSIONS ARE IN INCHES TOLERANCES: FRACTIONAL ± ANGULAR: MACH ± BEND ± TWO PLACE DECIMAL ± THREE PLACE DECIMAL ±	DRAWN	HOYER	9/11/13
	CHECKED		
	ENG APPR.		
	MFG APPR.		
INTERPRET GEOMETRIC TOLERANCING PER:	Q.A.		
MATERIAL D2 Steel	COMMENTS:		
FINISH			
DO NOT SCALE DRAWING			

TITLE: Cylinder Connecting Piece

SIZE	DWG. NO.	REV
A		0

SCALE: 1:1 | WEIGHT: | SHEET 1 OF 1

5 4 3 2 1

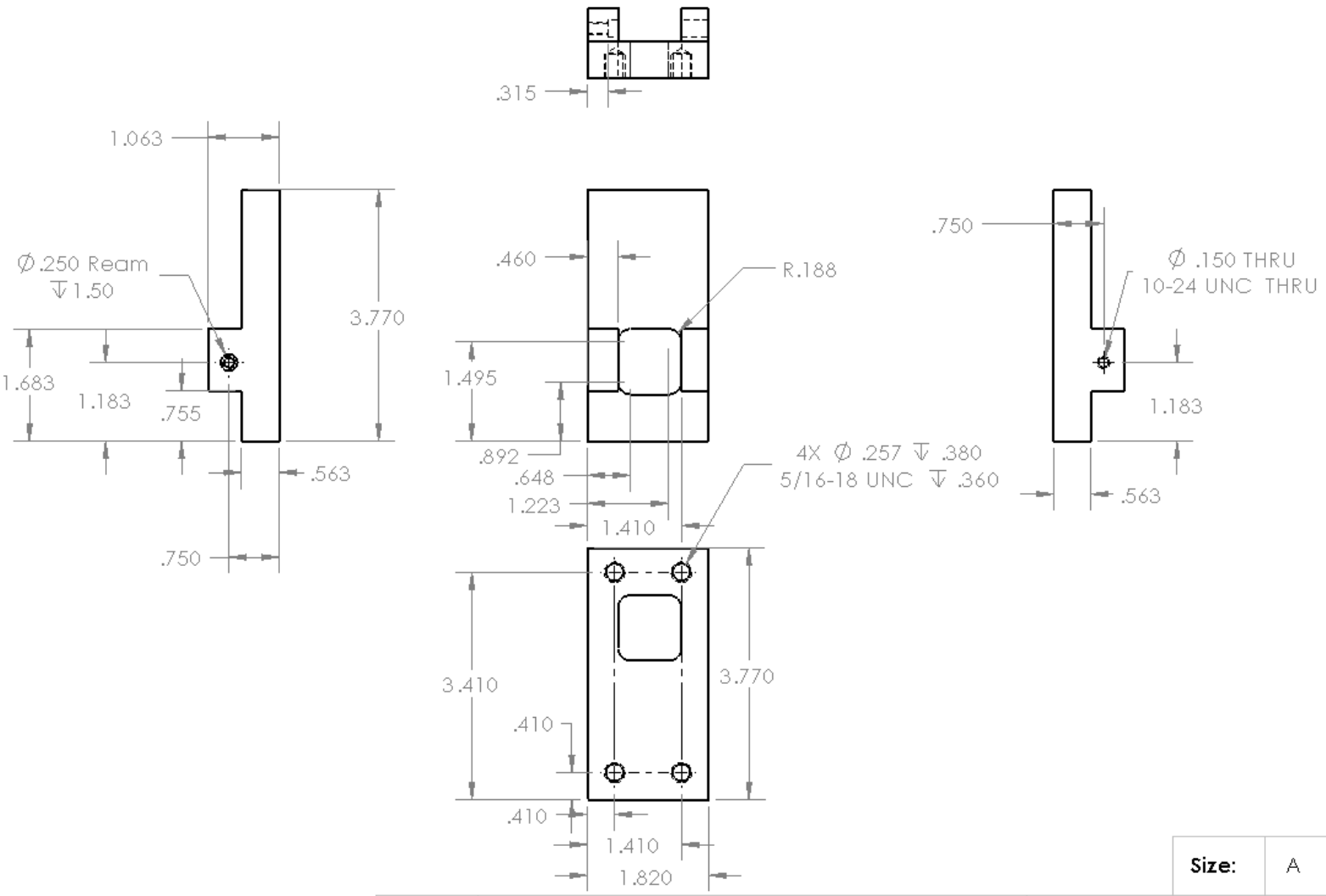

				Size:	A
Title:	FDMBaseSupport_correct		**QTY:** 4	**Scale:**	1:2
Material:	6061-T6	**Author:**	Jacob Harris		

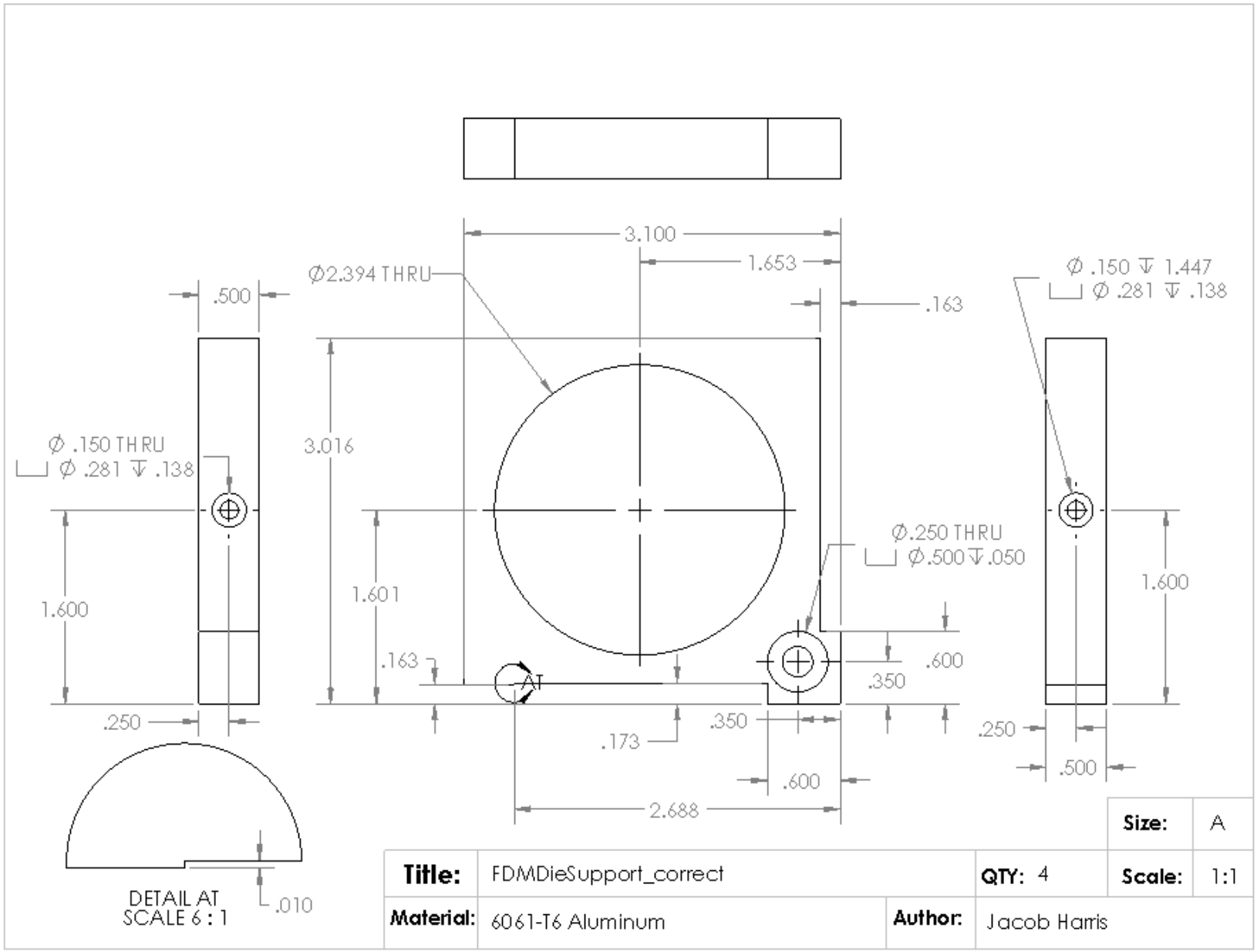
3.100
1.653
.163
.500
Ø2.394 THRU
Ø .150 ↧ 1.447
⌴ Ø .281 ↧ .138
Ø .150 THRU
⌴ Ø .281 ↧ .138
3.016
1.600
1.601
.163
Ø.250 THRU
⌴ Ø.500 ↧.050
.600
.350
.250
.173
.350
.600
2.688
1.600
.250
.500
DETAIL AT
SCALE 6 : 1
.010
Title: FDMDieSupport_correct
QTY: 4
Size: A
Scale: 1:1
Material: 6061-T6 Aluminum
Author: Jacob Harris

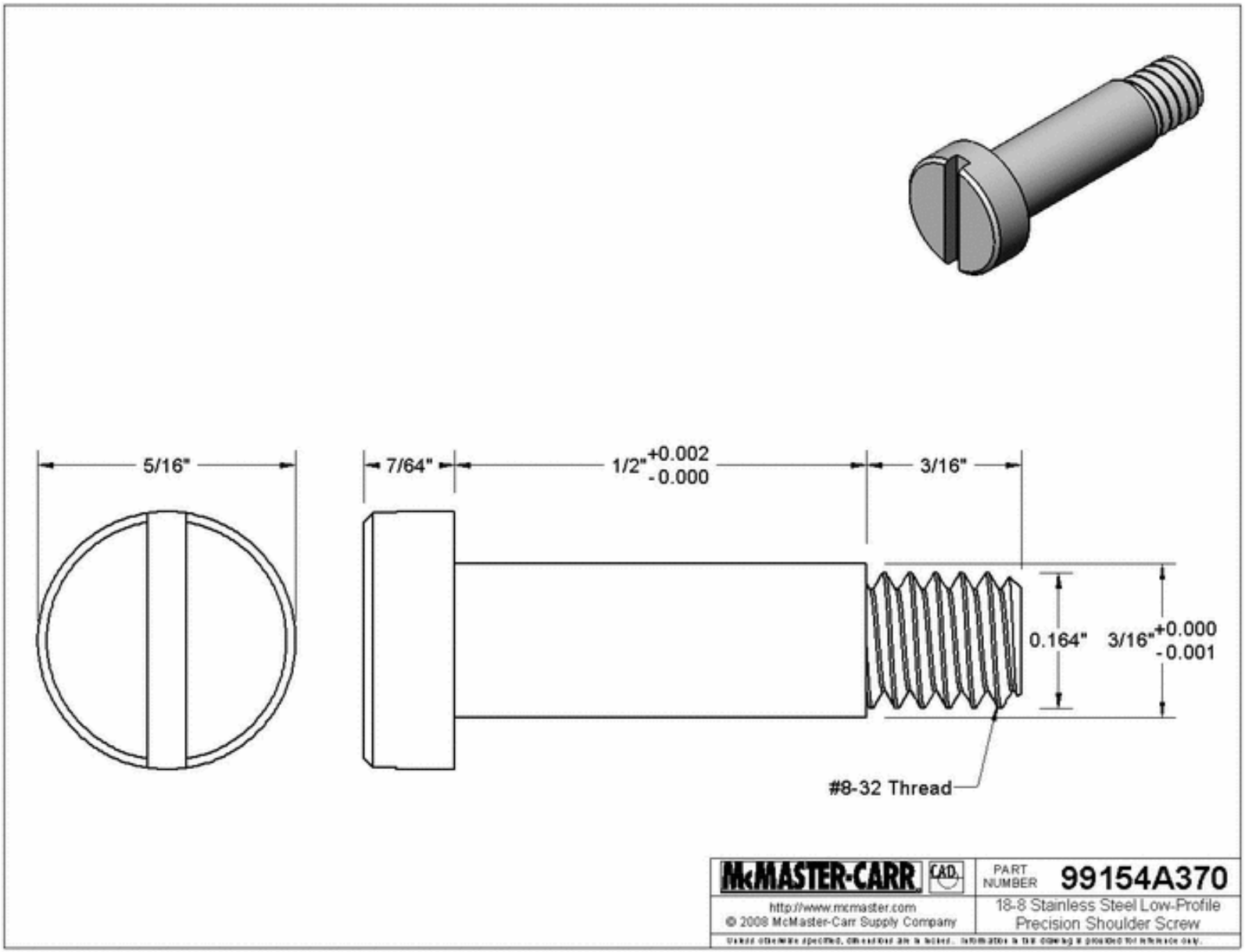
5/16"
7/64"
1/2" +0.002 -0.000
3/16"
0.164"
3/16" +0.000 -0.001
#8-32 Thread
McMASTER-CARR
CAD
PART NUMBER 99154A370
http://www.mcmaster.com
© 2008 McMaster-Carr Supply Company
18-8 Stainless Steel Low-Profile Precision Shoulder Screw

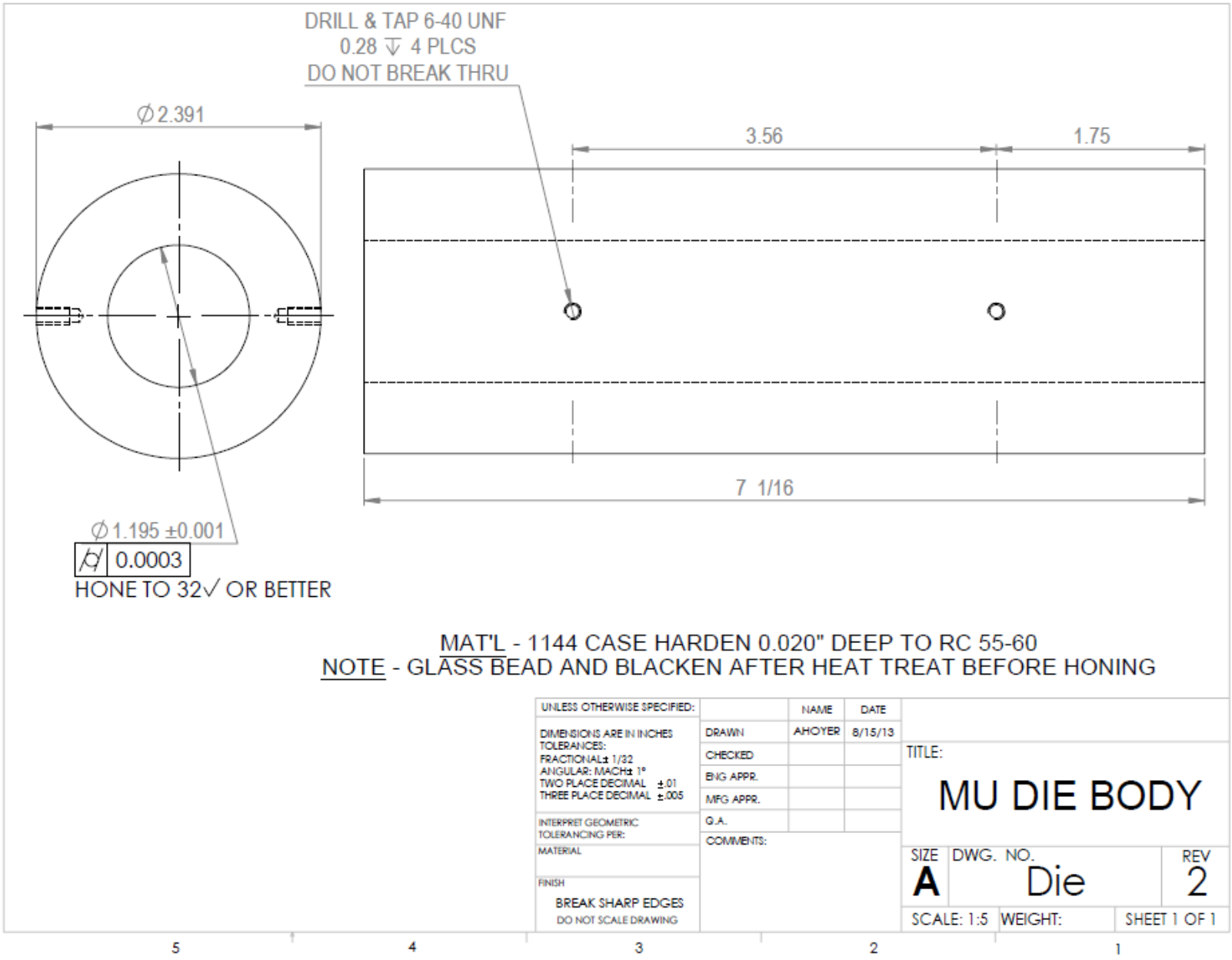
DRILL & TAP 6-40 UNF
0.28 ↧ 4 PLCS
DO NOT BREAK THRU
∅2.391
3.56
1.75
7 1/16
∅1.195 ±0.001
0.0003
HONE TO 32✓ OR BETTER
MAT'L - 1144 CASE HARDEN 0.020" DEEP TO RC 55-60
NOTE - GLASS BEAD AND BLACKEN AFTER HEAT TREAT BEFORE HONING
UNLESS OTHERWISE SPECIFIED:
DIMENSIONS ARE IN INCHES
TOLERANCES:
FRACTIONAL± 1/32
ANGULAR: MACH± 1°
TWO PLACE DECIMAL ±.01
THREE PLACE DECIMAL ±.005
INTERPRET GEOMETRIC TOLERANCING PER:
MATERIAL
FINISH
BREAK SHARP EDGES
DO NOT SCALE DRAWING
NAME
DATE
DRAWN
AHOYER
8/15/13
CHECKED
ENG APPR.
MFG APPR.
Q.A.
COMMENTS:
TITLE:
MU DIE BODY
SIZE
A
DWG. NO.
Die
REV
2
SCALE: 1:5
WEIGHT:
SHEET 1 OF 1
5
4
3
2
1

APPENDIX F

FUNCTION DIMENS

```
function dimens
% input method of calculating dimensions
% Option 1:
%      Keep smaller diameter = 0.800 inches
%      Make shaft longer

% Option 2:
%      Make smaller diameter bigger
%      Keep shaft same length = 1.17 inches

callmenu = menu('Choose an option:',...% Menu title
    'Run option 1 - LONGER SHAFT',...% case 1
    'Run option 2 - BIGGER DIAMETER',... % case 2
    'Clear Workspace and screen');  % case 3


switch callmenu
    case {1}
        prompt = {'Enter desired plug size 1.0xx:'...
            ,'Small diameter:'...
            ,'Shaft size:'};

        input = inputdlg(prompt,'Input for draw plug size',...
            1,{'1.046','0.800','1.17'});
        plugsize = str2num(input{1});
        small_dia = str2num(input{2});
        shaft = str2num(input{3});

        delx = plugsize - small_dia;
        sina = 0.246/shaft;
        NEW_Length = delx/sina
        fprintf('The new shaft length is %2.6f inches with diameter still
0.800',NEW_Length)
        fprintf('/n')
        dimens

    case {2}

        prompt = {'Enter desired plug size 1.0xx:'...
            ,'Small diameter:'...
            ,'Shaft size:'};

        input = inputdlg(prompt,'Input for draw plug size',...
            1,{'1.046','0.800','1.17'});
        plugsize = str2num(input{1});
        small_dia = str2num(input{2});
        shaft = str2num(input{3});

        sina = 0.246/shaft;
```

```
        delx = sina*shaft;
        small_dia = plugsize - delx;
        fprintf('The new diameter is %2.6f inches with shaft still
1.17"',small_dia)
        fprintf('/n')
        dimens

    case {3}
        clc
        fprintf('script has been terminated\n')
end
```

APPENDIX G

FOIL ORDER

APPENDIX H

FOIL SAFETY

Goodfellow
Ermine Business Park
Huntingdon PE29 6WR England
Telephone +44 1480 424 800
Fax +44 1480 424 900

Our reference LS378385 /M K S
Your order number Solbrekken DFF86
Stainless Steel - AISI 304 Foil

Version

14

Date

23-Sep-2009

Identification of the substance/preparation and company

Name

Stainless Steel - AISI 304
Foil

Synonyms

Fe/Cr18/Ni10

UN number

CAS number

7439-89-6 Iron, 7440-47-3 Chromium, 7440-02-0 Nickel

EINECS number

EEC number

Goodfellow
Ermine Business Park
HUNTINGDON PE29 6WR England
Tel: +44 (0) 1480 424 800
Fax: +44 (0) 1480 424 900
E-mail: info@goodfellow.com

Composition/information on ingredients

Purity/composition (weight %)

Iron 72% Chromium 18% Nickel 10% [nominal]

Ingredients contributing to any hazard

Iron Metal. Chromium. Nickel

Hazards identification

Hazards

May cause sensitization by skin contact. If further processing will result in fine particles then please request the MSDS for either the **ingredients contributing to any hazard** or the powder form of this material.

Risk phrases (EEC)

None applicable

Continued...

Goodfellow
Ermine Business Park
Huntingdon PE29 6WR England
Telephone +44 1480 424 800
Fax +44 1480 424 900

Our reference LS378385 /M K S
Your order number Solbrekken DFF86
Stainless Steel - AISI 304 Foil

First-aid measures

Fire-fighting measures

Accidental release measures

Handling and storage

Safety phrases (EEC)

None applicable

Exposure controls/personal protection

WEL - TWA 8 hours : 0.5 mg.m(-3)
TLV - ACGIH : 0.05 mg.m(-3)

Personal protection

Wear gloves when handling.

Physical and chemical properties

Steel grey metal. Hard.

Physical Data

Density : 7.93 g cm-3
Melting point : 1400-1455 C

Stability and reactivity

Toxicological information

Ecological information

Disposal considerations

Transport information

Regulatory information

Other information

This material is for use only in the workplace, it should be kept out of the reach of children and in a secure store accessible only to individuals with the technical expertise to understand this Material Safety Data Sheet. The material should be kept away from foodstuffs and the user should not eat, drink or smoke whilst using the material. The information detailed relates only to the material specified and may not be valid when it is used in combination with other materials or in any process. The information given is based on the latest information available to us and is, to the best of our knowledge, accurate and reliable at the time of preparation. However, no representation, warranty or guarantee is made as to its accuracy, reliability or completeness. Goodfellow assumes no responsibility and disclaims any liability incurred in using this information. The product is supplied on the condition the user accepts the responsibility to satisfy himself as to the suitability and completeness of such information for his own particular use. References: "Sax's Dangerous Properties of Industrial Materials" 9th Edition, Lewis, Richard j. Sr., Van Nostrand Reinhold New York, ISBN SET 0-442-02025-2. "Handbook of Reactive Chemical Hazards" Third Edition, L. Bretherick, Butterworths, ISBN 0-408-01388-5. The Royal Society of Chemistry "Chemical Safety Data Sheets" ISBN 0-85186-913-0 (1989), 0-85186-311-6 (1991), 0-85186-411-2 (1992). In accordance with 91/155/EEC directive. This MSDS is always current and, generally, complies with 2001/58/EC guidelines.

Material Safety Data Sheet

Goodfellow

Stainless Steel - AISI 304

1. Product and company identification

Product name : Stainless Steel - AISI 304

Supplier

Goodfellow Corporation
125 Hookstown Grade Road, Coraopolis, PA 15108-9302, USA
Telephone: +1 800 821 2870 (USA) or +1 724 695 7060
Fax: +1 800 283 2020 (USA) or +1 724 695 7063
e-mail: sds@goodfellowusa.com

Code : FE220

Validation date : 26/01/2012.

In case of emergency

Telephone number : Chemtrec +1 202 483 7616

Product type : Solid.

2. Hazards identification

Emergency overview

Physical state : Solid.

Signal word : WARNING!

Hazard statements : MAY CAUSE ALLERGIC SKIN REACTION. CONTAINS MATERIAL THAT MAY CAUSE TARGET ORGAN DAMAGE, BASED ON ANIMAL DATA. SUSPECT CANCER HAZARD - CONTAINS MATERIAL WHICH MAY CAUSE CANCER.

Precautionary measures : Do not handle until all safety precautions have been read and understood. Obtain special instructions before use. Do not eat, drink or smoke when using this product. Avoid prolonged or repeated contact with skin. Use personal protective equipment as required. Wash thoroughly after handling.

OSHA/HCS status : This material is considered hazardous by the OSHA Hazard Communication Standard (29 CFR 1910.1200).

Avoid inhalation of and contact with eyes by any dust produced during machining, cutting or processing (a safety data sheet for product in powder form is available on request).

Potential acute health effects

Skin : May cause sensitization by skin contact.

Potential chronic health effects

Chronic effects : Contains material that may cause target organ damage, based on animal data. Once sensitized, a severe allergic reaction may occur when subsequently exposed to very low levels.

Carcinogenicity : Contains material which may cause cancer. Risk of cancer depends on duration and level of exposure.

Target organs : Contains material which may cause damage to the following organs: kidneys, lungs, upper respiratory tract, skin, eyes, nose/sinuses.

Over-exposure signs/symptoms

Skin : Adverse symptoms may include the following:
irritation
redness

Medical conditions aggravated by over-exposure : Pre-existing skin disorders and disorders involving any other target organs mentioned in this MSDS as being at risk may be aggravated by over-exposure to this product.

See toxicological information (Section 11)

3. Composition/information on ingredients

Name	CAS number	%
chromium	7440-47-3	17 - 19
Nickel	7440-02-0	8 - 10

There are no additional ingredients present which, within the current knowledge of the supplier and in the concentrations applicable, are classified as hazardous to health or the environment and hence require reporting in this section.

4. First aid measures

Eye contact : Check for and remove any contact lenses. Immediately flush eyes with plenty of water for at least 15 minutes, occasionally lifting the upper and lower eyelids. Get medical attention immediately.

Skin contact : In case of contact, immediately flush skin with plenty of water for at least 15 minutes while removing contaminated clothing and shoes. Wash clothing before reuse. Clean shoes thoroughly before reuse. Get medical attention immediately.

Inhalation : Move exposed person to fresh air. If not breathing, if breathing is irregular or if respiratory arrest occurs, provide artificial respiration or oxygen by trained personnel. Loosen tight clothing such as a collar, tie, belt or waistband. Get medical attention immediately.

Ingestion : Wash out mouth with water. Do not induce vomiting unless directed to do so by medical personnel. Never give anything by mouth to an unconscious person. Get medical attention immediately.

Protection of first-aiders : No action shall be taken involving any personal risk or without suitable training. If it is suspected that fumes are still present, the rescuer should wear an appropriate mask or self-contained breathing apparatus. It may be dangerous to the person providing aid to give mouth-to-mouth resuscitation. Wash contaminated clothing thoroughly with water before removing it, or wear gloves.

Notes to physician : No specific treatment. Treat symptomatically. Contact poison treatment specialist immediately if large quantities have been ingested or inhaled.

5. Fire-fighting measures

Flammability of the product : No specific fire or explosion hazard.

Extinguishing media

Suitable : Use an extinguishing agent suitable for the surrounding fire.

Not suitable : None known.

Special exposure hazards : Promptly isolate the scene by removing all persons from the vicinity of the incident if there is a fire. No action shall be taken involving any personal risk or without suitable training.

Hazardous thermal decomposition products : Decomposition products may include the following materials:
metal oxide/oxides

Special protective equipment for fire-fighters : Fire-fighters should wear appropriate protective equipment and self-contained breathing apparatus (SCBA) with a full face-piece operated in positive pressure mode.

6. Accidental release measures

Personal precautions : No action shall be taken involving any personal risk or without suitable training. Evacuate surrounding areas. Keep unnecessary and unprotected personnel from entering. Do not touch or walk through spilled material. Provide adequate ventilation. Wear appropriate respirator when ventilation is inadequate. Put on appropriate personal protective equipment (see Section 8).

Environmental precautions : Avoid dispersal of spilled material and runoff and contact with soil, waterways, drains and sewers. Inform the relevant authorities if the product has caused environmental pollution (sewers, waterways, soil or air).

Methods for cleaning up

6. Accidental release measures

Small spill : Move containers from spill area. Vacuum or sweep up material and place in a designated, labeled waste container. Dispose of via a licensed waste disposal contractor.

Large spill : Move containers from spill area. Approach release from upwind. Prevent entry into sewers, water courses, basements or confined areas. Vacuum or sweep up material and place in a designated, labeled waste container. Dispose of via a licensed waste disposal contractor. Note: see section 1 for emergency contact information and section 13 for waste disposal.

7. Handling and storage

Handling : Put on appropriate personal protective equipment (see Section 8). Eating, drinking and smoking should be prohibited in areas where this material is handled, stored and processed. Workers should wash hands and face before eating, drinking and smoking. Remove contaminated clothing and protective equipment before entering eating areas. Persons with a history of skin sensitization problems should not be employed in any process in which this product is used. Avoid exposure - obtain special instructions before use. Do not get in eyes or on skin or clothing. Do not ingest. If during normal use the material presents a respiratory hazard, use only with adequate ventilation or wear appropriate respirator. Keep in the original container or an approved alternative made from a compatible material, kept tightly closed when not in use. Empty containers retain product residue and can be hazardous. Do not reuse container.

Storage : Store in accordance with local regulations. Store in original container protected from direct sunlight in a dry, cool and well-ventilated area, away from incompatible materials (see section 10) and food and drink. Keep container tightly closed and sealed until ready for use. Containers that have been opened must be carefully resealed and kept upright to prevent leakage. Do not store in unlabeled containers. Use appropriate containment to avoid environmental contamination.

8. Exposure controls/personal protection

Ingredient	Exposure limits
chromium	**OSHA PEL 1989 (United States, 3/1989).** TWA: 1 mg/m³ 8 hour(s). **NIOSH REL (United States, 6/2009).** TWA: 0.5 mg/m³ 10 hour(s). **ACGIH TLV (United States, 2/2010).** TWA: 0.5 mg/m³, (measured as Cr) 8 hour(s). Form: Inorganic **OSHA PEL (United States, 6/2010).** TWA: 1 mg/m³, (as Cr) 8 hour(s).
Nickel	**OSHA PEL 1989 (United States, 3/1989).** TWA: 1 mg/m³, (as Ni) 8 hour(s). **NIOSH REL (United States, 6/2009).** TWA: 0.015 mg/m³, (as Ni) 10 hour(s). **ACGIH TLV (United States, 2/2010).** TWA: 1.5 mg/m³ 8 hour(s). Form: Inhalable fraction **OSHA PEL (United States, 6/2010).** TWA: 1 mg/m³, (as Ni) 8 hour(s).

Recommended monitoring procedures : If this product contains ingredients with exposure limits, personal, workplace atmosphere or biological monitoring may be required to determine the effectiveness of the ventilation or other control measures and/or the necessity to use respiratory protective equipment.

Engineering measures : If user operations generate dust, fumes, gas, vapor or mist, use process enclosures, local exhaust ventilation or other engineering controls to keep worker exposure to airborne contaminants below any recommended or statutory limits.

8. Exposure controls/personal protection

Hygiene measures : Wash hands, forearms and face thoroughly after handling chemical products, before eating, smoking and using the lavatory and at the end of the working period. Appropriate techniques should be used to remove potentially contaminated clothing. Contaminated work clothing should not be allowed out of the workplace. Wash contaminated clothing before reusing. Ensure that eyewash stations and safety showers are close to the workstation location.

Personal protection

Respiratory : Use a properly fitted, air-purifying or air-fed respirator complying with an approved standard if a risk assessment indicates this is necessary. Respirator selection must be based on known or anticipated exposure levels, the hazards of the product and the safe working limits of the selected respirator.

Hands : Chemical-resistant, impervious gloves complying with an approved standard should be worn at all times when handling chemical products if a risk assessment indicates this is necessary.

Eyes : Safety eyewear complying with an approved standard should be used when a risk assessment indicates this is necessary to avoid exposure to liquid splashes, mists or dusts.

Skin : Personal protective equipment for the body should be selected based on the task being performed and the risks involved and should be approved by a specialist before handling this product.

Environmental exposure controls : Emissions from ventilation or work process equipment should be checked to ensure they comply with the requirements of environmental protection legislation. In some cases, fume scrubbers, filters or engineering modifications to the process equipment will be necessary to reduce emissions to acceptable levels.

9. Physical and chemical properties

Physical state : Solid.

Melting/freezing point : 1370°C (2498°F)

10. Stability and reactivity

Chemical stability : The product is stable.

Conditions to avoid : No specific data.

Incompatible materials : No specific data.

Hazardous decomposition products : Under normal conditions of storage and use, hazardous decomposition products should not be produced.

Possibility of hazardous reactions : Under normal conditions of storage and use, hazardous reactions will not occur.

11. Toxicological information

Acute toxicity

Conclusion/Summary : Not available.

Chronic toxicity

Conclusion/Summary : Not available.

Irritation/Corrosion

Conclusion/Summary : Not available.

Sensitizer

Conclusion/Summary : Not available.

Carcinogenicity

Conclusion/Summary : Not available.

Classification

11. Toxicological information

Product/ingredient name	ACGIH	IARC	EPA	NIOSH	NTP	OSHA
chromium	A4	3	-	-	-	-
Nickel	A5	2B	-	+	Possible	-

Mutagenicity

Conclusion/Summary : Not available.

Teratogenicity

Conclusion/Summary : Not available.

Reproductive toxicity

Conclusion/Summary : Not available.

12. Ecological information

Ecotoxicity : No known significant effects or critical hazards.

Aquatic ecotoxicity

Product/ingredient name	Result	Species	Exposure
chromium	Acute LC50 13.9 ppm Fresh water	Fish - Anguilla rostrata	96 hours
Nickel	Acute LC50 2.3 ppm Fresh water	Fish - Cyprinus carpio - Juvenile (Fledgling, Hatchling, Weanling) - 6 cm	96 hours
	Chronic NOEC 3.5 ug/L Fresh water	Fish - Cyprinus carpio - 13 months - 10.5 cm - 27.8 g	4 weeks

Conclusion/Summary : Not available.

Persistence/degradability

Conclusion/Summary : Not available.

13. Disposal considerations

Waste disposal : The generation of waste should be avoided or minimized wherever possible. Significant quantities of waste product residues should not be disposed of via the foul sewer but processed in a suitable effluent treatment plant. Dispose of surplus and non-recyclable products via a licensed waste disposal contractor. Disposal of this product, solutions and any by-products should at all times comply with the requirements of environmental protection and waste disposal legislation and any regional local authority requirements. Waste packaging should be recycled. Incineration or landfill should only be considered when recycling is not feasible. This material and its container must be disposed of in a safe way. Care should be taken when handling emptied containers that have not been cleaned or rinsed out. Empty containers or liners may retain some product residues. Avoid dispersal of spilled material and runoff and contact with soil, waterways, drains and sewers.

Disposal should be in accordance with applicable regional, national and local laws and regulations.

Refer to Section 7: HANDLING AND STORAGE and Section 8: EXPOSURE CONTROLS/PERSONAL PROTECTION for additional handling information and protection of employees.

14. Transport information

Regulatory information	UN number	Proper shipping name	Classes	PG*	Label	Additional information
DOT Classification	Not available.	Not available.	Not available.	-		-
TDG Classification	Not available.	Not available.	Not available.	-		-
Mexico Classification	Not available.	Not available.	Not available.	-		-

14. Transport information

ADR/RID Class	Not available.	Not available.	Not available.	-		-
IMDG Class	Not available.	Not available.	Not available.	-		-
IATA-DGR Class	Not available.	Not available.	Not available.	-		-

PG* : Packing group

15. Regulatory information

HCS Classification : Sensitizing material
Carcinogen
Target organ effects

U.S. Federal regulations : **TSCA 8(a) IUR Exempt/Partial exemption**: Not determined

United States inventory (TSCA 8b): All components are listed or exempted.

SARA 302/304/311/312 extremely hazardous substances: No products were found.
SARA 302/304 emergency planning and notification: No products were found.
SARA 302/304/311/312 hazardous chemicals: Nickel
SARA 311/312 MSDS distribution - chemical inventory - hazard identification: Nickel: Fire hazard, Immediate (acute) health hazard, Delayed (chronic) health hazard; iron: Fire hazard

Clean Water Act (CWA) 307: chromium; Nickel

Clean Air Act Section 112(b) Hazardous Air Pollutants (HAPs) : Not listed

Clean Air Act Section 602 Class I Substances : Not listed

Clean Air Act Section 602 Class II Substances : Not listed

DEA List I Chemicals (Precursor Chemicals) : Not listed

DEA List II Chemicals (Essential Chemicals) : Not listed

SARA 313

	Product name	CAS number	Concentration
Form R - Reporting requirements	chromium Nickel	7440-47-3 7440-02-0	17 - 19 8 - 10
Supplier notification	chromium Nickel	7440-47-3 7440-02-0	17 - 19 8 - 10

SARA 313 notifications must not be detached from the MSDS and any copying and redistribution of the MSDS shall include copying and redistribution of the notice attached to copies of the MSDS subsequently redistributed.

State regulations

Massachusetts : The following components are listed: CHROMIUM; NICKEL

New York : The following components are listed: Chromium; Nickel

New Jersey : The following components are listed: CHROMIUM; NICKEL

Pennsylvania : The following components are listed: CHROMIUM; NICKEL

California Prop. 65

WARNING: This product contains a chemical known to the State of California to cause cancer.

Ingredient name	Cancer	Reproductive	No significant risk level	Maximum acceptable dosage level

15. Regulatory information

Nickel	Yes.	No.	No.	No.

Canada inventory : All components are listed or exempted.

16. Other information

Label requirements : MAY CAUSE ALLERGIC SKIN REACTION. CONTAINS MATERIAL THAT MAY CAUSE TARGET ORGAN DAMAGE, BASED ON ANIMAL DATA. SUSPECT CANCER HAZARD - CONTAINS MATERIAL WHICH MAY CAUSE CANCER.

Hazardous Material Information System (U.S.A.) :

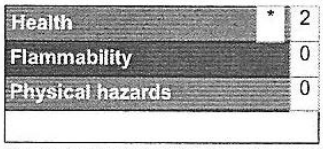

Caution: HMIS® ratings are based on a 0-4 rating scale, with 0 representing minimal hazards or risks, and 4 representing significant hazards or risks Although HMIS® ratings are not required on MSDSs under 29 CFR 1910.1200, the preparer may choose to provide them. HMIS® ratings are to be used with a fully implemented HMIS® program. HMIS® is a registered mark of the National Paint & Coatings Association (NPCA). HMIS® materials may be purchased exclusively from J. J. Keller (800) 327-6868.

The customer is responsible for determining the PPE code for this material.

National Fire Protection Association (U.S.A.) :

Date of issue : 26/01/2012.

Date of previous issue : 19/01/2012.

Version : 1.03

Indicates information that has changed from previously issued version.

Notice to reader

Further information

License granted to make unlimited paper copies for internal use only.

The above information is believed to be correct but does not purport to be all inclusive and shall be used only as a guide. It is based on the present state of our knowledge and is applicable to the product with regard to appropriate safety precautions. Employers should use this information only as a supplement to other information gathered by them and should make independent judgement of the suitability of this information to ensure proper use of the product and to protect the health and safety of their employees and the end-user(s) of the product.

Goodfellow Holdings Limited and any subsidiary or associated company supplies this information without warranty and any use of the product not in conformance with this Material Safety Data Sheet or in combination with any other product or process is the responsibility of the user. The Company does not represent any guarantee of the properties of the product or any suitability of the product for a given application.

Goodfellow Holdings Limited shall not be held liable for any damage resulting from handling or from contact with the product. See www.goodfellow.com or www.goodfellowusa.com for additional terms and conditions of sale.

The information contained in this document is only relevant for products supplied by Goodfellow Holdings Limited and any subsidiary or associated company.

Material Safety Data Sheet

Nickel

1. Product and company identification

Product name : Nickel

Supplier

Goodfellow Corporation
125 Hookstown Grade Road, Coraopolis, PA 15108-9302, USA
Telephone: +1 800 821 2870 (USA) or +1 724 695 7060
Fax: +1 800 283 2020 (USA) or +1 724 695 7063
e-mail: sds@goodfellowusa.com

Code : NI000

Validation date : 21/09/2012.

In case of emergency

Telephone number : Chemtrec +1 202 483 7616

Product type : Solid.

2. Hazards identification

Emergency overview

Physical state : Solid. [Lustrous solid.]

Color : Silvery.

Odor : Odorless.

Signal word : WARNING!

Hazard statements : MAY CAUSE ALLERGIC SKIN REACTION. MAY CAUSE TARGET ORGAN DAMAGE, BASED ON ANIMAL DATA. POSSIBLE CANCER HAZARD - MAY CAUSE CANCER, BASED ON ANIMAL DATA.

Precautionary measures : Do not handle until all safety precautions have been read and understood. Obtain special instructions before use. Do not eat, drink or smoke when using this product. Avoid prolonged or repeated contact with skin. Use personal protective equipment as required. Wash thoroughly after handling.

OSHA/HCS status : This material is considered hazardous by the OSHA Hazard Communication Standard (29 CFR 1910.1200).

Avoid inhalation of and contact with eyes by any dust produced during machining, cutting or processing (a safety data sheet for product in powder form is available on request).

Potential acute health effects

Skin : May cause sensitization by skin contact.

Potential chronic health effects

Chronic effects : May cause target organ damage, based on animal data. Once sensitized, a severe allergic reaction may occur when subsequently exposed to very low levels.

Carcinogenicity : May cause cancer, based on animal data. Risk of cancer depends on duration and level of exposure.

Target organs : May cause damage to the following organs: kidneys, lungs, upper respiratory tract, skin, nose/sinuses.

Over-exposure signs/symptoms

Skin : Adverse symptoms may include the following:
irritation
redness

Medical conditions aggravated by over-exposure : Pre-existing skin disorders and disorders involving any other target organs mentioned in this MSDS as being at risk may be aggravated by over-exposure to this product.

See toxicological information (Section 11)

3. Composition/information on ingredients

Name	CAS number	%
Nickel	7440-02-0	100

There are no additional ingredients present which, within the current knowledge of the supplier and in the concentrations applicable, are classified as hazardous to health or the environment and hence require reporting in this section.

4. First aid measures

Eye contact : Check for and remove any contact lenses. Immediately flush eyes with plenty of water for at least 15 minutes, occasionally lifting the upper and lower eyelids. Get medical attention immediately.

Skin contact : In case of contact, immediately flush skin with plenty of water for at least 15 minutes while removing contaminated clothing and shoes. Wash clothing before reuse. Clean shoes thoroughly before reuse. Get medical attention immediately.

Inhalation : Move exposed person to fresh air. If not breathing, if breathing is irregular or if respiratory arrest occurs, provide artificial respiration or oxygen by trained personnel. Loosen tight clothing such as a collar, tie, belt or waistband. Get medical attention immediately.

Ingestion : Wash out mouth with water. Do not induce vomiting unless directed to do so by medical personnel. Never give anything by mouth to an unconscious person. Get medical attention immediately.

Protection of first-aiders : No action shall be taken involving any personal risk or without suitable training. It may be dangerous to the person providing aid to give mouth-to-mouth resuscitation. Wash contaminated clothing thoroughly with water before removing it, or wear gloves.

Notes to physician : No specific treatment. Treat symptomatically. Contact poison treatment specialist immediately if large quantities have been ingested or inhaled.

5. Fire-fighting measures

Flammability of the product : No specific fire or explosion hazard.

Extinguishing media

Suitable : Use an extinguishing agent suitable for the surrounding fire.

Not suitable : None known.

Special exposure hazards : Promptly isolate the scene by removing all persons from the vicinity of the incident if there is a fire. No action shall be taken involving any personal risk or without suitable training.

Hazardous thermal decomposition products : Decomposition products may include the following materials:
metal oxide/oxides

Special protective equipment for fire-fighters : Fire-fighters should wear appropriate protective equipment and self-contained breathing apparatus (SCBA) with a full face-piece operated in positive pressure mode.

6. Accidental release measures

Personal precautions : No action shall be taken involving any personal risk or without suitable training. Evacuate surrounding areas. Keep unnecessary and unprotected personnel from entering. Do not touch or walk through spilled material. Provide adequate ventilation. Wear appropriate respirator when ventilation is inadequate. Put on appropriate personal protective equipment (see Section 8).

Environmental precautions : Avoid dispersal of spilled material and runoff and contact with soil, waterways, drains and sewers. Inform the relevant authorities if the product has caused environmental pollution (sewers, waterways, soil or air).

Methods for cleaning up

Small spill : Move containers from spill area. Vacuum or sweep up material and place in a designated, labeled waste container. Dispose of via a licensed waste disposal contractor.

6. Accidental release measures

Large spill : Move containers from spill area. Approach release from upwind. Prevent entry into sewers, water courses, basements or confined areas. Vacuum or sweep up material and place in a designated, labeled waste container. Dispose of via a licensed waste disposal contractor. Note: see section 1 for emergency contact information and section 13 for waste disposal.

7. Handling and storage

Handling : Put on appropriate personal protective equipment (see Section 8). Eating, drinking and smoking should be prohibited in areas where this material is handled, stored and processed. Workers should wash hands and face before eating, drinking and smoking. Remove contaminated clothing and protective equipment before entering eating areas. Persons with a history of skin sensitization problems should not be employed in any process in which this product is used. Do not get in eyes or on skin or clothing. Do not ingest. If during normal use the material presents a respiratory hazard, use only with adequate ventilation or wear appropriate respirator. Keep in the original container or an approved alternative made from a compatible material, kept tightly closed when not in use. Empty containers retain product residue and can be hazardous. Do not reuse container.

Storage : Store in accordance with local regulations. Store in original container protected from direct sunlight in a dry, cool and well-ventilated area, away from incompatible materials (see section 10) and food and drink. Keep container tightly closed and sealed until ready for use. Containers that have been opened must be carefully resealed and kept upright to prevent leakage. Do not store in unlabeled containers. Use appropriate containment to avoid environmental contamination.

8. Exposure controls/personal protection

Ingredient	Exposure limits
Nickel	**OSHA PEL 1989 (United States, 3/1989).** TWA: 1 mg/m³, (as Ni) 8 hour(s). **NIOSH REL (United States, 6/2009).** TWA: 0.015 mg/m³, (as Ni) 10 hour(s). **ACGIH TLV (United States, 2/2010).** TWA: 1.5 mg/m³ 8 hour(s). Form: Inhalable fraction **OSHA PEL (United States, 6/2010).** TWA: 1 mg/m³, (as Ni) 8 hour(s).

Recommended monitoring procedures : If this product contains ingredients with exposure limits, personal, workplace atmosphere or biological monitoring may be required to determine the effectiveness of the ventilation or other control measures and/or the necessity to use respiratory protective equipment.

Engineering measures : If user operations generate dust, fumes, gas, vapor or mist, use process enclosures, local exhaust ventilation or other engineering controls to keep worker exposure to airborne contaminants below any recommended or statutory limits.

Hygiene measures : Wash hands, forearms and face thoroughly after handling chemical products, before eating, smoking and using the lavatory and at the end of the working period. Appropriate techniques should be used to remove potentially contaminated clothing. Contaminated work clothing should not be allowed out of the workplace. Wash contaminated clothing before reusing. Ensure that eyewash stations and safety showers are close to the workstation location.

Personal protection

Respiratory : Use a properly fitted, air-purifying or air-fed respirator complying with an approved standard if a risk assessment indicates this is necessary. Respirator selection must be based on known or anticipated exposure levels, the hazards of the product and the safe working limits of the selected respirator.

Hands : Chemical-resistant, impervious gloves complying with an approved standard should be worn at all times when handling chemical products if a risk assessment indicates this is necessary.

8. Exposure controls/personal protection

Eyes : Safety eyewear complying with an approved standard should be used when a risk assessment indicates this is necessary to avoid exposure to liquid splashes, mists or dusts.

Skin : Personal protective equipment for the body should be selected based on the task being performed and the risks involved and should be approved by a specialist before handling this product.

Environmental exposure controls : Emissions from ventilation or work process equipment should be checked to ensure they comply with the requirements of environmental protection legislation. In some cases, fume scrubbers, filters or engineering modifications to the process equipment will be necessary to reduce emissions to acceptable levels.

9. Physical and chemical properties

Physical state : Solid. [Lustrous solid.]

Color : Silvery.

Odor : Odorless.

Molecular weight : 58.69 g/mole

Molecular formula : Ni

Boiling/condensation point : 2730°C (4946°F)

Melting/freezing point : 1453°C (2647.4°F)

Relative density : 8.9

10. Stability and reactivity

Chemical stability : The product is stable.

Conditions to avoid : No specific data.

Incompatible materials : No specific data.

Hazardous decomposition products : Under normal conditions of storage and use, hazardous decomposition products should not be produced.

Possibility of hazardous reactions : Under normal conditions of storage and use, hazardous reactions will not occur.

11. Toxicological information

Acute toxicity

Conclusion/Summary : Not available.

Chronic toxicity

Conclusion/Summary : Not available.

Irritation/Corrosion

Conclusion/Summary : Not available.

Sensitizer

Conclusion/Summary : Not available.

Carcinogenicity

Conclusion/Summary : Not available.

Classification

Product/ingredient name	ACGIH	IARC	EPA	NIOSH	NTP	OSHA
Nickel	A5	2B	-	+	Possible	-

Mutagenicity

Conclusion/Summary : Not available.

Teratogenicity

Conclusion/Summary : Not available.

Reproductive toxicity

Nickel

11. Toxicological information

Conclusion/Summary : Not available.

12. Ecological information

Ecotoxicity : No known significant effects or critical hazards.

Aquatic ecotoxicity

Product/ingredient name	Result	Species	Exposure
Nickel	Acute LC50 2.3 ppm Fresh water	Fish - Cyprinus carpio - Juvenile (Fledgling, Hatchling, Weanling) - 6 cm	96 hours
	Chronic NOEC 3.5 ug/L Fresh water	Fish - Cyprinus carpio - 13 months - 10.5 cm - 27.8 g	4 weeks

Conclusion/Summary : Not available.

Persistence/degradability

Conclusion/Summary : Not available.

13. Disposal considerations

Waste disposal : The generation of waste should be avoided or minimized wherever possible. Significant quantities of waste product residues should not be disposed of via the foul sewer but processed in a suitable effluent treatment plant. Dispose of surplus and non-recyclable products via a licensed waste disposal contractor. Disposal of this product, solutions and any by-products should at all times comply with the requirements of environmental protection and waste disposal legislation and any regional local authority requirements. Waste packaging should be recycled. Incineration or landfill should only be considered when recycling is not feasible. This material and its container must be disposed of in a safe way. Care should be taken when handling emptied containers that have not been cleaned or rinsed out. Empty containers or liners may retain some product residues. Avoid dispersal of spilled material and runoff and contact with soil, waterways, drains and sewers.

Disposal should be in accordance with applicable regional, national and local laws and regulations.

Refer to Section 7: HANDLING AND STORAGE and Section 8: EXPOSURE CONTROLS/PERSONAL PROTECTION for additional handling information and protection of employees.

14. Transport information

Regulatory information	UN number	Proper shipping name	Classes	PG*	Label	Additional information
DOT Classification	Not available.	Not available.	Not available.	-		Reportable quantity 100 lbs. (45.4 kg)
TDG Classification	Not available.	Not available.	Not available.	-		-
Mexico Classification	Not available.	Not available.	Not available.	-		-
ADR/RID Class	Not available.	Not available.	Not available.	-		-
IMDG Class	Not available.	Not available.	Not available.	-		-
IATA-DGR Class	Not available.	Not available.	Not available.	-		-

PG* : Packing group

15. Regulatory information

HCS Classification : Sensitizing material
Carcinogen
Target organ effects

U.S. Federal regulations : **TSCA 8(a) IUR Exempt/Partial exemption:** Not determined

United States inventory (TSCA 8b): This material is listed or exempted.

SARA 302/304/311/312 extremely hazardous substances: No products were found.
SARA 302/304 emergency planning and notification: No products were found.
SARA 302/304/311/312 hazardous chemicals: Nickel
SARA 311/312 MSDS distribution - chemical inventory - hazard identification: Nickel: Fire hazard, Immediate (acute) health hazard, Delayed (chronic) health hazard

Clean Water Act (CWA) 307: Nickel

Clean Air Act Section 112(b) Hazardous Air Pollutants (HAPs) : Not listed

Clean Air Act Section 602 Class I Substances : Not listed

Clean Air Act Section 602 Class II Substances : Not listed

DEA List I Chemicals (Precursor Chemicals) : Not listed

DEA List II Chemicals (Essential Chemicals) : Not listed

SARA 313

	Product name	CAS number	Concentration
Form R - Reporting requirements	Nickel	7440-02-0	100
Supplier notification	Nickel	7440-02-0	100

SARA 313 notifications must not be detached from the MSDS and any copying and redistribution of the MSDS shall include copying and redistribution of the notice attached to copies of the MSDS subsequently redistributed.

State regulations

Massachusetts : This material is listed.

New York : This material is listed.

New Jersey : This material is listed.

Pennsylvania : This material is listed.

California Prop. 65

WARNING: This product contains a chemical known to the State of California to cause cancer.

Ingredient name	Cancer	Reproductive	No significant risk level	Maximum acceptable dosage level
Nickel	Yes.	No.	No.	No.

Canada inventory : This material is listed or exempted.

16. Other information

Label requirements : MAY CAUSE ALLERGIC SKIN REACTION. MAY CAUSE TARGET ORGAN DAMAGE, BASED ON ANIMAL DATA. POSSIBLE CANCER HAZARD - MAY CAUSE CANCER, BASED ON ANIMAL DATA.

Hazardous Material Information System (U.S.A.) :

Health	*	2
Flammability		0
Physical hazards		0

Caution: HMIS® ratings are based on a 0-4 rating scale, with 0 representing minimal hazards or risks, and 4 representing significant hazards or risks Although HMIS® ratings are not required on MSDSs under 29 CFR 1910.1200, the preparer may choose to provide them. HMIS® ratings are to be used with a fully implemented HMIS® program. HMIS® is a registered mark of the National Paint & Coatings Association (NPCA). HMIS® materials may be purchased exclusively from J. J. Keller (800) 327-6868.

The customer is responsible for determining the PPE code for this material.

National Fire Protection Association (U.S.A.) :

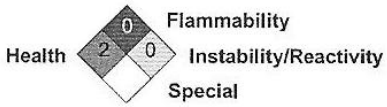

Reprinted with permission from NFPA 704-2001, Identification of the Hazards of Materials for Emergency Response Copyright ©1997, National Fire Protection Association, Quincy, MA 02269. This reprinted material is not the complete and official position of the National Fire Protection Association, on the referenced subject which is represented only by the standard in its entirety.

Date of issue : 21/09/2012.

Date of previous issue : 26/01/2012.

Version : 2

Indicates information that has changed from previously issued version.

Notice to reader

Further information

License granted to make unlimited paper copies for internal use only.

The above information is believed to be correct but does not purport to be all inclusive and shall be used only as a guide. It is based on the present state of our knowledge and is applicable to the product with regard to appropriate safety precautions. Employers should use this information only as a supplement to other information gathered by them and should make independent judgement of the suitability of this information to ensure proper use of the product and to protect the health and safety of their employees and the end-user(s) of the product.

Goodfellow Holdings Limited and any subsidiary or associated company supplies this information without warranty and any use of the product not in conformance with this Material Safety Data Sheet or in combination with any other product or process is the responsibility of the user. The Company does not represent any guarantee of the properties of the product or any suitability of the product for a given application.

Goodfellow Holdings Limited shall not be held liable for any damage resulting from handling or from contact with the product. See www.goodfellow.com or www.goodfellowusa.com for additional terms and conditions of sale.

The information contained in this document is only relevant for products supplied by Goodfellow Holdings Limited and any subsidiary or associated company.

APPENDIX I

VICE PART/ASSEMBLY DRAWINGS

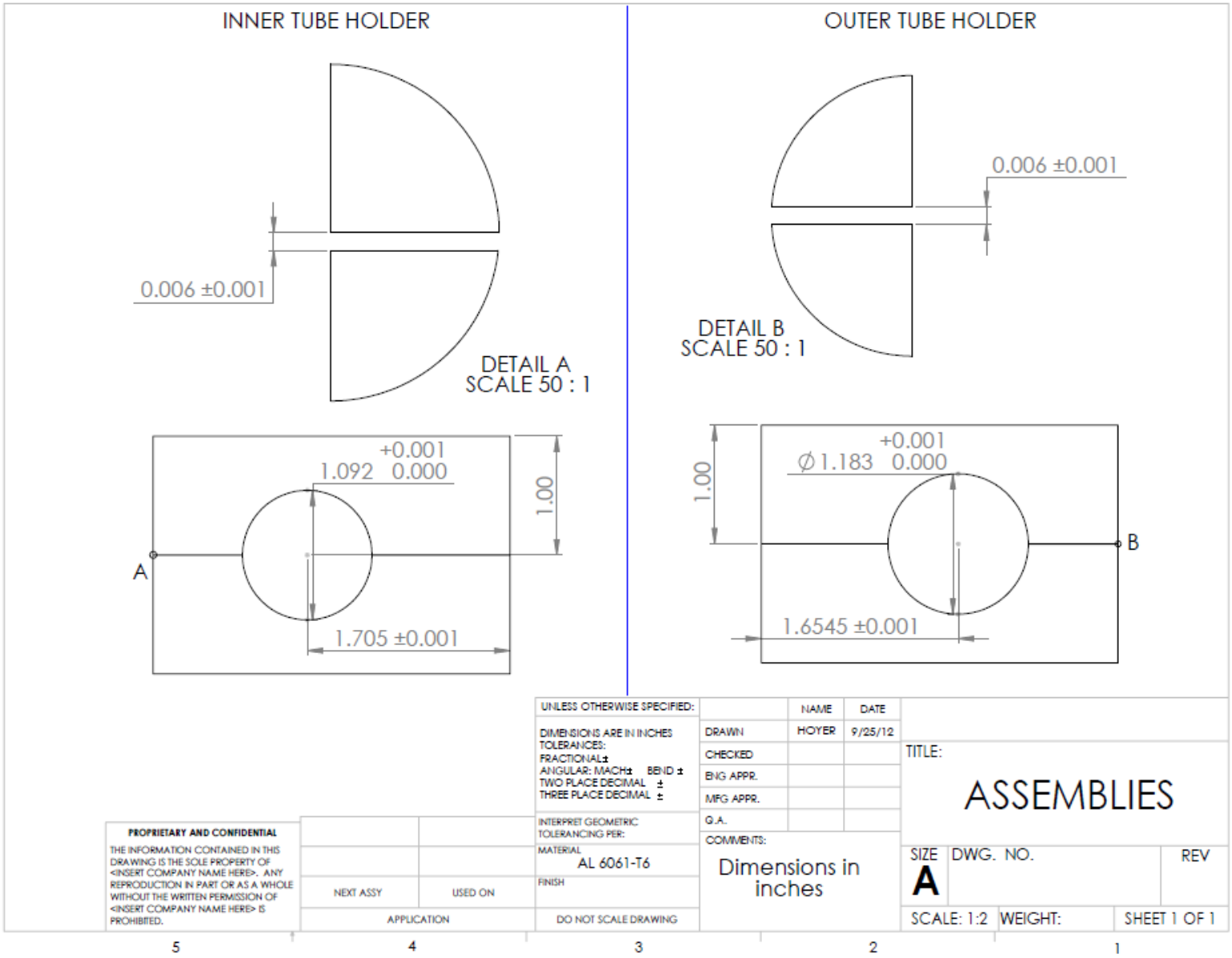
INNER TUBE HOLDER
0.006 ±0.001
DETAIL A
SCALE 50 : 1
+0.001
1.092 0.000
1.00
A
1.705 ±0.001
OUTER TUBE HOLDER
0.006 ±0.001
DETAIL B
SCALE 50 : 1
+0.001
Ø1.183 0.000
1.00
B
1.6545 ±0.001
UNLESS OTHERWISE SPECIFIED:
DIMENSIONS ARE IN INCHES
TOLERANCES:
FRACTIONAL ±
ANGULAR: MACH ± BEND ±
TWO PLACE DECIMAL ±
THREE PLACE DECIMAL ±
INTERPRET GEOMETRIC TOLERANCING PER:
MATERIAL
AL 6061-T6
FINISH
DO NOT SCALE DRAWING
NAME
DATE
DRAWN
HOYER
9/25/12
CHECKED
ENG APPR.
MFG APPR.
Q.A.
COMMENTS:
Dimensions in inches
TITLE:
ASSEMBLIES
SIZE
A
DWG. NO.
REV
SCALE: 1:2
WEIGHT:
SHEET 1 OF 1
PROPRIETARY AND CONFIDENTIAL
THE INFORMATION CONTAINED IN THIS DRAWING IS THE SOLE PROPERTY OF <INSERT COMPANY NAME HERE>. ANY REPRODUCTION IN PART OR AS A WHOLE WITHOUT THE WRITTEN PERMISSION OF <INSERT COMPANY NAME HERE> IS PROHIBITED.
NEXT ASSY
USED ON
APPLICATION
5
4
3
2
1

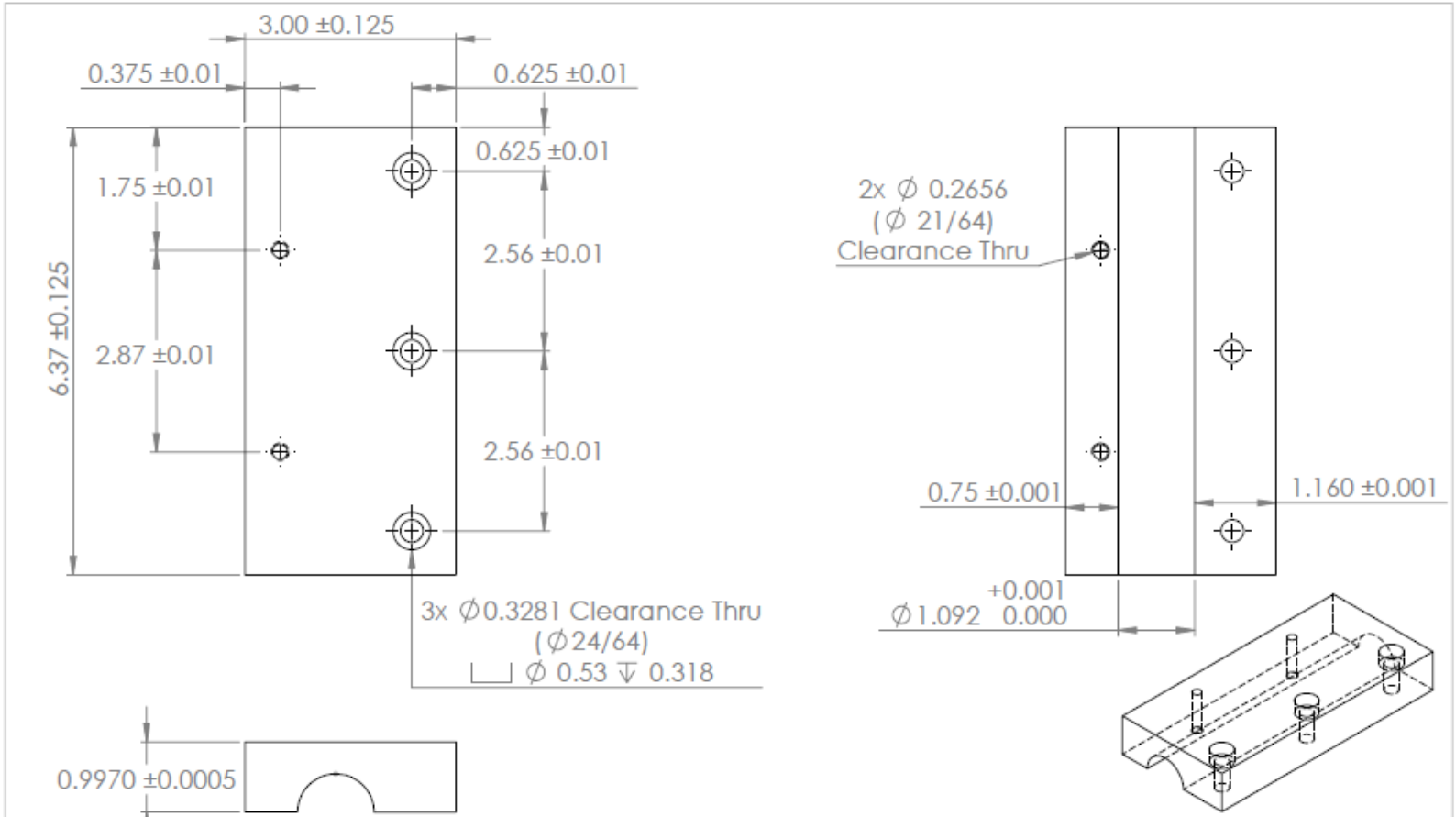

UNLESS OTHERWISE SPECIFIED:		NAME	DATE
DIMENSIONS ARE IN INCHES TOLERANCES: FRACTIONAL± ANGULAR: MACH± BEND ± TWO PLACE DECIMAL ± THREE PLACE DECIMAL ±	DRAWN	HOYER	9/24/12
	CHECKED		
	ENG APPR.		
	MFG APPR.		
INTERPRET GEOMETRIC TOLERANCING PER:	Q.A.		
MATERIAL AL 6061-T6	COMMENTS: Dimensions in inches		
FINISH			
DO NOT SCALE DRAWING			

QTY: 1

TITLE:

Inner_Hold_Front

SIZE	DWG. NO.	REV
A	1 of 4	
SCALE: 1:2	WEIGHT:	SHEET 1 OF 1

NEXT ASSY	USED ON
APPLICATION	

5 4 3 2 1

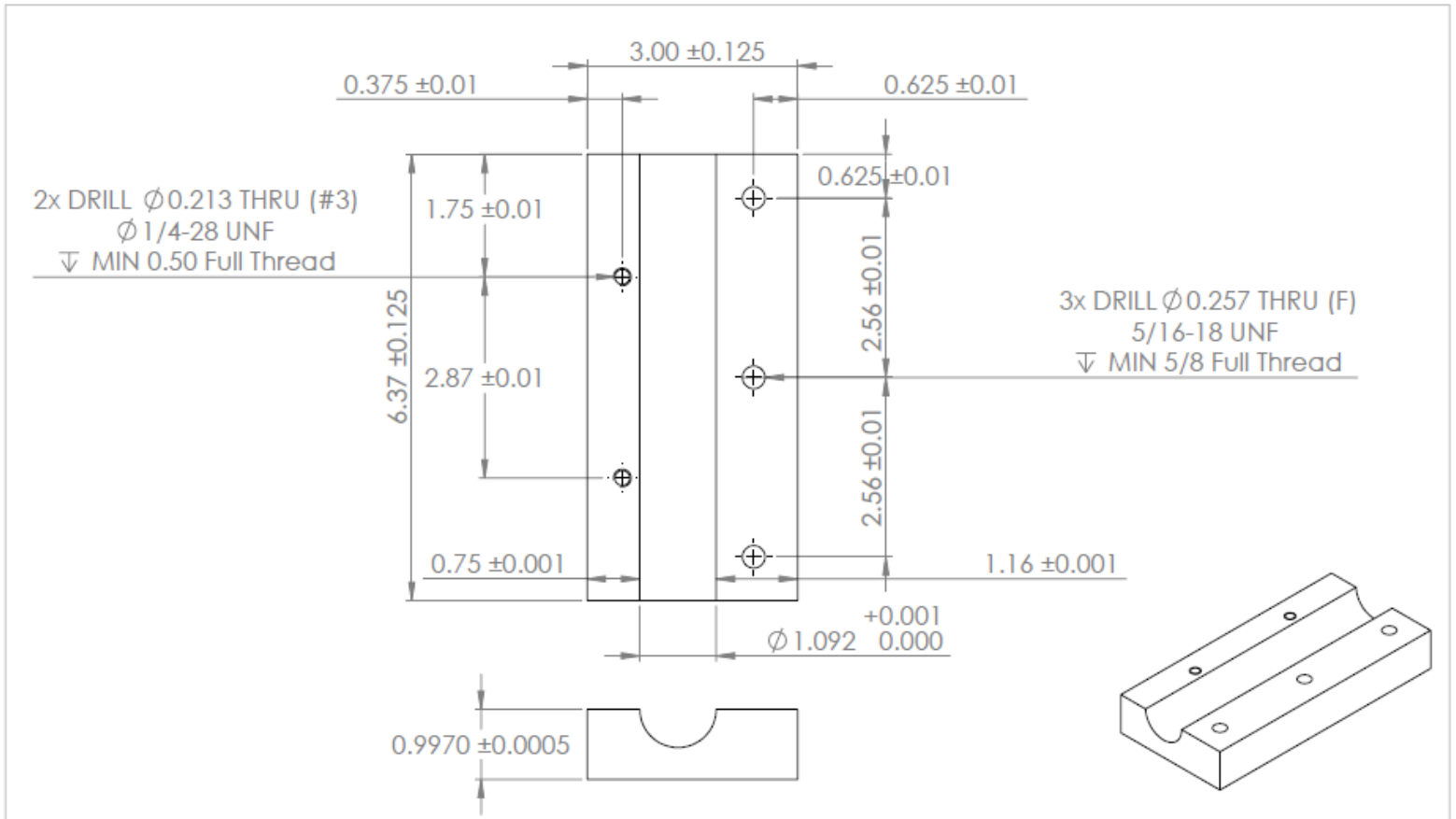

UNLESS OTHERWISE SPECIFIED:		NAME	DATE
DIMENSIONS ARE IN INCHES TOLERANCES: FRACTIONAL ± ANGULAR: MACH ± BEND ± TWO PLACE DECIMAL ± THREE PLACE DECIMAL ±	DRAWN	HOYER	9/24/12
	CHECKED		
	ENG APPR.		
	MFG APPR.		
INTERPRET GEOMETRIC TOLERANCING PER:	Q.A.		
MATERIAL AL 6061-T6	COMMENTS: Dimensions in inches		
FINISH			
DO NOT SCALE DRAWING			

QTY: 1

TITLE: Inner_Hold_Back

SIZE	DWG. NO.	REV
A	2 of 4	
SCALE: 1:2	WEIGHT:	SHEET 1 OF 1

NEXT ASSY	USED ON
APPLICATION	

5 4 3 2 1

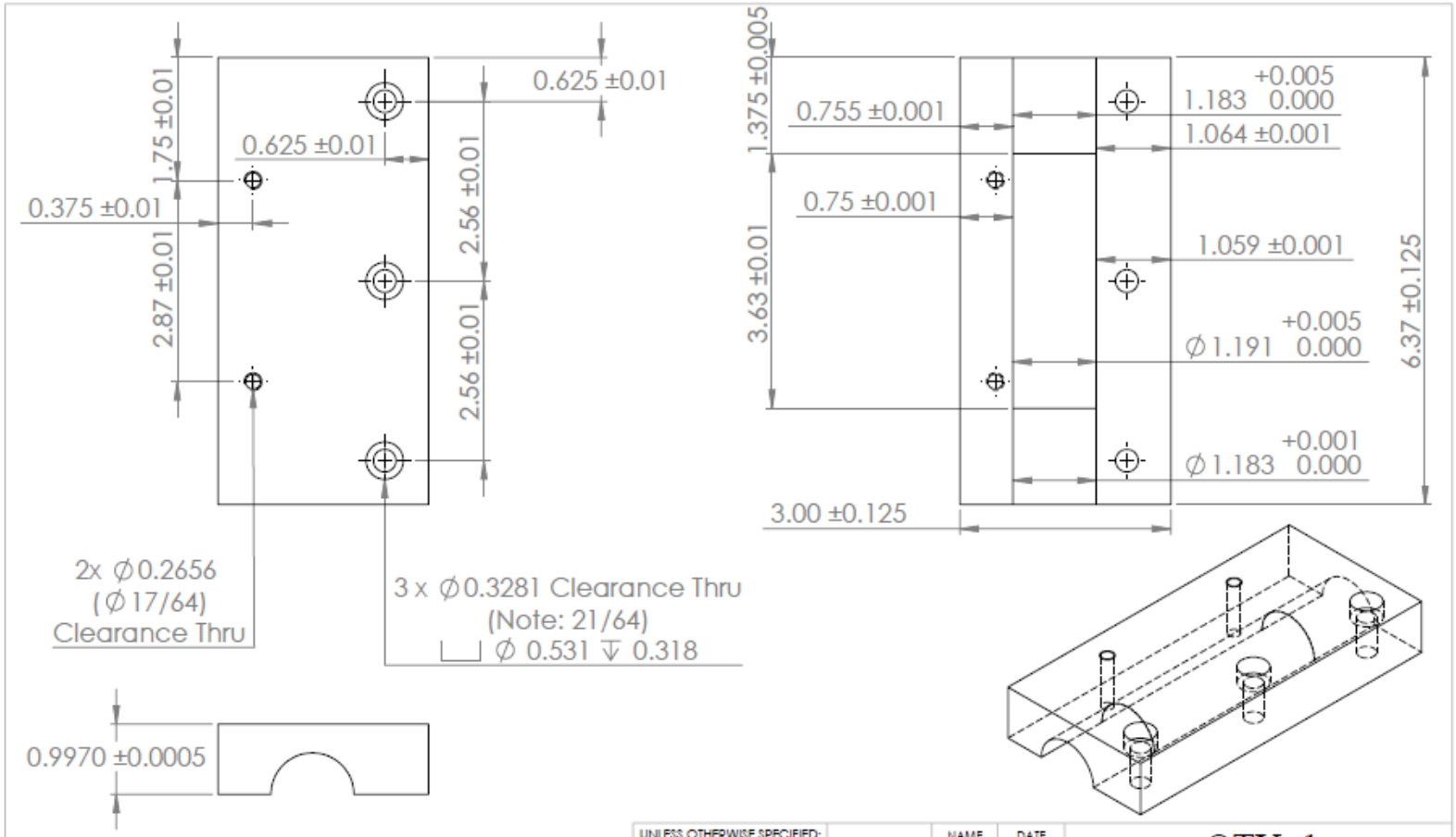

UNLESS OTHERWISE SPECIFIED:		NAME	DATE
DIMENSIONS ARE IN INCHES TOLERANCES: FRACTIONAL ± ANGULAR: MACH ± BEND ± TWO PLACE DECIMAL ± THREE PLACE DECIMAL ±	DRAWN	HOYER	9/25/12
	CHECKED		
	ENG APPR.		
	MFG APPR.		
INTERPRET GEOMETRIC TOLERANCING PER:	Q.A.		
MATERIAL AL 6061-T6	COMMENTS: Dimensions in inches		
FINISH			
DO NOT SCALE DRAWING			

QTY: 1

TITLE: Outer_Hold_Front

SIZE	DWG. NO.	REV
A	3 of 4	
SCALE: 1:2	WEIGHT:	SHEET 1 OF 1

NEXT ASSY	USED ON
APPLICATION	

5 4 3 2 1

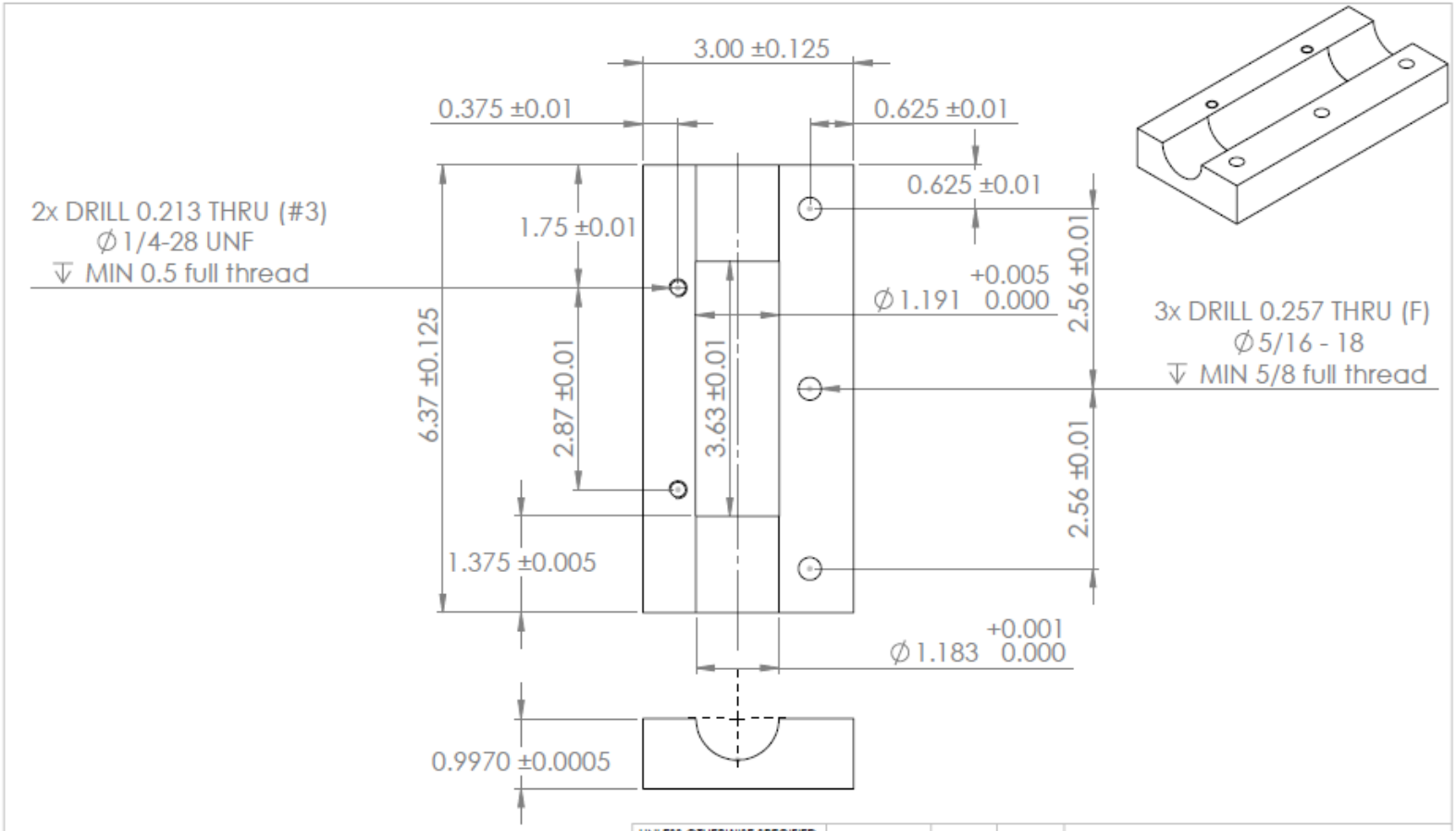
3.00 ±0.125
0.375 ±0.01
0.625 ±0.01
0.625 ±0.01
2x DRILL 0.213 THRU (#3)
Ø1/4-28 UNF
↧ MIN 0.5 full thread
1.75 ±0.01
+0.005
Ø1.191 0.000
2.56 ±0.01
3x DRILL 0.257 THRU (F)
Ø5/16 - 18
↧ MIN 5/8 full thread
6.37 ±0.125
2.87 ±0.01
3.63 ±0.01
2.56 ±0.01
1.375 ±0.005
+0.001
Ø1.183 0.000
0.9970 ±0.0005
UNLESS OTHERWISE SPECIFIED:
DIMENSIONS ARE IN INCHES
TOLERANCES:
FRACTIONAL ±
ANGULAR: MACH ± BEND ±
TWO PLACE DECIMAL ±
THREE PLACE DECIMAL ±
INTERPRET GEOMETRIC TOLERANCING PER:
MATERIAL
AL 6061-T6
FINISH
NEXT ASSY
USED ON
APPLICATION
DO NOT SCALE DRAWING
NAME
DATE
DRAWN
HOYER
9/24/12
CHECKED
ENG APPR.
MFG APPR.
Q.A.
COMMENTS:
Dimensions in inches
QTY: 1
TITLE:
Outer_Hold_Back
SIZE
A
DWG. NO.
4 of 4
REV
SCALE: 1:2
WEIGHT:
SHEET 1 OF 1
PROPRIETARY AND CONFIDENTIAL
THE INFORMATION CONTAINED IN THIS DRAWING IS THE SOLE PROPERTY OF <INSERT COMPANY NAME HERE>. ANY REPRODUCTION IN PART OR AS A WHOLE WITHOUT THE WRITTEN PERMISSION OF <INSERT COMPANY NAME HERE> IS PROHIBITED.
5
4
3
2
1

APPENDIX J

RELIABILITY TESTING

```
% script

clear all, close all
% Initial conditions:
prompt = {'Enter number of samples to test:'};
freq = inputdlg(prompt,'Number of Samples',...
    1,{'10000'});

dist_type = menu('Choose an distribution to test:',...% Menu title
    'Normal',...        % case 1
    'Exponential',...   % case 2
    'Lognormal');       % case 3

format compact;format long;clc
ns = str2double(freq{1});
tic

% conversions
in2mm = 25.4;

% Input design parameters
input_innerID = 1.026;
input_outerOD = 1.181;
input_foilID = 1.076;

% See background information in thesis to get explanation of equations


callmenu = menu('Choose an Deformation Size:',...% Menu title
    '0.009" - Diameter 1.046"',...  % case 1
    '0.010" - Diameter 1.047"',...  % case 2
    '0.011" - Diameter 1.048"');    % case 3

% Choose punch size
switch callmenu
    case {1}
        punch_dia = 1.046;
        small_dia = 0.8;
    case {2}
        punch_dia = 1.047;
        small_dia = 0.801;
    case {3}
        punch_dia = 1.048;
        small_dia = 0.802;
end

switch dist_type
    case {1}    % Normal
```

```
        % generate random normal tube diameters...
        design = [input_innerID input_outerOD];
        std_design = design*0.0116;
        %range = [0.005 0.01 0.05]
        newdesign = zeros(length(design),ns);

        ic = 1;
        for ii = 1:length(design)
            newdesign(ic,:) = design(ii) +
real(std_design(ii)*randn(1,ns));
            ic = ic + 1;
        end

        for ii = 1:length(design)
            max_dia(ii) = max(newdesign(ii,:));
            min_dia(ii) = min(newdesign(ii,:));
        end

        % here step into forming calculations
        k(1:2,1) = 0;
        for jj = 1:ns
            innerID = newdesign(1,jj);
            outerOD = newdesign(2,jj);
            [sigma_dr,UTS] =
forming_pressure_ends(punch_dia,innerID,outerOD);

            % Working with outputs
            output3(jj,1) = real(sigma_dr);       % fill column



            % Checking constraints: failure
            if sigma_dr > UTS | sigma_dr < 1E7
                k(1,jj) = 1;
            end
        end

        idk = k;
        yay = sum(idk(:)~=0);

        failure_rate = yay/ns

        useful_output1 = output3(:,1);


        useful_output1(useful_output1<0)=[];

        mu = zeros(1,1); stdv = zeros(1,1);

        useful_mu(1,1) = mean(useful_output1)
        useful_stdv(1,1) = std(useful_output1)


        mu(1,1) = mean(output3(:,1));
```

```
        stdv(1,1) = std(output3(:,1));



        %   Plot histograms based on number of values used.

        nb_bars = 60;
        figure(1);
        [N,Zout] = hist(useful_output1,nb_bars);
        bar(Zout,N/max(N));
        hold on

%         x = (useful_mu(1) -
3*useful_stdv(1)):useful_stdv(1)/15:useful_mu(1) + 3*useful_stdv(1);
%         y = (1/(useful_stdv(1)*sqrt(2*pi))).*exp(-((x-
useful_mu(1)).^2)/(2*useful_stdv(1).^2));
%         plot(x,y);

        xlabel('Forming Stress');ylabel(['Occurrance at NS =
',num2str(ns)]);
        title(['Forming stress Plug Size ',num2str(punch_dia), '
inches']);
        hold off

        toc
        fprintf('Nominal Inner ID\t\tNominal Outer OD\n')
        fprintf('\t%2.3f \t\t\t\t %2.3f \n',design(1), design(2))
        fprintf('Maximum Inner ID\t\tMaximum Outer OD\n')
        fprintf('\t%2.3f \t\t\t\t %2.3f \n',max_dia(1), max_dia(2))
        fprintf('Minimum Inner ID\t\tMinimum Outer OD\n')
        fprintf('\t%2.3f \t\t\t\t %2.3f \n',min_dia(1), min_dia(2))


    case {2}    % Exponential
        % --------------------- EXP ---------------------------------- %

        % generate random normal tube diameters...
        design = [input_innerID input_outerOD];
        std_design = design*0.004272;
        %range = [0.011 0.05]
        newdesign = zeros(length(design),ns);

        ic = 1;
        for ii = 1:length(design)
            newdesign(ic,:) = design(ii) +
real(std_design(ii)*(exprnd(design(ii),[1,ns])));
            ic = ic + 1;
        end

         for ii = 1:length(design)
            max_dia(ii) = max(newdesign(ii,:));
            min_dia(ii) = min(newdesign(ii,:));
        end
```

```
        % here step into forming calculations
        k(1:2,1) = 0;
        for jj = 1:ns
            innerID = newdesign(1,jj);
            outerOD = newdesign(2,jj);
            [sigma_dr,UTS] =
forming_pressure_ends(punch_dia,innerID,outerOD);

            % Working with outputs
            output3(jj,1) = real(sigma_dr);       % fill column



            % Checking constraints: failure
            if sigma_dr > UTS | sigma_dr < 1E7
                k(1,jj) = 1;
            end
        end

        idk = k;
        yay = sum(idk(:)~=0);

        failure_rate = yay/ns

        useful_output1 = output3(:,1);


        useful_output1(useful_output1<0)=[];

        mu = zeros(1,1); stdv = zeros(1,1);

        useful_mu(1,1) = mean(useful_output1)
        useful_stdv(1,1) = std(useful_output1)


        mu(1,1) = mean(output3(:,1));
        stdv(1,1) = std(output3(:,1));



        %   Plot histograms based on number of values used.

        nb_bars = 60;
        figure(1);
        [N,Zout] = hist(useful_output1,nb_bars);
        bar(Zout,N/max(N));
        hold on

        xlabel('Forming Stress');ylabel(['Occurrance at NS =
',num2str(ns)]);
        title(['Forming stress Plug Size ',num2str(punch_dia), '
inches']);
        hold off
```

```
        toc
        fprintf('Nominal Inner ID\t\tNominal Outer OD\n')
        fprintf('\t%2.3f \t\t\t\t %2.3f \n',design(1), design(2))
        fprintf('Maximum Inner ID\t\tMaximum Outer OD\n')
        fprintf('\t%2.3f \t\t\t\t %2.3f \n',max_dia(1), max_dia(2))
        fprintf('Minimum Inner ID\t\tMinimum Outer OD\n')
        fprintf('\t%2.3f \t\t\t\t %2.3f \n',min_dia(1), min_dia(2))


    case {3}    % Lognormal
        % -------------------- Lognormal -------------------------%
        % random_log = random('Lognormal',mu_log,sigma_log,[1,ns]);



        % generate random normal tube diameters...
        design = [input_innerID input_outerOD];
        std_design = design*0.0093;
        %range = [0.011 0.05]
        newdesign = zeros(length(design),ns);

        ic = 1;
        for ii = 1:length(design)
            newdesign(ic,:) = design(ii) +
real(std_design(ii)*log(randn(1,ns)));
            ic = ic + 1;
        end

        for ii = 1:length(design)
            max_dia(ii) = max(newdesign(ii,:));
            min_dia(ii) = min(newdesign(ii,:));
        end

        % here step into forming calculations
        k(1:2,1) = 0;
        for jj = 1:ns
            innerID = newdesign(1,jj);
            outerOD = newdesign(2,jj);
            [sigma_dr,UTS] =
forming_pressure_ends(punch_dia,innerID,outerOD);

            % Working with outputs
            output3(jj,1) = real(sigma_dr);       % fill column



            % Checking constraints: failure
            if sigma_dr > UTS | sigma_dr < 1E7
                k(1,jj) = 1;
            end
        end

        idk = k;
        yay = sum(idk(:)~=0);
```

```
        failure_rate = yay/ns

        useful_output1 = output3(:,1);


        useful_output1(useful_output1<0)=[];

        mu = zeros(1,1); stdv = zeros(1,1);

        useful_mu(1,1) = mean(useful_output1)
        useful_stdv(1,1) = std(useful_output1)


        mu(1,1) = mean(output3(:,1));
        stdv(1,1) = std(output3(:,1));



        %   Plot histograms based on number of values used.

        nb_bars = 60;
        figure(1);
        [N,Zout] = hist(useful_output1,nb_bars);
        bar(Zout,N/max(N));
        hold on

        xlabel('Forming Stress');ylabel(['Occurrance at NS =
',num2str(ns)]);
        title(['Forming stress Plug Size ',num2str(punch_dia), '
inches']);
        hold off

        toc
        fprintf('Nominal Inner ID\t\tNominal Outer OD\n')
        fprintf('\t%2.3f \t\t\t\t %2.3f \n',design(1), design(2))
        fprintf('Maximum Inner ID\t\tMaximum Outer OD\n')
        fprintf('\t%2.3f \t\t\t\t %2.3f \n',max_dia(1), max_dia(2))
        fprintf('Minimum Inner ID\t\tMinimum Outer OD\n')
        fprintf('\t%2.3f \t\t\t\t %2.3f \n',min_dia(1), min_dia(2))
end




% function [sigma_dr,UTS] =
forming_pressure_foil(punch_dia,foilID,outerOD)

% Conversion
r2d = 180/pi;
d2r = 1/r2d;
in2mm = 25.4;
```

```
punch_dia = 1.046;
outerOD = 1.181;
foilID = 1.076;

punch_dia = punch_dia*in2mm;
outerOD = outerOD*in2mm;
innerID = foilID*in2mm;


% -- Geometry Calculations -- %
dh = in2mm*(punch_dia - innerID)/2; % Change in height punch dia.
shaft_len = 1.17*in2mm;             % Length of punch, mm
L = sqrt(shaft_len^2 + dh^2);       % Hypotenuse for angle, mm
alpha = atan2(dh,shaft_len)*r2d;    % Angle of punch ascent

% -- Stress Calculations -- %
% Tensile stress: Al 6061-T6
UTS = 310e6;                        % Pascals

% Drawing stress: Al 6061-T6

A0 = (pi/4)*(outerOD^2 - innerID^2);
A1 = (pi/4)*(outerOD^2 - punch_dia^2);
strain = log(A0/A1);
h = (innerID + punch_dia)/2;
phi = 0.88 + 0.12*(h/L);

mu = 0.3;                           % coeff of friction (die & Al 6061)
Qfr = 1 + mu*cot(alpha*d2r);        % forming multiplication factor

sigma_dr = UTS*Qfr*phi*strain;      % drawing stress, Pa
sigma_dr


% end
```